

CAA PAPER 2001/2

**CRASHWORTHINESS OF HELICOPTER
EMERGENCY FLOTATION SYSTEMS**

Study I (Main Study)

Study II (Supplementary Study)

CIVIL AVIATION AUTHORITY, LONDON

Price £30.00

CAA PAPER 2001/2

CRASHWORTHINESS OF HELICOPTER EMERGENCY FLOTATION SYSTEMS

Study I (Main Study)

Prepared by W S Atkins Consultants Ltd
Author: P J Murrell

Study II (Supplementary Study)

Prepared by BMT Fluid Mechanics Ltd
Authors: R G Standing
R Eichaker

© Civil Aviation Authority 2001

ISBN 0 86039 810 2

Printed and distributed by
Documedia, 37 Windsor Street, Cheltenham, England

General Foreword

The research reported in this paper was funded by the Safety Regulation Group of the UK Civil Aviation Authority (CAA). The work was instigated at WS Atkins Consultants Limited (WSA) and BMT Fluid Mechanics Limited (BMT), primarily in response to the conclusions and recommendations of earlier research performed for CAA by GKN Westland Helicopters Limited. This earlier work was commissioned by CAA in response to recommendations made in the HARP Report (Report of the Helicopter Airworthiness Review Panel - CAP 491), and was published as CAA Paper 96005 in July 1996. In addition, impetus was added to the project by the recommendation (Recommendation 14.2 (g)) in the RHOSS Report (Review of Helicopter Offshore Safety and Survivability - CAP 641) that *"Particular account should be taken [in the CAA's ongoing research programme on helicopter crashworthiness and ditching stability] of the need to improve provision for flotation after a severe impact, including the possibility of installing extra flotation devices specifically to cater for a crash"*.

This paper contains unabridged versions of the following WSA and BMT final project reports, each covering their respective parts of the research:-

I. WS Atkins Consultants Ltd. Report No.AM3504/R006, Issue 04

This study included: a review of accident data and public domain literature relating to water impact; the development and validation of finite element modelling (FEM) techniques to predict airframe accelerations and forces during water impact; the modelling of three helicopter water impact scenarios (based on actual accidents) using the proprietary FEM code LS-DYNA3D; a review of helicopter emergency flotation equipment design; a top-level cost-benefit analysis of a number of proposed modifications; a review of the requirements and advisory material relating to water impact, ditching and occupant egress.

II. BMT Fluid Mechanics Ltd. Document No.44134r55 Release 5

This study comprised an assessment of the range and variability of impact loads experienced by typical emergency flotation systems during water impact, using a Monte Carlo simulation procedure based on simplified empirical and theoretical formulae. The purpose of this study was to complement the finite element analysis performed by WSA.

The principal conclusions of these studies included:-

- The most effective means of significantly improving the crashworthiness of helicopter emergency flotation systems is through the addition of flotation unit redundancy (preferably through the addition of flotation units at the top of the airframe to provide a side-floating attitude).
- The consequences of a significant proportion of helicopter water impacts could be mitigated through the introduction of automatic arming and deployment of emergency flotation systems.
- The finite element analysis techniques used show significant limitations when attempting to accurately model impacts between complex deformable structures and fluids.
- The nature of drag and planing forces in the water impact loading process are not fully understood, and their magnitudes are likely to be significant in mainly horizontal impacts.

The results of the research reported in this paper are being progressed through the JAA/FAA requirement development and harmonisation procedures. They have been presented to and considered by the JAA/FAA Joint Harmonisation Working Group on helicopter water impact and ditching, and the JAA Helicopter Offshore Safety and Survivability (HOSS) Working Group. Recommendations for changes to the requirements and advisory material have been made by both of these groups to the JAA.

Safety Regulation Group

03 January 2001

Study I (Main Study)

Prepared by W S Atkins Consultants Ltd

Summary

This document reports on an investigation of the crashworthiness of helicopter emergency flotation systems (EFS), commissioned and funded by the Safety Regulation Group of the UK Civil Aviation Authority (CAA).

The work follows on from GKN Westland Helicopters Limited (GKN WHL) studies into civil and military water impacts. The work was given greater importance following the Review of Offshore Safety and Survival, commissioned by the CAA, which recommended that the provision for flotation after a severe but survivable impact be improved.

This report details the work performed by WS Atkins comprising a complete review of EFS design and associated requirements (JARs), with a particular emphasis on crashworthiness issues.

A review of accident data and public domain literature relating to water impact was undertaken. The aims of this task were to determine the nature and extent of any relevant work that had been conducted elsewhere, identify accidents where a failure of the EFS system contributed to the consequences and to obtain water impact data from actual accidents and research activities.

Finite element modelling techniques were then developed with a view to predicting accelerations and forces on the airframe during a water impact. Using this approach, siting of the EFS to reduce damage on impact could be investigated. The technique was validated against a variety of full and scale model test programmes. The correlation between analysis and test was found to be variable, and highlighted water mesh density and model complexity as the main controlling factors. Questions also arose regarding the validity of some of the test data used for validation.

Three full scale helicopter water impact scenarios were explicitly modelled using LS-DYNA3D to determine the response of a typical airframe during water entry. These scenarios were based on actual accidents which were outside the Federal Aviation Authority's proposed 95% survivability ditching envelope, but for which there were a significant number of survivors.

From the literature reviews, causes for failure of EFS deployment other than impact damage were identified. A number of modifications to the EFS were proposed and a cost-benefit analysis carried out. Advice was sought from helicopter manufacturers, EFS suppliers and regulatory bodies to ensure their implementation would be practical.

Finally, regulatory requirements for water impact, ditching and occupant egress were reviewed. A series of recommendations, based on the conclusions from all the stages of the project, are made to improve the crash performance of EFS and the associated regulatory requirements and guidance material.

Contents

	<i>Page</i>	
1	INTRODUCTION	1
2	Description of Emergency Flotation Systems	2
3	Literature review	2
3.1	Introduction	2
3.2	Methodology	2
3.3	Results of Literature Review	3
3.4	Results of Accident Review	4
3.4.1	Air Accident Investigation Branch (AAIB)	4
3.4.2	Royal Navy Flight Safety and Accident Investigation Centre (RNFAIC)	5
3.4.3	CAA Flight Safety Data Department	5
3.4.4	Aircraft Insurance Companies	5
3.4.5	Federal Aviation Administration (FAA)	6
3.5	Summary of UK Civil Water Impacts	
3.5.1	G-BIJF, Bell 212, 12/8/81, North Sea (Dunlin Alpha) [12]	7
3.5.2	G-ASWI, Wessex 60, 13/8/81, North Sea [AAIB]	7
3.5.3	G-BDIL, Bell 212, 14/09/82, North Sea (Murchison Platform) [13]	7
3.5.4	G-BEON, Sikorsky S61N, 16/7/83, St Marys (Isles of Scilly) [14]	7
3.5.5	G-BJJR, Bell 212, 20/11/84, North Sea [AAIB]	8
3.5.6	G-BEWL, Sikorsky S61N, 25/07/90, North Sea (Brent Spar) [15]	8
3.5.7	G-TIGH AS 332L Super Puma, 14/03/92 North Sea (Cormorant 'A' Platform) [16]	8
3.5.8	Non Fatal Accidents	9
3.6	Conclusions	9
4	COMPUTER modelling	10
4.1	Introduction	10
4.2	Modelling Methods	11
4.3	Validation of Helicopter Model	12
4.4	Validation of Water Model for Vertical Impacts – Capsule Model	14
4.5	Validation of Water Model for Horizontal Impacts – Orbiter Model	15
4.6	Validation of Water Model for Horizontal Impacts– Seaplane Hull Model	17
4.7	Validation Conclusions	19
4.8	Helicopter Water Impact Scenarios	19
4.8.1	Brent Spar (Lagrangian Water)	21
4.8.2	Cormorant Alpha (Lagrangian Water)	22
4.8.3	Isles of Scilly (Lagrangian Water)	23
4.8.4	Eulerian Modelling	23
4.8.5	Comparison of Panel Loads Against Empirical Predictions	24
4.9	Modelling Conclusions	25
5	Emergency Flotation DESIGN Review	26
5.1	Introduction	26
5.2	Emergency Flotation Problems	26
5.2.1	Floats Not Armed	27
5.2.2	Floats Armed But Not Activated	27
5.2.3	Floats Activated But Not Deployed	28

5.2.4	Uneven Float Deployment	28
5.2.5	Incomplete Inflation Due to Adverse Ambient Conditions	29
5.2.6	Float Damage Upon Impact	30
5.2.7	Floats Deployed But Helicopter Immediately Overturns	31
5.3	Summary of Design Recommendations to Improve Emergency Flotation System Crashworthiness	32
6	Cost Benefit Analysis	33
6.1	Overview	33
6.2	Causes of EFS Failure	34
6.2.1	Float Deployment	34
6.2.2	Accident Data	34
6.3	EFS Design Modifications	35
6.4	Assessment of Benefits	36
6.4.1	Effect on Outcome	36
6.4.2	Effect on Fatalities	37
6.5	Determination of Implementation Costs	39
6.6	Cost-Benefit	39
6.7	Discussion of Results	40
7	REVIEW OF REGULATORY REQUIREMENTS	41
7.1	JAR 29.801: Ditching	41
7.2	JAR 29.563: Structural Ditching Provisions	43
7.3	JAR 29.561: Emergency Landing Conditions	44
7.4	JAR 29.562: Emergency Landing Dynamic Conditions	44
7.5	JAR 29.807: Passenger Emergency Exits	44
7.6	Recommendations For Regulation Changes	44
8	CONCLUSIONS	45
9	RECOMMENDATIONS	47
	Acknowledgements	48
	References	49
	Appendix A: Royal Navy Accident Records	87
	Appendix B: Space Capsule and Orbiter Modelling Data	91
	Appendix C: Joint Airworthiness Requirements and Advisory Material	93
	Appendix D: Cost Benefit Study – NTSB Accident Summaries	111
	Appendix E: Cost Benefit Study – UK Accident Summaries	131
	Appendix F: Cost Benefit Study – Worked Example	135

List of figures

Figure 1:	WG30 Finite Element Model	51
Figure 2:	Cut Away of WG30 Model after Ground Impact, Together With Lynx Test Comparison	52
Figure 3:	Acceleration Time History Pulse Recorded at Cabin Floor	53
Figure 4:	Acceleration Time History Pulse Recorded at Main Rotor Gearbox	54
Figure 5:	Arrangement of the Space Capsule Impact Scenario	55
Figure 6:	Acceleration of Space Capsule from Test and Analysis	56
Figure 7:	Vertical Displacement of Space Capsule from Test and Analysis	57
Figure 8:	Finite Element Mesh of Orbiter Space Shuttle	58
Figure 9:	Lateral Acceleration of Orbiter using Lagrangian Mesh	59
Figure 10:	Set-up for the two Hull Scenarios Showing Differences in Trim Angle and Flight Path	60
Figure 11:	Vertical Displacement of Hull for Case 1	61
Figure 12:	Vertical Acceleration of Hull for Case 1	62
Figure 13:	Vertical Velocity of Hull for Case 1	63
Figure 14:	Vertical Displacement of Hull for Case 2	64
Figure 15:	Vertical Acceleration of Hull for Case 2	65
Figure 16:	Vertical Velocity of Hull for Case 2	66
Figure 17:	Brent Spar – Global Acceleration at Full Speed	67
Figure 18:	Brent Spar – Full Speed: Maximum Plastic Strain Throughout Time Period	68
Figure 19:	Brent Spar – Half Speed: Maximum Plastic Strain Throughout Time Period	69
Figure 20:	Comparison of Nodal Velocity for Rigid and Non-Rigid Analysis	70
Figure 21:	Nodal Acceleration Before and After Filtering	71
Figure 22:	Location of Nodes for Monitoring Acceleration	72
Figure 23:	Filtered Vertical Acceleration for Gearbox, Floor and Side Panel	73
Figure 24:	Cormorant Alpha – Global Acceleration at Full Speed	74

Figure 25: Cormorant Alpha – Full Speed: Maximum Plastic Strain Throughout Time Period	75
Figure 26: Cormorant Alpha – Half Speed: Maximum Plastic Strain Throughout Time Period	76
Figure 27: Isles of Scilly – Global Acceleration at Full Speed	77
Figure 28: Isles of Scilly – Full Speed: Maximum Plastic Strain Throughout Time Period	78
Figure 29: Isles of Scilly – Half Speed: Maximum Plastic Strain Throughout Time Period	79
Figure 30: Global Accelerations For Full Speed Scenarios, Eulerian Water Models	80
Figure 31: Plastic Strain for Full Speed Brent Spar Scenario, Eulerian Water Model	81
Figure 32: Plastic Strain for Full Speed Scilly Isles Scenario, Eulerian Water Model	82
Figure 33: Plastic Strain for Full Speed Cormorant Alpha Scenario, Eulerian Water Model	83
Figure 34: Location of Side Panels Under Consideration	84
Figure 35: Sequence of Events in Successful Float Deployment	85
Figure 36: Probability Tree for Deployment of EFS	86

INTRODUCTION

The Safety Regulation Group of the Civil Aviation Authority is currently investigating the crashworthiness of helicopter emergency flotation systems (EFS). The work follows on from GKN Westland Helicopters Limited (GKN WHL) studies into civil and military water impacts [1,2]. The work was given greater importance following the Review of Offshore Safety and Survival [3], commissioned by the Civil Aviation Authority (CAA), which recommended that the provision for flotation after a severe but survivable impact be improved.

CAA commissioned WS Atkins (Contract 084/SRG/R&AD) to undertake a crashworthiness review of EFS design, operation and legislation. The work was divided into the five key tasks summarised below:

- **Task 1 – Literature Review:** The aim of this task was to determine the nature and extent of any relevant work that had been conducted elsewhere, identify accidents where a failure of the EFS system contributed to the consequences and to obtain water impact data from actual accidents and research activities.
- **Task 2 – Computer Modelling:** The aim of this task was to understand and to predict the loadings generated in a typical helicopter airframe during a water impact using finite element (FE) modelling techniques. The techniques were validated against a variety of full scale and model test programmes. The method was then applied to three specific accident scenarios for which there were a significant number of survivors, but which were outside the Federal Aviation Authority's proposed 95% survivability ditching envelope.

In addition to the WS Atkins modelling work, supporting work was undertaken by BMT Fluid Mechanics Ltd [4]. BMT's work examined the highly variable nature of water impacts. Their method used an empirical statistical approach to determine the range of possible loadings on single airframe panels and sponsons, over a large variety of impact orientations, speeds and sea states.

- **Task 3 – Review of EFS Design:** A review of typical EFS designs was undertaken and proposals developed to improve overall system functionality, reliability and operation following a water impact.
- **Task 4 – Cost and Benefits Analysis:** The proposals developed under Task 3 were assessed against estimated cost of implementation and potential benefit in terms of reductions of the probability of EFS failure to determine their relative merit.
- **Task 5 – Review of Regulatory Requirements:** Finally, the airworthiness and operational requirements relating to water impact, ditching and occupant egress were reviewed, and recommendations for improvements proposed.

This report describes the work carried out by WS Atkins whilst undertaking these tasks, concluding with a series of recommendations for improving the crashworthiness of emergency flotation systems.

2 DESCRIPTION OF EMERGENCY FLOTATION SYSTEMS

In order to provide additional buoyancy upon ditching, helicopters which operate over water are fitted with emergency flotation devices. They are designed to maintain the emergency exits above water level long enough for the occupants to escape and board the life rafts.

The system comprises two or more inflatable bags mounted either onto the helicopter lower fuselage or to the landing skids. During normal operation the floats are stowed and packed within a protective cover until activation. Different helicopters have different numbers, sizes and locations of flotation units, depending on the inherent buoyancy and stability of the fuselage. Typical mounting locations are outrigger sponsons (S61N), pods (AS332L rear), fuselage (AS332L nose) and skids (Bell 206).

The floats are inflated from canisters of pressurised gas. The mechanism for inflating the devices relies on two stages. The first stage is arming the inflation system. This is necessary to prevent inadvertent inflation while in flight. Some systems have additional safeguards that prevent inflation outside certain flight conditions. The second stage is deployment, which is triggered either by manual operation or by immersion switches and/or inversion switches.

3 LITERATURE REVIEW

3.1 Introduction

The purpose of this stage of the work was to develop an understanding of the water impact response of helicopters from inspection of historical records and published research. The objectives of this stage were:

- 1 To identify potential improvements to the EFS.
- 2 To provide an indication of the potential benefit resulting from improvements to the EFS.
- 3 To provide validation data for Task 2 of the project which involved computer simulation of helicopter water impacts.

The aim of the review was therefore to examine accidents that were considered survivable, but where failure of the EFS for whatever reason increased the likelihood of occupants drowning. In addition, a literature search of relevant research papers and reports was also carried out.

3.2 Methodology

The main purpose of the study was to establish the data associated with accidents where fatalities occurred due to failure of the EFS. Accidents considered non-survivable were disregarded, as the impact in these cases often resulted in gross failure of the fuselage.

The review utilised the following sources:

- Relevant information from the literature search.
- Review of information held in the CAA library.
- Review of Air Accident Investigation Reports.
- Communication with the CAA Safety Data Department
- Communication and meetings with the UK Air Accident Investigation Branch (AAIB).
- Communication with Royal Navy Flight Safety and Investigation Centre.
- Review of information held at Royal Navy Flight Safety and Investigation Centre.
- Communication with helicopter insurers.
- Communication with US Federal Aviation Authority (FAA).

The results from the different sources are described in Section 3.4.

The main information sought from each source was as follows:

- Whether the flotation systems functioned correctly.
- Whether the accident was deemed survivable, i.e. the fuselage remained relatively intact.
- The consequence of EFS failure in terms of casualties.
- Aircraft loading and impact parameters.
- Structural damage.
- Sea state at the time of the accident.

In addition to the above requirements, the study concentrated on medium to large helicopter types such as the Sikorsky S61-N and AS332L Super Puma, although relevant data on other helicopter types is also included.

3.3 **Results of Literature Review**

An on-line search was carried out on three different databases. A general engineering database, an aviation database and a US government publication database. For all searches the combination of keywords used were:

(helicopter or rotorcraft) and (flotation or floatation or ditching or impact or crash)

This generated a title search of some 300 articles.

The most noteworthy result of the search is that little new information was discovered. A similar exercise had been carried out by GKN Westland Helicopters Ltd (GKN WHL) in 1993 [1] and partly in 1995 [2], to provide information for general structural response to helicopter impacts. The current review served to confirm the results of these studies. In addition it was already known that the US FAA were also engaged in sponsoring work relating to helicopter EFS [5,6,7].

The review also highlighted some research work being carried out in the National Aerospace Laboratory in The Netherlands [8,9]. The work considers design of compliant composite panels for use in a helicopter floor to withstand water impact. This work is of interest to this study, particularly in the latter stages considering mitigation, but is not of direct relevance.

The work being carried out in the US was researched further during an American Helicopter Society (AHS) Conference in Phoenix during September 1998. General discussions were held on the current status of US research into helicopter crashworthiness including helicopter airbags, energy absorbing seats and composite energy absorbing design. Of particular interest were papers from Sikorsky [10] using MSC/DYTRAN to model helicopter water impact and a paper on the developments of hybrid approaches [11]. The general conclusion was that the work being carried out in the US was at a similar stage to research in the UK. The conference agreed that there was a lack of good validation data; the US DoD announced that they were in the process of funding some full scale drop tests of helicopters onto water which would hopefully fulfil this need.

3.4 **Results of Accident Review**

As mentioned in Section 3.3, a number of sources were contacted to establish data relating to ditched or impacted helicopters where failure of the EFS had increased the chances of fatalities due to drowning. The quality and quantity of data held by these sources is discussed below.

3.4.1 *Air Accident Investigation Branch (AAIB)*

The AAIB investigates UK civil and also military aircraft accidents. The main aim of each investigation is to establish the cause of the accident and to recommend proposals to address any operational or design shortcomings highlighted by the investigation.

The findings of significant accidents are published in AAIB reports. Since the primary issue of the investigation is to establish cause of the accident, the areas of interest to this study are not generally addressed in any detail. This approach is changing though, and more recent accident reports present additional data. Some of the additional information is as a consequence of helicopters now carrying flight data recorders. These provide information regarding the helicopter orientation and velocity at the point of impact that previously had often to be based on judgement.

In addition to the reports, the AAIB was approached to establish what additional data might be held. Unfortunately the information required by this study is often not gathered or is not kept beyond the investigators' personal copies. Some further information is available for the most recent accidents, but this diminishes rapidly for events that occurred more than 5 or 6 years ago.

Discussions were held with several of the investigating engineers on 9th January 1997 at Farnborough. The main source of additional data gathered related to video footage of the wreckage of G-TIGH (accident near the Cormorant Alpha platform) lying on the sea bed and during recovery. The footage shows the relatively intact fuselage and EFS system. Damage to the nose section is visible but it is difficult to establish if damage occurred during the initial impact with the sea or subsequently with the sea bed. This is a factor in most accidents where the airframe sank. Often, further damage is caused during recovery of the airframe.

3.4.2 *Royal Navy Flight Safety and Accident Investigation Centre (RNFAIC)*

The RNFAIC performs a similar role to the AAIB for Royal Navy (RN) accidents. They investigate accidents and produce a report to establish the cause. The RN operate the Sea King, from which the civilian Sikorsky S61-N was derived. The search was therefore restricted to this helicopter type, although consideration was also given to accidents involving the Wessex helicopter which is of a similar size to the Sea King.

A review of the available accident reports from 1980 was carried out at the RNFAIC. Of the 10 accidents reviewed only one matched the requirements but the fuselage sank in very deep water and was not recovered. The survivors were also unsure as to the precise condition of the helicopter after the accident. Some of the accidents, where the airframe broke up on impact, were considered not survivable. A list of the corresponding accidents and associated descriptions is given in Appendix A for completeness.

The amount of historical data available was generally better than for the AAIB records. The main reporting on structural damage recorded major damage such as fuselage break-up or loss of sponsons. It was concluded however that, apart from data for the assessment of benefit (Task 4), the only useful data related to the retention, or otherwise, of the Sea King forward sponsons for modelling validation purposes.

3.4.3 *CAA Flight Safety Data Department*

The CAA maintain a database of all UK civil aircraft accidents. The database also contains some military accidents as well as some non-UK accidents. The database contains only basic information similar to the International Civil Aircraft Organisation (ICAO) database, with additional CAA comments.

The database is, however, useful in ensuring that no obvious accident records are missed, and in identifying overseas accidents of interest to the study. For those countries which publish air accident reports it was considered by the CAA Safety Data Department that the level of information would be comparable to the UK reports and would therefore be of limited value. It was not considered feasible to pursue non-US overseas accident data.

3.4.4 *Aircraft Insurance Companies*

The helicopter insurers also keep records relating to helicopter accidents and associated damage. One of the major companies, Air Claims, were contacted to establish the quantity and quality of records they kept. In addition to records similar to the ICAO database, they also have limited information relating to the extent of damage for accidents where they were the acting loss adjusters. This information

relates more to the cost of repairs, and does not distinguish between damage caused at different stages of the accident or subsequent salvage. Where the helicopter is not considered economically viable to repair, the reports are more limited as the loss equates to the cost of the complete helicopter. This is often the case for those helicopters where flotation systems failed and the helicopter sank.

It was considered that it was not worthwhile pursuing data from this source at this stage.

3.4.5 *Federal Aviation Administration (FAA)*

The FAA have sponsored work reviewing helicopter ditching and water related impacts [5,6]. As a result of these studies, occupant drowning was identified as the most significant post impact hazard and resulted in additional research work [7], which concentrated on the performance of EFS and possible areas of improvement. A brief summary of the data held within these reports relevant to this study is given below.

The data used in the reports relates to 67 accidents that occurred in the US between 1982 and 1989. The report considers all types of helicopter, therefore some small and some very large helicopter accidents are included in the results. The sample sizes for the individual helicopter types included, however, do not allow meaningful comparisons to be made. The report identifies 26 fatalities that occurred in survivable or partially survivable accidents. These were composed of 19 fatalities due to drowning, 1 due to exposure and 6 through impact related injuries. In considering these figures it should be noted that a significant proportion of US over water flights take place over the Gulf of Mexico, where sea conditions are considerably less harsh than the North Sea.

The problems with the EFS were categorised by failure type and the number of occurrences of each. Of a sample size of 35 float-equipped helicopters, the problems and associated frequencies of occurrence can be summarised as follows:

- no problems (11);
- damaged by impact (7), (3 of which deployed unevenly);
- did not deploy after activation (3);
- uneven deployment (2);
- other problems (2);
- floats armed but not activated (2);
- floats not armed (8).

The majority of the impact damage to floats occurred with systems where the float was inflated prior to impact with the water. For the three EFS that failed to deploy, one suffered electrical damage caused by the impact, and no reason was given for the failure of the remaining two.

Unfortunately, no direct correlation can be made between the number of fatalities.

The research also highlights the fact that occupants survived impacts where the helicopters' vertical and horizontal velocities far exceed the FAA's proposed 95% survivability envelope. However, occupants often encountered post-impact difficulties and drowned.

3.5 **Summary of UK Civil Water Impacts**

A summary and discussion of the UK civil helicopter fatal water impacts since 1980 is given below. The list is confined to medium to large helicopter types that are of relevance to this study. A description of each fatal accident is provided in this section. In addition, Section 3.5.8 gives a brief description of relevant non-fatal impacts.

3.5.1 *G-BIJF, Bell 212, 12/8/81, North Sea (Dunlin Alpha) [12]*

- *Conditions:* Helicopter hit the water with an unknown rate of descent (>1.5m/s). Helicopter inverted almost immediately. Helicopter remained upturned but floating and was used as support for survivors.
- *Damage:* No significant damage to the cabin space. Lower fuselage skins stoved and fuselage frames, keel members and cabin floor suffered extensive damage.
- *Flotation System:* EFS automatically deployed but damage sustained during impact had caused the right feeder pipe to rupture.
- *Casualties:* 1 fatality due to exposure out of 14 occupants.

3.5.2 *G-ASWI, Wessex 60, 13/8/81, North Sea [AAIB]*

- *Conditions:* Helicopter crashed into sea following loss of power to main rotor gearbox. Helicopter crashed from 1500ft.
- *Casualties:* All 13 occupants were killed. This was considered a non-survivable impact.

3.5.3 *G-BDIL, Bell 212, 14/09/82, North Sea (Murchison Platform) [13]*

- *Conditions :* Impact with water with significant forward speed, considered non survivable accident.
- *Damage:* Damage typical of high speed forward impact.
- *Flotation System:* No mention of EFS in AAIB report.
- *Casualties:* All six occupants died.

3.5.4 *G-BEON, Sikorsky S61N, 16/7/83, St Marys (Isles of Scilly) [14]*

- *Conditions:* Aircraft flew into water in straight horizontal flight on approach to landing.
- *Damage:* Both sponsons broke off. Water entered the cabin forcibly, and water pressure burst two freight bay hatches in floor. Water also destroyed the aircraft

hull for most of its length below floor level. Helicopter then rolled over and sank.

- *Impact Conditions:* Aircraft slightly nose down and banked slightly to port. Forward airspeed 80 to 100 knots (41 – 51m/s), low rate of descent. Large number of seat failures (post accident testing suggest that this occurs at longitudinal accelerations >12g). Sea State calm.
- *Flotation System:* The flotation systems were attached to the sponsons and were therefore unavailable for deployment.
- *Casualties:* 6 survivors, 20 fatalities. No incapacitating injuries, all fatalities caused by drowning.

3.5.5 G-BJJR, Bell 212, 20/11/84, North Sea [AAIB]

- *Conditions:* Control of helicopter lost following decay of rotor RPM. Helicopter then fell into sea. Considered non-survivable accident.
- *Casualties:* Both crew died in the accident.

3.5.6 G-BEWL, Sikorsky S61N, 25/07/90, North Sea (Brent Spar) [15]

- *Conditions:* Helicopter tail rotor struck handrail on Brent Spar. Helicopter struck helideck, causing damage to left-hand sponson and fuselage, and causing left hand emergency escape hatch to enter cabin. Helicopter then fell off platform almost vertically into the water where it sank almost immediately.
- *Damage:* Damage to left hand sponson consistent with large lateral force (not vertical) on deck impact. Right hand sponson detached in rearward direction and nose of sponson damaged indicating impact with the water. Fuselage suffered failure from close to cockpit bulkhead to just aft of cargo door (station 120 to station 170). Tail boom failed and folded to left. Damage to seats indicated that impact with water was mainly vertical but had some longitudinal and lateral components. Impact less severe in rear of cabin.
- *Impact Conditions:* Helicopter fell through 95 feet, therefore impact velocity was 75 feet/s (50 mph, 22m/s), pitch 5° to 10° below horizon and roll 10° to right of horizontal. Estimated deceleration 20-25g at cabin floor. Sea State calm.
- *Flotation System:* Intact and attached to damaged sponsons, however it was not deployed.
- *Casualties:* 7 survivors, 6 fatalities. Two suffered severe injuries as a result of the impact. The remainder suffered less severe injuries but were unable to escape and drowned.

3.5.7 G-TIGH AS 332L Super Puma, 14/03/92 North Sea (Cormorant 'A' Platform) [16]

- *Conditions:* Aircraft struck the water when flying between two platforms. The aircraft entered an uncontrolled descent which pilot attempted to recover. After impact with water aircraft rolled over to an inverted position and then sank within a minute or two of impact.

- *Damage:* Damage to aircraft suggests initial impact occurred into a wave on the right side of the nose area. Report indicates crushing damage to fuselage.
- *Impact Conditions:* Pitch 4.1° nose up, roll 0.3° left. Rate of descent 25 feet/second (7.6 m/s) and derived ground speed of 43 Kt. Severe wind and snow, Sea State high (significant wave height 7 – 8 metres, max. 11 – 13 metres, period 8 – 10 seconds).
- *Flotation System:* Two bags mounted in collar around nose, and one each at structural frames at the sponsons. System was armed and post accident testing revealed the system was working but required firing by pilots. No water immersion switches.
- *Casualties:* 6 survivors, 11 fatalities. All injuries were slight and should not have affected the ability of an individual to escape from the helicopter. Five of the fatalities were trapped inside the cabin.

3.5.8 Non Fatal Accidents

G-ASNL, Sikorsky S61N, 11/03/83, North Sea [AAIB]

Controlled ditching. EFS successfully deployed. No fatalities but helicopter sank during attempted recovery.

G-BDII, Sikorsky S61N, 17/10/88, Handa Island [17]

Helicopter inadvertently flown into sea. Starboard side of boat hull damaged due to impact with water at approximately 5° nose down pitch, banked 15° to right and slipping to the right. Helicopter moving forward at no more than 5 Kt. and descending in excess of 1000 fpm (5.1 m/s) at point of impact. Ruptures in skin in areas below cockpit, boat hull badly creased. Starboard sponson torn away. Helicopter subsequently sank. Calm sea. Crew escaped, no fatalities. No mention of flotation system in AAIB report.

G-BDES, Sikorsky S61N, 10/11/88, North Sea [AAIB]

Helicopter ditched but overturned in strong winds. All passengers and crew escaped. Helicopter remained afloat but inverted for 24 hours before eventually sinking.

G-TIGK, AS332L Super Puma, 19/01/95 [AAIB]

Helicopter underwent successful auto-rotational ditching following lightning strike. EFS deployed and all occupants evacuated safely into a liferaft.

3.6 Conclusions

A survey of UK Civil and Royal Navy helicopter water impacts has been conducted with regard to performance of emergency flotation systems. In addition, a world-wide literature search has been carried out to identify existing research into helicopter emergency flotation systems.

The conclusions of the data review are:

- Little 'new' data to that already known at the start of the review is available.
- The accident data is almost exclusively limited to the information published in the accident reports, especially for accidents more than 8 years ago.
- Where levels of damage are supplied, they are often too general for detailed comparison with computer modelling techniques.
- Sponson mounted emergency flotation systems, such as the S61N, are particularly vulnerable to impact damage.
- Pod mounted emergency flotation systems are less prone to damage.
- Significant fatalities were observed in accidents where the EFS had failed to arm and/or deploy.

4 COMPUTER MODELLING

4.1 Introduction

The review of crash data and EFS performance, reported in Section 3, indicated that the location of the floats may have an effect on whether or not they are damaged on impact.

It was proposed that the impact of a helicopter with water would be modelled using finite element techniques (FE), so that the loads and accelerations on different panels of the aircraft could be investigated. In this way, the best location for minimal damage could be established for both location of floats and pipe routing. It was also anticipated that the method could be used to determine the panel force levels during actual survivable impacts with a view to defining a maximum panel force design limit.

A non-linear FE model of a WG30 helicopter was developed from data supplied by GKN WHL. This aircraft was considered to represent a typical design of medium weight helicopter. Water models using two separate modelling techniques were also developed.

The finite element software LS-DYNA 3D was chosen to model a variety of impacts between the helicopter and water models. LS-DYNA 3D is widely used to assess the plastic response of structures under extreme loads and has a variety of fluid modelling methods.

In order to gain confidence in the modelling results, it was necessary to validate both the responses of the WG30 and water models.

For the airframe used in the assessment, no water or ground drop test results were available. A survey of available test data highlighted that, for most helicopters where ground drop test data was available, the landing gear was usually deployed. The load paths for impacts with the gear deployed are very different from water impacts. For ground impact conditions, the initial contact normally occurs on the landing gear

(when deployed) which absorbs some of the impact energy. The load is then transferred to the airframe at discrete points where the undercarriage is attached. When an impact occurs with water, the load is transferred over the entire fuselage area in contact with the water. The only useful validation data available was that of a drop test of a similar airframe (GKN WHL Lynx) onto a flat concrete surface, with the landing gear retracted [18]. This was therefore used for the validation of the airframe model.

The water modelling methodology was validated by analysing re-entry space capsule impacts for which test data existed [19]. This was to validate the suitability of the water modelling method for vertical drop type scenarios. For impacts with longitudinal as well as vertical motion, the water modelling method was validated against Sea Plane Hull and Space Shuttle test data [20,21].

To summarise, due to the lack of helicopter water impact data, it was proposed that four simulated impacts would be validated. These were:

- Helicopter model validation against a level drop test of a similar helicopter with landing gear retracted.
- Water model validation against the NASA Gemini space capsule drop tests for impacts with main component of velocity vertical.
- Water model validation against space shuttle orbiter data for impacts with large longitudinal velocities.
- Water model validation against Sea Plane Hull and Space Shuttle data for impacts with vertical and longitudinal velocities.

Once the validation procedure was completed, three specific helicopter water impact scenarios were analysed. These were the accidents that occurred at the Brent Spar, the Cormorant Alpha and the Scilly Isles [15,16,14]. These scenarios represented water impacts that were known to have a significant number of survivors, but which were considerably outside the FAA's proposed 95% survivability curve. Panel loadings and structural accelerations were compared against damage described in the accident reports. Both full speed and half speed impact conditions were considered to try to understand trends in the response of the structure.

In addition to the WS Atkins modelling work, supporting work [4] was undertaken by BMT Fluid Mechanics Ltd (BMT). Their method used an empirical statistical approach to determine the range of possible loadings on single airframe panels and sponsons in isolation. The aim of BMT's work was to consider the likely loadings over a very large number of possible impact scenarios and parameter variation using a Monte Carlo simulation approach. The work was intended to complement the specific accident modelling being performed by WS Atkins. Panel force results predicted by the two methods for the Brent Spar and Cormorant Alpha incidents were made for comparison purposes.

4.2 **Modelling Methods**

LS-DYNA3D contains two processing techniques, Lagrangian and Eulerian, which can be coupled together. In both techniques, the equations of motion are integrated in time using central differences. The method requires very small time steps for a stable

solution. Thus, it is particularly suitable to assessing the crash behaviour of aircraft structures. These analyses are complex in that they involve both non-linear dynamic material response and large structural deformations. It is widely used in the automotive and rail industries to develop crashworthy designs.

The main advantage of this explicit method is that the governing equations are coupled allowing an 'element by element' solution, requiring no global stiffness matrix assembly or inversion. The method is generally recognised to be very robust for highly non-linear problems.

The LS-DYNA3D code contains many material models and, importantly for crash analysis, contact in the structure is efficiently handled by introducing temporary 'penalty forces' as additional external forces to resist penetration and control sliding.

Structural Modelling (Lagrangian)

The Lagrangian method is the most common finite-element processing technique for engineering applications.

Grid points are located on the body being analysed. Elements of material with constant (invariant) mass connect the grid points, forming a mesh. As the body deforms, the grid points move with the body and the elements (mesh) distort. The LS-DYNA3D Lagrangian processor uses explicit formulation and allows large deflection with material and geometric non-linearities. The helicopter, space capsule, orbiter and seaplane hull models were all constructed using Lagrangian elements.

Fluid Modelling (Lagrangian)

Fluids may be modelled in a similar way to structures using Lagrangian elements. The fluid is defined using an elastic material with zero shear modulus, which effectively allows neighbouring elements to slide relative to each other. Only the bulk modulus and density have to be defined to capture the shock wave through the fluid.

Fluid Modelling (Eulerian)

The Eulerian method may also be used for analysing fluids. The grid points remain fixed in space, defining fixed volumes, or elements. As the fluid moves through these Euler elements or mesh, the mass, momentum, and energy of the fluid is transported from one element to another. The LS-DYNA3D Eulerian processor is essentially an explicit in-viscid computational fluid dynamics code.

4.3 **Validation of Helicopter Model**

The airframe used in the analysis was based on the GKN WHL WG30 helicopter. This aircraft is a medium weight helicopter (c.4500 kg), constructed from riveted aluminium ribs, stringers and panels.

Airframe Model

The FE model of the WG30 was constructed by adapting an existing model used by GKN WHL to undertake vibration assessments. The model incorporated all the important structural components, including the main ring frames and outer fuselage

panels. The mesh density in the model was increased in the lower fuselage and roof sections, where large deformations were expected. The detail in these sections extended to the explicit modelling of the stringers, ribs and panel stiffeners.

The final helicopter model is shown in Figure 1. It utilises some 6,000 elements, mainly four noded shell elements for the main structure, plus a few beam elements to represent the tail rotor assembly. An elastic-plastic material was used to model the majority of helicopter fuselage. The following assumptions were applied in the model construction to ensure that reasonable development and analysis time-scales could be achieved.

- Failure was not included in the material model since, by assessing the levels of plastic strain in the model, it is possible to predict the extent of failure, if any, in the material.
- The rivets connecting the fuselage components were not modelled explicitly; instead a continuous mesh was used.
- The modelling detail extends to the individual stringers in the lower regions of the fuselage, however beam elements were used in the upper structure to provide stiff connections in the engine, gearbox and rotor head.
- Point masses were added to the model to represent the large mechanical items such as the engines, gearboxes and fuel.

It was considered that the simplifications listed above were not important given the types of results required and the levels of deformation observed in the accidents.

Validation Method

The airframe model was validated using data from a drop test of the Lynx helicopter onto a flat concrete surface with the landing gear retracted [18]. The Lynx and WG30, although not identical, are very similar in terms of weight, size and main structural components. The WG30 design uses many of the same components and design features as the Lynx, as it was the next helicopter that GKN WHL designed of this size. Both helicopters have their two engines, main rotor gearbox (MRGB) and rotor assembly mounted across two forged aluminium ring frames, located either side of the passenger compartment doorway. The airframes date from the same era and use the same fabrication techniques and materials.

The test results for the Lynx were therefore considered sufficiently representative for validation of predicted deformations of the main fuselage structure and levels of deceleration experienced in important areas.

The test configuration was simply represented in the analysis by modelling the ground as a rigid surface. The model was given the same vertical impact velocity as the test airframe of 8.2m/s, with no discernible pitch or roll.

The data recorded in the test were acceleration and relative displacements within the cabin. In addition, several high-speed cameras were used to record the event from different directions. Despite the differences in the designs of the tested and analysed helicopters, their behaviour was remarkably similar.

Results

Figure 2 shows a cut-away view of the WG30 helicopter model after impact with the ground. Structural deformation can be seen in the cockpit floor and rear bulkhead with buckling of the main ring frames. It can also be seen that the cabin roof has dropped, due to the mass of the engine, gearbox and rotor head in this region. This ties in well with observations of the Lynx drop test (see lower plate in Figure 2), showing similar levels of deformations in the key areas.

The acceleration time histories recorded at the cabin floor during the test and analysis are shown in Figure 3. Both curves exhibit a short peak, followed by a period of low acceleration as the cabin floor oscillates. The test result showed a double peak, whereas the analysis showed only a single peak. The double peak in the test is likely to be a result of the fuselage initially striking the ground remotely from the accelerometer location. The peak values of acceleration for both curves are around 110-120 g.

The accelerations recorded at the MRGB for the test and analysis helicopters are shown in Figure 4. The test helicopter exhibited a peak acceleration of nearly 80 g whilst the analysis peak was only around 25 g. The variation was considered to be caused by the stiffer structural design of the test airframe compared to that employed in the analysis and the simplified connections between the MRGB and main structure assumed in the FE model.

Conclusion

Given the structural differences between model and test sample, these results were considered encouraging in the context of predicting generic deformation modes and local accelerations.

4.4 **Validation of Water Model for Vertical Impacts – Capsule Model**

The water model was validated against a drop test performed by NASA on the Gemini space capsule [19]. The test report investigates the water landing characteristics of a conical shaped re-entry capsule having a segment of a sphere as its base.

Capsule Model

The geometry of the space capsule was relatively straightforward and a rigid surface FE model of the capsule was created. The physical data on the capsule can be found in Table 1 of Appendix B. The correct mass and inertia properties were explicitly attached to the capsule in the FE model. The capsule was modelled with water represented by both Eulerian and Lagrangian meshes.

Impact Conditions

The arrangement of the Space Capsule impact scenario is shown in Figure 5. It consists of a body of water 6x6x4m with an average element length of 300mm.

The NASA test report recorded both acceleration and displacement time histories for the capsule. The report, however, did not detail the instrumentation used in the test

or the level of filtering employed. Therefore, some judgement was used in interpreting the LS-DYNA3D results and an SAE 180Hz filter was applied to the analysis data.

Comparison of Acceleration Results

The comparison of accelerations for the test capsule and the two FE analyses is shown in Figure 6. These are for an impact velocity of 9m/s in the vertical direction, with no inclination of the capsule.

The accelerations predicted in the analyses were in good agreement with the test results for both the Eulerian and Lagrangian water models. Both analyses reproduced the correct shape of test curve, but with more noise being exhibited by the Eulerian model. The peak acceleration recorded in the test was 41m/s^2 , compared to the FE prediction of 42m/s^2 for the Lagrangian model and 44m/s^2 for the Eulerian model.

For the Lagrangian model, the peak acceleration was delayed by approximately 0.01 seconds. This was not considered to be significant and within the tolerances of the analysis and test instrumentation.

Comparison of Displacement Results

A comparison of the test and analysis displacements of the capsule are shown in Figure 7. As with the accelerations, the curves generally show good agreement.

The Lagrangian model under predicts the displacements, especially towards the end of the analysis, where the results start to diverge. The results show that the Lagrangian mesh formulation used to model the water is 'too hard' towards the latter stages of the analysis. This is due to its inability to model fluidity effects, which require significant displacement of the water.

The Eulerian model shows very good agreement with the test data. Initially the impact is slightly "harder" than the test results leading to an underestimate of displacement. However, at the end of the analysis, the displacement is overestimated compared to the test results. This was considered to be due to the omission of buoyancy, which will tend to reduce the displacement into the water.

Conclusion

Both the Eulerian and Lagrangian water models gave good predictions for the initial peak deceleration for vertical water impacts.

The Eulerian model was better at predicting displacements over the duration of the analysis due to its ability to model more accurately fluid flow effects. Towards the end of the analysis, the Eulerian mesh predicted too large a displacement due to the omission of buoyancy forces within the model.

4.5 **Validation of Water Model for Horizontal Impacts – Orbiter Model**

The Orbiter validation model is shown in Figure 8. The test arrangement [21] was based on a 1/20th scale model of a 'rigid' space shuttle. The test arrangement was very different to the capsule, as the shuttle had a large forward velocity and it skimmed across the water surface.

Orbiter Model

In a similar manner to the capsule model, the Orbiter model was constructed from rigid shells that represented the outer surface only. Appropriate mass and inertia properties were applied to the rigid body geometry. The physical data on the orbiter is summarised in Table 2 of Appendix B.

Impact Conditions

The impact conditions for the model was a forward velocity of 78m/s, 2.3m/s vertical velocity and 12° nose-up. The large forward velocity required a large water model, 200x54x5m in size.

As with the capsule modelling, the Orbiter test report documented accelerations and displacements of the test model. Again, both Lagrangian and Eulerian water models were considered. One of the issues with the fly in incident was that the event had a long duration relative to the vertical drop. The Orbiter also bounced along the surface and therefore spent a significant amount of time travelling through air. The long event duration resulted in long simulation run times.

Results

The results for the Lagrangian water mesh are shown in Figure 9. Initially, the rear section of the Orbiter hit the water (at 0.02s), and then bounced upwards. Whilst in the air and still travelling at a large longitudinal velocity, the nose rotated downwards before descending and striking the water for a second time (0.8s onwards).

The initial deceleration, where the rear of the Orbiter struck the water, for both the test and analysis occurred at the same time (0.02 s). A peak of 0.5g was predicted by the analysis compared to 0.25g in the test. However, in the analysis the deceleration pulse was sharper and of shorter duration.

The nose of the Orbiter contacted the water again in both cases at approximately 0.8s, indicating the correct flight time between the impacts was predicted. However, the maximum deceleration for the analysis was much larger, 13g compared to 5.5g for the test. Similarly, the analysis deceleration pulse was extremely sharp compared to the sustained deceleration observed in the test. This was due to the nose of the Orbiter not digging into the water in the analysis. The Lagrangian water model could not accommodate significant fluid displacements and planing effects, hence, the Orbiter was not sufficiently retarded and skimmed across the water's surface in the analysis.

The model was re-run with an Eulerian water formulation. Due to the large size of the water model, it was only possible to use a coarsely refined mesh. Even with a coarse mesh the run times were excessively long. After several weeks of solving, no useful data had been produced. The size of the problem was simply too big to be solved effectively with the current level of computing power. (Silicon Graphics Origin 2000 with four parallel microprocessors)

Conclusions

The Lagrangian water model was found not to be capable of modelling impacts with large components of horizontal velocity. The orbiter did not plough into the water due to the inability of the Lagrangian mesh to capture large fluid flow effects.

For the Eulerian model, no usable results were obtained due to the high speed of the Orbiter, long analysis times and the low density of the water mesh.

4.6 **Validation of Water Model for Horizontal Impacts– Seaplane Hull Model**

The Orbiter work had shown the Lagrangian water model to be unsuitable for impacts with large longitudinal velocities, and the model was too large and complex to solve with the Eulerian water model. Therefore, in order to assess the suitability of the Eulerian model, a smaller problem with a slower impact speed was required. Work performed on seaplane hulls landing on water was therefore chosen to validate the Eulerian water for planing impacts.

The experimental data on seaplane hull impacts was obtained from a literature review carried out by BMT [20]. The experiments were performed at the NASA Langley Laboratory and the data contained results from tests on seaplane hulls for impacts with both longitudinal and vertical velocities.

The data supplied with the BMT report included the following information:

- Geometrical drawings of the seaplane hulls.
- Graphs of vertical displacement, velocity and acceleration versus time.
- Data on trim angle and flight path angle.

Methodology

Two hull impact scenarios were modelled using the Eulerian water modelling method. Figure 10 shows the finite element mesh for the two cases studied. This figure also shows the differences in flight path angle and trim angle. The configurations are summarised in Table 1 below. They represent extremes of hull-water approach used in the tests. Case 1 had a small trim angle with a steep flight path, whilst Case 2 had a large trim angle and a shallow flight path.

	Case 1	Case 2
Resultant Velocity at contact with water	13.8 m/s	29.4 m/s
Trim angle	3°	12°
Flight path angle	6.22°	1.13°

Table 1 : Seaplane Hull Impact Conditions.

The hull was modelled from drawings supplied in the report, again using rigid shell elements.

Case 1 was modelled for 0.09 seconds with four different setups:

- Zero gravity, normal mesh
- Zero gravity and refined mesh
- Gravity on hull only, normal mesh
- Gravity on water only, normal mesh

Case 2 was modelled for 0.09 seconds with two different setups:

- Gravity on hull, normal mesh
- Zero gravity, normal mesh

The results were compared for velocity, displacement and acceleration in the vertical direction against those from the test.

Results

The results for Case 1 are shown in Figures 11 to 13. The basic analysis results (zero gravity), show that the displacements and velocities were lower than the test results. The accelerations (Figure 12) exhibited a large initial peak that was not shown in the test data.

Increasing the mesh density increased the accuracy of the results, but they were still significantly different to the test data. The large initial acceleration pulse still remained.

Applying gravity to the hull only slightly reduced the vertical accelerations, resulting in larger vertical velocities and displacements. Applying gravity only to the water had little effect on the results.

The results for Case 2 are shown in Figures 14 to 16. The results show that good agreement was made between test and analysis when zero gravity was applied. Applying gravity to the hull increased the levels of acceleration, velocity and displacement.

Discussion

The results of the analyses for the two cases were considerably different. This may be due to the characteristics of the impact being different. Case 2 was travelling about twice the speed of Case 1. Also Case 1 was closer to a vertical drop situation, whereas in Case 2 the back of the hull hits the water rather than the underside of the hull.

Characterising different types of impact for complicated aircraft structures could prove difficult. In these situations, mesh refinement would have to be carried out until convergence of the solution had been obtained. However, for large models this is likely to result in mesh densities that are beyond the scope of today's computing power.

Other questions arise of the validity of the test data. The tests were carried out in the late 1940s and early 1950s. The test apparatus, described in the BMT report [20], included a 'buoyancy engine' as part of the dropping mechanism. This buoyancy engine was to "represent aerodynamic lift, and thereby control the vertical velocity of the model after contact with the water". However, no detailed description is given of the degree of aerodynamic lift given, nor of the accuracy and repeatability of the lift. All that can be determined is that the lift is somewhere between free fall and zero gravity – the bounds of the analysis. According to the BMT report, there also seems to be some question as to the accuracy of the device used to measure the velocity and displacement. It is apparent that the sample rate of the test data may not have been fast enough to capture the initial high accelerations encountered by the seaplane hull.

Given these factors, there is doubt over the suitability of the data for validation of the analysis methodology.

4.7 Validation Conclusions

Given the differences between the model and the airframe under test, good validation was achieved for the response of the WG30 airframe model.

Both the Lagrangian and Eulerian water models were found to be suitable for vertical impacts. However, the Lagrangian approach only gave correlation over the initial impact duration. Longer duration events, or impacts with large horizontal velocity components require the accurate representation of fluid flow effects, which cannot be accurately modelled using the Lagrangian approach.

It was concluded from the seaplane hull and Orbiter work that the Eulerian approach was more suitable for planning impacts. However, it appears likely that for most cases, fine mesh densities would be required to give good answers. This would be difficult to achieve given the limitations of current computer hardware.

4.8 Helicopter Water Impact Scenarios

Three actual accident scenarios were modelled using both Eulerian and Lagrangian meshes to represent the water. The three cases are summarised in Table 2 below:

	Craft Velocity m/s			Pitch	Roll	Sea Conditions
	x	y	z			
Brent Spar	0	0	-22	7.5° down	10° right	Calm
Cormorant Alpha	22	0	-7.6	4.1° up	0.3° right	14 m/s receding waves at 60° to craft
Isles of Scilly	41	0	0	0.5° down	0°	Calm

Table 2 : Helicopter Impact Conditions.

Each scenario represents a helicopter/sea accident which resulted in a full accident investigation by the AAIB, [14, 15, 16]. Both full (actual) and half speed impact conditions were analysed to determine trends in the response of the airframe.

The Brent Spar scenario essentially represents a vertical drop; the Isles of Scilly an impact with longitudinal motion only; and Cormorant Alpha an impact with both longitudinal and vertical motion.

It should be noted that the helicopters involved in the actual accidents were considerably stronger than the WG30 model used in the FE analysis:

- A Sikorsky S61N was involved in the Brent Spar and Isle of Scilly accidents. This helicopter has four main structural ring frames as opposed to just two on the WG30. It also has its engines and gearbox mounted on separate frames rather than having all the massive items supported in one place.
- A Super Puma was involved in the Cormorant Alpha accident which also has a more robust ring frame arrangement and more generous distribution of massive items.

Both these helicopters were therefore designed to survive much higher impact loadings than the WG30. It was anticipated that some of the scenarios, although survivable for stronger airframes, may result in gross structural failure of the WG30 model.

Post Processing

The results for the impact scenarios were post processed using a combination of four different methods:

- 1 *Global Acceleration*: The overall response of the airframe can be examined by looking at the global acceleration of the model over the duration of the impact. The global acceleration is the average of the resultant accelerations of each element in the model. It only has a magnitude, although the direction can be estimated from the model's general retardation and flight path. The method averages out any local effects in the structure to give the overall response. It is useful for assessing general behaviour and gives a degree of confidence in the overall performance of the model.
- 2 *Plastic Strain*: The likelihood of failure of parts of the structure can be predicted by looking at plastic strain. For aluminium structures, tensile strains above 0.1% can be considered to result in initiation of structural failure.
- 3 *Contact Forces*: The hydrodynamic forces on the panels of the airframe can be assessed by examining the contact forces between the airframe and water elements. This method was used to compare results with empirical predictions obtained by BMT [4] for the Brent Spar and Cormorant Alpha scenarios.
- 4 *Nodal Accelerations*: Local loads in the airframe can be estimated by extracting accelerations of appropriate nodes in the model. They are particularly useful for examining local effects which may be masked in the overall global response. However, they tend to be more "noisy" as data from a single point includes significant high frequency/high amplitude vibrations. The results are therefore

typically filtered to remove the high frequency components. This problem is more pronounced for high speed impacts due to the larger shock waves oscillating through the structure.

4.8.1 *Brent Spar (Lagrangian Water)*

Global Response

The global accelerations for the full and half speed impacts are shown in Figure 17. For the full speed case, a peak acceleration of 23 g is observed before dropping off to around 12 g. The accident report for this accident estimated, from the damage that the cabin floor had experienced, the peak deceleration was between 20 and 25 g. The acceleration levels for the half speed case are approximately half.

Airframe Failure

The areas of possible failure in the structure were investigated by looking at the maximum plastic strain in each element throughout the whole time period. These results are shown in Figures 18 and 19 for the full and half speed impact conditions respectively.

For the full speed case (Figure 18), large parts of the airframe have strains well above 0.1 %. This indicates that the main structural ring frames and tail boom are likely to fail. This is due to the high inertia and mass of the engines, rotor and MRGB causing the cabin roof to collapse downwards.

In the actual accident, the fuselage cockpit bulkhead aft of the cargo door and tail boom failed. Less severe damage occurred in the rear of the cabin than at the front. Clearly, the WG30 would have sustained far greater level of structural damage. The full speed Brent Spar conditions are considered to be unsurvivable for a WG30 airframe.

For the half speed case (Figure 19), less damage is sustained. However, areas above 0.1% strain exist in the main structural ring frames and the tail. A considerable amount of damage is therefore expected to occur in these areas at the half impact speed.

Panel Forces

The panel force results and comparison with BMTs empirical predictions are discussed in Section 4.8.5 below.

Local Loadings

The results for the nodal accelerations were less promising. The Brent Spar impact conditions proved to provide a very hard landing for the WG30, resulting in large structural deformation of the cabin roof. The level of damage was exacerbated by the lack of fluidity in the Lagrangian water formulation. The nodal accelerations and deformations of parts of the helicopter were very high. The hardness of the landing and the flexible nature of the airframe model combined to give nodal results that were very noisy due to excessive vibration of the mesh nodes on impact. This was demonstrated by changing all of the airframe materials to rigid.

Figure 20 compares the vertical velocities of a node in the floor for both the rigid and non-rigid airframe models. It can be seen that the rigid model does not vibrate and therefore does not show the large peaks in velocity and therefore acceleration. Heavy filtering would be necessary to extract appropriate accelerations from the deformable model. However, excessive filtering was shown to excessively distort the results.

Figure 21 shows the vertical acceleration of a node in the aircraft floor before and after filtering with SAE 60 Hz and 180 Hz filters. It can be seen that the 60 Hz filtered acceleration reaches approximately 800 g. However, this peak value can be changed by the level of filtering. The overall acceleration levels can therefore not clearly be determined due to the noise levels.

Figure 22 shows the locations of the three nodes that were used to monitor acceleration. Figure 23 shows the filtered signals (SAE 60 Hz) for these nodes on the floor, side panel and gearbox. The initial impact occurs close to the floor panel and the acceleration reaches 2000 g. The side panel acceleration peaks approximately 0.005 seconds later at about 800 g. The gearbox acceleration (17 g, 0.07 seconds after initial contact) is comparably low as it is farther away from the impact site and has a large inertia. Figure 23 shows the timing of the peak values relative to each other but, as described in the paragraph above, it does not give reliable quantitative acceleration values due to excessive nodal vibrations and the heavy filtering.

4.8.2 *Cormorant Alpha (Lagrangian Water)*

The results for the Cormorant Alpha scenario should be treated as being indicative only. The impact has a significant horizontal velocity component. The validation work had shown that the Lagrangian water model was not suited to "fly-in" scenarios, due to its inability in modelling large fluid flow effects. The initial peak loads are considered to be representative, but the analysis becomes less representative and less conservative once the water has had time to flow a significant distance.

Global Response

The global accelerations for the full and half speed Cormorant Alpha scenarios are shown in Figure 24. For the full speed case, a peak acceleration of approximately 3 g is predicted, then dropping off to around 1.2 g. The acceleration levels for the half speed case are approximately half.

Airframe Failure

Maximum plastic strains for the full and half speed impacts are shown in Figures 25 and 26.

For the full speed case (Figure 25), strains above 0.1% occur around the tail boom, engine/rotor/MRGB connections to the main ring frames and locally around the point of impact on the nose. Therefore, limited failure in these regions would be expected.

In the actual accident, crushing damage was observed to the forward and right of the fuselage, the tail boom folded and the right hand side cabin door failed. This level of damage is consistent with that predicted by the WG30 model.

For the half speed case (Figure 26), strains over 0.1% were predicted around the tail boom.

Panel Forces and Local Loadings

The panel force results and comparison with BMT's empirical predictions are discussed in Section 4.8.5 below.

In a similar manner to the Brent Spar results, noise prevented useful data being extracted from the nodal accelerations.

4.8.3 *Isles of Scilly (Lagrangian Water)*

The Isles of Scilly scenario is a "fly-in" accident. Therefore, the results should be treated as being indicative only due to the inability of the Lagrangian water model to predict large fluid flow effects. The initial peak loads are considered to be representative, but the analysis becomes less representative and less conservative once the water has had time to flow.

Global Response

The global accelerations for the full and half speed scenarios are shown in Figure 27. For the full speed case, a peak acceleration of 9 g is predicted, then dropping off to around 2 g. The acceleration levels for the half speed case are approximately a third of the full speed results.

The accident report for this accident estimated the peak deceleration to be greater than 12 g. This was based on failure of the seat connections to the cabin floor.

Airframe Failure

Maximum plastic strains for the full and half speed impacts are shown in Figures 28 and 29.

For the full speed case (Figure 28), strains above 0.1% occur in the panels around the nose wheel retraction holes, the edges of the floor and in the middle of the main ring frame. Failure was also predicted around the tail boom. Failure of the floor panels and subsequent water ingress is not included in the model. Once a floor panel had failed it would be likely that the influx of water would cause significant damage to the remaining floor panels.

In the actual accident the sponsons detached and all the hull below the cabin floor was destroyed.

For the half speed case (Figure 29), minimal areas of failure were predicted.

Panel Forces and Local Loadings

No empirical predictions were made by BMT for this scenario, therefore no data was extracted from the FE model for comparison.

In a similar manner to the Brent Spar results, noise prevented useful data being extracted from the nodal accelerations.

4.8.4 *Eulerian Modelling*

The three impact scenarios were repeated with the Eulerian water mesh. The results for the full speed impacts are shown in Figures 30 to 33.

Global Response

The global acceleration responses (Figure 30) for the Brent Spar and Cormorant Alpha scenarios were much higher than with the Lagrangian water model. Large and sustained levels of acceleration were observed in both cases.

The Scilly Isles result exhibited a short duration peak, followed by a sustained period of small negative acceleration.

These spurious accelerations were considered to be a result of problems with the software code. The solver appears to have difficulty in coupling the deformation in the airframe structures with the mass transfer through the Eulerian water mesh.

Structural Failure

The results for the plastic strains (Figures 31 to 33) were also not realistic. For the Brent Spar and Cormorant Alpha scenarios, all the damage was located in the upper part of the airframe. There was relatively little damage predicted at the primary impact locations around the nose.

Conversely for the Scilly Isles scenarios, only two very localised failures are predicted on the nose of the airframe.

Conclusion

It was concluded that the Eulerian water model was not suitable for complex deformable models. The airframe model consisted of deformable materials, lumped masses and beam elements, whereas the validation models had only contained rigid shell elements. A considerable amount of development work would be necessary to fully understand the limitations of the Eulerian water methodology which was beyond the scope of this study.

4.8.5 *Comparison of Panel Loads Against Empirical Predictions*

Table 3 summarises the panel contact force results for the Lagrangian Brent Spar and Cormorant Alpha scenarios. Two panels near to the impact point on the nose of the airframe were considered. The location of the side and base panels are shown in red in Figure 34.

Scenario		FE Modelling		Empirical Approach	
		Base Panel Load	Side Panel Load	Base Panel Load	Side Panel Load
Brent Spar	Full Speed	481 kN	23 kN	594 kN	176 kN
	Half Speed	219 kN	10 kN	149 kN	44 kN
Cormorant Alpha	Full Speed	70 kN	No Data	250 kN (Stationary Wave)	59 kN 45 kN (Receding Wave)

Table 3: Comparison of Panel Forces

Supporting work was undertaken by BMT Fluid Mechanics Ltd [4]. Their method used an empirical statistical approach to determine the range of possible loadings on single airframe panels and sponsons over a large variety of impact orientations. The results from the BMT study for the two specific impact scenarios and appropriate panels are included in Table 3 for comparison.

For the full speed Brent Spar impact a peak load of 481 kN was predicted for the base panel by the FE modelling. This agreed extremely well with the empirical prediction of 594 kN. A similar level of correlation was observed for the half speed cases.

The correlation for the side panel was less satisfactory. The empirical results were much higher than those predicted by the FE model. This was due to two factors:

- The empirical approach assumed the side panel to be the primary impact point. In reality, the side panel was not the first point of contact. The FE model was geometrically accurate with the base of the airframe contacting the water first. Therefore, the FE results would be expected to be lower as the side panel did not take the full impact force.
- The lack of “fluidity” in the Lagrangian mesh would contribute to under-predicting the side panel force, as less water would be in contact with the sides of the airframe. However, over the small timescale of the initial impact this effect would be small.

For the Cormorant Alpha scenario, the FE base panel results were lower than the empirical approach. This was attributed to the fact the base panel was not the primary impact point in the actual accident.

For the side panel, no FE data was obtained, as the panel did not contact the water during the initial impact. The empirical results were considered to overestimate the actual load seen by the panel. It should be noted that the both the empirical and FE methods are less reliable for planing type impacts due to poor understanding of drag and planing effects.

Although both approaches were not fully validated, they did predict loadings of similar magnitudes. Given the large differences in the two approaches and uncertainties in the analyses, the results were considered encouraging.

4.9 **Modelling Conclusions**

From the FE validation work, it was concluded that:

- 1 The only relevant validation data for the WG30 airframe was of a Lynx impact onto the ground with the undercarriage retracted. The WG30 and Lynx airframes were considered similar in terms of mass distribution and main structural members. The response of WG30 model exhibited good correlation with the test data. Local acceleration levels at the MRGB were a factor of five less than those observed in the cabin floor.
- 2 The Lagrangian and Eulerian water models were validated against a variety of test data. Rigid bodies were used to model both vertical and horizontal impacts.

- The Lagrangian water model was only suitable for determining initial accelerations during vertical impacts. It was not suited to fly-in impacts or impacts that occurred over a significant period of time as it cannot model large fluid displacements.
- The Eulerian water model was more suited to both vertical and fly-in impacts. However, very refined meshes were required to achieve converged results for the validation cases. The number of elements required for high speed impacts or complex models, such as the WG30 model, proved to be prohibitively large, resulting in very long analysis times. There were some doubts as to the validity of the test data used for the seaplane hull validation work. Further work would be required to gain sufficient confidence in the accuracy of the Eulerian method.

From the Brent Spar, Cormorant Alpha and Scilly Isles scenarios, it was concluded that:

- 1 The Eulerian water model produced no useful data for impacts with deformable structures. The WG30 model included complex geometry, elastic-plastic materials, shell and beam elements and lumped masses. The Eulerian modelling technique is considered insufficiently mature to accurately model complex water/deformable structure impacts.
- 2 The Lagrangian water model was only suitable for determining initial acceleration levels for vertical impacts such as the Brent Spar scenario. Global responses and strain levels were generally consistent with damage detailed in the accident reports. However, results for local accelerations were too noisy to extract any useful information. Large nodal vibrations occurred on impact and resulted in large local accelerations of very small duration. This resulted in the need for heavy filtering, which removed useful information from the data. Reasonable correlation with empirical methods was achieved using panel force data for the Brent Spar and Cormorant Alpha scenarios.

5 EMERGENCY FLOTATION DESIGN REVIEW

5.1 Introduction

The purpose of this task was to review current EFS design in light of the findings of Sections 3 and 4, and to propose modifications to improve EFS crashworthiness.

5.2 Emergency Flotation Problems

The problems associated with emergency flotation systems are well understood and discussed in the Survey and Analysis of Helicopter Flotation Systems [7] commissioned by the FAA. This section summarises these problems and then adds to the discussion. The main problems that are associated with float deployment are listed below. Each of these problems is then addressed in the following sections.

- Floats are not armed.
- Floats are armed but not activated.

- Floats are activated but do not deploy.
- Uneven float deployment.
- Incomplete inflation due to adverse ambient conditions.
- Floats damaged upon impact.
- Floats deployed but helicopter overturns.

Four of the incidents reported in the FAA report were ditchings where the EFS had failed to deploy. The information relating to the ditching cases (approximately 6%) could not be clearly distinguished from the main data but, since a ditching is effectively a "gentle" impact, system failures that occur under these less onerous conditions are of interest to this study.

5.2.1 *Floats Not Armed*

To prevent inadvertent float deployment in flight, current flotation systems typically require a two-step process for inflation. First, the inflation circuit must be armed and second, the inflation is activated either automatically (e.g. water immersion switches) or by a trigger operated by the pilot. The fact that many helicopters equipped with emergency flotation systems impact the water with the floats unarmed is a cause of concern. FAA guidelines recommend that the inflation system be safeguarded against inadvertent activation by using a separate float arming circuit. Unfortunately, the pilot is often preoccupied with controlling and landing the helicopter during an emergency situation and thus may fail to arm the inflation system before contacting the water. Therefore, another method for preventing inadvertent float deployment would be desirable.

One solution is to provide an override function that senses the condition that makes float deployment unsafe. For example, if the airspeed must be below a certain value for safe deployment, then the airspeed indicator would be used to send a bypass signal to the arming circuit. The float arming circuit would effectively be automatic in that the floats could be activated at any time during a flight provided the helicopter is within the safe deployment envelope (based on sensor input). A backup manual arming system is also recommended.

5.2.2 *Floats Armed But Not Activated*

Flotation systems fitted with activation circuits that must be triggered by the pilot suffer from the same problems as manually operated arming circuits. The pilot often does not have time, does not remember, or is physically unable to activate the floats. In addition, pilot activated floats suffer from timing problems. Activating the floats too early will make them more vulnerable to damage during the impact. Activating the floats too late will mean that, by the time the floats are fully inflated, water ingress may be too far advanced. The floats may then not be able to maintain the stability of the floating helicopter for the desired time period. Therefore, floats activated by automatic means (e.g. water immersion switches) are more desirable. However, again, a backup manual activation switch is recommended.

5.2.3 *Floats Activated But Not Deployed*

One reason for all floats failing to deploy after activation is electrical wiring faults. FAA guidelines recommend a mechanical backup system for electrically activated systems, but also allow backup electrical systems provided they are shown to be independent and of high reliability. In either case, thought should be given to protecting wiring by avoiding routes through areas which are most likely to be damaged. For example, wires should not be run next to the lower fuselage skin, which is likely to tear during impacts involving significant horizontal velocities. Use should be made of flexible armoured cable racing.

Inflation devices (bottles) store compressed gas at high pressures and are used to inflate the bags rapidly. The bottles are typically 'fired' by a pyrotechnic charge that punctures a diaphragm in the bottle, causing the gas to release. Use of multiple bottles or redundant firing mechanisms is desirable in the event that a bottle does not fire. The firing mechanism and the controlling electronics should be tested and certified to the shock acceleration levels likely to be seen in the area in which they are located during a partially survivable water impact. Electronics and firing mechanisms should be upgraded if necessary or, alternatively, bottles could be located higher up the fuselage where acceleration levels are likely to be much lower.

5.2.4 *Uneven Float Deployment*

The three main causes of uneven deployment, are as follows:

- Inflation bottles failing to fire.
- Bags failing to fully inflate.
- Failure of the flow line connecting the bags to the inflation bottles.

Bottle Failure

FAA guidelines recommend use of either a single inflation bottle or use of a multiple bottle system, interconnected to help prevent uneven deployment. Single bottle systems however, suffer from the problem that the entire system fails if the bottle does not fire (see above). Therefore, multiple-interconnected bottles are recommended. Thought should be given to bottle positioning. Placing bottles too near to airframe members which could deform and puncture the bottles should be avoided.

Bag Failure

Where an inflation system is interconnected, the gas will follow the path of least resistance. If a float bag is severely damaged (torn), then more flow will be diverted to that float causing less inflation for the intact float chambers. Float inflation systems, however, operate under high pressure and high flow velocities are developed in the distribution lines. Therefore, most of the flow resistance is in the flow distribution lines and not in the resistance associated with inflating the bag. The amount of gas actually lost due to a ripped chamber is thus small. Therefore, it is important to design the flow distribution lines with equal resistance and/or use flow distributing valves to ensure equal float deployment in all eventualities.

Bags should be divided into multiple cells to limit the buoyancy volume lost due to small tears in inflation bags. When considering uneven deployment, it is important to assess the implications of uneven inflation times and not just uneven final inflation volumes.

Flow Line Failure

Flow lines severing during impact present more of a problem. If the break is near to the high pressure gas supply, then the path to the break will be of significantly less resistance and will result in a problematic loss of gas volume. Thus, care should be taken to route flow lines away from areas most likely to be damaged in a water impact. Full use should be made of flexible high pressure wire coated hoses. Rigid flow lines should be avoided as the deforming airframe could easily lead to pipe rupture.

For the three impact scenarios considered in Section 4, the maximum strains experienced in the model are shown in Figures, 22, 23, 25, 26, 28 and 29. The highly strained regions indicate parts of the aircraft that would deform significantly or experience gross structural failure. These areas are not suitable for the routing of any pipe work, as deformation of the structure would lead to breakage and rupture of pipe lines. These are primarily the main ring frames of the airframe, which support massive items in the roof, the floor skin and the tail boom connection to the fuselage.

Mounting bottles near to bags will reduce the length of flow line required, thus reducing the risk of pipe rupture. However, the likelihood of damaging the bottles would be increased, as they would be located in more vulnerable areas of the airframe. This arrangement also makes cross feeding between bottles more difficult. Careful consideration should be given to the trade off between redundancy with interconnected bottles, the higher risk associated with longer pipe runs and vulnerability of equipment.

5.2.5 *Incomplete Inflation Due to Adverse Ambient Conditions*

The types of gases used to inflate the flotation systems are typically nitrogen or helium. The gases are compressed to approximately 3000 psi and expanded to approximately 2.25 psi in the inflated floats. The pressure of the compressed gas within the bottle must be adjusted before flight to take account of variations in ambient temperature. However, ambient conditions may change during flight which can mean that the pressure supplied to the floats drops by plus or minus 1.5 psi [7] resulting in incomplete inflation.

The American Navy H-46 system is designed to work without a pyrotechnic charge [7]. In this case, a solid propellant is burned to warm pressurised/liquefied carbon dioxide contained within a Kevlar reinforced aluminium pressure vessel. The pressure within the vessel is raised until a burst valve releases the gas into the float bags. This inflation method automatically adjusts the amount of solid propellant burned depending upon the ambient conditions. This ensures that the gas supplied to the floats has a uniform and constant temperature and pressure regardless of the prevailing ambient conditions.

5.2.6 *Float Damage Upon Impact*

Emergency floats are stored in a packed position in some form of protective cover until activated. The floats tend to be positioned to produce a slight nose-up attitude in water to prevent the cockpit and cabin from being submersed under water. In general, the floats are configured either as a skid-mounted or fuselage-mounted system, depending on the landing gear configuration.

Skid Mounted Floats

Skid mounted float systems tend to have very simple storage methods. Each float is folded and stored in a protective cover, typically made of a waterproof material such as nylon, and mounted on top of the landing gear skid. The float bag covers for these systems are fitted with snaps that pop open upon float deployment.

The main problem with skid mounted flotation systems is that the skids are attached to the underside of the fuselage and are therefore vulnerable in an impact. In an impact the skids would initially take the full force and may break away from the airframe. In this event the floats would become separated from the fuselage.

Fuselage Mounted Floats

Heavier helicopters that do not use skid landing gear require more sophisticated and thus heavier fuselage-mounted systems.

Nose floats may be stored inside fuselage skin flaps. These storage compartments are hinged on one side and remain attached to the fuselage upon deployment of the floats. The main landing gear floats are usually stored inside the main landing gear doors, requiring the doors to blow out to the fully open position upon deployment of the floats.

Fuselage-mounted floats that are activated before impact are often damaged by high water entry forces. Flotation systems which do not deploy until after impact are not subjected to these forces, resulting in fewer cases of float system damage caused by the impact.

Location of Flotation Equipment

The results presented in Section 4 indicate that the degree of damage experienced by the EFS would depend on their location on the fuselage. Panel forces reported in Section 4.8.5 (Table 3) show that side panels typically experience a much lower force than base panels. Additionally, the airframe validation work had shown that for a vertical drop, accelerations at the rotor gearbox were a factor of five less than those experienced by the cabin floor.

Positioning the EFS such that it is not located at likely impact locations or on parts of the structure which are likely to fail, would result in an increased chance of post impact survivability. The nose, tail boom and underside of the aircraft are particularly vulnerable during water impacts.

Attachment and Structural Design Loads

The loads experienced by the floats, their attachments and the surrounding airframe can be extremely high during water impacts. The integrity of the floats and surrounding structure is therefore an important consideration.

Work performed by BMT [4], suggests that the current design loads are more than adequate for ditching scenarios. However for severe impacts, doubling the design loads for airframe panels would have little effect on improving survivability. Primary impact loads are too large to allow the development of practical design solutions given the material and weight constraints of an airframe. Greater benefit would be obtained through the provision of redundant flotation.

Parts of the airframe that are claimed to provide passive buoyancy (i.e. sealed spaces such as fuel tanks) should be shown to remain intact and attached to the passenger cabin during a severe but survivable impact. In all the scenarios analysed in Section 4.8 the tail boom consistently failed. Some aircraft manufacturers claim voids in the tail boom as passive flotation. In an impact the tail boom is very likely to fail and any buoyancy it provides would, thus, be of no benefit.

Float Redundancy

Currently, redundant flotation is only provided by sub-compartments within a bag. During a severe but survivable impact the complete bag is likely to be lost, thus negating both the redundant and normal flotation capacity.

If redundancy was provided at bag level, then the likelihood of significant loss of flotation capacity would be greatly reduced. Work performed by BMT [4], predicts that the provision of redundant bags would significantly improve the chances of the EFS continuing to perform its function following an impact.

The redundant flotation should be located in areas less likely to experience high loads during a severe impact, such as the upper part of the airframe.

5.2.7 Floats Deployed But Helicopter Immediately Overturns

Immediate overturning of helicopters upon impact is the most common cause of occupant drowning in an otherwise survivable accident. Helicopters have a natural tendency to invert in water because of their relatively high centre of gravity. Combining this inherent instability with wave action, high winds, and impacting the water at a significant velocity or improper attitude, greatly increases the chance of overturning. Once a helicopter has capsized the cabin quickly fills with water and the helicopter will totally invert. There is little time for the occupants to escape.

Currently, emergency flotation devices are designed to keep the helicopter upright to facilitate egress in the event of a controlled ditching. The requirement is to keep at least one exit on either side of the airframe above the water line. This necessitates the location of flotation equipment near to the underside of the airframe. However, this area is typically most prone to damage in an impact and also results in just two stable flotation attitudes.

In an accident, lives would be saved if a second aim became to keep the cabin partially dry in the event of significant damage to the primary flotation system. This would require the location of additional flotation equipment in areas of the airframe around the sides or top of the cabin. This additional flotation could be designed to allow the helicopter to float on its side [22], whilst still achieving an acceptable egress route for the occupants.

This would prevent total inversion following capsizing, retaining an air pocket within the cabin and maintaining a number of escape routes above the water surface. Additionally it would provide redundant flotation located in a less vulnerable area of the airframe.

5.3 **Summary of Design Recommendations to Improve Emergency Flotation System Crashworthiness**

- EFS should have automatic arming.
- A manual independent backup arming system is recommended, where automatic arming systems are used.
- Floats should be activated automatically by immersion switches.
- A manual, independent, backup activation system is recommended where automatic activation systems are used.
- Distribution lines should be designed with equal resistance and/or flow distributing valves should be used to ensure equal float deployment, even with a bag ruptured.
- Flexible hoses should be used for flow distribution lines.
- Bags should be divided into multiple cells to limit the effect of small bag ruptures.
- Inflation systems that limit the effect of varying ambient conditions should be considered.
- Systems which require inflation should be deployed after impact.
- Floats should be designed for balanced deployment (timing as well as volume), even with system damage.
- Where possible, floats should be located away from likely primary impact sites, such as the nose, sponsons and floor of the airframe.
- Distribution hoses and wiring should not be routed through areas of the airframe likely to undergo severe deformation or failure during an impact. Short pipework, or individual gas bottles located near each bag would reduce the risk of flow line failure due to structural deformation. However, careful consideration should be given to the trade off between redundancy with interconnected bags and the higher risk associated with longer pipe runs.
- Redundant flotation should be provided at bag level, as well as compartments within a bag.

- To take account of severe but survivable impacts, redundant flotation bags should be located in the upper part of the airframe to minimise the risk of damage. These could also be arranged to allow the helicopter to float on its side retaining an air pocket in the cabin and maintaining a number of escape routes above the water surface, rather than capsizing into a fully inverted position.
- Finally, any claimed passive buoyancy (e.g. fuel tanks or tail boom voids) for ditching should only be allowed if it can be demonstrated that the appropriate part of the airframe remains attached to the passenger compartment during and after an impact.

6 COST BENEFIT ANALYSIS

This section develops a methodology for determining the benefits of modifications to the EFS in the context of their implementation costs and potential for saving life.

6.1 Overview

The raw data for the cost benefit study was obtained from a search of helicopter water impacts contained in the NTSB database and from UK accident reports. The search provided information as to how actual EFS had failed for a range of helicopter types and accident scenarios. Only accidents where both the EFS failed and where fatalities were sustained were considered.

From the data an EFS failure deployment tree was constructed. The tree quantified how various EFS failure modes contributed to whether the helicopter maintained an air pocket in the cabin with an over-water escape route, inverted or sank.

A variety of modifications were proposed for various stages of the EFS deployment process aimed at improving the likelihood of successful operation. These modifications were based on the findings of Section 5 of this report.

The benefit for each modification, in terms of affecting the probabilities of sinking and inversion, was assessed using the failure event tree. This change in functional effectiveness was translated into an occupant survival number. Modifications which improved the chances of maintaining an air pocket in the cabin with an over water escape route were assumed to provide the greatest benefit in terms of occupant survivability. Modifications that reduced the chances of sinking, but increased the probability of inversion, were assumed to be less effective.

The estimated costs of each modification were obtained from an EFS manufacturer and a helicopter manufacturer.

Finally, a cost benefit study was undertaken for the current UK offshore helicopter support fleet to determine whether implementation of the modifications would be cost effective in terms of potential lives saved over the remaining service life of the fleet. A worked example of a cost benefit calculation is given in Appendix F.

6.2 Causes of EFS Failure

6.2.1 Float Deployment

The successful deployment of the EFS can be described as a sequence of events, each of which has to be carried out successfully if the EFS is to deploy correctly. If any event is not successfully carried out, the EFS will not inflate correctly. Figure 35 shows the sequential path of events. The desired aim is to keep the helicopter afloat, with an air pocket in the passenger cabin and an over-water escape route, long enough to enable all the occupants to board the liferafts.

The first stage in the deployment sequence is to arm the system. If the system is not switched on then it cannot operate. The system then needs to be activated. If either of these stages do not occur the helicopter will sink. For the purposes of this study, the stages of arming and activation have been grouped together as the pilot is assumed to be a common failure mode.

Once the system is activated, the compressed air needs to be discharged from the bottles and to reach the floats. If the gas is not discharged then the helicopter will sink. If the floats, pipe work between the floats or the storage bottles have been damaged then all, some, or none of the floats may inflate. If none of the floats inflate then the helicopter will sink, if some inflate then the asymmetric inflation is likely to cause the helicopter to invert and possibly sink.

Finally, if all the floats correctly inflate the helicopter can still invert and/or sink due to external factors such as bad weather or impact attitude/velocity.

6.2.2 Accident Data

An on-line search of the NTSB accident database, between 1982 and 1999, identified 20 accidents where the EFS had failed and where fatalities were sustained (Appendix D).

A search of UK accidents, between 1980 and 1999, identified four accidents (Brent Spar, Cormorant Alpha, Dunlin Alpha and Scilly Isles) which fulfilled the criteria (Appendix E).

For each of the 24 relevant accidents the failure mode of the EFS was determined. Appendices D and E provide details of each accident and the assumptions made as to the likely EFS failure mode. Table 4 summarises the results of the EFS failure modes.

Stage	Failure Event	Number of Cases	Outcome		
			Sink	Invert	Air Pocket in Cabin with Over-water Escape Route
1	EFS not armed or not activated	12	12	0	0
2	Gas did not discharge from bottles	0	0	0	0
3	All gas did not reach all floats	2	0	2	0
4	Damaged floats	6	4	2	0
5	Helicopter affected by external factors	4	0	4	0
Totals		24	16	8	0

Table 4 : Summary of Relevant Accidents

In half of the cases considered the EFS failed to activate, resulting in 12 sinkings. In all the cases where the EFS activated, the air discharged successfully from the storage bottles. However, in two cases the gas did not reach the floats and the helicopters inverted. Six cases sustained varying levels of float damage leading to four sinkings and two inversions. In the remaining four cases, where the EFS deployed successfully, the helicopters inverted due to external factors.

No cases resulted in an air pocket in the cabin and an over-water escape route. This is not surprising as the study is specifically concerned with EFS failures that resulted in fatalities.

Using the above data, a probability tree was constructed (Figure 36) in order to analyse the EFS deployment process. The upper branches indicate the probability of success for each stage, given the previous event has been performed successfully. The lower branches indicate the probabilities of failure at each stage.

The overall probability for each of the three outcomes was determined by multiplying together the probabilities along each branch and adding those which lead to the outcome of interest.

6.3 EFS Design Modifications

A list of possible modifications to the EFS was drawn up, based on the findings of Section 5 of this report. The modifications comprised:

- *Arm System:* Float activation system is armed at all times, except during flight conditions in which activation of floats would be hazardous. It was considered that the best way to achieve this was to manually arm the system on takeoff with any subsequent disarming being automatic. This modification would improve the probability of successfully completing the first stage of the deployment process (Modification A, Figure 36).
- *Activate System:* Floats activated automatically by immersion switches. Hence, the floats are deployed after impact with the water. A manual independent backup activation system would be provided. This modification would improve the probability of successfully completing the first stage of the deployment process (Modification B, Figure 36).
- *Bottle Redundancy:* Systems that have either more than one bottle or a redundant activation system within a single bottle, and in which the firing electronics are designed to survive the impact shock. This modification would improve the probability of successfully completing the second stage of the deployment process (Modification C, Figure 36).
- *Ambient Conditions:* Inflation system that minimises the effect of varying ambient conditions on the quantity of gas leaving bottles. This modification would improve the probability of ensuring that the correct quantity of gas reaches the floats and hence successfully completing the third stage of the deployment process (Modification D, Figure 36).
- *Flexible Hoses:* Flexible hoses used for flow distribution lines to minimise damage caused by impact. This modification would improve the probability of

successfully completing the third stage of the deployment process (Modification E, Figure 36).

- *Even Flow*: Flow distribution lines designed with equal resistance, and/or use of flow valves to achieve even bag deployment in the event of small ruptures. Floats are designed for balanced deployment (timing as well as volume), even with bottle damage. Bags divided into multiple cells to limit effect of small ruptures. These modifications would improve the probability of successfully completing the third stage of the deployment process (Modification F, Figure 36).
- *Float Attachment/Protection*: Increased float attachment design loads and protection from impact. These modifications would reduce the chances of the existing floats being damaged during an impact. They would improve the probability of successfully completing the fourth stage of the deployment process (Modification G on Figure 36).
- *Float Location*: Re-location of existing floats to regions of the airframe less susceptible to impact damage. This modification would improve the probability of successfully completing the fourth stage of the deployment process (Modification H, Figure 36).
- *Float Redundancy*: Systems that incorporate complete flotation unit redundancy, additional to the existing floats required for ditching. Redundant floats can be added anywhere on the airframe, apart from at the top (see below). This modification includes the advantages of both float location and float redundancy as it necessitates the location of additional flotation away from the underside of the airframe which experiences the highest impact loads. This modification would improve the probability of successfully completing the fourth stage of the deployment process (Modification I, Figure 36).
- *Side Floating*: This is a specific case of redundancy as floats are located at the top of the airframe. This additional flotation allows the helicopter to float on its side, preventing total inversion while retaining an air pocket in the cabin and maintaining an over-water escape route to the surface. This modification includes the advantages of both float location and float redundancy as it necessitates the location of additional flotation at the top of the airframe which sees lower impact loads. It will also reduce the likelihood of inversion in high sea states or adverse impact conditions. This modification would therefore improve the probability of successfully completing the fourth and final stages of the deployment process (Modification J, Figure 36).

6.4 **Assessment of Benefits**

6.4.1 *Effect on Outcome*

The benefit for each modification alone, in terms of reducing the probabilities of sinking and inversion, was assessed using the failure event tree (Figure 36).

Implementation of each modification was assumed to result in the successful completion of the appropriate stage of deployment (i.e. the probability of failure was reduced to zero). In this way, the effect of each modification on the probabilities of the three outcomes could be quantified. Table 5 shows the results of this exercise.

Modification	Probability of Above Water Escape Route	Craft Inverted	Craft Sinks
No Modifications	0.0	0.3	0.7
A+B – Arming and Activation	0.0	0.7	0.3
C – Bottle Redundancy	0.0	0.3	0.7
D – Ambient Conditions	0.0	0.3	0.7
E – Flexible Hoses	0.0	0.3	0.7
F – Even Flow	0.0	0.3	0.7
G – Float Attachment/Protection	0.0	0.5	0.5
H – Float Location	0.0	0.5	0.5
I – Float Redundancy	0.0	0.5	0.5
J – Side Floating	0.3	0.2	0.5

Table 5: Probabilities of An Above Water Escape Route, Craft Inverting or Sinking for each Modification.

Automatic arming and activation produced the greatest benefits in terms of reducing the probability of the helicopter sinking. Increased float attachment and protection, float re-location and additional redundancy all produced lesser benefits in this regard. Side floating not only reduced the probabilities of sinking and of inversion, but also increased the probability of maintaining an over water escape route. The remaining modifications produced no benefit.

6.4.2 *Effect on Fatalities*

In order to interpret these changes in functional effectiveness in terms of their potential for saving life, it was necessary to consider what effect they would have if they were installed on an actual fleet of helicopters. The UK helicopter offshore support fleet was chosen for this exercise because of the relatively high quantity of data available.

As at 15th December 1999, there were 79 helicopters in the UK offshore support fleet [23]. The fleet consists of a variety of different helicopter types with varying degrees of remaining service life. There have been four serious accidents (Brent Spar, Cormorant Alpha, Dunlin Alpha and Scilly Isles) over the last 20 years (the period of the data search), that resulted in fatalities and where the EFS had failed to operate correctly.

A total of 38 occupants were killed in the four UK accidents. 12 of these fatalities were known to have been due to impact injuries or due to exposure following escape from the helicopter. These 12 cases were therefore discounted, as successful operation of the EFS would not have prevented these deaths. The remaining 26 fatalities were assumed to have been caused by EFS failure, which had resulted in drowning due to insufficient time being available to escape. This yields an average fatality rate of 1.3 per annum. (The assumed causes of death for the four UK accidents are summarised in Appendix E).

The change in functional effectiveness derived for each individual modification from the EFS deployment tree was translated into an occupant survival number (see Appendix F). The modifications were assumed to improve the probability of survival for all of the 26 fatalities caused by EFS failure in proportion to their estimated benefits (see Table 5), adjusted as described below. The small sample size of only four accidents precluded a case by case benefit analysis.

Modifications which improved the chances of maintaining an air pocket in the cabin with an over water escape route were assumed to provide the greatest benefit in terms of occupant survival. These modifications would increase the time available for escape, and facilitate escape through the provision of over-water escape routes. It was assumed that these modifications would be 90% effective in reducing the number of fatalities.

Modifications that reduced the chances of sinking, but did not reduce the probability of inversion, were assumed to be less effective as egress would be more hazardous. These modifications were assumed to be 50% effective in reducing fatality levels.

Given the above assumptions a proportion of “occupant” benefit for each modification could be derived. Table 6 summarises the number of lives saved for each modification.

Modification	Number of Lives Saved
A+B – Arm and Activate System	4.3
C – Bottle Redundancy	0
D – Ambient Conditions	0
E – Flexible Hoses	0
F – Even Flow	0
G – Float Attachment/Protection	2.2
H – Float Location	2.2
I – Float Redundancy	2.2
J – Side Floating	5.1

Table 6: Lives Saved for each Modification

Side floating provided the greatest benefit as this prevents total inversion. It also incorporates the benefits of redundancy and locating floats in less vulnerable areas, as it would necessitate the location of flotation equipment at the top of the airframe. Arming and activating the system provided a similarly high level of benefit. Float Attachment/Protection, Float Location and Float Redundancy all gave a lower level of benefit. The remaining modifications did not provide a benefit.

Determination of Implementation Costs

The cost of each modification was determined by consultation with helicopter manufacturer GKN WHL, and EFS manufacturer FPT Industries. They provided estimates of the relative cost of implementing each modification for retro-fit onto existing designs.

The costs were provided as a proportion of the cost of the whole flotation system by the manufacturers. The exception to this was the costs for float location. WS Atkins estimated this at 50%. This modification entails the removal of existing floats and moving them to less vulnerable areas and represents a major change to the EFS and possibly the airframe.

The cost of an EFS for a JAR29 helicopter was estimated to be in the region of £200,000 by CAA following discussions with a major North Sea helicopter operator. This figure was used to convert the relative costs into absolute figures. Table 7 details the proportionate cost of each modification and the cost of implementing each modification on the current UK Offshore Support Fleet of 79 helicopters.

Modification	Proportion EFS Cost (JAR29)	Cost of Implementation on UK Offshore Fleet (79 Aircraft)
A + B – Arm and Activate System	0.07	£1,106,000
C – Bottle Redundancy (2 Extra Bottles)	0.10	£1,580,000
D – Ambient Conditions	0.07	£1,106,000
E – Flexible Hoses	0.05	£790,000
F – Even Flow	0.01	£158,000
G – Float Attachment/Protection	0.15	£2,370,000
H – Float Location	0.50	£7,900,000
I – Float Redundancy	0.15	£2,370,000
J – Side Floating	0.3	£4,740,000

Table 7: Costs For Each Modification.

Cost-Benefit

The cost-benefit of each modification to the EFS was quantified in terms of cost per life saved. The cost of retro-fitting the modifications on the UK offshore support fleet was divided by the number of lives the modification would save over the remainder of the fleet's service life. Values of £2,000,000 per life and an average 20 year remaining service life were assumed in the calculation. The cost per life saved figures for each modification are summarised in Table 8.

Modification	Cost/Life Saved	Cost Effective?
A + B – Arm and Activate System	£255,000	Yes
C – Bottle Redundancy (2 Extra Bottles)	No Benefit	No
D – Ambient Conditions	No Benefit	No
E – Flexible Hoses	No Benefit	No
F – Even Flow	No Benefit	No
G – Float Attachment/Protection	£1,094,000	Yes
H – Float Location	£3,646,000	No
I – Float Redundancy	£1,094,000	Yes
J – Side Floating	£938,000	Yes

Table 8: Cost per Life Saved for Each Modification.

6.7 Discussion of Results

Arming and activating the system, float attachment, redundancy and side floating all provided cost effective options in terms of their potential for saving life.

Float location was not cost effective due to the large cost associated with moving floats on the airframe. This modification would also cause problems with the existing ditching requirements, which specify that at least one exit on each side of the cabin should be maintained above water level.

Although the other modifications did not provide any benefit, it should be noted that the small sample size resulted in only very few failures being attributed to these stages of the deployment process. Therefore, it is not surprising that they produced no benefit as the modifications cannot improve on the existing successful outcomes. It should also be noted that bottle redundancy, flexible hoses and even flow are considered to be standard features on modern EFS designs.

The costs for each modification were based on retro-fitting them to existing helicopters. It is anticipated that costs for new build would be lower as the benefit of the full service life would be accrued and that they would be easier and therefore less expensive to implement on a helicopter which is being built, rather than making retrospective changes to existing designs.

The costs accounted for in the study were installation and material costs only. They did not include indirect costs such as design costs, helicopter down time, labour, costs and increases in operating costs due to added weight or drag. In order to address these detailed cost issues a type specific study would be required to be undertaken on a particular helicopter.

However, the study clearly shows that there are significant benefits to be made by implementing automatic arming and activation, side floating, redundancy and improved float protection or attachment to helicopters in the UK offshore fleet.

A key assumption in the study was that each modification would be 100% reliable in terms of its operation. This assumption was necessary due to the small sample size

and the lack of information on system reliability during an impact. Although this is slightly non-conservative, the cost-benefit for the four key modifications are well below £2,000,000 per life. Therefore, even if the modifications were assumed to be just 50% reliable they would still be cost effective in terms of their potential for saving life.

7 REVIEW OF REGULATORY REQUIREMENTS

The regulatory body for rotorcraft in the UK is the Civil Aviation Authority (CAA). The CAA has adopted the Joint Aviation Authority (JAA) requirements (JARs) for certification of rotorcraft.

The JAA requirements for rotorcraft ditching are effectively tied to the American Federal Aviation Authority (FAA) requirements (FARs). These regulatory bodies are responsible for maintaining and enforcing airworthiness and operational requirements to ensure an acceptable level of safety is achieved for helicopter design, manufacture and operation. As the FARs are largely identical to the JARs for water ditching, only the JAR requirements are discussed in detail in this section.

The following JARs relate to water ditching, flotation, emergency landing conditions and evacuation issues:

- JAR 29.801: Ditching
- JAR 29.563: Structural Ditching Provisions
- JAR 29.561: Emergency Landing Conditions
- JAR 29.562: Emergency Landing Dynamic Conditions
- JAR 29.807: Passenger Emergency Exits

For certain JARs, where advisory material has not been explicitly provided, the FAA's Advisory Circulars (AC) have been adopted to clarify the intent of the requirements. It should be noted that these documents are intended to give an acceptable means, but not the only means of achieving compliance with the requirements. FAA AC 29-2B relates to the sections listed above.

The JAR text and relevant sections of AC 29-2B are given in Appendix C. A brief discussion of each of the above sections is given below, followed by a series of recommendations for improvements. The main JARs directly related to crashworthiness are the emergency landing conditions. However, the other JARs have been reviewed as they impinge indirectly on crashworthiness and survivability issues.

7.1 JAR 29.801: Ditching

This clause specifies the general ditching requirements. Its main concern is protecting the occupants and ensuring that there is an adequate escape route. Ditching is defined as:

“An emergency landing on water, deliberately executed, with the intent of abandoning the rotorcraft as soon as possible. The rotorcraft is assumed to be intact prior to water entry with all controls and essential systems, except engines, functioning properly”

Ditching is therefore assumed to be a controlled water entry, rather than at an uncontrolled/inappropriate attitude and velocity which would occur in an impact. The JAR only gives broad guidance using phrases like “*minimise the probability of injury*” and “*probable behaviour*”, and provides little specific guidance. The basic requirement is for the helicopter to remain afloat in a mainly upright position, long enough to allow the occupants to exit the helicopter and board the liferafts, under the most likely sea conditions for the intended area of operation.

Ditching certification is not required unless requested by the applicant. Certification is demonstrated either by scale model tests, or by comparison with helicopters of similar design.

The AC gives considerably more detail than the JAR, and discusses four main certification areas for ditching:

- 1 *Water Entry*: Model tests or direct comparison with craft of similar design with proven ditching characteristics should be used to determine the optimum behaviour of the helicopter in a water ditching. During ditching the helicopter is assumed to be auto-rotating and rotor lift of up to two thirds of the maximum design weight is assumed to act through the centre of gravity. The following parameters are used to establish the worst case ditching loads:
 - Probable variation from the optimum pitch angle.
 - Forward speeds up to the knee in the helicopter's height velocity diagram, reduced by the wind speed associated with each applicable sea state.
 - Vertical descent velocity of 5 ft/s (1.52 m/s).
 - Yaw attitudes up to 15 degrees.
 - Wave heights up to and including Sea State 4 are given as examples for North Sea operation.

The structural integrity of the floats and their attachments are then required to be demonstrated under the most onerous ditching condition. The effects of the vertical and drag loads may be considered to act independently. Probable failure of windows, doors, skins and panels should also be considered.

- 2 *Flotation Systems*: For fixed (normally inflated) flotation systems, consideration should be given to the following loadings on the floats.
 - Air loads throughout the approved flight envelope.
 - Water entry loads.
 - Water loads after entry.

For floats that are normally deflated, flotation bags are only required to be assessed against water loads after water entry. A manual or fully automatic activation system is required, together with a redundant alternative. It should be demonstrated that inflation at any flight condition within the approved operating envelope is not hazardous unless a very reliable safeguard is in place. The AC gives an example of a manual arming circuit as a reliable inflation safeguard. A means should also be available to check the gas cylinder pressures and the status of the EFS prior to take off.

The inflation system should be designed to minimise the probability of floats inflating improperly. The inflation time should be short enough to prevent the helicopter from becoming partially submerged. Additionally, the AC recommends that the floats should be shown to inflate (without puncture) when subjected to static water pressure.

- 3 *Flotation and Trim:* Flotation and trim characteristics should be demonstrated to be satisfactory to at least Sea State 4. This is typically achieved using scale models with solid floats. Probable damage to the airframe should be considered when demonstrating compliance against the trim requirements. Adequate flotation and trim characteristics should also be demonstrated at Sea State 2 for a rupture in the most critical flotation bag compartment.
- 4 *Occupant Egress and Survival:* The ability of the occupants to deploy and board the liferafts should be demonstrated. This can be achieved either by a full scale helicopter test on calm water or, more typically, by a "representative" ground based test. The flotation bags should not obstruct occupant egress.

7.2 **JAR 29.563: Structural Ditching Provisions**

The structural ditching provisions define the landing condition for a controlled ditching, and loading requirements for the emergency floats.

The AC recommends that the helicopter support structure, floats and attachments should be substantiated for rational limit and ultimate ditching loads. The ditching event is defined slightly differently to that in clause 29.801. Namely a forward velocity of up to 30 Knots (15.4 m/s) with a minimum vertical velocity of 1.52 m/s, in a Sea State 4 condition. The attitude of the helicopter and the likely variation in yaw and pitch angles should also be considered. The AC recommends that flight tests should be undertaken to confirm the auto-rotation attitude and variability in yaw and pitch angles.

For floats that are fixed or deployed prior to impact, the floats and attachments are required to be designed against the buoyancy load developed by a fully immersed float. Consideration should also be given to restoring moments induced by side winds, asymmetrical helicopter loading, inertia, wave action and probable damage sustained under the ditching requirements of 29.801. For floats deployed in flight, the air loads should be "substantiated" and an air speed safety factor of 1.11 applied to the maximum deployment speed. The AC recommends that landing load factors and likely water distribution are determined from water drop tests or validated analysis.

For floats deployed after impact, the same immersion loadings as for fixed floats apply. In addition, they must be capable of resisting a combined vertical and drag load generated by a relative speed of 20 Knots (10.3 m/s) between the helicopter and

water. This requirement is different to the loads specified in 29.801, which states that the vertical and drag loads can be treated independently.

7.3 JAR 29.561: Emergency Landing Conditions

This section relates to emergency landings onto both land and water. It is primarily concerned with protecting the occupants from serious injury during a crash landing. To this end it specifies inertial loads for items within the passenger cabin which would be likely to injure occupants if they became detached from the airframe. Additionally, ultimate inertial load factors are defined for heavy equipment such as rotors, engines and fuel tanks, which although not inside the cabin may intrude into the passenger compartment during the impact. As EFS are typically sited in non-occupied areas and are of relatively low mass, they would not be capable of intruding into the cabin and therefore would not be covered by this section.

7.4 JAR 29.562: Emergency Landing Dynamic Conditions

This requirement is concerned with protecting occupants from excessive shock loadings during an emergency landing. This is achieved by specifying design and loading requirements for the passenger seats and attachments. Acceptable levels of injury to the occupant are also defined. This clause does not, therefore, apply to EFS.

7.5 JAR 29.807: Passenger Emergency Exits

This clause is concerned with the number and size of emergency exits. The criteria are based on the number of passenger seats in the airframe. In all cases at least one exit in each side of the rotorcraft should remain above the waterline. The flotation devices must not obstruct the exits, and a test must be conducted to demonstrate the proper functioning of all exits.

7.6 Recommendations For Regulation Changes

- The main focus of the JARs is on controlled water entry rather than crashworthiness. It is recommended that guidance on good design practices for accident or high energy impacts should be incorporated in the AC.
- Redundant flotation should be specified at bag level as well as individual compartment level. In an impact, where high loads would be experienced, if one compartment has been ruptured the whole bag is likely to have been damaged.
- A requirement for secondary flotation bags away from the underside of the structure should be considered. The floor region experiences the greatest loads in a water impact, as it is typically the primary impact site. Location away from the underside of the helicopter would greatly improve survivability of the flotation bags.
- Consideration should be given to relaxing the requirement to maintain at least one emergency exit on each side of the helicopter above the water line for severe but survivable impacts. Work being undertaken by CAA is investigating the benefits of side floating in terms of occupant egress. Side floating would help mitigate the effects of capsizing following an impact. It should be used in conjunction with, rather than an alternative to floating upright.

- Identical sea state conditions should be specified for both redundant and normal flotation configurations to improve flotation times following an impact.
- Shock loadings should be specified for all safety critical equipment. Currently impact loads are only defined for passengers, or items likely to injure occupants or penetrate the cabin. These loads should be limited by human survivability criteria. There would be little advantage in having a system which functions if the occupants have not survived.
- The use of automatic arming and deployment devices should be incorporated into the JAR design requirements. This would dramatically improve the reliability of the system. These measures would negate the need to involve a conscious decision by the pilot to activate or deploy the flotation bags. Following an accident, the pilot will likely be in shock and disorientated. Historical evidence has shown that the pilot may fail to deploy the flotation system following an uncontrolled water entry. The use of manual backup/override systems would improve reliability and redundancy.
- The regulatory material should be improved by removing the duplication and inconsistencies between the ACs on 29.801 and 29.563. The definition of ditching should be made consistent throughout the text.
- The JARs should be better defined. In particular the applicability of the AC guidance should be more explicit.

8 CONCLUSIONS

A comprehensive review of the crashworthiness of helicopter EFS, their design and regulation has been performed.

A survey of EFS performance in UK Civil and Royal Navy helicopter water impacts was undertaken. In addition, a world-wide literature search was carried out to identify existing research into helicopter EFS.

Little 'new' data to that already known at the start of the survey was found. The accident data was almost exclusively limited to the information published in the accident reports, especially for accidents more than eight years ago. Where levels of damage were supplied, they were often too general to be of use for detailed assessments.

Historically, sponson mounted EFS, such as on the S61N, were found to be particularly vulnerable to impact damage. Pod mounted EFS were less prone to damage. Significant fatalities were observed in accidents where the EFS had not been armed and/or deployed.

A detailed assessment of the behaviour of a generic helicopter under a variety of water impact scenarios was performed using non-linear FE methods. The scenarios were based on actual accidents which were outside the FAA's proposed 95% survivability envelope, but which had a significant number of survivors.

The airframe and water body FE models were validated against a variety of drop tests and various scale model tank tests. The only relevant validation data for the airframe was of a Lynx impact onto the ground with the undercarriage retracted. Given the minor differences between the Lynx and modelled airframe, good correlation with the test data was observed.

Two water models were developed using Lagrangian and Eulerian formulations. For validation purposes, rigid bodies were used to model both vertical and fly-in impacts. The Lagrangian water model was found only to be suitable for determining initial accelerations during vertical impacts. It was not suited to fly-in impacts or impacts that occurred over a significant period of time, as it is incapable of modelling large fluid displacements. The Eulerian water model was more suited to both vertical and fly-in impacts. However, very refined meshes were required to achieve a converged result. The number of elements required for high speed impacts or complex models proved to be prohibitively large, resulting in very long analysis times. There were doubts as to the validity of the test data used for some of the water model validation work.

The Eulerian modelling technique is considered not mature enough to accurately model complex water deformable structure impacts. The Lagrangian water model was only suitable for determining initial acceleration levels for vertical impacts such as the Brent Spar scenario. Global responses and strain levels were generally consistent with damage detailed in the accident reports. However, results for local accelerations were too noisy to extract any useful information. Reasonable correlation with empirical results performed by BMT was achieved.

A review of the design and operation of EFS was performed. This was based on limited data produced by the FAA on US water impacts between 1982 and 1989. Several design modifications were proposed to improve the performance of EFS following a severe impact.

A general cost benefit study was performed to assess whether implementation of any of the modifications would be cost effective in terms of their potential for saving life if they were fitted to the current UK offshore fleet. Automatic arming and activation, redundancy, side floating and increased float protection/attachment all provided cost per life saved figures of £1,000,000 or less. All these modifications offer significant cost-effective methods for saving life and should be considered in further detail in a type specific study.

Several of the proposed modifications are now considered as industry standard and are fitted to the majority of new EFS. These include automatic activation, even gas distribution, flexible hoses and bottle redundancy. The fact that some of the modifications are incorporated voluntarily into current designs does not obviate the need to mandate them in future design requirements. Due to the evolution of EFS design, a study of modern helicopter water impacts may uncover a different list of reasons for failure of the EFS and fatalities. However, only limited data is likely to be available.

The regulatory requirements relating to water ditching, flotation, emergency landing conditions and evacuation issues were reviewed, with an emphasis on crashworthiness issues. A series of recommendations for EFS design and regulatory changes were then made. These are summarised in Section 9 of this report.

RECOMMENDATIONS

The crashworthiness of EFS can be improved by incorporating the following design features:

- 1 Automatic arming.
- 2 Automatic activation of floats by immersion switches.
- 3 Provision of a manual, independent, backup activation and arming system where automatic systems are used.
- 4 Distribution lines designed with equal resistance and/or flow distribution valves used to ensure equal float deployment, even with a bag ruptured.
- 5 Flexible hoses used for flow distribution lines.
- 6 Bags divided into multiple cells to limit the effect of small bag ruptures.
- 7 Inflation systems designed to limit the effect of varying ambient conditions.
- 8 Systems which require inflation to be deployed after impact.
- 9 Floats designed for balanced deployment (timing as well as volume), even with system damage.
- 10 Where possible, floats located away from likely primary impact sites, such as the nose, sponsons and floor of the airframe.
- 11 Distribution hoses and wiring not routed through areas of the airframe likely to undergo severe deformation or failure during an impact. Short pipework, or individual gas bottles located near each bag used to reduce the risk of flow line failure due to structural deformation. NB: Careful consideration should be given to the trade off between redundancy with interconnected bags and the higher risk associated with longer pipe runs.
- 12 Redundant flotation provided at bag level, as well as compartments within a bag.
- 13 Redundant flotation bags should be located in the upper part of the airframe to minimise the risk of damage. These could be arranged to allow the helicopter to float on its side retaining an air pocket in the cabin and maintaining a number of escape routes above the water surface, rather than capsizing into a fully inverted position.
- 14 Any claimed passive buoyancy (e.g. fuel tanks or tail boom voids) for ditching is only allowed if it can be demonstrated that the appropriate part of the airframe remains attached to the passenger compartment during an impact.

To improve regulatory requirements, the following changes to the Joint Airworthiness Requirements (JARs) and/or Advisory Circulars (ACs) are recommended:

- 15 The main focus of the JARs is on controlled water entry rather than crashworthiness. It is recommended that guidance on good design practices for accidental or high energy impacts should be incorporated in the AC.
- 16 Redundant flotation should be specified at bag level as well as at individual compartment level. In an impact, where high loads would be experienced, if one compartment has been ruptured the whole bag is likely to have been damaged.
- 17 A requirement for secondary flotation bags away from the underside of the structure should be considered. The floor region experiences the greatest loads in a water impact, as it is typically the primary impact site. Location away from the underside of the helicopter would greatly improve survivability of the flotation bags.
- 18 Consideration should be given to relaxing the requirement to maintain at least one emergency exit on each side of the helicopter above the water line for severe but survivable impacts. Work being undertaken by CAA is investigating the benefits of side floating in terms of occupant egress.
- 19 Identical sea state conditions should be specified for both redundant and normal flotation configurations to improve flotation times following a severe impact.
- 20 Shock loadings should be specified for all safety critical equipment. Currently impact loads are only defined for passengers, or items likely to injure occupants or penetrate into the cabin. These loads should be limited by human survivability criteria. There would be little advantage in having a system which functions if the occupants have not survived.
- 21 The use of automatic arming and deployment devices should be incorporated into the JAR design requirements. This would dramatically improve the reliability of the system. These measures would negate the need to involve a conscious decision by the pilot to activate or deploy the flotation bags. Following an accident, the pilot will likely be in shock and disorientated. Historical evidence has shown that the pilot may forget to deploy the flotation system following an uncontrolled water entry. The use of manual backup/override systems would improve reliability and redundancy.
- 22 The regulatory material should be improved by removing the duplication and inconsistencies between the ACs on 29.801 and 29.563. The definition of ditching should be made consistent throughout the text.

The JARs should be better defined. In particular the applicability of the AC guidance should be more explicit.

ACKNOWLEDGEMENTS

WS Atkins would like to thank GKN Westland Helicopters Ltd, BMT Fluid Mechanics, AAIB, RNFSIC, Air Claims, FAA and FPT Industries for helping in the completion of this work.

REFERENCES

- 1 A Review of UK Military and World Civil Helicopter Water Impacts over the Period 1971-1992, Westland Helicopters Ltd., November 1993. Also published as CAA paper 96005 "Helicopter Crashworthiness", Civil Aviation Authority July 1996.
- 2 An Analysis of the Response of Helicopter Structures to Water Impact, Westland Helicopters Ltd., March 1995. Also published as CAA paper 96005 "Helicopter Crashworthiness", Civil Aviation Authority July 1996.
- 3 Review of Helicopter Offshore Safety and Survival, CAP 641 Civil aviation Authority, 1995.
- 4 Crashworthiness of Helicopter Emergency Flotation Systems : Final Summary Report, BMT Fluid Mechanics Ltd, Project 44134/00, 30th June 1999.
- 5 Rotorcraft Ditchings and Water-Related Impacts that Occurred from 1982 to 1989 – Phase I, DOT/FAA/CT-92/13, US Federal Aviation Authority, October 1993.
- 6 Rotorcraft Ditchings and Water-Related Impacts that Occurred from 1982 to 1989 – Phase II, DOT/FAA/CT-92/14, US Federal Aviation Authority, October 1993.
- 7 Survey and Analysis of Rotorcraft Flotation Systems, DOT/FAA/AR-95/53, US Federal Aviation Administration, May 1996.
- 8 A Tensor-Skin Concept for Crashworthiness of Helicopters in Case of Water Impact, Thuis and Wiggendaad, National Aerospace Laboratory NLR, Pub. American Helicopter Society 50th Annual Forum, Crash Safety Session, 1994.
- 9 Sub-Floor Skin Panels for Improved Crashworthiness of Helicopters in Case of Water Impact, Thuis et al, National Aerospace Laboratory NLR, Pub. American Helicopter Society 51st Annual Forum, May 1995.
- 10 The Development of a Rotorcraft Water Impact Analysis Methodology, C. W. Clark, Y-C Shen, Sikorsky Aircraft Corporation, Stratford CT. Presented at AHS National Crashworthiness Specialist Meeting September 14-16 1998 Phoenix Az.
- 11 Hybrid Modelling with DRI/KRASH, G. Wittlin et al. Dynamic Response Inc, Presented at AHS National Crashworthiness Specialist Meeting September 14-16 1998 Phoenix Az.
- 12 Report on the Accident to Bell 212 G-BIJF in the North Sea, South East of the Dunlin Alpha Platform, on 12 August 1981, AAIB Report 10/82.
- 13 Report on the Accident to Bell 212, G-BDIL 14 Miles from the Murchison Platform on 14 September 1982, AAIB Report 2/84.
- 14 Report on the Accident to British Airways Sikorsky S-61N, G-BEON in the Sea Near St Mary's Aerodrome, Isles of Scilly, on 16 July 1983, AAIB Report 8/84.
- 15 Report on the Accident to Sikorsky S61N, G-BEWL at Brent Spar, East Shetland Basin on 25 July 1990, AAIB Report 2/91.

- 16 Report on the Accident to AS 332L Super Puma, G-TIGH, near Cormorant 'A' Platform, East Shetland Basin, on 14 March 1992, AAIB Report 2/93.
- 17 Report on the Accident to the Sikorsky S61N Helicopter G-BDII Near Handa Island off the Northwest Coast of Scotland on 17 October 1988, AAIB Report 3/89.
- 18 The Lynx Crashworthiness Drop Test Programme, S. Clifford, GKN Westland Ltd, Contract No A26B/28, February 1984.
- 19 Water Landing Characteristics of a Re-entry Capsule, NASA Memo 5-23-59L, NASA, June 1959.
- 20 Crashworthiness of Helicopter Emergency Flotation Systems: Model Test Validation Information, BMT Fluid Mechanics Ltd, Project 44134/00 Report 4 Rel2., 26 March, 1999.
- 21 Ditching Investigation of a 1/20-Scale Model of the Space Shuttle Orbiter. NASA Contractor Report 2593, October 1975, WL Thomas.
- 22 Devices to Prevent Helicopter Total Inversion Following a Ditching, BMT Fluid Mechanics Ltd, Project 44117/00 Report 3 Rel.2, 12 May, 1997. Also published as CAA paper 97010 "Devices to Prevent Helicopter Total Inversion Following a Ditching", Civil Aviation Authority December 1997.
- 23 Email from CAA to WS Atkins Consultants Ltd, 4th April 2000.

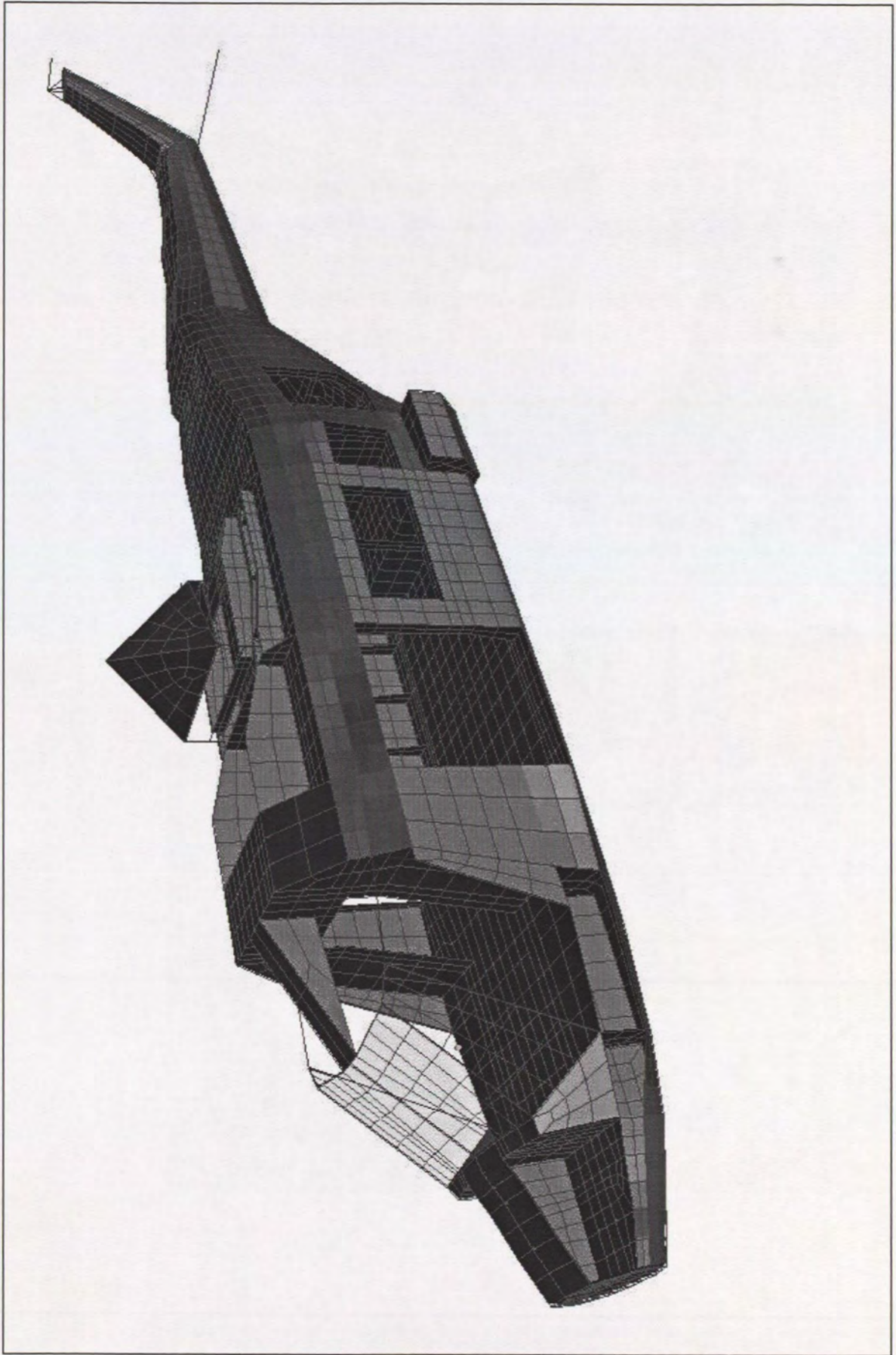


Figure 1: WG30 Finite Element Model

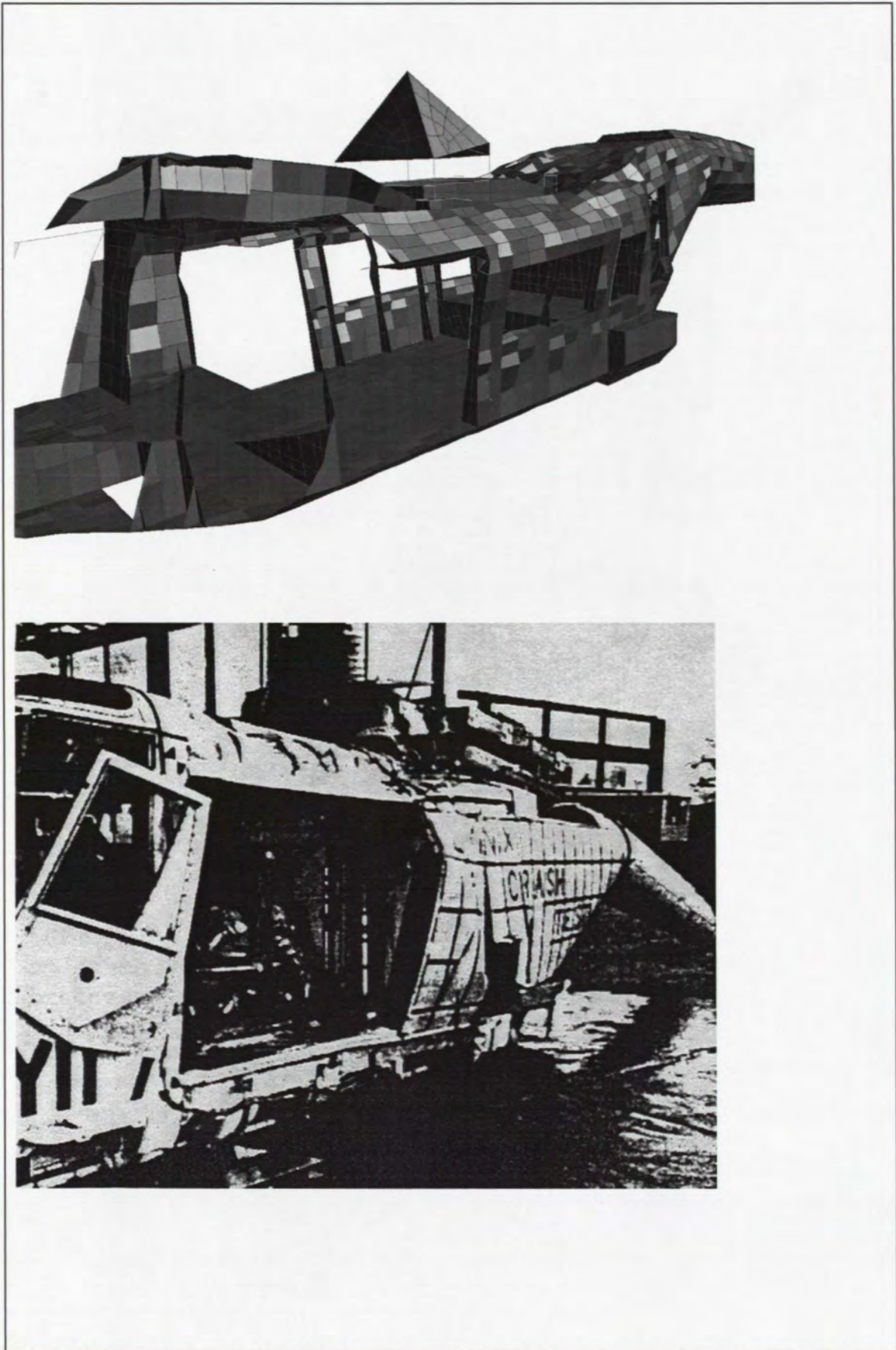


Figure 2: Cut Away of WG30 Model after Ground Impact, Together With Lynx Test Comparison

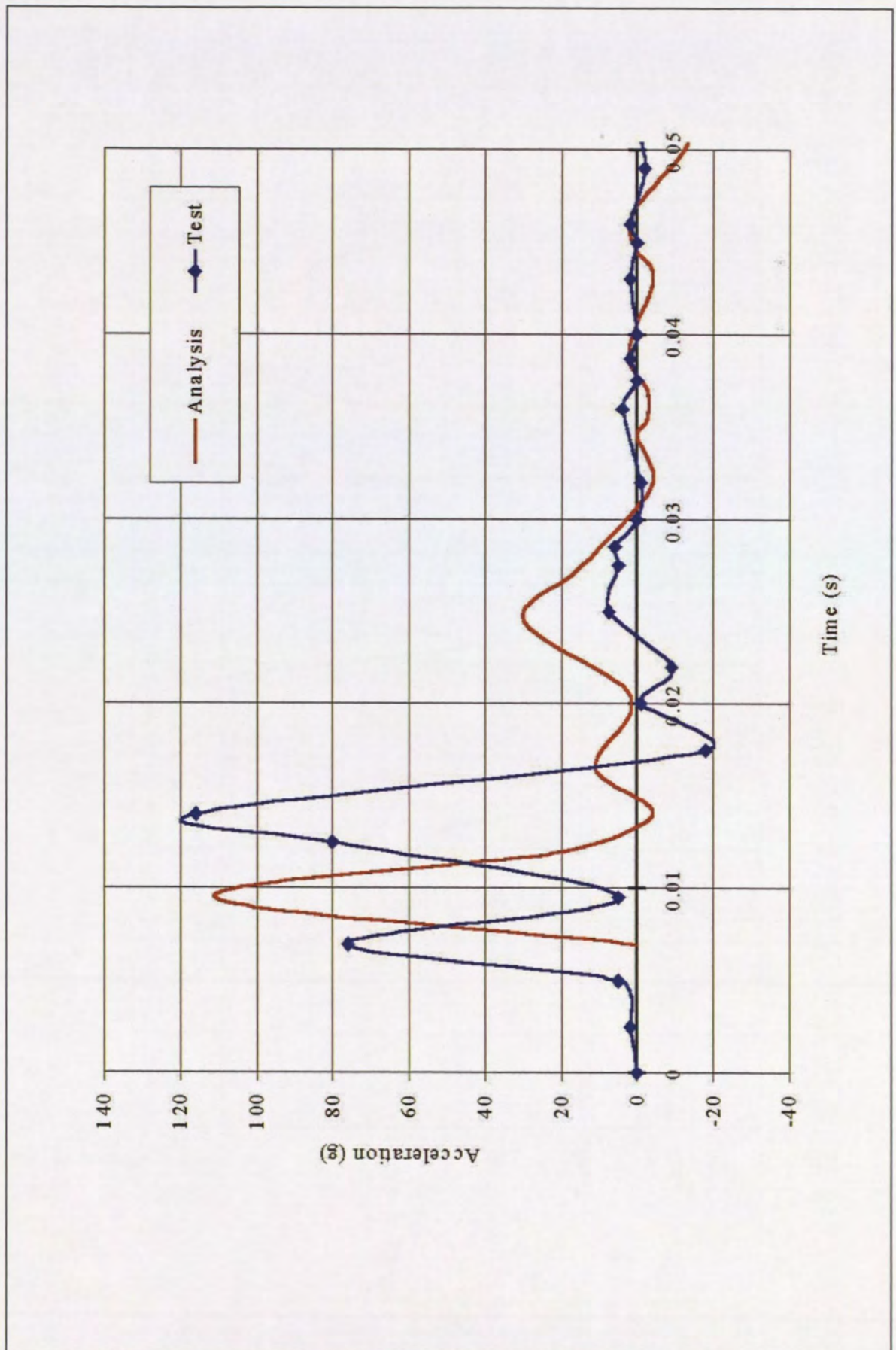


Figure 3: Acceleration Time History Pulse Recorded at Cabin Floor

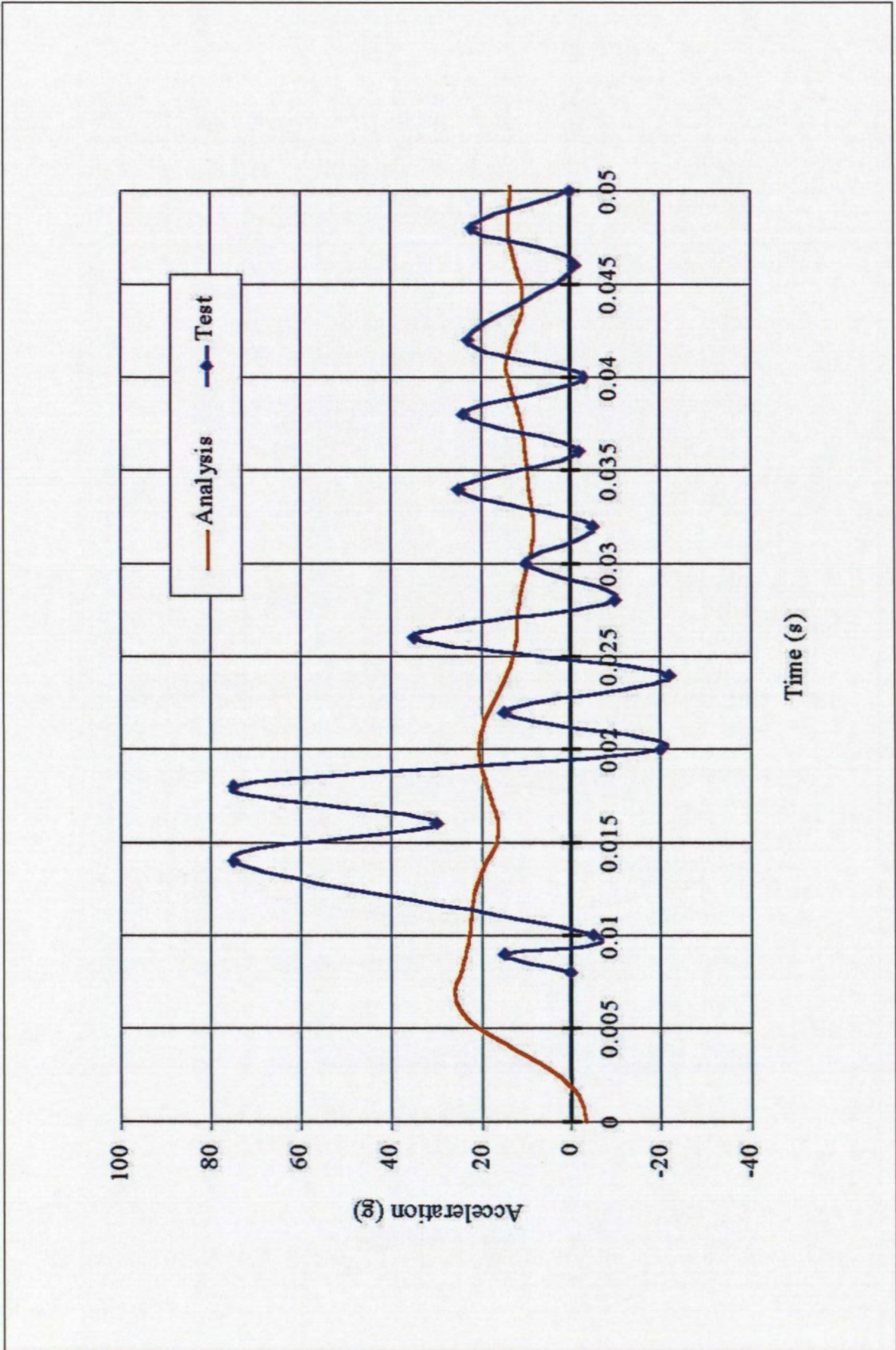


Figure 4: Acceleration Time History Pulse Recorded at Main Rotor Gearbox

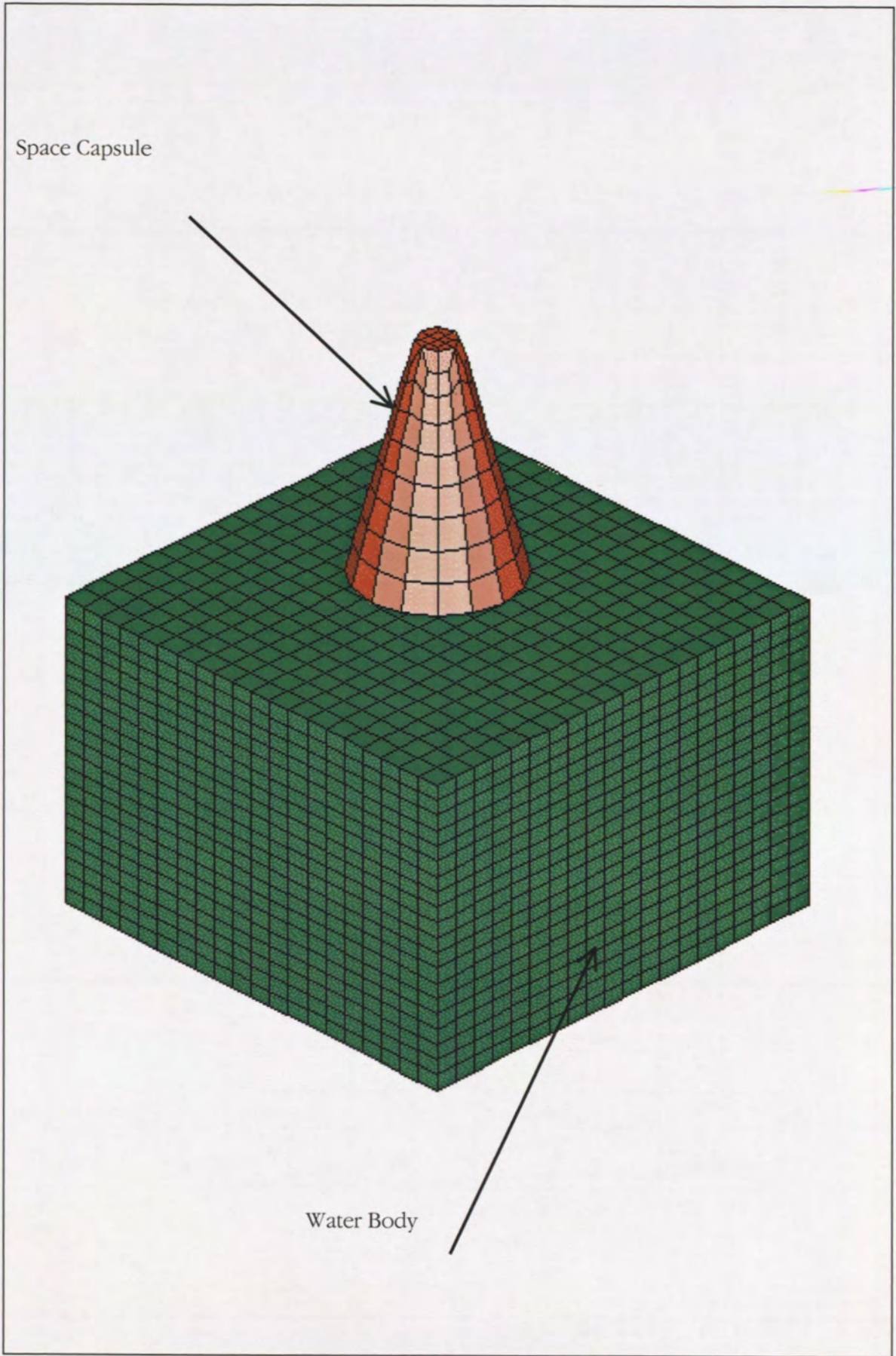


Figure 5: Arrangement of the Space Capsule Impact Scenario

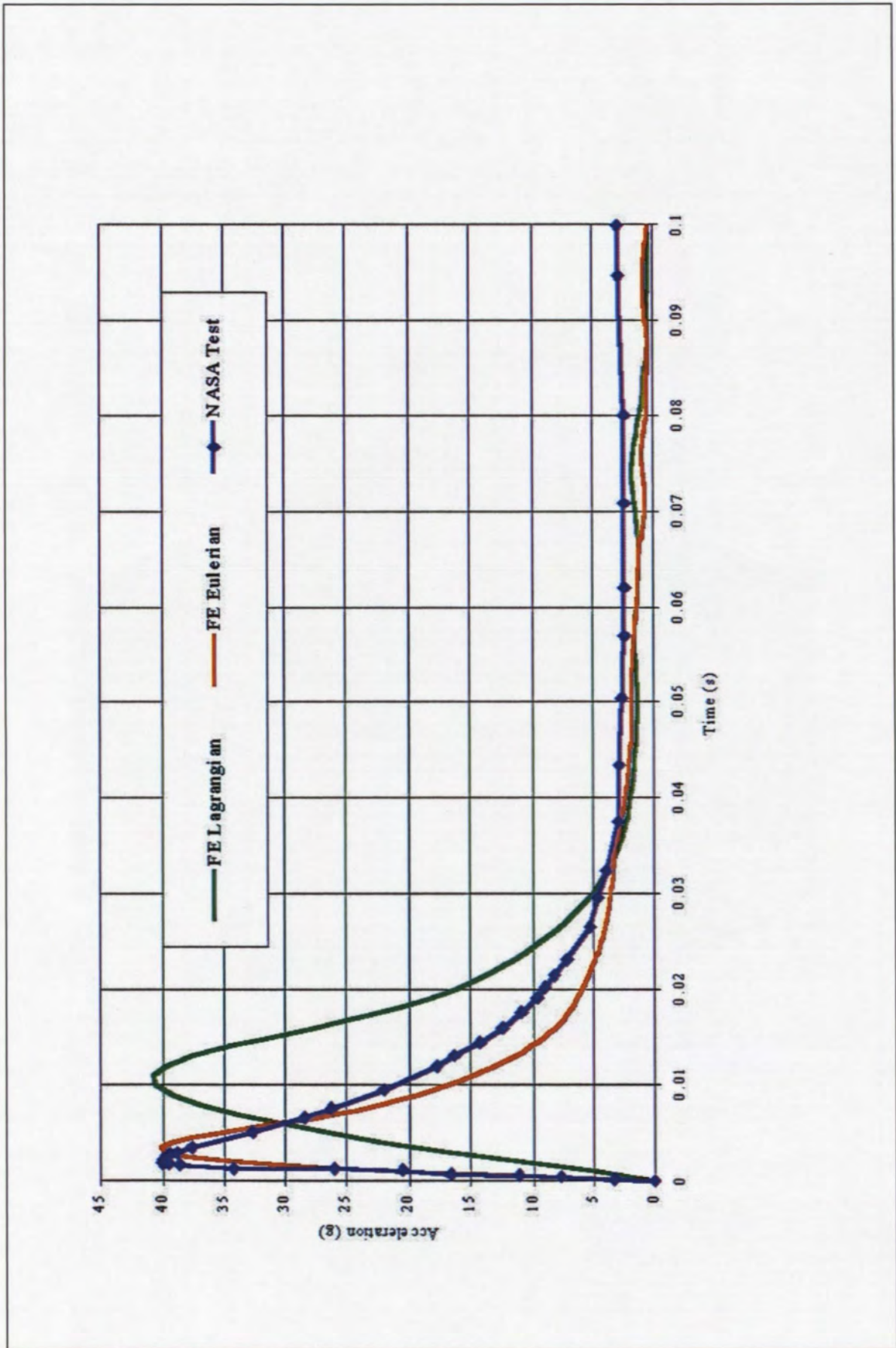


Figure 6: Acceleration of Space Capsule from Test and Analysis

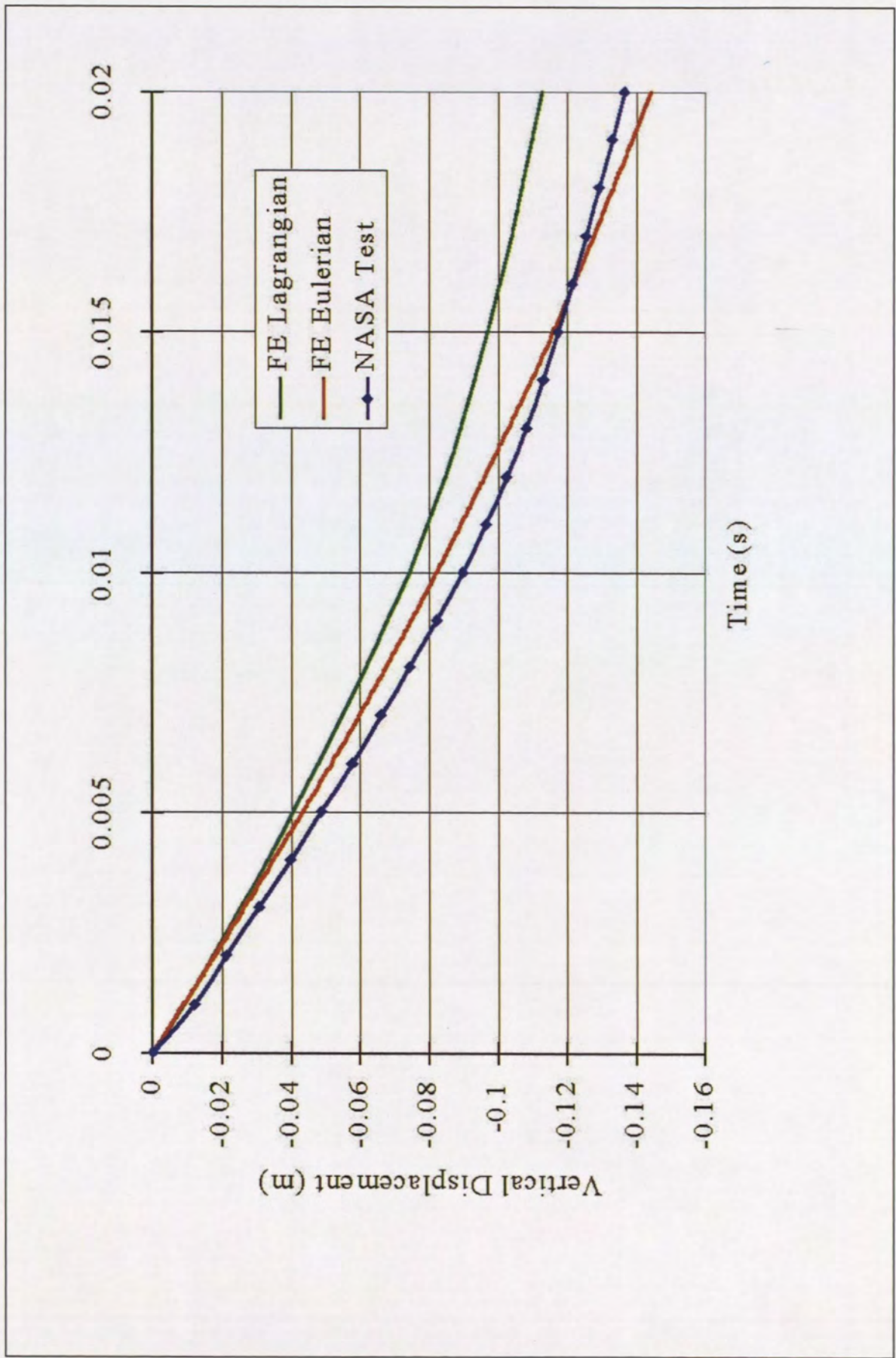


Figure 7: Vertical Displacement of Space Capsule from Test and Analysis

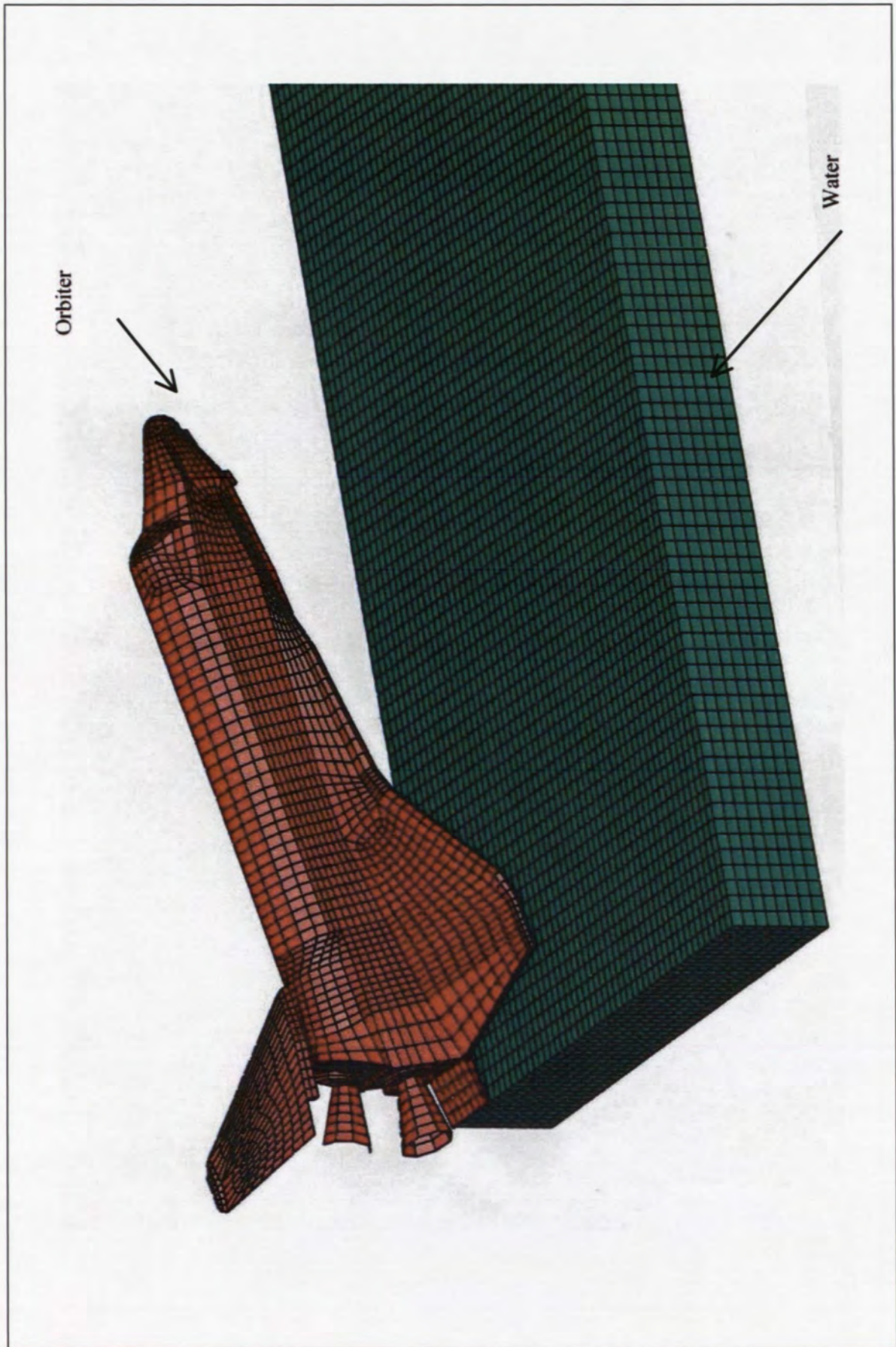


Figure 8: Finite Element Mesh of Orbiter Space Shuttle

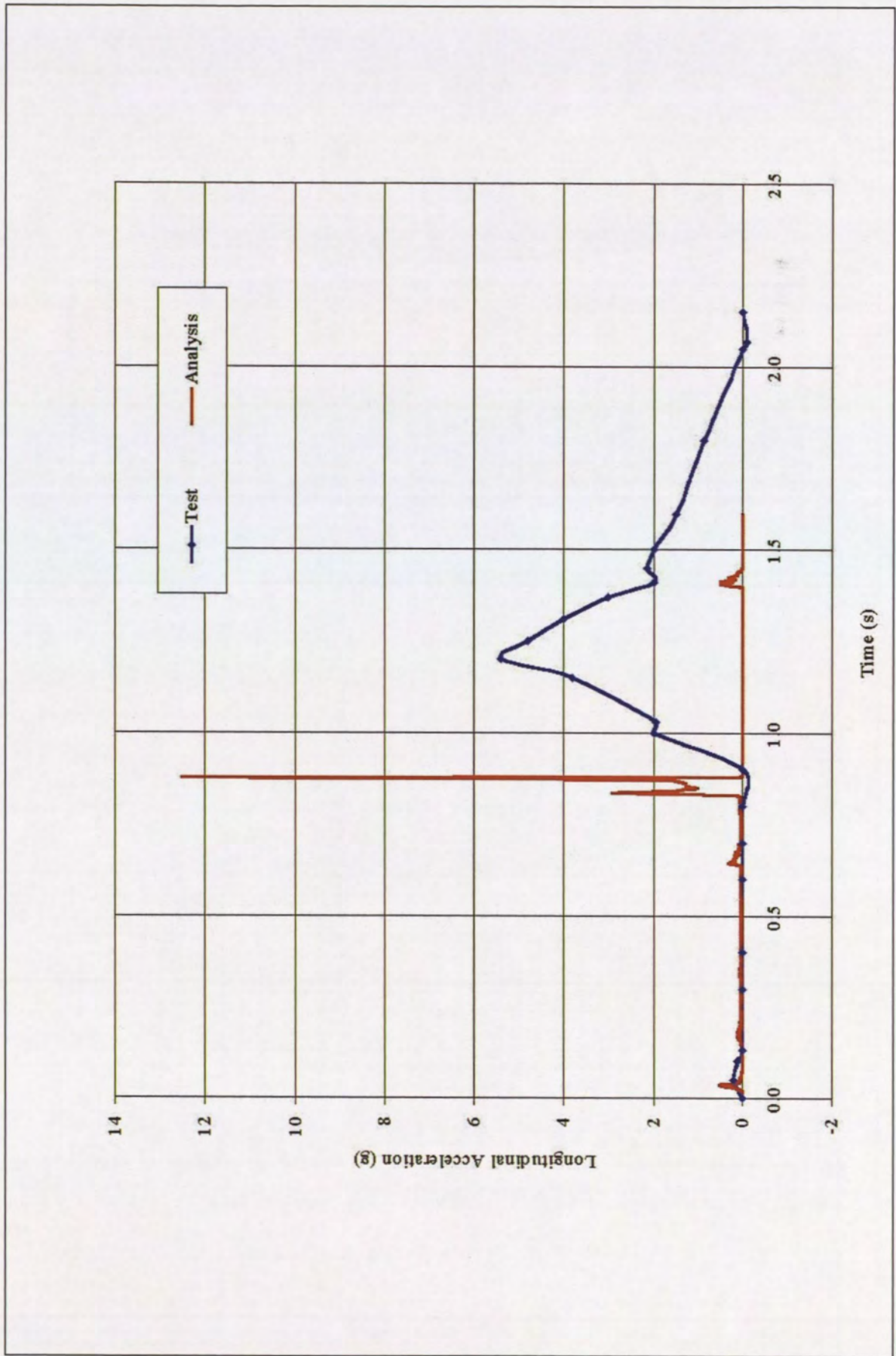


Figure 9: Lateral Acceleration of Orbiter using Lagrangian Mesh

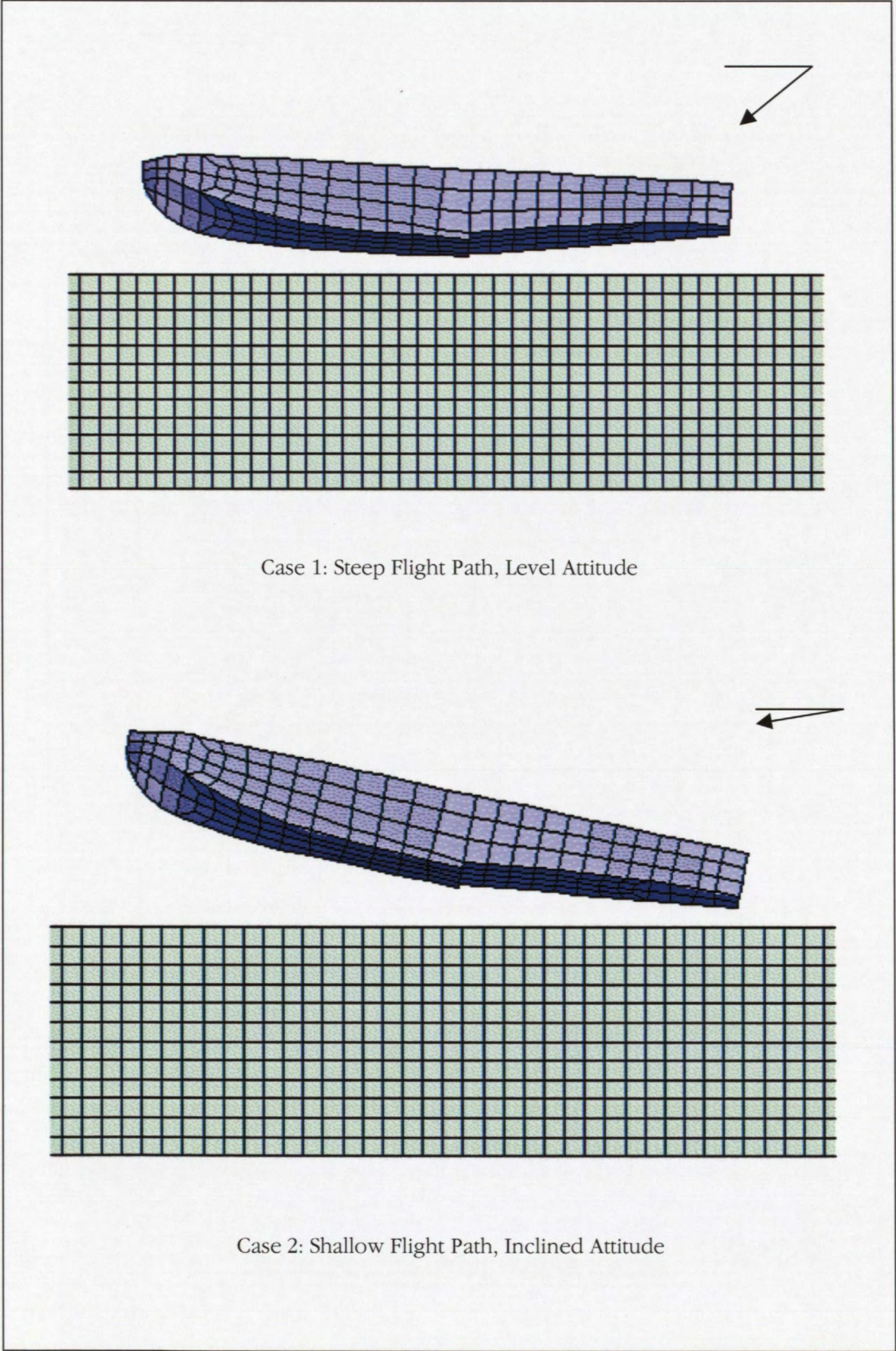


Figure 10: Set up of Two Hull Scenarios Showing Differences in Trim Angle and Flight Path

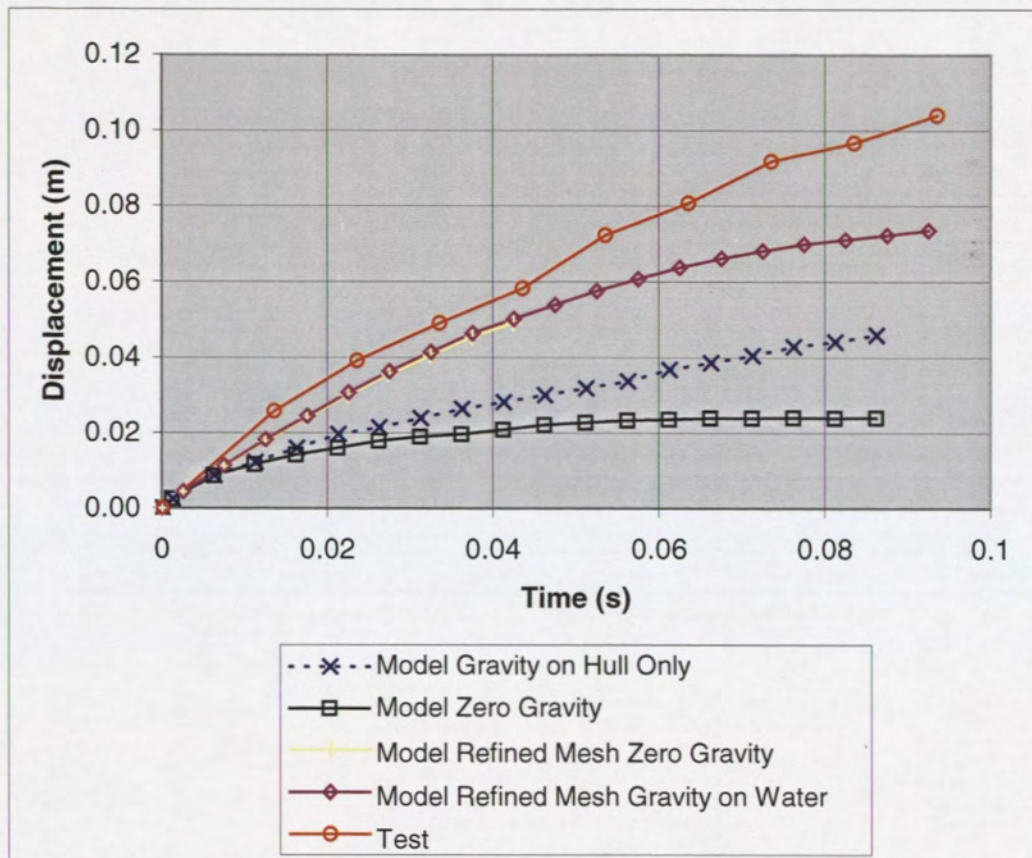


Figure 11: Vertical Displacement of Hull for Case 1

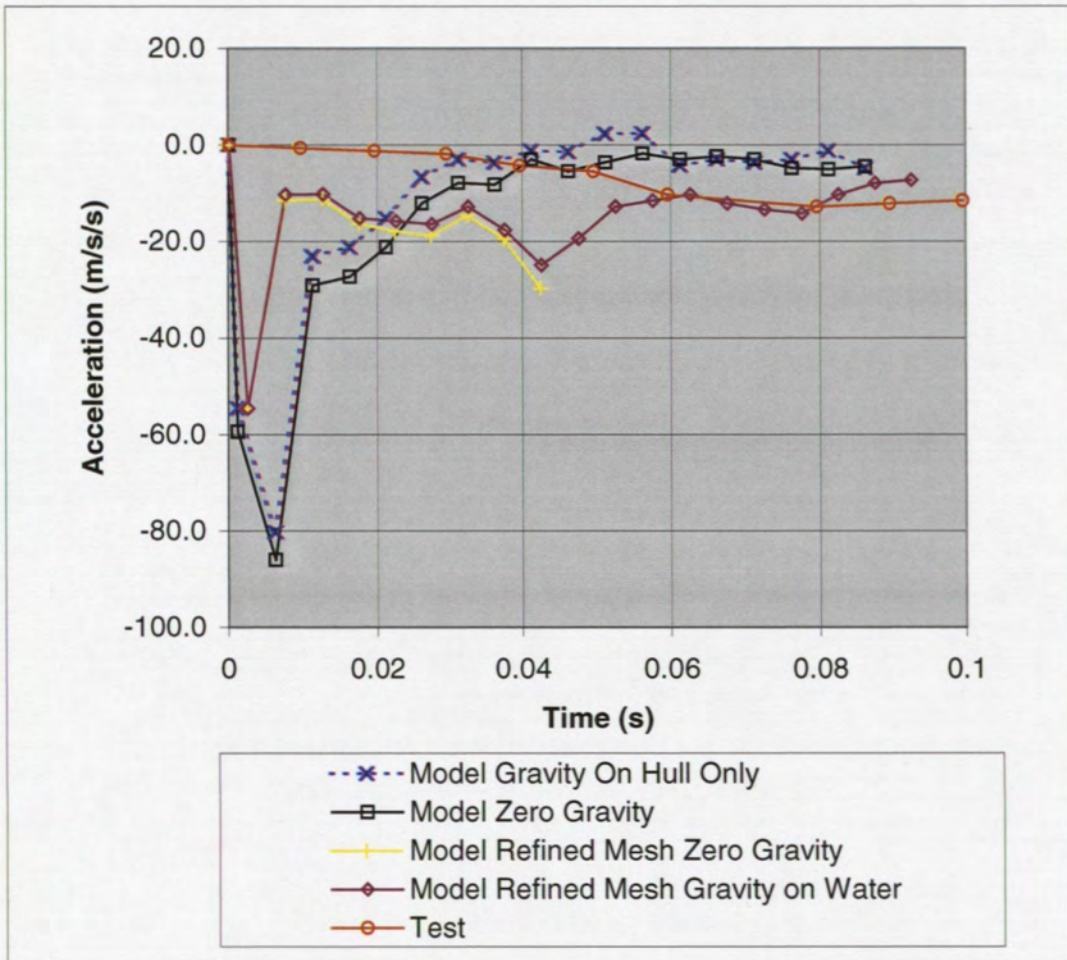


Figure 12: Vertical Acceleration of Hull for Case 1

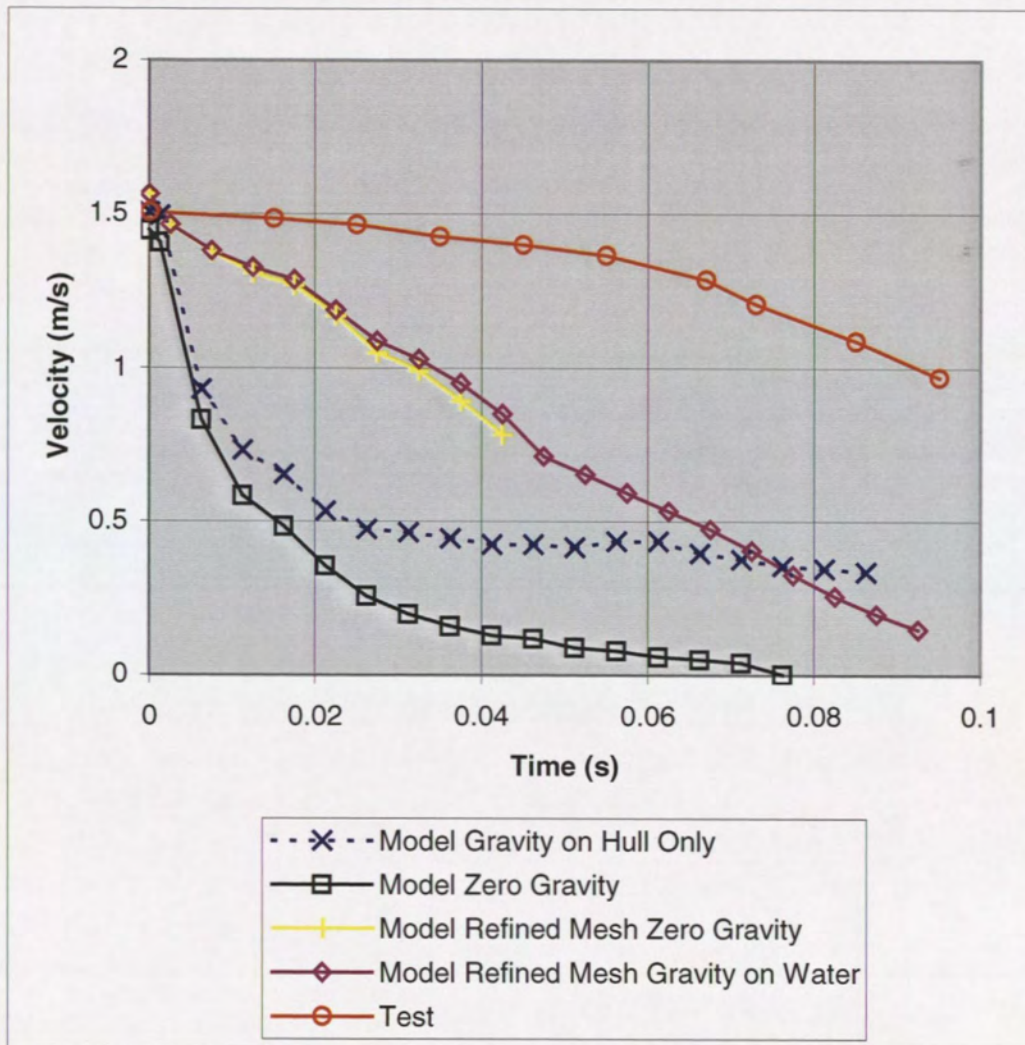


Figure 13: Vertical Velocity of Hull for Case 1

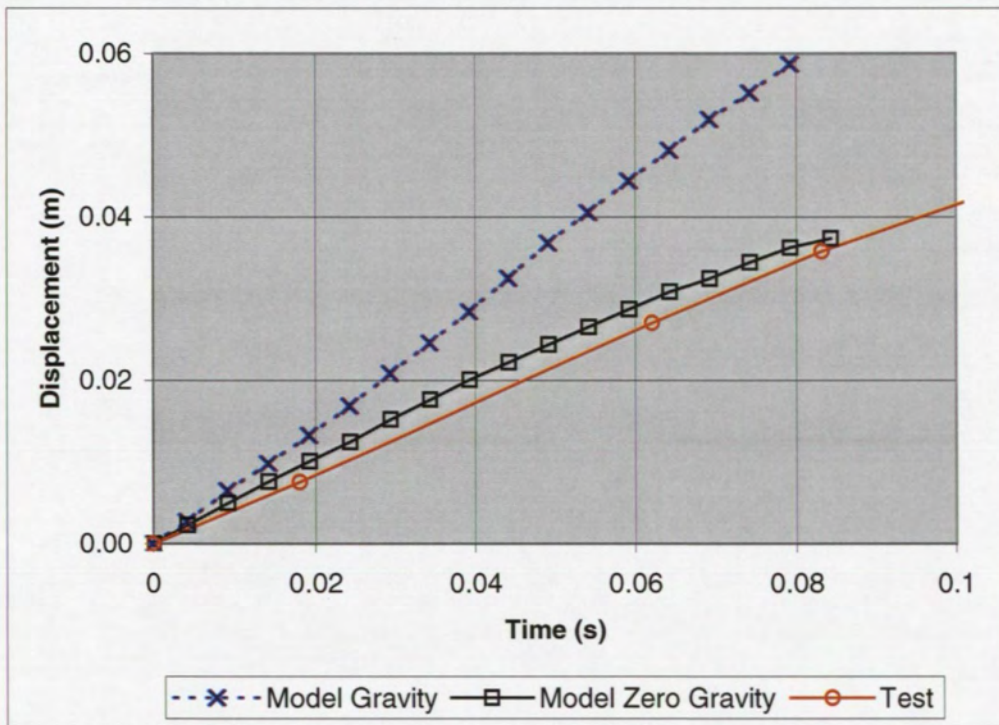


Figure 14: Vertical Displacement of Hull for Case 2

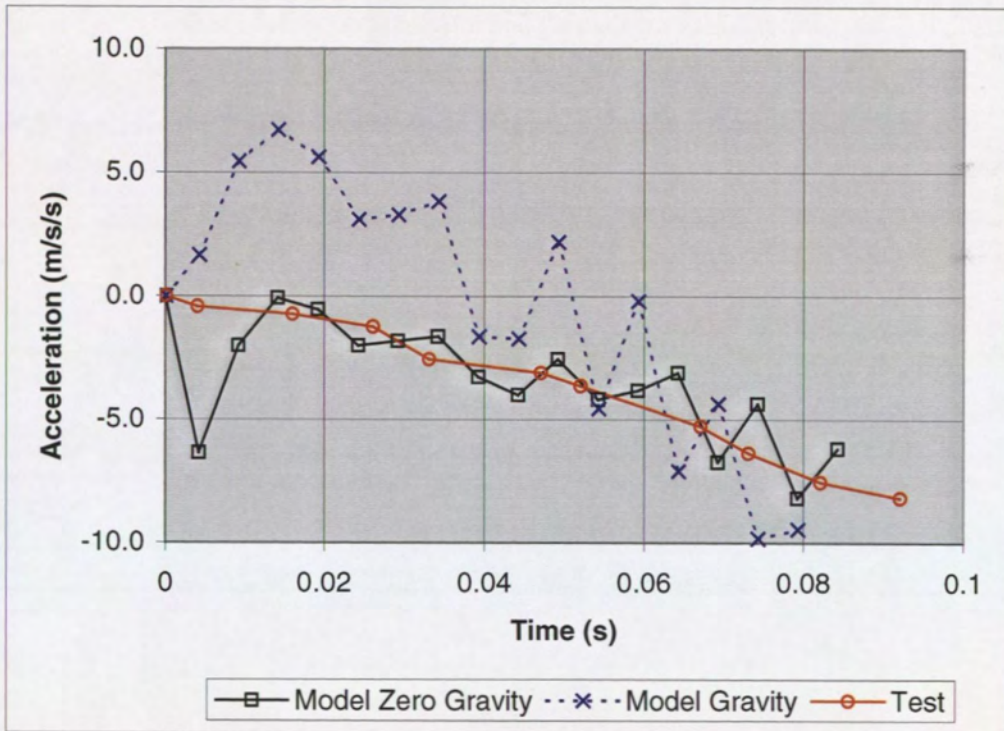


Figure 15: Vertical Acceleration of Hull for Case 2

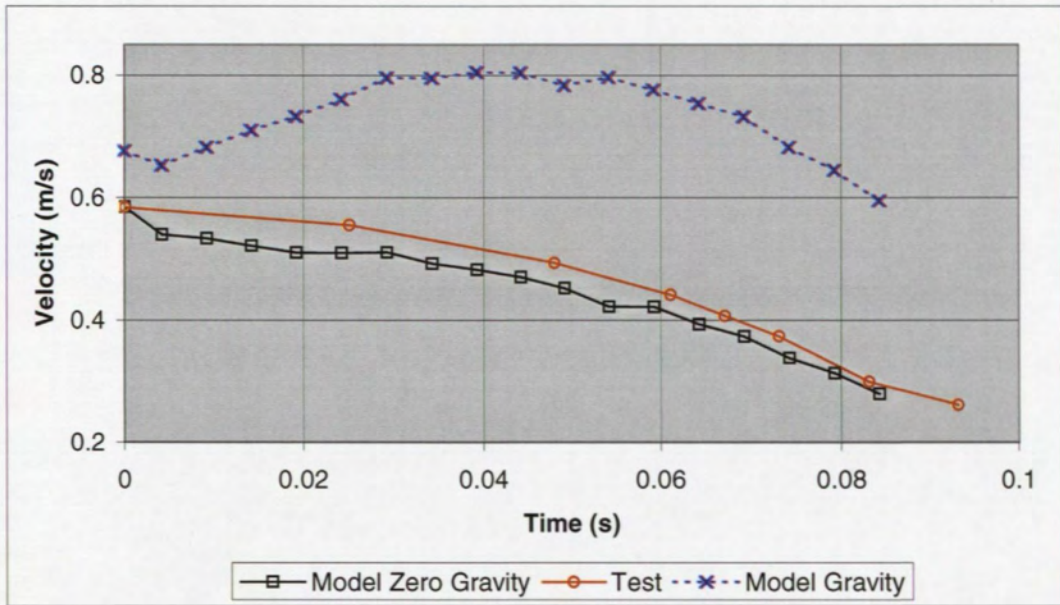


Figure 16: Vertical Velocity of Hull for Case 2

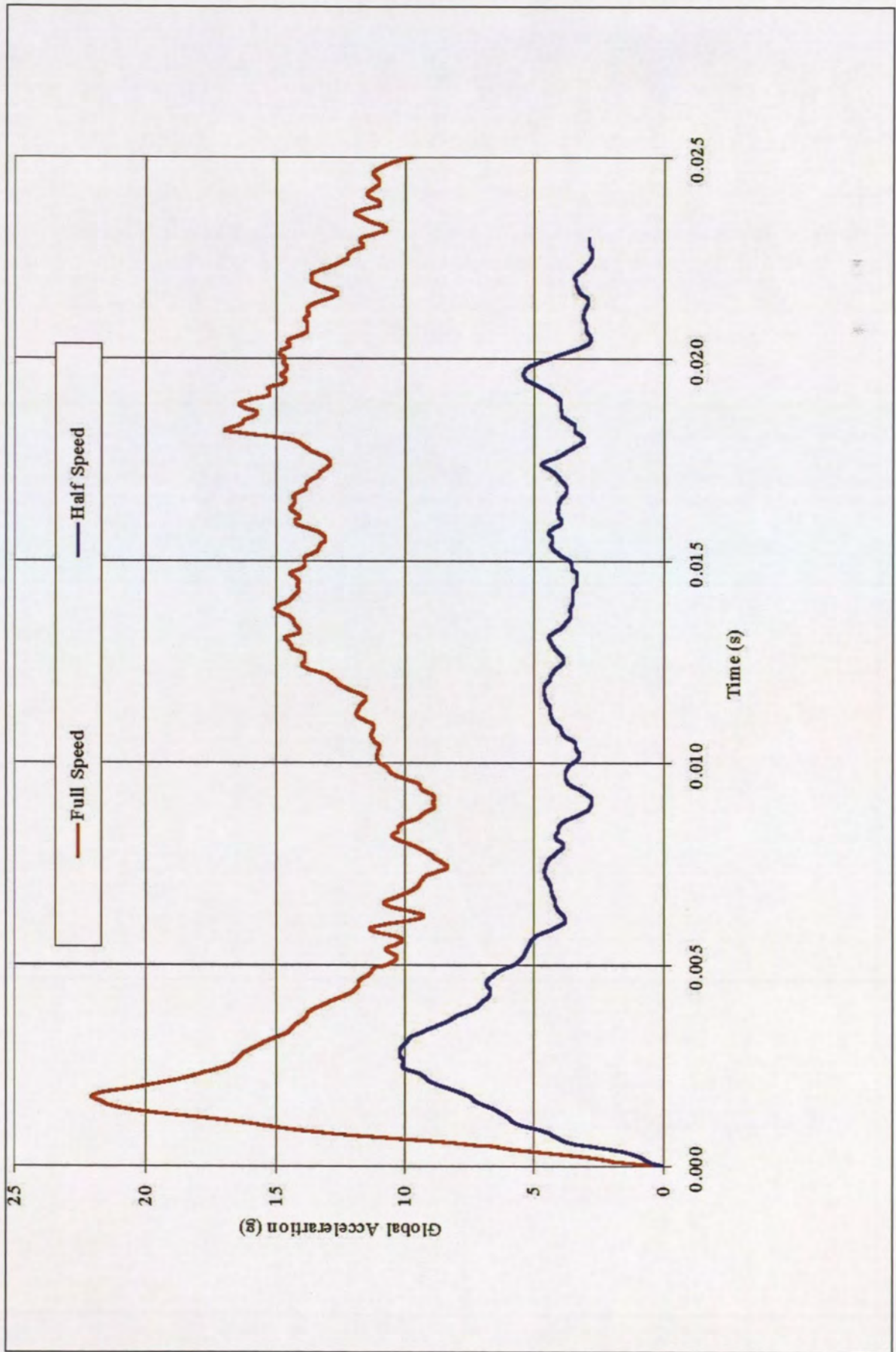


Figure 17: Brent Spar – Global Acceleration at Full and Half Speed



Figure 18: Brent Spar – Full Speed: Maximum Plastic Strain Throughout Time Period

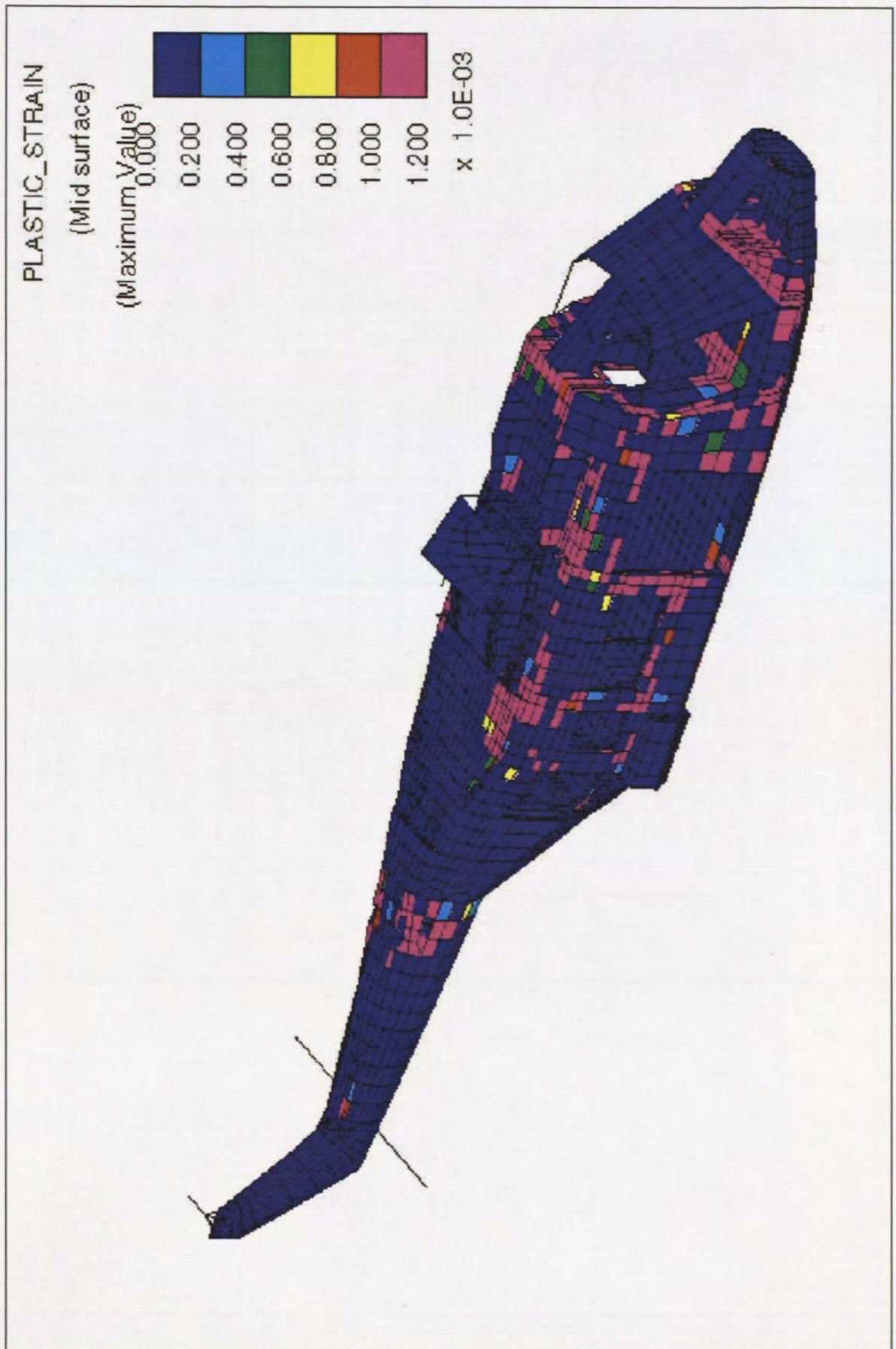


Figure 19: Brent Spar – Half Speed: Maximum Plastic Strain Throughout Time Period

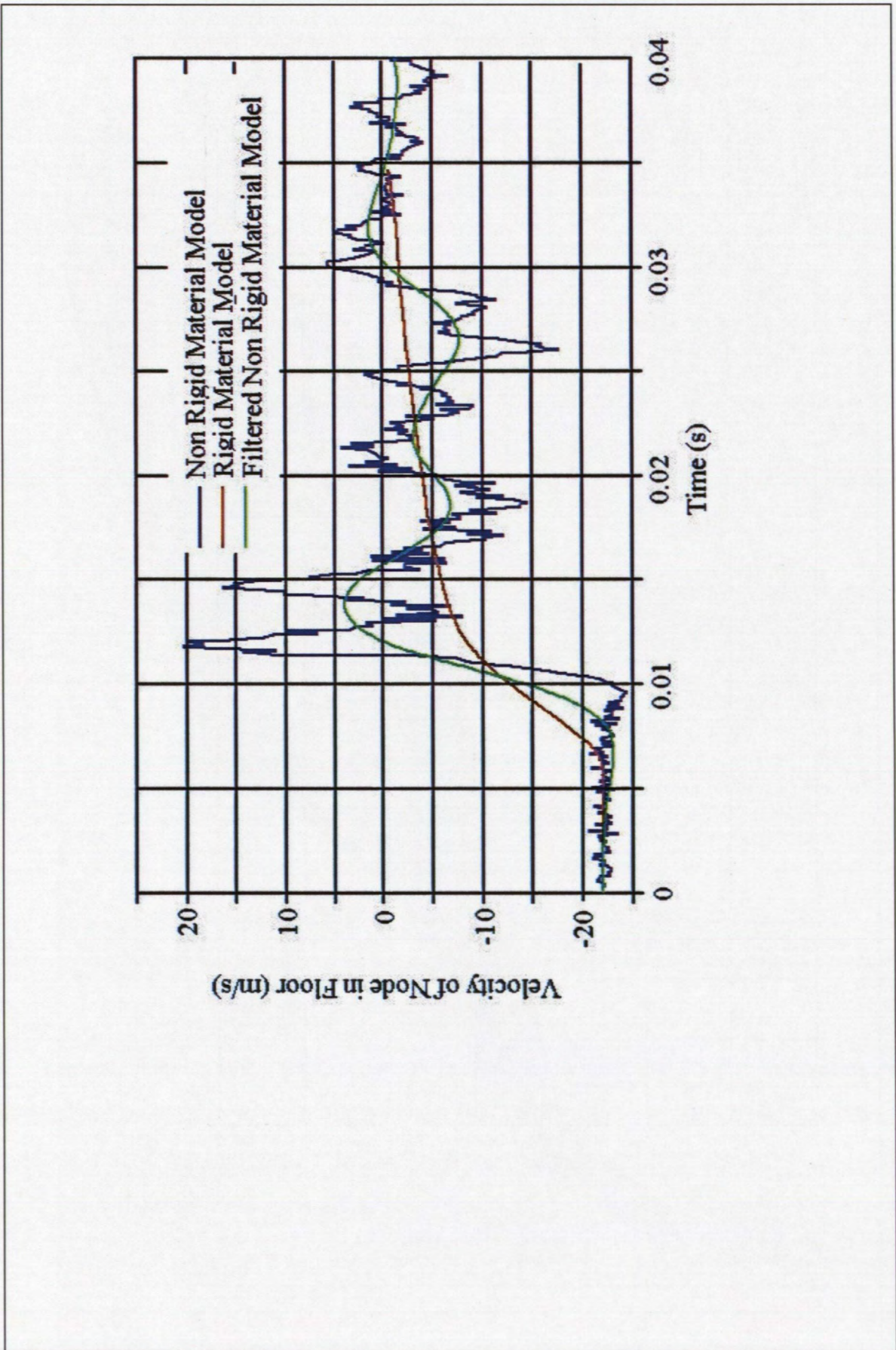


Figure 20: Comparison of Nodal Velocity for Rigid and Non-Rigid Analysis

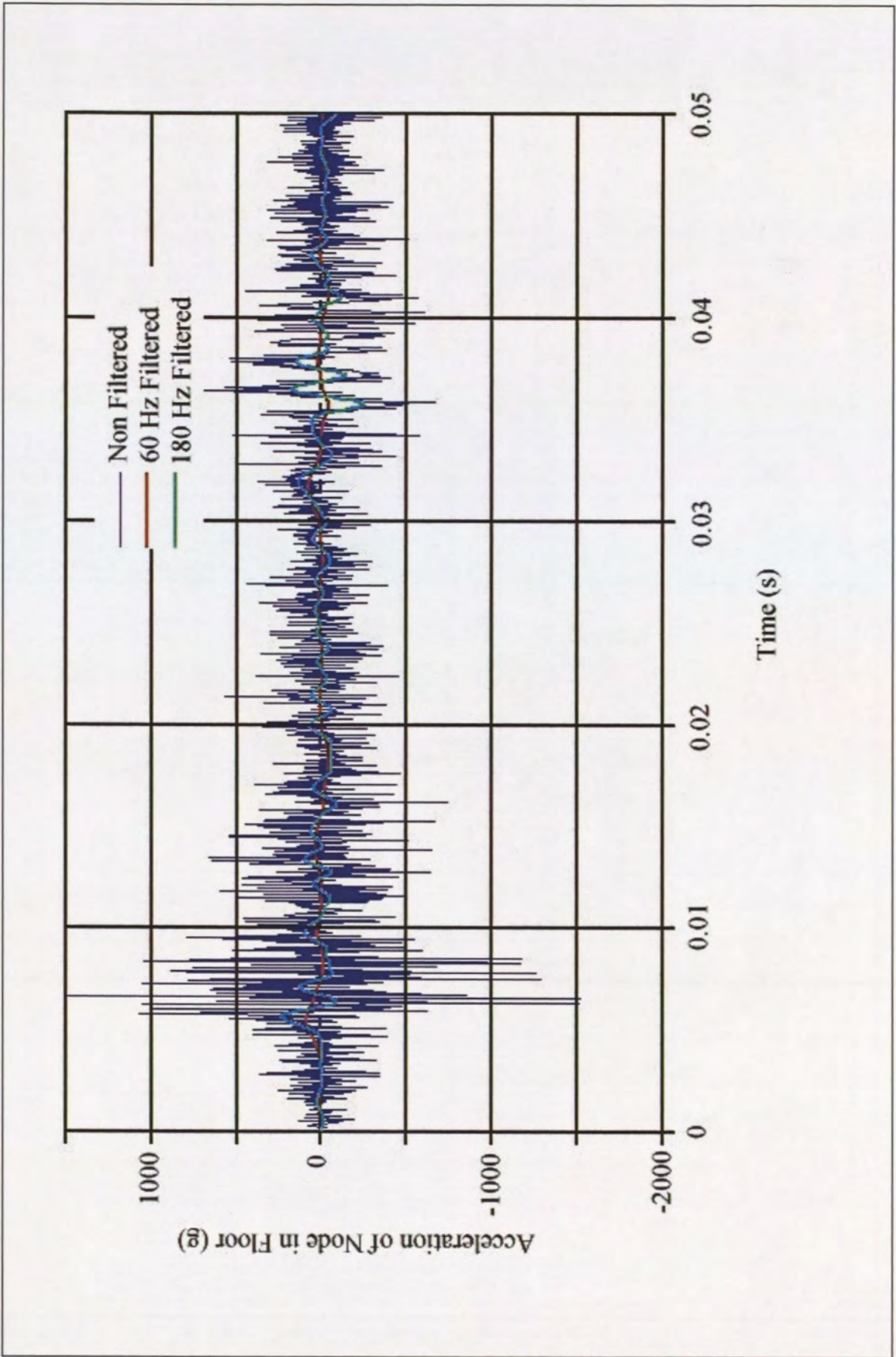


Figure 21: Nodal Acceleration Before and After Filtering

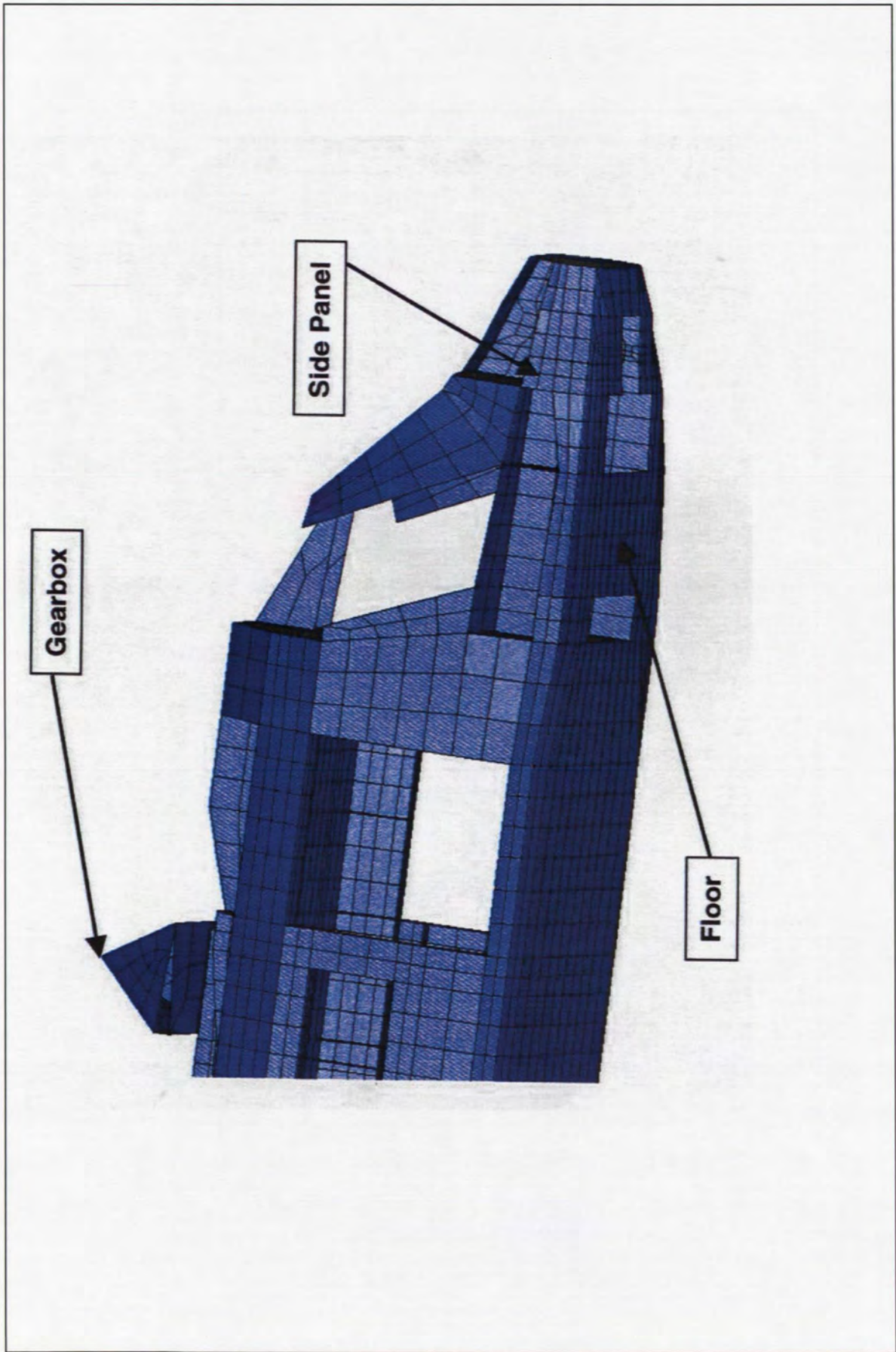


Figure 22: Location of Nodes for Monitoring Acceleration

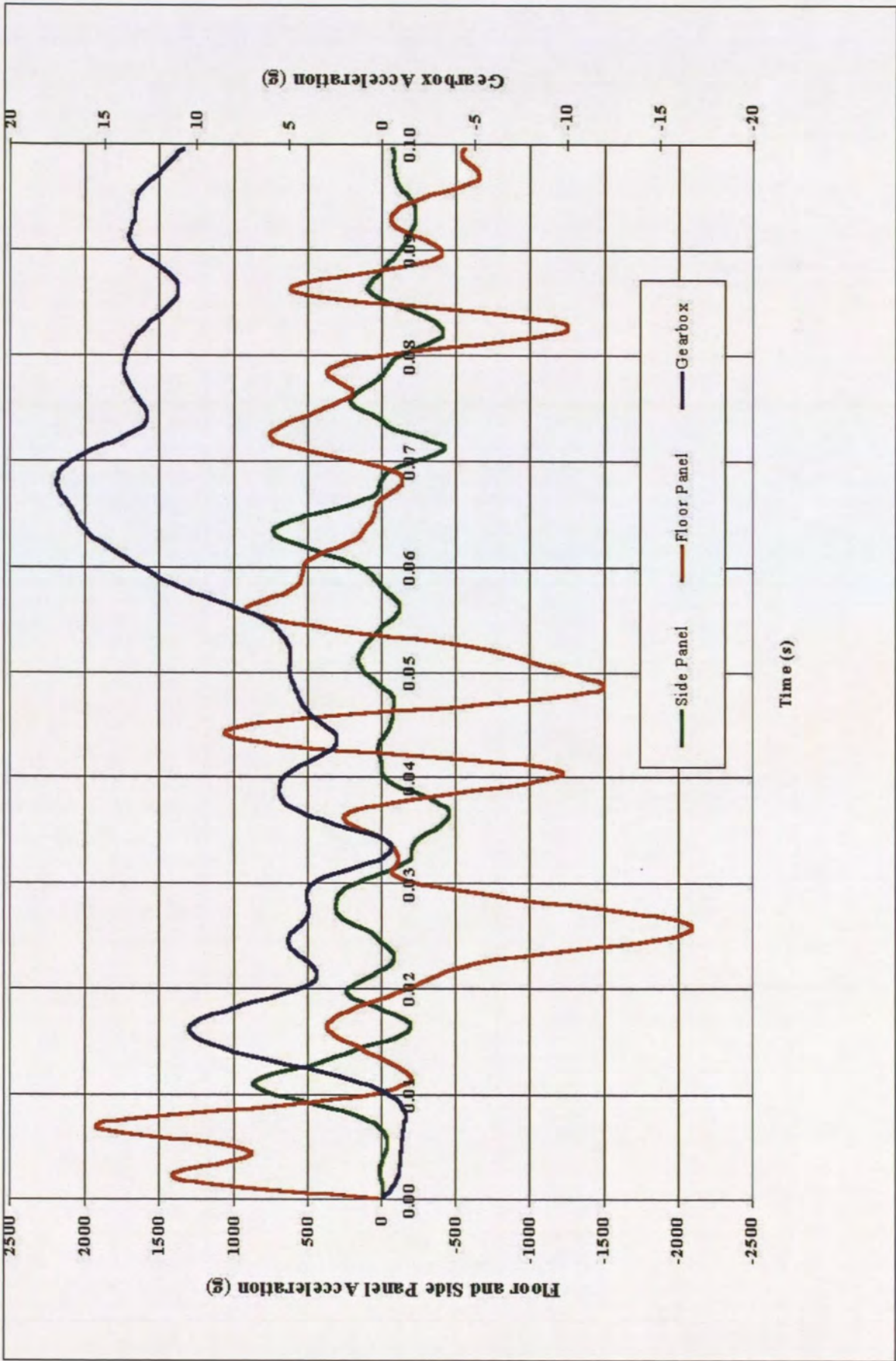


Figure 23: Filtered Vertical Acceleration for Gearbox, Floor and Side Panels

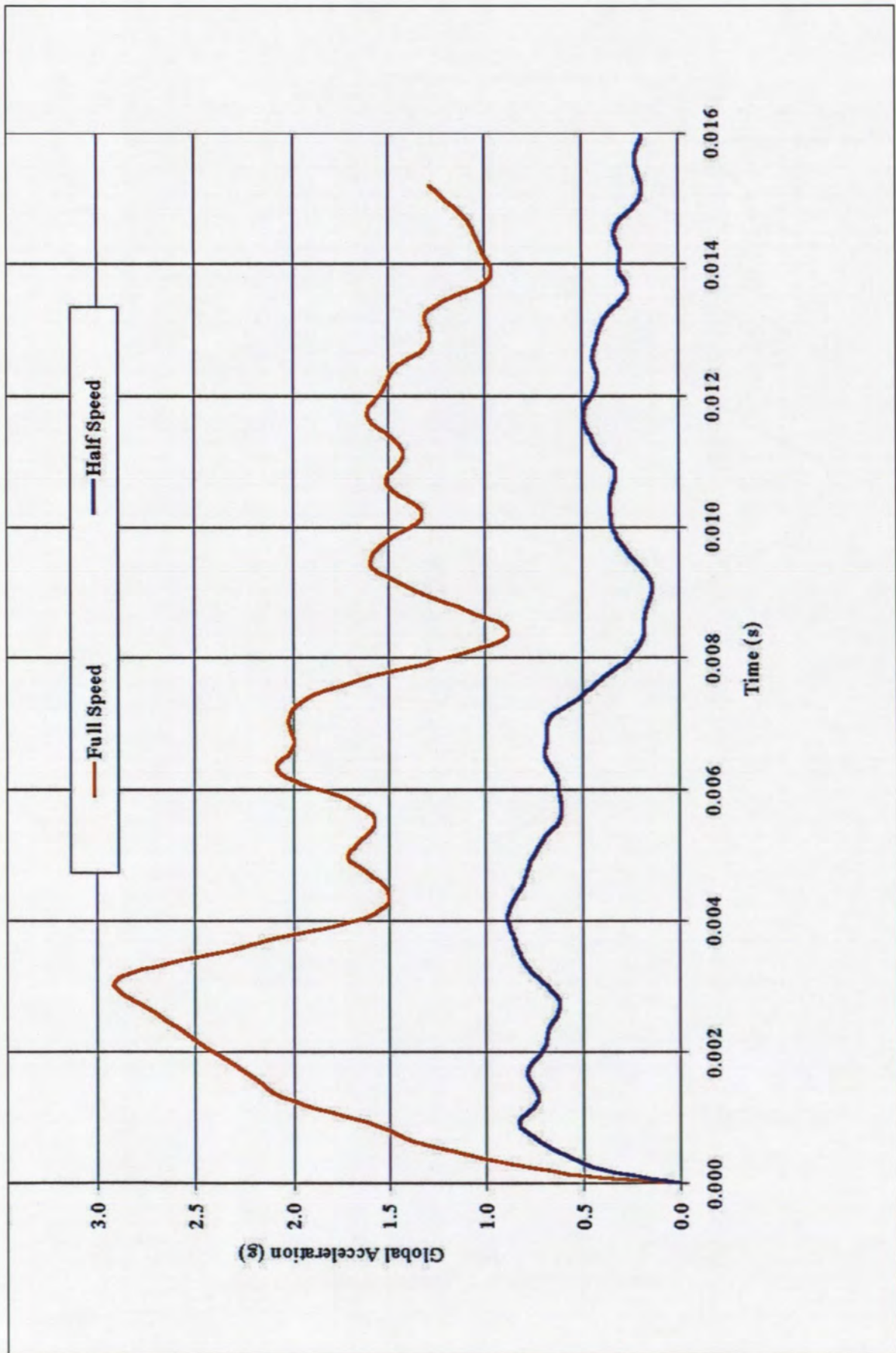


Figure 24: Cormorant Alpha – Global Acceleration at Full and Half Speed

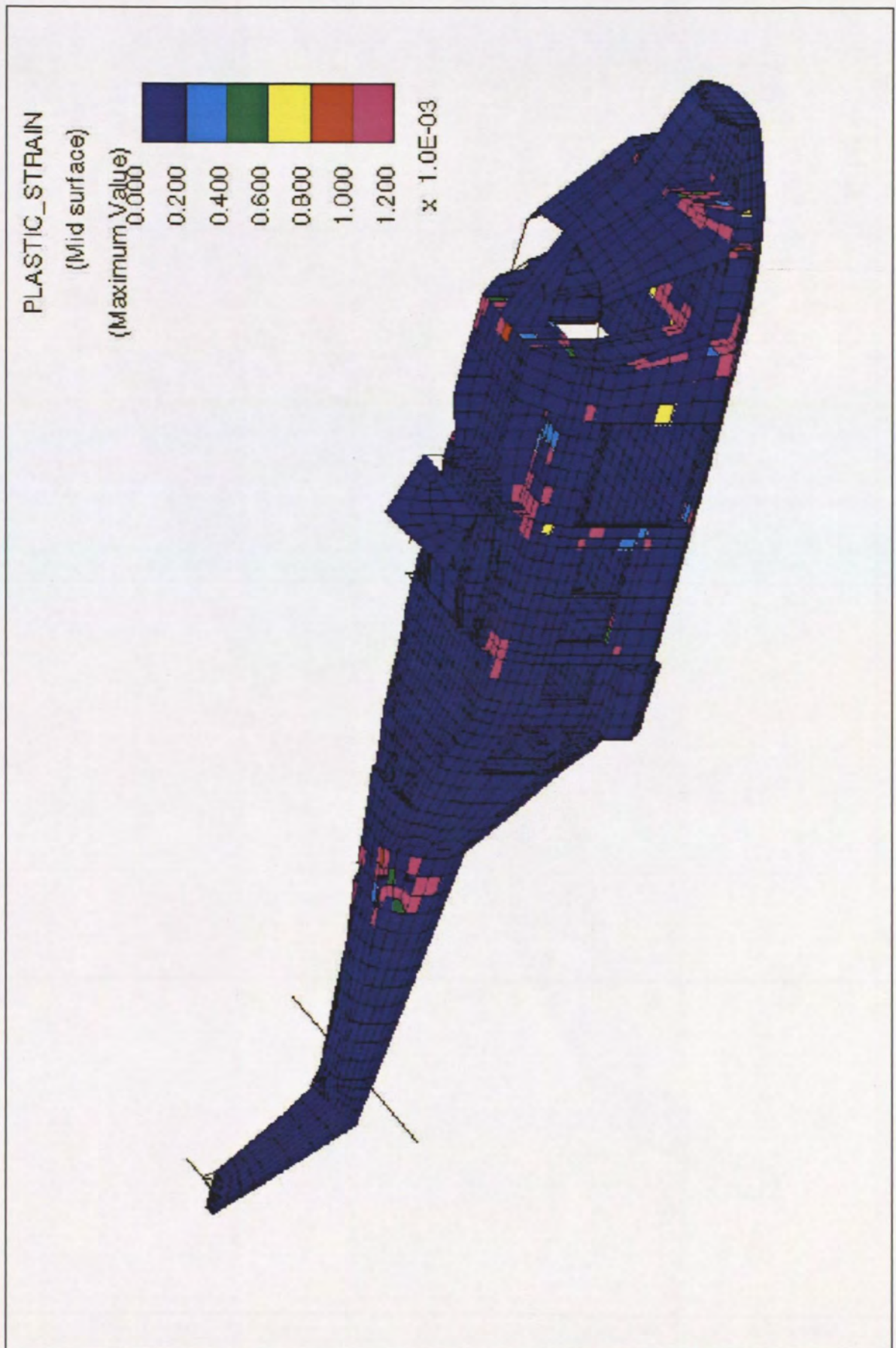


Figure 25: Cormorant Alpha – Full Speed: Maximum Plastic Strain Throughout Time Period

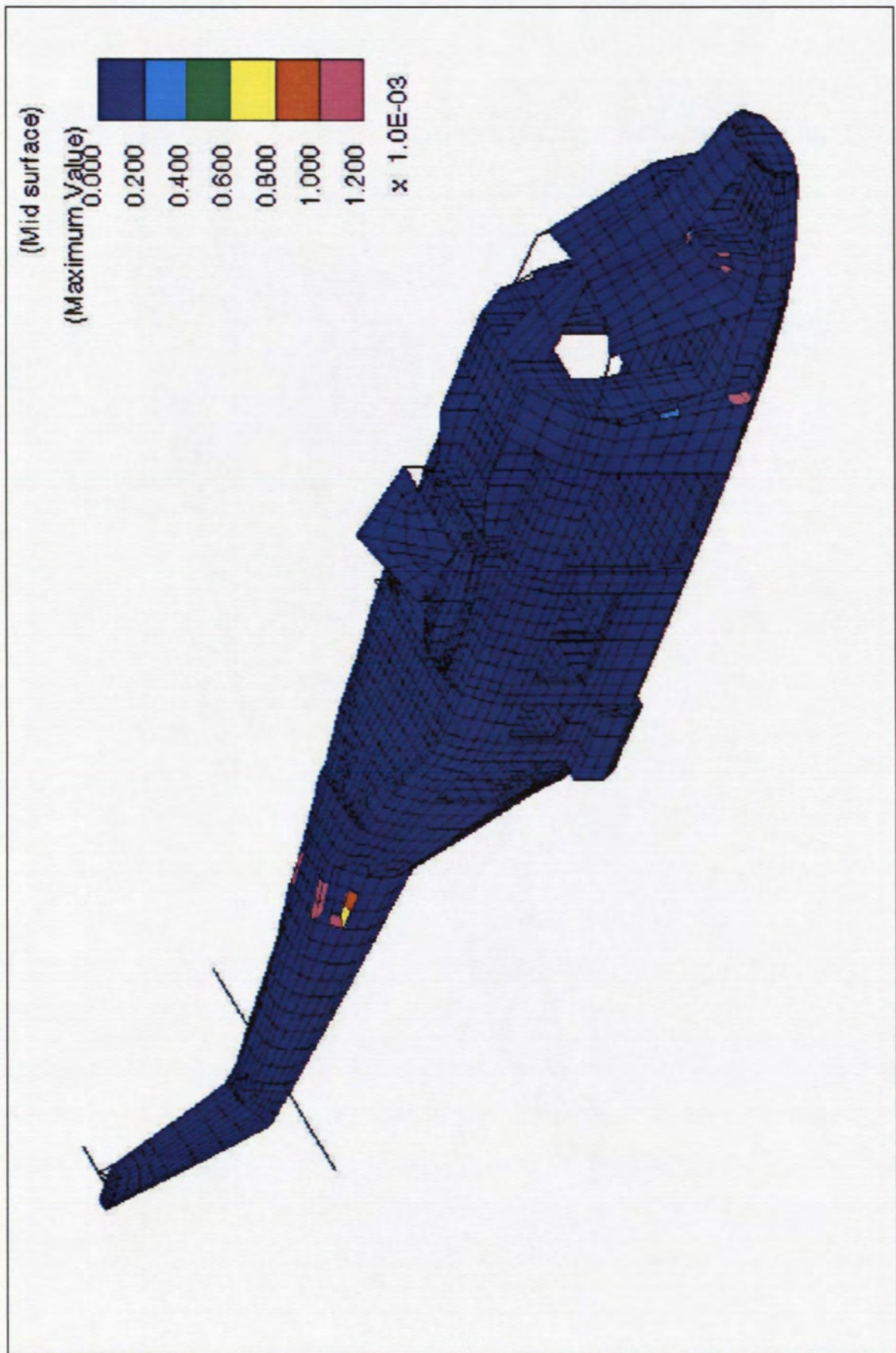


Figure 26: Cormorant Alpha – Half Speed: Maximum Plastic Strain Throughout Time Period

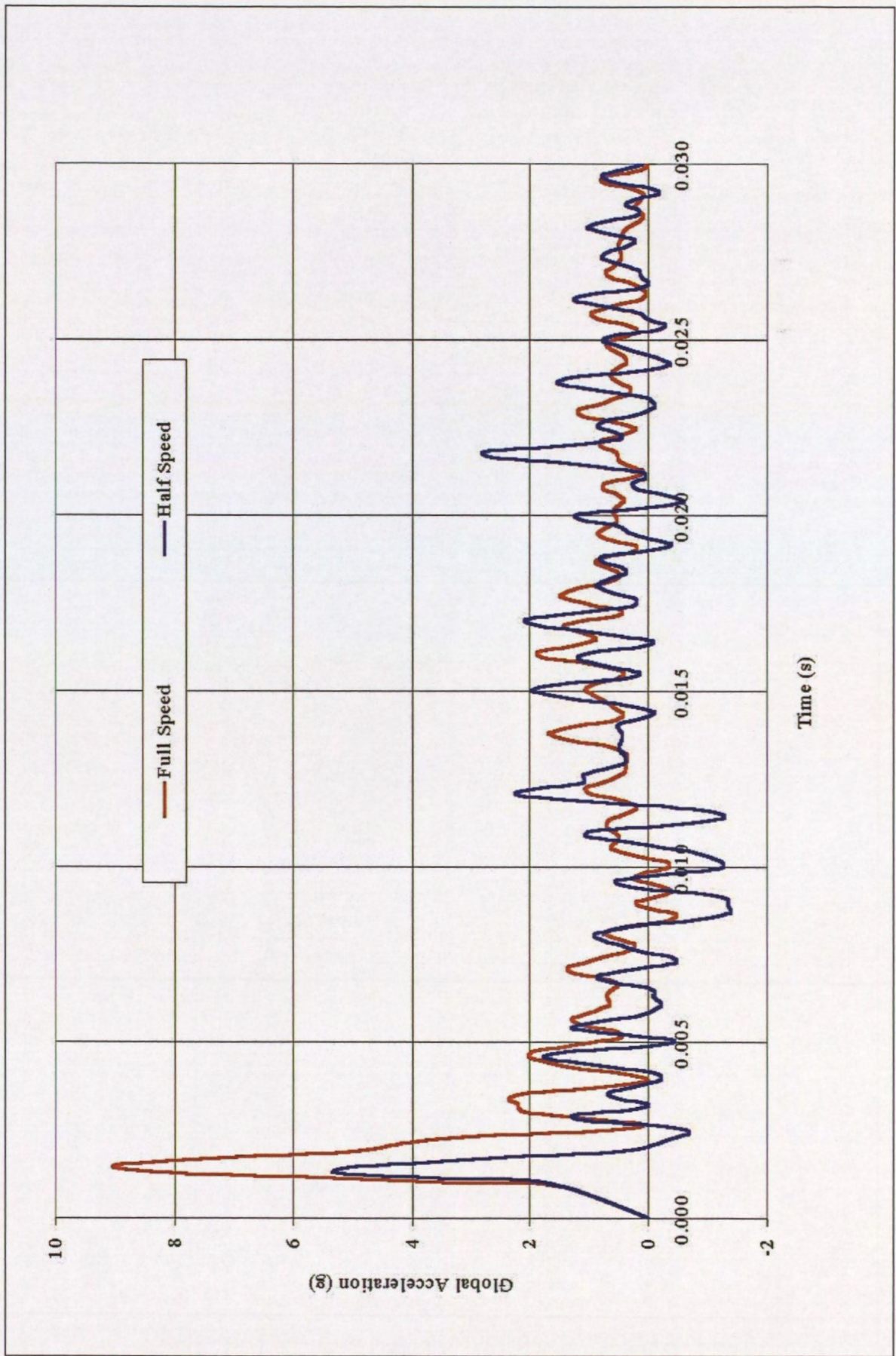


Figure 27: Isles of Scilly – Global Acceleration at Full Speed

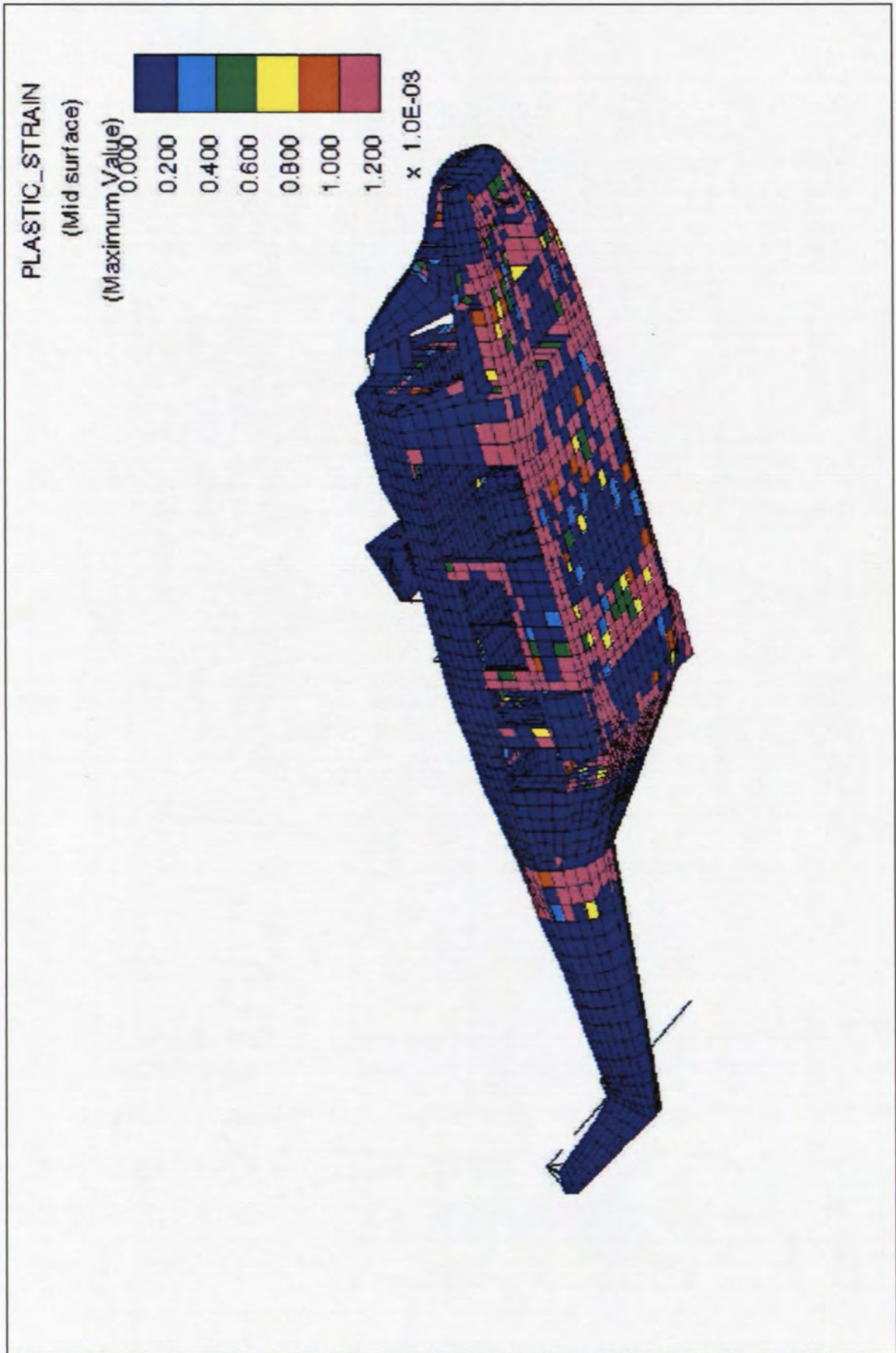


Figure 28: Isles of Scilly – Full Speed: Maximum Plastic Strain Throughout Time Period

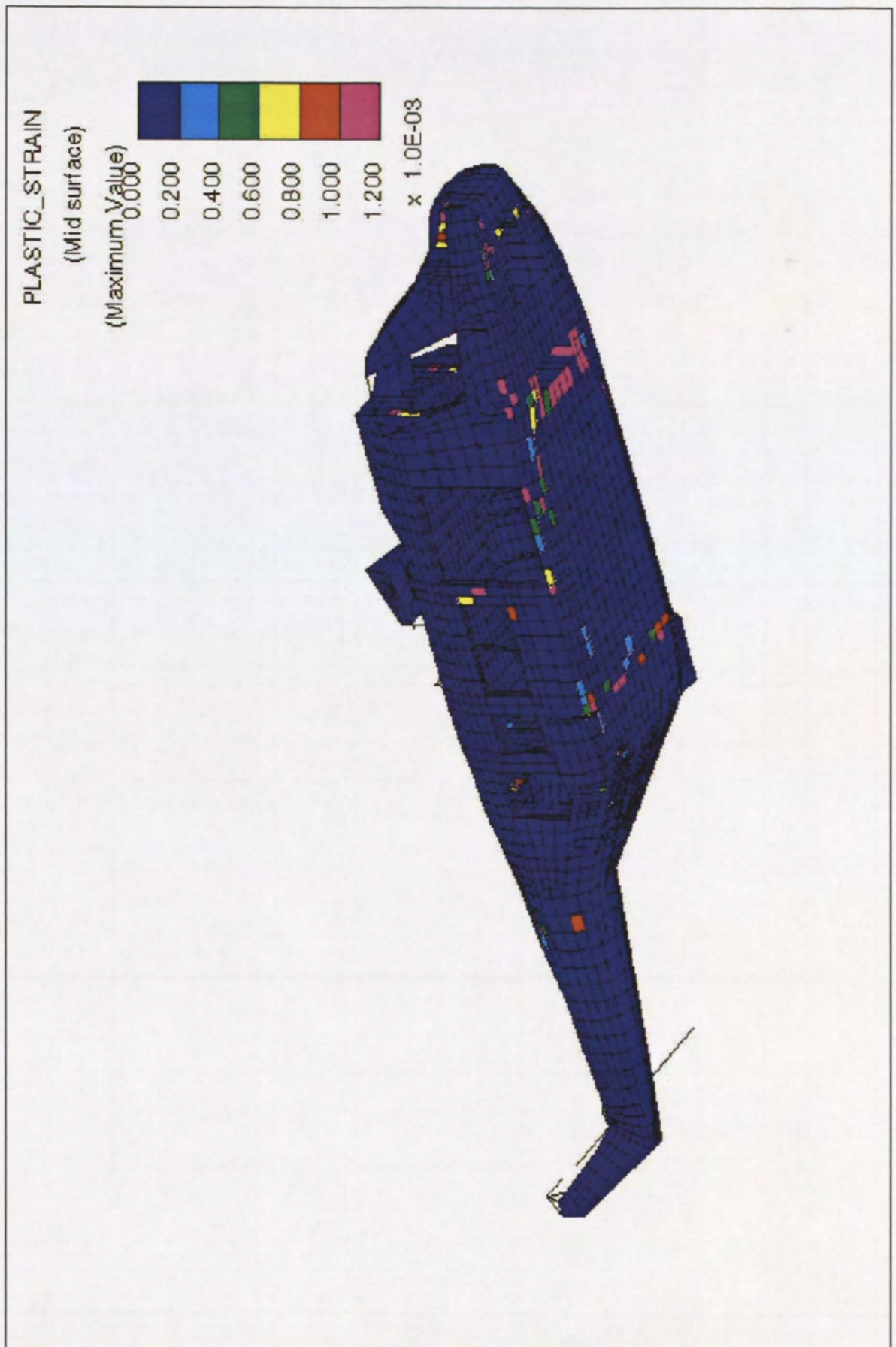


Figure 29: Isles of Scilly – Half Speed: Maximum Plastic Strain Throughout Time Period

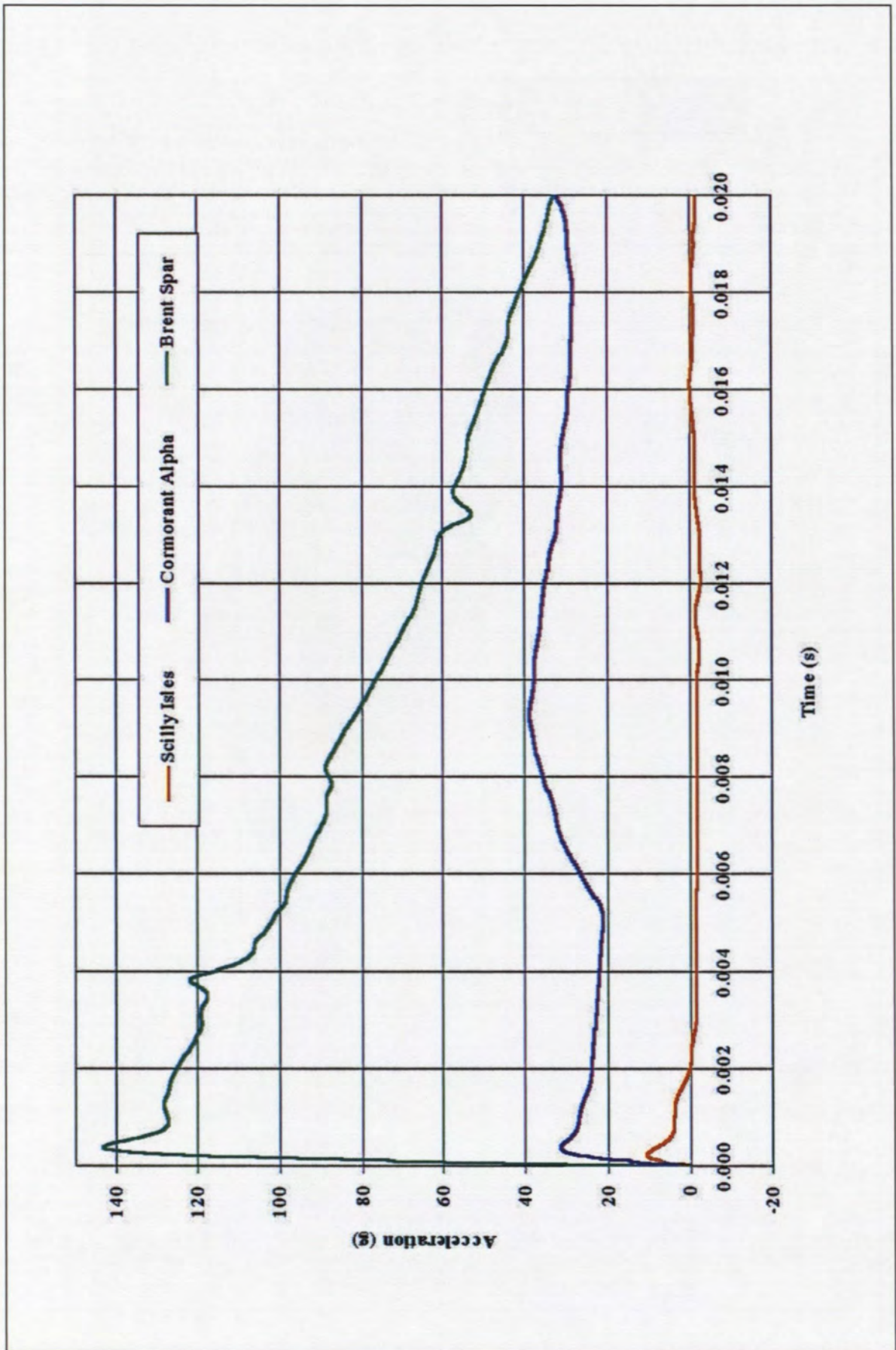


Figure 30: Global Accelerations For Full Speed Scenarios Eulerian Water Models



Figure 31: Plastic Strain for Full Speed Brent Spar Scenario Eulerian Water Model



Figure 32: Plastic Strain for Full Speed Scilly Isles Scenario Eulerian Water Model



Figure 33: Plastic Strain for Full Speed Cormorant Alpha Scenario Eulerian Water Model

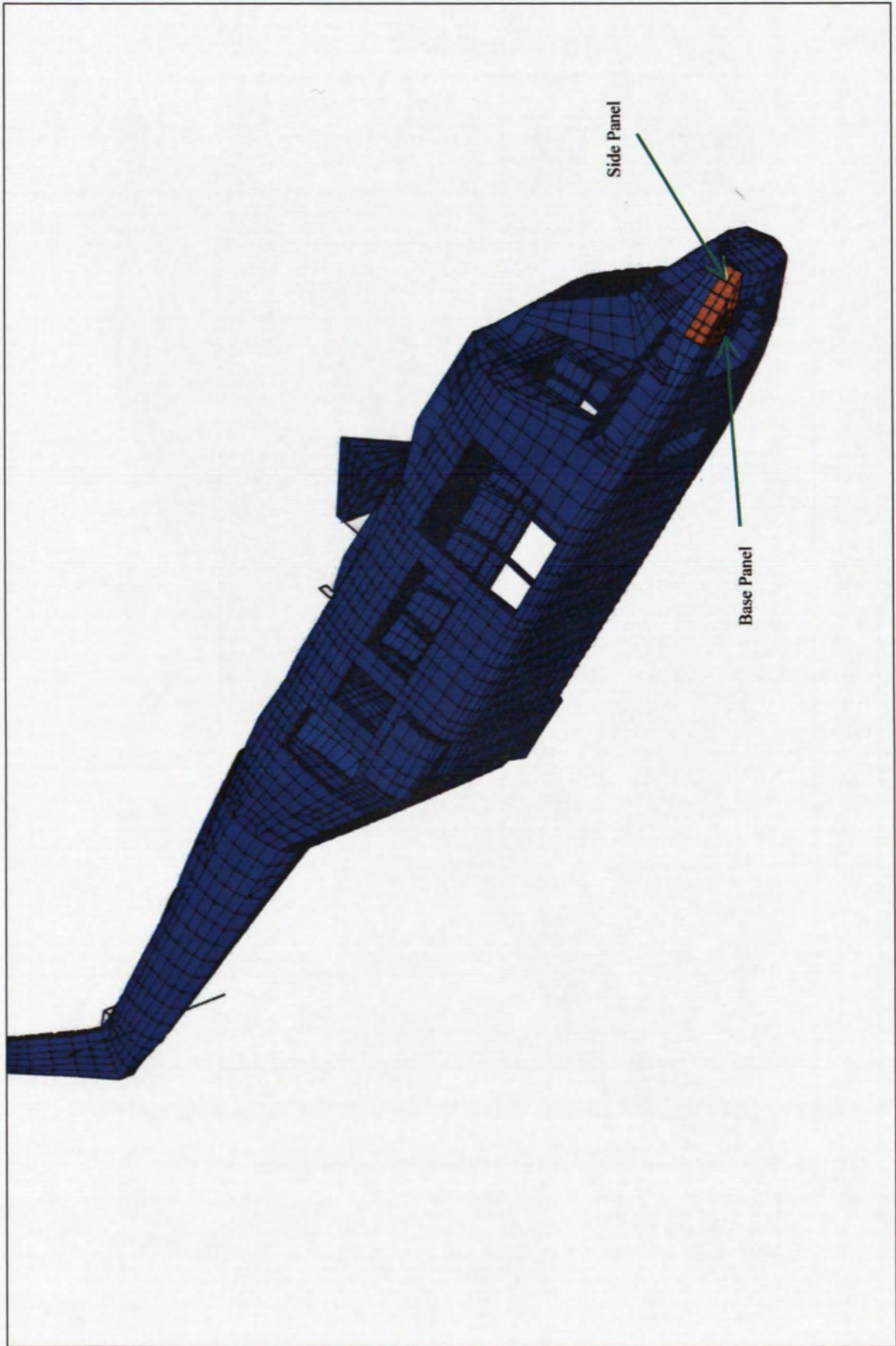


Figure 34: Location of Side Panels Under Consideration

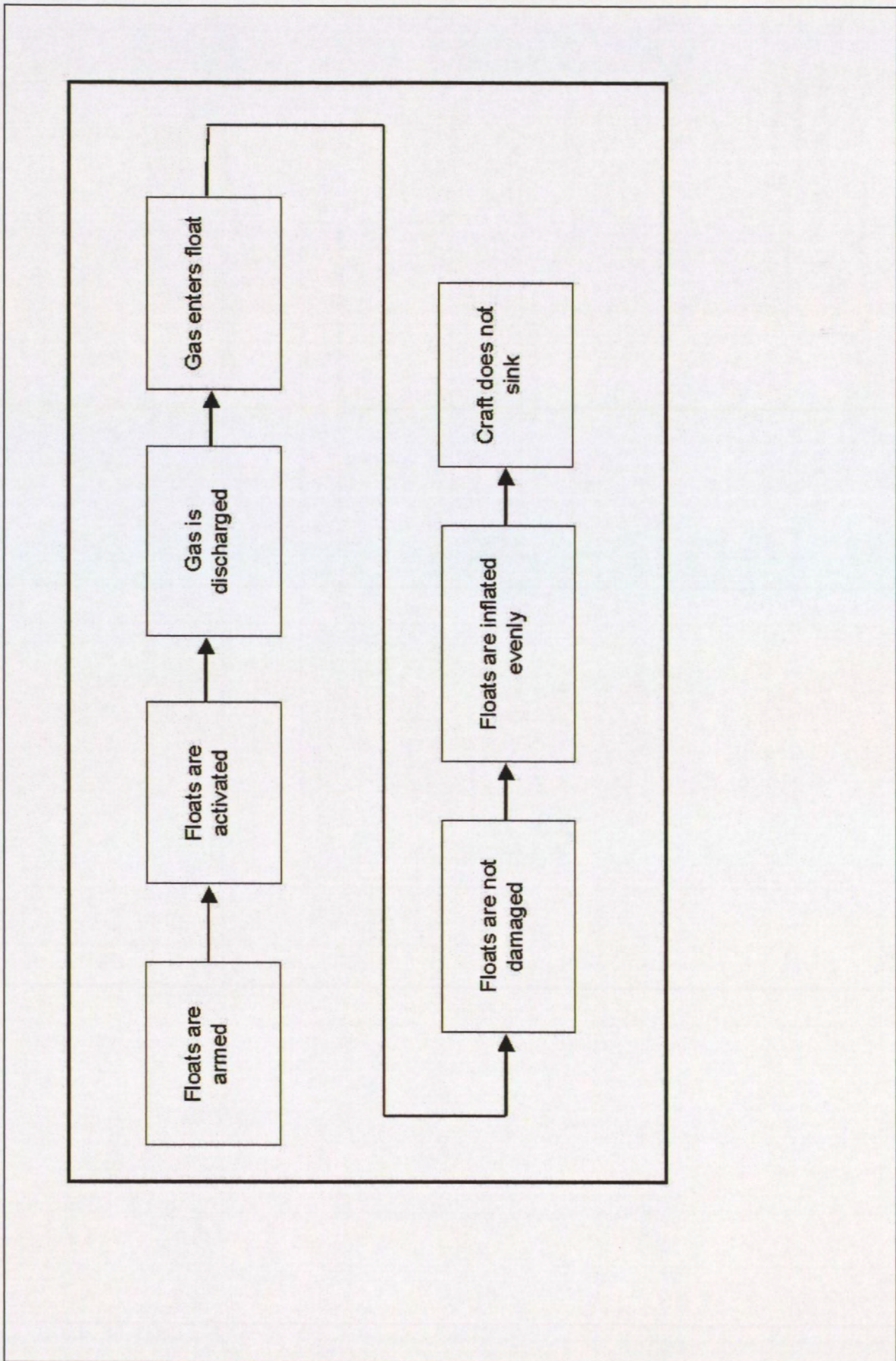


Figure 35: Sequence of Events in Successful Float Deployment

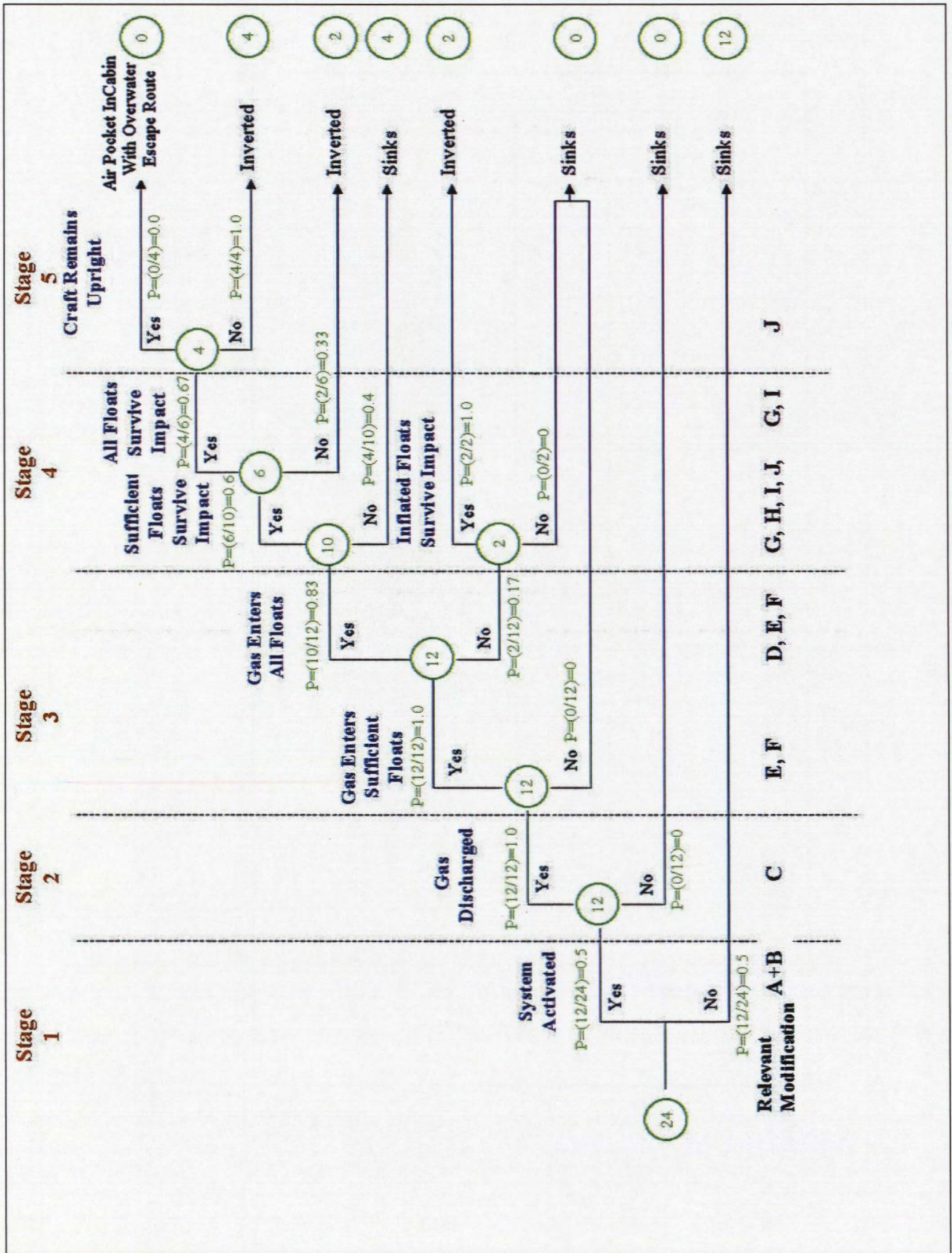


Figure 36: Probability Tree for Deployment of EFS

Appendix A Royal Navy Accident Records

The following information was gathered as a result of a visit to Royal Navy Flight Safety and Accident Investigation Centre at RNAS Yeovilton on 18/2/97. After each accident a discussion of the main accident features relevant to this study are given.

1 21/1/81 Sea King XV665 RN Report 2/81 – Gulf of Oman

- Yaw control failure.
- 4 occupants, 0 injuries.
- Nose down, 10knts forward, 0 down speed, auto rotation controlled ditching.
- Slight damage to 6 sub frames below cockpit floor and panel torn, no window breakage.
- 1 EFS bag fired, the other did not due to manual switch not fully depressed.

2 18/2/81 Sea King RN Report 3/81 – Falmouth

- Controlled ditching. Very little information found.
- 7 occupants, 4 minor injuries.

3 6/3/81 Sea King RN Report 4/81 – Oman

- Mid air collision between two Sea Kings.
- 4 occupants in one helicopter, 4 fatalities.
- No attempt at flotation heavy impact with water, considered non survivable.
- 4 occupants in other helicopter, 1 fatality, 1 minor injury.
- Impacted water from 20ft with 30knt ground speed into Sea State 4. Occupants thought it was drifting right.
- Helicopter inverted and tail broke off.
- 1 EFS bag fired. No more additional information found.

4 8/11/85 Sea King, RN Report 4/85

- Controlled descent from 40ft following failure of main rotor gearbox.
- 4 occupants, no injuries.
- EFS deployed, no record of damage.

5 22/10/86 Sea King XD632 RN Report 3/86

- Helicopter ditched after fuel starvation.
- 3 occupants, 1 minor injury.
- 20knt forward speed, nose up attitude.
- On striking the water the tail broke off and helicopter sank in 2300 fathoms, no recovery attempt made.
- It was thought that one maybe both sponsons were broken off on impact.
- Sea state 2/3, slight with 15knt wind.

6 24/2/87 Sea King, RN Report 2/87

- Sudden impact 35knots in acute nose down attitude.
- 3 occupants, 3 fatalities
- Large structural damage to fuselage, right hand sponson torn off disrupting fuselage frames. Fuselage broke up into 3 section. Forward part of lower boat hull remained attached by cables. Aft fuselage section at rear of internal floor separated. Tail cone separated aft of rear undercarriage. Rotor head and gearbox remained attached.
- No attempt at EFS, considered non-survivable due to major structural break-up.

7 16/10/87 Wessex, RN Report 4/87

- Uncontrolled descent, leading to 4.5g impact, no forward speed.
- 3 occupants, 1 injury.
- EFS deployed but helicopter inverted after 5 minutes.

8 13/10/88 Sea King, RN Report 3/88

- Heavy impact at 87knts forward speed.
- 4 occupants, 2 fatalities, 1 minor injury.
- Helicopter broke up on impact, severe damage.

9 10/9/91 Sea King ZD631, RN Report 3/91

- Controlled ditching following failure of MRGB.
- 4 occupants, no fatalities or injuries.
- EFS deployed successfully.
- Rough seas caused helicopter to sink after 20 minutes, rough weather also prevented salvage of helicopter.

10 6/11/93 Sea King ZE419, RN Report 5/93 – Islay

- 27knts backwards impact, 2.2m/s descent, nose up 12°.
- 4 occupants, 1 fatality, 1 serious (breathing gear used in escape)
- Helicopter broke into 3 sections, across the tail and at mid fuselage. 1 sponson severely damaged.
- EFS did not operate due to immediate loss of electric power (EFS on auto deploy system). Investigation held view that if it had fired it would have been ineffective.
- Sea State 3.

Appendix B Space Capsule And Orbiter Modelling Data

Weight	975 kg
Height (overall)	3.20 m
Radius of spherical bottom	3.20 m
Base diameter	2.13 m
Centre-of-Gravity location (height from bottom)	0.710 m
Moments of Inertia Pitch	731 kgm ²
Moments of Inertia Yaw	731 kgm ²

Table 1: Pertinent Physical Properties Of Space Capsule

Weight	85,464 kg
Centre-of-Gravity location (height from base)	0.378 m
Centre-of-Gravity location (length from rear)	11.09 m
Moments of Inertia Pitch	7.95x10 ⁶ kgm ²
Moments of Inertia Yaw	8.21x10 ⁶ kgm ²
Moments of Inertia Roll	1.09x10 ⁶ kgm ²

Table 2: Pertinent Physical Properties Of Space Shuttle Orbiter

Appendix C Joint Airworthiness Requirements and Advisory Material

1.1 JAR 29.561 General

(a) The rotorcraft, although it may be damaged in emergency landing conditions on land or water, must be designed as prescribed in this section to protect the occupants under those conditions.

(b) The structure must be designed to give each occupant every reasonable chance of escaping serious injury in a crash landing when -

(1) Proper use is made of seats, belts, and other safety design provisions;

(2) The wheels are retracted (where applicable); and

(3) Each occupant and each item of mass inside the cabin that could injure an occupant is restrained when subjected to the following ultimate inertial load factors relative to the surrounding structure:

(i) Upward - 4 g

(ii) Forward -16 g

(iii) Sideward - 8 g

(iv) Downward - 20 g, after the intended displacement of the seat device.

(c) The supporting structure must be designed to restrain under any ultimate inertial load factor up to those specified in this paragraph, any item of mass above and/or behind the crew and passenger compartment that could injure an occupant if it came loose in an emergency landing. Items of mass to be considered include, but are not limited to, rotors, transmission and engines. The items of mass must be restrained for the following ultimate inertial load factors:

(1) Upward - 1.5 g

(2) Forward - 8 g

(3) Sideward - 2 g

(4) Downward - 4 g

(d) Any fuselage structure in the area of internal fuel tanks below the passenger floor level must be designed to resist the following ultimate inertia factors and loads, and to protect the fuel tanks from rupture, if rupture is likely when those loads are applied to that area:

(1) Upward - 1.5 g

(2) Forward - 4.0 g

(3) Sideward - 2.0 g

(4) Downward - 4.0 g

1.2 Advisory Circular 29-2B: JAR 29.561 General

218. § 29.561 GENERAL.

a. Explanation.

(1) The occupants should be protected as prescribed from serious injury during an emergency/minor crash landing on water or land for the conditions prescribed in the standard. The standard states that each occupant should be given every reasonable chance of escaping serious injury in a minor crash landing.

(2) Section 29.561(b)(3) specifies certain ultimate inertial load factors but allows a lesser downward vertical load factor by virtue of a 5 FPS ultimate rate of descent at maximum design weight.

(3) In addition, the occupants must be protected from items of mass inside the cabin as well as outside the cabin. For example, a cabin fire extinguisher must be restrained for the load factors prescribed in this section. A transmission or engine must be restrained to the load factors in § 29.561(b)(3) if located adjacent to, above, or behind the occupants.

(4) For aircraft equipped with retractable landing gear, the landing gear must be retracted for compliance.

(5) Fuel tank protection.

(i) Underfloor fuel tanks are specifically addressed in § 29.561(d). The fuselage structure must be designed to resist crash impact loads prescribed in § 29.561(b)(3) and to also protect the fuel tank from rupture as prescribed. The landing gear must be retracted if the rotorcraft is equipped with retractable gears.

(ii) Section 29.963(b), a general rule tank design standard, also refers to § 29.561. This standard specifies that each tank and its installation must be designed or protected to retain fuel without leakage under the emergency landing conditions in § 29.561. Paragraph 454 of this AC relates to this standard.

(6) The minor crash conditions contained in § 29.561(b)(3) must also be considered in designing doors and exits (§ 29.783(d) and (g), and § 29.809(e)).

b. Procedures.

(1) The design criteria report or another similar report of the rotorcraft structural limits should contain the (ultimate) minor crash condition load factors.

(2) Section 29.785 (Paragraph 336 of this AC) concerns application of this design standard to seats (berths, litters), belts, and harnesses.

(3) The ultimate design landing and maneuvering load factors may exceed the minor crash condition load factors. The highest load factor derived must be used.

(i) For example, for light weight conditions, the ultimate maneuvering load factor may be 5.25g as specified in § 29.337.

(ii) The ultimate vertical landing load factors derived from §§ 29.471 through 29.521, whichever are appropriate for the design, may exceed the 4.0g down load factor in this section. The rotorcraft landing case design limit contact velocity must be at least 6.5 FPS (see §§ 29.473 and 29.725).

(4) As specified in § 29.561(b)(3)(iv), the downward load factor is 4.0, or a lower design load factor may be used at maximum design weight.

(i) The lower load factor relates to a rotorcraft impacting a flat, hard landing surface at 5 FPS (ultimate) vertical rate of descent. The load factor derived for each unique design is a function of the rotorcraft impact/crushing characteristics.

(ii) The 4.0 g down load factor case is related to either a fixed or retractable gear rotorcraft. This condition is not dependent on impact characteristics of the rotorcraft.

(iii) As noted in Paragraph b(3) above, the design landing load factors may exceed each of the two previous cases and would then become the prominent design (vertical load) parameter for seats, transmissions, fire extinguishers, and so forth.

(5) Items of mass such as fire extinguishers, radio equipment, liferafts, engines, and/or transmissions must be restrained for the appropriate load factors.

(6) Cargo/baggage compartments separated from the passenger compartment must be designed for load factors specified in § 29.787. The conditions in § 29.561 are excepted from that standard.

(7) Each fuel tank and its installation are subject to the loads stated in this standard whether "under floor" or located elsewhere. (See § 29.963(b) also.) Under-floor fuel tanks are specifically addressed in § 29.561(d); however, an acceptable means of compliance with CAR 7.261 which is identical to and preceded § 29.561(d) is quoted here for information.

NOTE: Fuselage keels whose design and structural strength are such as to resist crash impacts associated with the emergency landing conditions of § 7.260 (§ 29.561) without extreme distortion which might tend to rupture the fuel tank may be considered to comply with the requirements of this section (7.261).

Puncture resistant "bladder" fuel cells that are adequately designed and also protected from the stated impact loads imposed on the fuselage may also satisfy the standards.

(8) For rotorcraft with retractable landing gear, alternative landing gear positions and the resulting effects on potential fuel release should be evaluated.

218A. § 29.561 (Amendment 29-29 EMERGENCY LANDING CONDITIONS - GENERAL.

a. Explanation. Amendment 29-29 adds or increases the design static load factors of § 29.561 in three different areas:

(1) The design static load factors for the cabin in § 29.561(b)(3) are increased in concert with the dynamic test requirements of new § 29.562.

(2) Design static load factors are added in § 29.561(c) for external items of mass located above and/or behind the crew and passenger compartment.

(3) The static load factors, which were formerly only referenced in § 29.561(d), are now included explicitly in § 29.561(d) for substantiation of internal fuel tanks which are below the passenger floor.

b. Procedures. The procedures of Paragraph 218, § 29.561, continue to apply except the new load factors of § 29.561 should be used. Penetration of any items of mass into the cabin or occupied areas should be prevented.

218B. § 29.561 (Amendment 29-38) EMERGENCY LANDING CONDITIONS-GENERAL.

a. Explanation. Amendment 29-38 adds a new rearward emergency load factor of 1.5g to both §§ 29.561(b)(3)(v) and 29.561(c)(5). The addition of the 1.5g rearward load factor in § 29.561(b)(3)(v) is to provide an aft ultimate load condition for substantiation of the restraints required for retention of both occupants and significant items of mass inside the cabin that could otherwise come loose and cause injuries in an emergency landing. The addition of the 1.5g rearward load factor to § 29.561(c)(5) is to provide an aft ultimate load condition for substantiation of the support structure for retention of significant items of mass above and forward of the occupied volume(s) of the rotorcraft that could otherwise come loose and injure an occupant in an emergency landing. Amendment 29-38 also increases the forward, sideward, and downward emergency load factors of § 29.561(c)(2), (c)(3), and (c)(4), respectively, for retention of items of mass above and behind the occupied volume(s) that could otherwise come loose and injure an occupant in an emergency landing.

b. Procedures. The procedures of Paragraphs 218 and 218A continue to apply except the newly specified load factors must be used. A list of the significant items of mass to be considered should be compiled by the applicant and approved by the certifying authority.

INTENTIONALLY BLANK

2.1 JAR 29.562 Emergency Landing Dynamic Conditions

(a) The rotorcraft, although it may be damaged in a crash landing, must be designed to reasonably protect each occupant when -

- (1) The occupant properly uses the seats, safety belts, and shoulder harnesses provided in the design; and
- (2) The occupant is exposed to loads equivalent to those resulting from the conditions prescribed in this section.

(b) Each seat type design or other seating device approved for crew or passenger occupancy during take-off and landing must successfully complete dynamic tests or be demonstrated by rational analysis based on dynamic tests of a similar type seat in accordance with the following criteria. The tests must be conducted with an occupant simulated by a 77 kg (170-pound) anthropomorphic test dummy (ATD), sitting in the normal upright position.

(1) A change in downward velocity of not less than 9.1 metres per second (30ft/s) when the seat or other seating device is oriented in its nominal position with respect to the rotorcraft's reference system, the rotorcraft's longitudinal axis is canted upward 60°, with respect to the impact velocity vector, and the rotorcraft's lateral axis is perpendicular to a vertical plane containing the impact velocity vector and the rotorcraft's longitudinal axis. Peak floor deceleration must occur in not more than 0.031 seconds after impact and must reach a minimum of 30g.

(2) A change in forward velocity of not less than 12.8 metres per second (42ft/s) when the seat or other seating device is oriented in its nominal position with respect to the rotorcraft's reference system, the rotorcraft's longitudinal axis is yawed 10°, either right or left of the impact velocity vector (whichever would cause the greatest load on the shoulder harness), the rotorcraft's lateral axis is contained in a horizontal plane containing the impact velocity vector, and the rotorcraft's vertical axis is perpendicular to a horizontal plane containing the impact velocity vector. Peak floor deceleration must occur in not more than 0.071 seconds after impact and must reach a minimum of 18.4g.

(3) Where floor rails or floor or sidewall floor attachment devices are used to attach the seating devices to the airframe structure for the conditions of this section, the rails or devices must be misaligned with respect to each other by at least 10°, vertically (i.e. pitch out of parallel) and by at least a 10°, lateral roll, with the directions optional, to account for possible floor warp.

(c) Compliance with the following must be shown:

(1) The seating device system must remain intact although it may experience separation intended as part of its design.

(2) The attachment between the seating device and the airframe structure must remain intact, although the structure may have exceeded its limit load.

(3) The ATD's shoulder harness strap or straps must remain on or in the immediate vicinity of the ATD's shoulder during the impact.

(4) The safety belt must remain on the ATD's pelvis during the impact.

(5) The ATD's head either does not contact any portion of the crew or passenger compartment, or if contact is made, the head impact does not exceed a head injury criteria (HIC) of 1000 as determined by this equation.

$$HIC = (t_2 - t_1) \left[\frac{1}{(t_2 - t_1)} \int_{t_1}^{t_2} a(t) dt \right]^{2.5}$$

Where – a(t) is the resultant acceleration at the centre of gravity of the head form expressed as a multiple of g (the acceleration of gravity) and t₂–t₁ is the time duration, in seconds, of major head impact, not to exceed 0.05 seconds.

(6) Loads in individual shoulder harness straps must not exceed 794 kg (1750 pounds). If dual straps are used for retaining the upper torso, the total harness strap loads must not exceed 907 kg (2000 pounds).

(7) The maximum compressive load measured between the pelvis and the lumbar column of the ATD must not exceed 680 kg (1500 pounds).

(d) An alternate approach that achieves an equivalent or greater level of occupant protection, as required by this section, must be substantiated on a rational basis.

2.2 Advisory Circular 29-2B: JAR 29.562 Emergency Landing Dynamic Conditions

219. § 29.562 EMERGENCY LANDING DYNAMIC CONDITIONS.

a. Explanation. Amendment 29-29 adds new requirements for the dynamic testing of all seats in rotorcraft.

b. Procedures. AC 20-137, "Dynamic Evaluation of Seat Restraint Systems and Occupant Restraint for Rotorcraft (Normal and Transport)," provides procedures for complying with § 29.562 using the 170-pound anthropomorphic test dummy specified in § 29.562(b). Those seats not occupied for takeoff and landing, and so placarded and identified in the rotorcraft flight manual (RFM), may be excluded from compliance.

INTENTIONALLY BLANK

3.1 JAR 29.563 Structural ditching provisions

If certification with ditching provisions is requested, structural strength for ditching must meet the requirements of this section and JAR 29.801(e).

(a) Forward speed landing conditions. The rotorcraft must initially contact the most critical wave for reasonably probable water conditions at forward velocities from zero up to 30 knots in likely pitch, roll, and yaw attitudes. The rotorcraft limit vertical descent velocity may not be less than 1.52 metres per second (5ft/s) relative to the mean water surface. Rotor lift may be used to act through the centre of gravity throughout the landing impact. This lift may not exceed two-thirds of the design maximum weight. A maximum forward velocity of less than 30 knots may be used in design if it can be demonstrated that the forward velocity selected would not be exceeded in a normal one-engine-out touchdown.

(b) Auxiliary or emergency float conditions

(1) Floats fixed or deployed before initial water contact. In addition to the landing loads in sub-paragraph (a) of this paragraph, each auxiliary or emergency float, or its support and attaching structure in the airframe or fuselage, must be designed for the load developed by a fully immersed float unless it can be shown that full immersion is unlikely. If full immersion is unlikely, the highest likely float buoyancy load must be applied. The highest likely buoyancy load must include consideration of a partially immersed float creating restoring moments to compensate the upsetting moments caused by side wind, unsymmetrical rotorcraft loading, water wave action, rotorcraft inertia, and probable structural damage and leakage considered under JAR 29.801 (d). Maximum roll and pitch angles determined from compliance with JAR 29.801 (d) may be used, if significant, to determine the extent of immersion of each float. If the floats are deployed in flight, appropriate air loads derived from the flight limitations with the floats deployed shall be used in substantiation of the floats and their attachment to the rotorcraft. For this purpose, the design airspeed for limit load is the float deployed airspeed operating limit multiplied by 1.11.

(2) Floats deployed after initial water contact. Each float must be designed for full or partial immersion prescribed in sub-paragraph (b)(1) of this paragraph. In addition, each float must be designed for combined vertical and drag loads using a relative limit speed of 20 knots between the rotorcraft and the water. The vertical load may not be less than the highest likely buoyancy load determined under paragraph (b) (1) of this paragraph.

3.2 Advisory Circular 29-2B: JAR 29.563 Structural Ditching Provisions

220. § 29.563 (Amendment 29-12) STRUCTURAL DITCHING PROVISIONS.

a. Explanation. Amendment 29-12 included certification requirements for ditching approvals. The rotorcraft must be able to sustain an emergency landing in water as prescribed by § 29.801(e).

b. Procedures. Refer to Paragraph 337, § 29.801, for procedures.

220A. § 29.563 (Amendment 29-30) STRUCTURAL DITCHING PROVISIONS.

a. Explanation. Amendment 29-30 added specific structural conditions to be considered to support the overall ditching requirements of § 29.801. These conditions are to be applied to rotorcraft for which over-water operations and associated ditching approvals are requested.

(1) The forward speed landing conditions are specified as:

(i) The rotorcraft should contact the most critical wave for reasonable, probable water conditions in the likely pitch, roll, and yaw attitudes.

(ii) The forward velocity relative to wave surface should be in a range of 0 to 30 knots with a vertical descent rate of not less than 5 FPS relative to the mean water surface.

NOTE: A forward velocity of less than 30 knots may be used for multiengine rotorcraft if it can be demonstrated that the forward velocity selected would not be exceeded in a normal one-engine-out touchdown.

(iii) Rotor lift of not more than two-thirds of the design maximum weight may be used to act through the CG throughout the landing impact.

(2) For floats fixed or deployed before water contact, the auxiliary or emergency float conditions are specified in § 29.563(b)(i). Loads for a fully immersed float should be applied (unless it is shown that full immersion is unlikely). If full immersion is unlikely, loads resulting from restoring moments are specified for sidewind and unsymmetrical rotorcraft landing.

(3) Floats deployed after water contact are normally considered fully immersed during and after full inflation. An exception would be when the inflation interval is long enough that full immersion of the inflated floats does not occur; e.g., deceleration of the rotorcraft during water impact and natural buoyancy of the hull prevent full immersion loads on the fully inflated floats.

b. Procedures.

(1) The rotorcraft support structure, structure-float attachments, and floats should be substantiated for rational limit and ultimate ditching loads.

(2) The most severe wave heights for which approval is desired are to be considered. A minimum of Sea State 4 condition wave heights should be considered (reference Paragraph 337 (§ 29.801) of this AC for a description of Sea State 4 conditions).

(3) The landing structural design consideration should be based on water impact with a rotor lift of not more than two-thirds of the maximum design weight acting through the center of gravity under the following conditions:

(i) Forward velocities of 0 to 30 knots (or a reduced maximum forward velocity if it can be demonstrated that a lower maximum velocity would not be exceeded in a normal one-engine-out landing).

(ii) The rotorcraft pitch attitude that would reasonably be expected to occur in service. Autorotation flight tests or one-engine-inoperative flight tests, as applicable, should be used to confirm the attitude selected. This information should be included in the Type Inspection Report.

(iii) Likely roll and yaw attitudes.

(iv) Vertical descent velocity of 5 FPS or greater.

(4) Landing load factors and water load distribution may be determined by water drop tests or analysis based on tests.

(5) Auxiliary or emergency float loads should be determined by full immersion or the use of restoring moments required to react upsetting moments caused by sidewind, asymmetrical rotorcraft landing, water wave action, rotorcraft inertia, and probable structure damage and punctures considered under § 29.801. Auxiliary or emergency float loads may be determined by tests or analysis based on tests.

(6) Floats deployed after initial water contact are required to be substantiated by tests or analysis for the specified immersion loads (same as for (5) above and for the specified combined vertical and drag loads).

4.1 JAR 29.801 Ditching

- (a) If certification with ditching provisions is requested, the rotorcraft must meet the requirements of this paragraph and JAR 29.807 (d), 29.1411 and 29.1415.
- (b) Each practicable design measure, compatible with the general characteristics of the rotorcraft, must be taken to minimise the probability that in an emergency landing on water, the behaviour of the rotorcraft would cause immediate injury to the occupants or would make it impossible for them to escape.
- (c) The probable behaviour of the rotorcraft in a water landing must be investigated by model tests or by comparison with rotorcraft of similar configuration for which the ditching characteristics are known. Scoops, flaps, projections, and any other factors likely to affect the hydrodynamic characteristics of the rotorcraft must be considered.
- (d) It must be shown that, under reasonably probable water conditions, the flotation time and trim of the rotorcraft will allow the occupants to leave the rotorcraft and enter the life rafts required by JAR 29.1415. If compliance with this provision is shown by buoyancy and trim computations, appropriate allowances must be made for probable structural damage and leakage. If the rotorcraft has fuel tanks (with fuel jettisoning provisions) that can reasonably be expected to withstand a ditching without leakage, the jettisonable volume of fuel may be considered as buoyancy volume.
- (e) Unless the effects of the collapse of external doors and windows are accounted for in the investigation of the probable behaviour of the rotorcraft in a water landing (as prescribed in sub-paragraphs (c) and (d) of this paragraph), the external doors and windows must be designed to withstand the probable maximum local pressures.

4.2 Advisory Circular 29-2B: JAR 29.801 Ditching

337. § 29.801 (Amendment 29-12) DITCHING.

a. Explanation.

- (1) Ditching certification is accomplished only if requested by the applicant.
- (2) Ditching may be defined as an emergency landing on the water, deliberately executed, with the intent of abandoning the rotorcraft as soon as practical. The rotorcraft is assumed to be intact prior to water entry with all controls and essential systems, except engines, functioning properly.
- (3) The regulation requires demonstration of the flotation and trim requirements under "reasonably probable water conditions." The FAA/AUTHORITY has determined that a sea state 4 is representative of reasonably probable water conditions to be encountered. Therefore, demonstration of compliance with the ditching requirements for at least sea state 4 water conditions is considered to satisfy the reasonably probable requirement.
- (4) A sea state 4 is defined as a moderate sea with significant wave heights of 4 to 8 feet with a height-to-length ratio of:
- (i) 1:12.5 for Category A rotorcraft.
 - (ii) 1:10 for Category B rotorcraft with Category A engine isolation.
 - (iii) 1:8 for Category B rotorcraft.
- The source of the sea state definition is the World Meteorological Organization (WMO) Table. (See Table 337-1).
- (5) Ditching certification encompasses four primary areas of concern: rotorcraft water entry, rotorcraft flotation and trim, occupant egress, and occupant survival.

(6) The rule requires that after ditching in reasonably probable water conditions, the flotation time and trim of the rotorcraft will allow the occupants to leave the rotorcraft and enter liferafts. This means that the rotorcraft should remain sufficiently upright and in adequate trim to permit safe and orderly evacuation of all personnel.

(7) For a rotorcraft to be certified for ditching, emergency exits must be provided which will meet the requirements of § 29.807(d).

(8) The safety and ditching equipment requirements are addressed in §§ 29.1411, 29.1415, and 29.1561 and specified in the operating rules (Parts 91, 121, 127, and 135). As used in § 29.1415, the term ditching equipment would more properly be described as occupant water survival equipment. Ditching equipment is required for extended overwater operations (more than 50 nautical miles from the nearest shoreline and more than 50 nautical miles from an offshore heliport structure). However, ditching certification should be accomplished with the maximum required quantity of ditching equipment regardless of possible operational use.

(9) Current practices allow wide latitude in the design of cabin interiors and consequently, the stowage provisions for safety and ditching equipment. Rotorcraft manufacturers may deliver aircraft with unfinished (green) interiors that are to be completed by the purchaser or modifier. These various "configurations" present problems for certifying the rotorcraft for ditching.

(i) In the past, "segmented" certification has been permitted to accommodate this practice. That is, the rotorcraft manufacturer shows compliance with the flotation time, trim, and emergency exit requirements while the purchaser or modifier shows compliance with the equipment provisions and egress requirements with the completed interior. This procedure requires close cooperation and coordination between the manufacturer, purchaser or modifier, and the FAA/AUTHORITY.

(ii) The rotorcraft manufacturer may elect to establish a "token" interior for ditching certification. This interior may subsequently be modified by a supplemental type certificate or a field approval. Compliance with the ditching requirements should be reviewed after any interior configuration and limitations changes where applicable.

(iii) The Rotorcraft Flight Manual and supplements deserve special attention if a "segmented" certification procedure is pursued.

b. Procedures. The following guidance criteria has been derived from past FAA/AUTHORITY certification policy and experience. Demonstration of compliance to other criteria may produce acceptable results if adequately justified by rational analysis. Model tests of the appropriate ditching configuration may be conducted to demonstrate satisfactory water entry and flotation and trim characteristics where satisfactory correlation between model testing and flight testing has been established. Model tests and other data from rotorcraft of similar configurations may be used to satisfy the ditching requirements where appropriate.

(1) Water entry.

(i) Tests should be conducted to establish procedures and techniques to be used for water entry. These tests should include determination of optimum pitch attitude and forward velocity for ditching in a calm sea as well as entry procedures for the highest sea state to be demonstrated (e.g., the recommended part of the wave on which to land). Procedures for all engines operating, one engine inoperative, and all engines inoperative conditions should be established. However, only the procedures for the most critical condition (usually all engines inoperative) need to be verified by water entry tests.

(ii) The ditching structural design consideration should be based on water impact with a rotor lift of not more than two-thirds of the maximum design weight acting through the center of gravity under the following conditions:

(A) For entry into a calm sea –

(1) The optimum pitch attitude as determined in 337(b)(1)(i) with consideration for pitch attitude variations that would reasonably be expected to occur in service;

(2) Forward speeds from zero up to the speed defining the knee of the height-velocity (HV) diagram;

(3) Vertical descent velocity of 5 feet per second; and

(4) Yaw attitudes up to 15°.

(B) For entry into the maximum demonstrated sea state –

(1) The optimum pitch attitude and entry procedure as established in (b)(1)(i);

(2) The forward speed defined by the knee of the HV diagram reduced by the wind speed associated with each applicable sea state;

(3) Vertical descent velocity of 5 feet per second; and

(4) Yaw attitudes up to 15°.

(C) The float system attachment hardware should be shown to be structurally adequate to withstand water loads during water entry when both deflated and stowed and fully inflated (unless in-flight inflation is prohibited). Water entry conditions should correspond to those established in Paragraphs 337(b)(1)(ii)(A) and (B). The appropriate vertical loads and drag loads determined from water entry conditions (or as limited by flight manual procedures) should be addressed. The effects of the vertical loads and the drag loads may be considered separately for the analysis.

(D) Probable damage due to water impact to the airframe/hull should be considered during the water entry evaluations; i.e., failure of windows, doors, skins, panels, etc.

(2) Flotation Systems.

(i) Normally inflated. Fixed flotation systems intended for emergency ditching use only and not for amphibian or limited amphibian duty should be evaluated for:

(A) Structural integrity when subjected to:

(1) Air loads throughout the approved flight envelope with floats installed;

(2) Water loads during water entry; and

(3) Water loads after water entry at speeds likely to be experienced after water impact.

(B) Rotorcraft handling qualities throughout the approved flight envelope with floats installed.

(ii) Normally deflated. Emergency flotation systems which are normally stowed in a deflated condition and inflated either in flight or after water contact during an emergency ditching should be evaluated for:

(A) Inflation. The float activation means may be either fully automatic or manual with a means to verify primary actuation system integrity prior to each flight. If manually inflated, the float activation switch should be on one of the primary flight controls and should be safeguarded against spontaneous or inadvertent actuation for all flight conditions.

(1) The inflation system design should minimize the probability of the floats not inflating properly or inflating asymmetrically. This may be accomplished by use of a single inflation agent container or multiple container system interconnected together. Redundant inflation activation systems will also normally be required. If the primary actuation system is electrical, a mechanical backup actuation system will usually provide the necessary reliability. A Secondary electrical actuation system may also be acceptable if adequate electrical system independence and reliability can be documented.

(2) The inflation system should be safeguarded against spontaneous or inadvertent actuation for all flight conditions. It should be demonstrated that float inflation at any flight condition within the approved operating envelope will not result in a hazardous condition unless the safeguarding system is shown to be extremely reliable. One safeguarding method that has been successfully used on previous certification programs is to provide a separate float system arming circuit which must be activated before inflation can be initiated.

(3) The maximum airspeeds for intentional in-flight actuation of the float system and for flight with the floats inflated should be established as limitations in the RFM unless in-flight actuation is prohibited by the RFM.

(4) The inflation time from actuation to neutral buoyancy should be short enough to prevent the rotorcraft from becoming more than partially submerged assuming actuation upon water contact.

(5) A means should be provided for checking the pressure of the gas storage cylinders prior to takeoff. A table of acceptable gas cylinder pressure variation with ambient temperature and altitude (if applicable) should be provided.

(6) A means should be provided to minimize the possibility of overinflation of the float bags under any reasonably probable actuation conditions.

(7) The ability of the floats to inflate without puncture when subjected to actual water pressures should be substantiated. A full-scale rotorcraft immersion demonstration in a calm body of water is one acceptable method of substantiation. Other methods of substantiation may be acceptable depending upon the particular design of the flotation system.

(B) Structural Integrity. The flotation bags should be evaluated for loads resulting from:

(1) Airloads during inflation and fully inflated for the most critical flight conditions and water loads with fully inflated floats during water impact for the water entry conditions established under Paragraph 337(b)(1)(ii) for rotorcraft desiring float deployment before water entry; or

(2) Water loads during inflation after water entry.

(C) Handling Qualities. Rotorcraft handling qualities should be verified to comply with the applicable regulations throughout the approved operating envelopes for:

(1) The deflated and stowed condition;

(2) The fully inflated condition; and

(3) The in-flight inflation condition.

(3) Flotation and Trim. The flotation and trim characteristics should be investigated for a range of sea states from zero to the maximum selected by the applicant and should be satisfactory in waves having height/length ratios of 1:12.5 for Category A rotorcraft, 1:10 for Category B rotorcraft with Category A engine isolation, and 1:8 for Category B rotorcraft.

(i) Flotation and trim characteristics should be demonstrated to be satisfactory to at least sea state 4 conditions.

(ii) Flotation tests should be investigated at the most critical rotorcraft loading condition.

(iii) Flotation time and trim requirements should be evaluated with a simulated, ruptured deflation of the most critical float compartment. Flotation characteristics should be satisfactory in this degraded mode to at least sea state 2 conditions.

(iv) A sea anchor or similar device should not be used when demonstrating compliance with the flotation and trim requirements but may be used to assist in the deployment of liferafts. If the basic flotation system has demonstrated compliance with the

minimum flotation and trim requirements, credit for a sea anchor or similar device to achieve stability in more severe water conditions (sea state, etc.) may be allowed if the device can be automatically, remotely, or easily deployed by the minimum flightcrew.

(v) Probable rotorcraft door/window open or closed configurations and probable damage to the airframe/hull (i.e. failure of doors, windows, skin, etc.) should be considered when demonstrating compliance with the flotation and trim requirements.

(4) Float System Reliability. Reliability should be considered in the basic design to assure approximately equal inflation of the floats to preclude excessive yaw, roll, or pitch in flight or in the water.

(i) Maintenance procedures should not degrade the flotation system (e.g., introducing contaminants which could affect normal operation, etc.).

(ii) The flotation system design should preclude inadvertent damage due to normal personnel traffic flow and excessive wear and tear. Protection covers should be evaluated for function and reliability.

(5) Occupant Egress and Survival. The ability of the occupants to deploy liferafts, egress the rotorcraft, and board the liferafts should be evaluated. For configurations which are considered to have critical occupant egress capabilities due to liferaft locations and/or ditching emergency exit locations and floats proximity, an actual demonstration of egress may be required. When a demonstration is required, it may be conducted on a full-scale rotorcraft actually immersed in a calm body of water or using any other rig/ground test facility shown to be representative. The demonstration should show that floats do not impede a satisfactory evacuation.

(6) Rotorcraft Flight Manual. The Rotorcraft Flight Manual is an important element in the approval cycle of the rotorcraft for ditching. The material related to ditching may be presented in the form of a supplement or a revision to the basic manual. This material should include:

(i) The information pertinent to the limitations applicable to the ditching approval. If the ditching approval is obtained in a segmented fashion (i.e., one applicant performing the aircraft equipment installation and operations portion and another designing and substantiating the liferaft/lifevest and ditching safety equipment installations and deployment facilities), the RFM limitations should state "Not Approved for Ditching" until all segments are completed. The requirements for a complete ditching approval not yet completed should be identified in the "Limitations" section.

(ii) Procedures and limitations for flotation device inflation.

(iii) Recommended rotorcraft water entry attitude, speed, and wave position.

(iv) Procedures for use of emergency ditching equipment.

(v) Ditching egress and raft entry procedures.

TABLE 337-1
SEA STATE CODE
(WORLD METEOROLOGICAL ORGANIZATION)

Sea State Code	Description of Sea	Significant Wave Height		Wind Speed
		Meters	Feet	Knots
0	Calm (Glassy)	0	0	0-3
1	Calm (Rippled)	0 to 0.1	0 to 1/3	4-6
2	Smooth (Wavelets)	0.1 to 0.5	1/3 to 1 2/3	7-10
3	Slight	0.5 to 1.25	1 2/3 to 4	11-16
4	Moderate	1.25 to 2.5	4 to 8	17-21
5	Rough	2.5 to 4	8 to 13	22-29
6	Very Rough	4 to 6	13 to 20	28-47
7	High	6 to 9	20 to 30	48-55
8	Very High	9 to 14	30 to 45	56-63
9	Phenomenal	Over 14	Over 45	64-118

INTENTIONALLY BLANK

5.1 JAR 29.807 Passenger Emergency Exits

(a) Type. For the purpose of this Part, the types of passenger emergency exit are as follows:

(1) Type I. This type must have a rectangular opening of not less than 609.6 mm wide by 1.219 m (24 inches wide by 48 inches) high, with corner radii not greater than one-third the width of the exit, in the passenger area in the side of the fuselage at floor level and as far away as practicable from areas that might become potential fire hazards in a crash.

(2) Type II. This type is the same as Type I, except that the opening must be at least 508 mm wide by 1.12 m (20 inches wide by 44 inches) high.

(3) Type III. This type is the same as Type I, except that -

(i) The opening must be at least 508 mm wide by 914.4 mm (20 inches wide by 36 inches) high; and

(ii) The exits need not be at floor level.

(4) Type IV. This type must have a rectangular opening of not less than 482.6 mm wide by 660.4 mm (19 inches wide by 26 inches) high, with corner radii not greater than one-third the width of the exit, in the side of the fuselage with a step-up inside the rotorcraft of not more than 736.6 mm (29 inches). Openings with dimensions larger than those specified in this section may be used, regardless of shape, if the base of the opening has a flat surface of not less than the specified width.

(b) Passenger emergency exits: side-of-fuselage. Emergency exits must be accessible to the passengers and, except as provided in sub-paragraph (d) of this paragraph, must be provided in accordance with the following table:

Passenger Seating Capacity	Emergency Exits For Each Side of The Fuselage			
	(Type I)	(Type II)	(Type III)	(Type IV)
1 to 10				1
11 to 19			1 or	2
20 to 39		1		1
40 to 59	1			1
60 to 79	1		1 or	2

(c) Passenger emergency exits; other than side-of-fuselage. In addition to the requirements of sub-paragraph (b) of this paragraph -

(1) There must be enough openings in the top, bottom, or ends of the fuselage to allow evacuation with the rotorcraft on its side; or

(2) The probability of the rotorcraft coming to rest on its side in a crash landing must be extremely remote.

(d) Ditching emergency exits for passengers. If certification with ditching provisions is requested, ditching emergency exits must be provided in accordance with the following requirements and must be proven by test, demonstration, or analysis unless the emergency exits required by sub-paragraph (b) of this paragraph already meet these requirements:

(1) For rotorcraft that have a passenger seating configuration, excluding pilots seats, of nine seats or less, one exit above the waterline in each side of the rotorcraft, meeting at least the dimensions of a Type IV exit.

(2) For rotorcraft that have a passenger seating configuration, excluding pilots seats, of 10 seats or more, one exit above the waterline in a side of the rotorcraft meeting at least the dimensions of a Type III exit, for each unit (or part of a unit) of 35 passenger seats, but no less than two such exits in the passenger cabin, with one on each side of the rotorcraft. However, where it has been shown through analysis, ditching demonstrations, or any other tests found necessary by the Authority, that the evacuation capability of the rotorcraft during ditching is improved by the use of larger exits, or by other means, the passenger seat to exit ratio may be increased.

(3) Flotation devices, whether stowed or deployed, may not interfere with or obstruct the exits.

(e) Ramp exits. One Type I exit only, or one Type II exit only, that is required in the side of the fuselage in sub-paragraph (b) of this paragraph, may be installed instead in the ramp of floor ramp rotorcraft if -

(1) Its installation in the side of the fuselage is impractical; and

(2) Its installation in the ramp meets JAR 29.813.

(f) Tests. The proper functioning of each emergency exit must be shown by test.

5.2 Advisory Circular 29-2B JAR 29.807 Passenger Emergency Exits

340. § 29.807 (Amendment 29-12) PASSENGER EMERGENCY EXITS.

a. Explanation. The normal passenger exits (type and number in each side of fuselage) are specified as follows:

(1) For overland operations.

Passenger Seating Capacity	Emergency exits (rectangular with corner radii of width/3) For each side of the fuselage			
	Floor level			Step-up -29" Max
	Type I 24" x 48"	Type II 20" x 44"	Type III 20" x 36"	Type IV 19" x 26"
1 through 10				1
11 through 19			1 or	2
20 through 39		1		1
40 through 59	1			1
60 through 79	1		1 or	2

(2) For overwater operations (related to ditching an optional standard).

Passenger Seating Capacity	Emergency exits (rectangular with corner radii of width/3) For each side of the fuselage	
	Threshold Above Waterline	
	Type III 20" x 36"	Type IV 19" x 26" w/step-up - 29" MAX
1 through 9		1
10 through 35	1*	
Each Additional or Partial Unit of 35	1*	

*The passenger seat-to-exit ratio may be increased by using larger exits if proven by analyses or tests.

(3) For crash rollover conditions. Sufficient top, bottom, or ends of fuselage exits are to be provided for evacuation unless the probability of the rotorcraft coming to rest on its side in a crash landing is extremely remote.

(4) Ramp exits to replace Type I or II exits are permitted.

(5) Each emergency exit must be functionally tested.

b. Procedures

(1) The number and size of overland and overwater operation exits will be as specified. The use of oversize exits is allowed if the threshold is flat and of the specified width.

(2) The top, bottom, or end fuselage exits should be provided unless features of design are provided which prevent the rotorcraft from coming to rest on its side in a crash landing, and unless sufficient fail-safe and fatigue tests and analyses are conducted of the landing gear and support structure to show it is unlikely that the rotorcraft will come to rest on its side as a result of a single structural failure. An analysis is generally necessary to prove compliance with § 29.807(c).

(3) Ramp exits may be used in place of one Type I or one Type II exit if the required Type I or Type II exit is impractical, and if the § 29.813 exit access requirements are met by ramp exits.

(4) Each emergency exit is to be opened from the inside and the outside as a functional test. Interior panels and seats should be installed for the exit functional tests to check for interferences and other effects. Section 29.813 pertains to access to the exits.

340A. § 29.807 (Amendment 29-30) EMERGENCY EXITS.

a. Explanation. Amendment 29-30 added § 29.807(d)(3) which requires proof that all ditching configuration exits will be free of interference from emergency flotation devices, whether stowed or deployed (inflated). The threshold for each of these "ditching" exits should be above the water line in calm water.

b. Procedures.

(1) Test, demonstration, compliance inspection, or analysis is required to show freedom from interference from stowed and deployed emergency flotation devices. In the event an analysis is insufficient or a given design is questionable, a demonstration may be required. Such a demonstration would consist of an accurate, full-size replica (or true representation) of the rotorcraft and the flotation devices while stowed and after their deployment.

Appendix D Cost Benefit Study – NTSB Accident Report Summaries

Report Number:	LAX83FA277
Date:	06/10/1983
City:	Goleta (CA)
Make/Model:	Bell BHT-212-XXX
Weight Class:	C (FAR 29)
Registration Number:	59636
Conditions:	Wind Speed 4 Knots. Assumed Sea State 1 based on wind speed.
Sequence of Events:	As the helicopter approached the oil rig and reduced power to begin descent the tail rotor pedals began to vibrate. Pilot further reduced power and planned his decent so that the helicopter was closer to the water in case of complete tail rotor failure. The aircraft unexpectedly hit the water and immediately rolled over.
Damage:	Substantial. The main rotor and tail rotor assemblies, vertical fin and upper transmission were not recovered
Flotation System:	The impact with the water occurred before the pilot armed the automatically actuated Emergency Flotation Bags. The bags are made from nylon. It is assumed they are located on the skids as shown in figure 16 of the FAA report.
Casualties:	Two passengers died. The pilot and another passenger had minor injuries.
Stage of Failure:	Stage 1: Flotation system activated.
Relevant Modifications:	A, B

Report Number:	FTW84LA166
Date:	03/12/1984
City:	Gulf of Mexico
Make/Model:	Bell BHT-206-L1
Weight Class:	B (FAR 27)
Registration Number:	1076N
Conditions:	Wind speed 25 Knots, blowing spray and rain. Assumed Sea State 5 based on wind speed.
Sequence of Events:	The helicopter was preparing to leave the oil rig. The engine was being started when it was blown off the platform and into the water by a gust of wind. The aircraft impacted the water in a tail first attitude. Given that the engine had only just been started it is assumed that the pilot had not armed the emergency flotation system.
Damage:	Destroyed
Flotation System:	6 Floats capable of in flight inflation were fitted on this helicopter. They need to be armed using a switch mounted on the overhead console. The system is activated using a trigger switch on the collective stick.
Casualties:	4 fatalities, 1 passenger seriously injured.
Stage of Failure:	Stage 1: Flotation system activated.
Relevant Modifications:	A, B

Report Number:	LAX85FA091
Date:	12/28/1984
City:	San Diego (CA)
Make/Model:	Bell BHT-47-G3B
Weight Class:	B (FAR 29)
Registration Number:	474MP
Sequence of Events:	Helicopter landed on a moored tuna boat. After touchdown the helicopter appeared to be repositioning when the main rotor blades contacted a crane being used to load the boat. It is assumed that the helicopter then hit the water and the floats were not deployed
Damage:	Substantial
Flotation System:	There was a flotation system fitted on the helicopter. It is assumed that the flotation bags are located on the skids in the positions shown in figure 14 of the FAA report. Assumed that the emergency flotation system required the pilot to arm it and that this was not done given the unexpected collision.
Casualties:	1 fatality, 1 serious injury.
Stage of Failure:	Stage 1: Flotation system activated
Relevant Modifications:	A, B

Report Number:	DCA85AA020
Date:	04/26/1985
City:	New York (NY)
Make/Model:	Aerospatiale SA-360-C
Weight Class:	C (FAR 29)
Registration Number:	49505
Conditions:	Wind speed 16 Knots. Assumed Sea State 3 based on wind speed.
Sequence of Events:	The helicopter was taking off from a heliport on the west bank of the river. As the aircraft climbed there was a 'popping' sound and there was a loss of engine power and main rotor rpm. Aircraft began settling but impacted the water, rolled over and sank.
Damage:	Substantial
Flotation System:	Pilot attempted to deploy the emergency floats but did not have time.
Casualties:	One passenger did not egress and drowned with seat belt fastened. The other passengers and crew received either minor or no injuries.
Stage of Failure:	Stage 1: Flotation system activated
Relevant Modifications:	A, B

Report Number:	LAX86MA050A
Date:	11/30/1985
City:	San Pedro (CA)
Make/Model:	Bell BHT-206-L1
Weight Class:	B (FAR 27)
Registration Number:	5759Y
Conditions:	Wind speed 7 Knots. Assumed Sea State 2 based on wind speed
Sequence of Events:	Mid air collision between two helicopters approaching a floating restaurant. 5759Y impacted the water. 3913Z hit the edge of the heliport and rolled over. It is assumed that the pilot did not arm/activate emergency flotation system because attention was directed to controlling the aircraft following the in flight collision.
Damage:	Destroyed
Flotation System:	An emergency flotation system was fitted to the helicopter. Assumed flotation bags mounted on the skids as shown in FAA report for Bell 206.
Casualties:	1 passenger died, four had serious injuries, 7 minor
Stage of Failure:	Stage 1: Flotation system activated
Relevant Modifications:	A, B

Report Number:	LAX87FA017
Date:	10/16/1986
City:	Lompoc (CA)
Make/Model:	Bell BHT-206-B
Weight Class:	B (FAR 27)
Registration Number:	3182V
Conditions:	Wind Speed 7 Knots. Assumed Sea State 2 based on wind speed.
Sequence of Events:	On taking off from the helipad deck at the stern of a barge the helicopter's left skid became caught in a rope net. The helicopter came free but banked to left and collided with the structures on the barge. It then fell overboard and sank. Assumed the emergency flotation system was either not armed or not activated because the pilot had not yet taken off.
Damage:	Destroyed. The skids and other wreckage were found caught up on the davit.
Flotation System:	Pontoons or stowed floats capable of in-flight inflation are available on this helicopter as optional kits. There was an emergency flotation system fitted on the helicopter. If the flotation system was armed given the damage to the skids it is unlikely the flotation bags would have inflated.
Casualties:	2 fatalities, 2 serious injuries
Stage of Failure:	Stage 1: Flotation system activated
Relevant Modifications:	A, B

Report Number:	FTW87LA057
Date:	02/05/1987
City:	Gulf of Mexico
Make/Model:	Bell BHT-206-L1
Weight Class:	B (FAR 27)
Registration Number:	5012Z
Conditions:	
Sequence of Events:	The helicopter took off from an oil rig shortly afterwards the pilot transmitted a 'Mayday'. The pilot told a passenger to get the raft out and the helicopter subsequently impacted rough water and sank.
Damage:	Substantial
Flotation System:	The flotation bags are located on the skids on the 206. The helicopter was not recovered but a float inflation bottle was found. It was fully charged and the squib had not been fired. It cannot be confirmed that the failure of the inflation bottle to discharge the gas was due to a mechanical failure. The system could not have been armed. It is assumed that the flotation system was not armed or not activated.
Casualties:	All occupants of the helicopter were retrieved although 2 later died from injuries.
Stage of Failure:	Stage 1: Flotation system activated
Relevant Modifications:	A+B

Report Number:	BFO87FA057
Date:	08/21/1987
City:	Washington DC
Make/Model:	Bell BHT-206-B
Weight Class:	B (FAR 27)
Registration Number:	83080
Conditions:	Wind Speed 3 Knots. Assumed Sea State 0 based on wind speed.
Sequence of Events:	The helicopter was on a sight seeing flight. Whilst hovering over the Potomac river the engine lost power. The pilot initiated an autorotation and deployed the emergency floats. The aircraft impacted the water and rolled over. Given the sea state it is unlikely that the helicopter overturning was initiated by a wave. Therefore the floats deployed unevenly due to an equipment failure. The helicopter was hovering at 200' when it lost power. The flight manual recommends that hovering at this height should be avoided to allow for successful autorotation landing in the event of a power loss. This implies that the autorotation carried out could cause damage to the aircraft. Therefore it is assumed that the failure of the floats to deploy evenly was due to impact damage.
Damage:	Destroyed
Flotation System:	Pontoons or stowed floats capable of in-flight inflation are available on this helicopter as optional kits. The helicopter was supported upside down in the water by the floats
Casualties:	All 3 passengers died, the pilot had serious injuries.
Stage of Failure:	Stage 4: Floats partially survive impact.
Relevant Modifications:	G, J, I, H

Report Number:	NYC88FA133
Date:	05/01/1988
City:	Long Island City
Make/Model:	Bell BHT-206-XXX
Weight Class:	B (FAR 27)
Registration Number:	7094J
Conditions:	Wind Speed 8 Knots. Assumed Sea State 2 based on wind speed.
Sequence of Events:	The helicopter was on a sightseeing flight when it experienced a low rotor rpm situation. The pilot made a forced landing in the river. The pilot and 3 passengers exited the aircraft and clung to the floats.
Damage:	Destroyed
Flotation System:	The floats were inflated and separated from the aircraft. Assumed that the floats separated from the aircraft during impact.
Casualties:	One passenger did not escape and died of drowning. The other occupants experienced minor injuries.
Stage of Failure:	Stage 4: Floats survive impact
Relevant Modifications:	G, J, I, H

Report Number:	FTW88FA131
Date:	07/14/1988
City:	Gulf of Mexico
Make/Model:	SNIAS SA-330-J
Weight Class:	D (FAR 29)
Registration Number:	47307
Conditions:	Wind Speed 10 Knots. Assumed Sea State 2 based on wind speed.
Sequence of Events:	During take off from an oil rig the helicopter began a slow uncommanded left turn. The pilot attempted corrective action but the helicopter impacted the water in a left bank, nose down attitude. Given that the pilot was concentrating on controlling the helicopter and it was in take off it is assumed that the EFS was either not armed or not activated. The latter is more likely as arming the EFS is a take-off pre-flight check.
Damage:	Destroyed
Flotation System:	The floats were not inflated.
Casualties:	1 fatality, 1 serious injury, 14 occupants had no injuries.
Stage of Failure:	Stage 1: Flotation system activated
Relevant Modifications:	A, B

Report Number:	FTW89FA013
Date:	11/04/1988
City:	Gulf of Mexico
Make/Model:	Aerospatiale AS-355-F1
Weight Class:	B (FAR 27)
Registration Number:	355EH
Conditions:	Wind Speed 25 Knots. Assumed Sea State 5 based on wind speed.
Sequence of Events:	The helicopter was taking off from an offshore platform when it experienced a complete loss of tail rotor and helicopter control. Recovery was not possible. It is assumed the emergency flotation system was either not armed or not activated. The latter is more likely as arming the EFS is a take-off pre-flight check.
Damage:	Destroyed
Flotation System:	There was a flotation system fitted on the helicopter.
Casualties:	4 fatalities, 2 serious injury
Stage of Failure:	Stage 1: Flotation system activated.
Relevant Modifications:	A, B

Report Number:	MIA90FA081
Date:	03/08/1990
City:	Miami
Make/Model:	SNIAS AS-350-D
Weight Class:	B (FAR 27)
Registration Number:	5778W
Conditions:	Wind Speed 20 Knots, rough water. Assumed Sea State 4 based on wind speed.
Sequence of Events:	The helicopter was in cruise flight over the ocean when it experienced a loss of engine power. At 100 feet above the water the pilot deployed the emergency floats and successfully landed the helicopter. A wave hit the helicopter and it rolled over. Assumed that floats deployed evenly and the wave caused it to turn over.
Damage:	Destroyed
Flotation System:	
Casualties:	Two passengers died from drowning. The pilot survived but suffered serious injuries.
Stage of Failure:	Stage 5: Craft remains upright
Relevant Modifications:	J

Report Number:	FTW91FA155
Date:	08/26/1991
City:	Gulf of Mexico
Make/Model:	Bell BHT-412-XXX
Weight Class:	D (FAR 29)
Registration Number:	3909F
Conditions:	Wind Speed 3 Knots. Assume Sea State 0 based on wind speed.
Sequence of Events:	The helicopter was on a final approach to an oil rig when tail rotor authority and directional control were lost. The crew began an autorotation to the water when the helicopter spun out of control to the right. It made 2 or 3 revolutions and impacted the water. The helicopter rolled over.
Damage:	Substantial
Flotation System:	The right flotation gear deployed. The left flotation gear did not deploy because the pneumatic lines were pulled apart during impact.
Casualties:	One passenger was incapacitated due to injuries from the impact and drowned. The other 10 occupants received some injuries.
Stage of Failure:	Stage 3: Gas enters some floats.
Relevant Modifications:	E, F

Report Number:	FTW94LA021
Date:	10/29/1993
City:	
Make/Model:	Bell BHT-206-B
Weight Class:	B (FAR 27)
Registration Number:	360S
Conditions:	Wind Speed 35 knots. Assumed Sea State 6 based on wind speed.
Sequence of Events:	The Pilot was attempting to fly to an off shore platform when he encountered bad weather. In an attempt to avoid the weather he set up an orbit. During the orbit he slowed the aircraft down and it began to descend. A 15 foot swell struck the aircraft and it rolled into the water. Pilot was not in an emergency situation so it is assumed that the flotation system was either not armed or activated. The latter is more likely as arming the EFS is a take-off pre-flight check.
Damage:	Destroyed
Flotation System:	An emergency flotation system was fitted on the aircraft.
Casualties:	1 Fatality and 2 minor injuries.
Stage of Failure:	Stage 1: Flotation system activated
Relevant Modifications:	A, B

Report Number:	BFO94FA013
Date:	11/19/1993
City:	Portland
Make/Model:	Bell BHT-206-L1
Weight Class:	B (FAR 27)
Registration Number:	911ME
Conditions:	Wind Speed 13 Knots. Water rough. Assumed Sea State 4 based on wave height.
Sequence of Events:	The helicopter experienced a loss of engine power due to fuel exhaustion. The helicopter ditched in the ocean. The helicopter landed hard in "rough water" with 6 foot waves. It inverted and sank. It was assumed that the EFS operated with some success as the helicopter inverted. It was also assumed that there was sufficient time for some occupants to escape before the helicopter sank
Damage:	Destroyed
Flotation System:	During the autorotation the pilot deployed the floats attached to the skids.
Casualties:	All 3 passengers died, the pilot received serious injuries.
Stage of Failure:	Stage 5: Craft remains upright
Relevant Modifications:	J

Report Number:	FTW99FA001A
Date:	10/05/1998
City:	Gulf of Mexico
Make/Model:	Bell BHT-407-XXX
Weight Class:	B (FAR 27)
Registration Number:	403PH
Conditions:	Wind Speed 25 knots. Assumed Sea State 5 based on wind speed.
Sequence of Events:	403PH collided in flight with 5792H. 403PH executed an autorotation landing into the water. The float system was deployed. The helicopter stayed upright for about thirty seconds and the rolled over. Assumed roll over was caused by wave.
Damage:	Destroyed
Flotation System:	The emergency flotation bags were mounted on the skids.
Casualties:	The pilot of 5792H died, the pilot of 403PH survived.
Stage of Failure:	Stage 5: Craft remains upright
Relevant Modifications:	J

Report Number:	LAX98LA079
Date:	01/24/1998
City:	Pacific Ocean
Make/Model:	Hughes HU-369-D
Weight Class:	B (FAR 27)
Registration Number:	521ZZ
Conditions:	Wind Speed 15 knots. Assumed Sea State 3 based on wind speed.
Sequence of Events:	The helicopter crashed into the ocean and sank. This was due to pilot error.
Damage:	Destroyed
Flotation System:	One float broke off the other was seriously damaged.
Casualties:	The pilot died, the other crew member was uninjured.
Stage of Failure:	Stage 4: Floats survive impact
Relevant Modifications:	G, J, I, H

Report Number:	FTW99FA094
Date:	03/17/1999
City:	Gulf of Mexico
Make/Model:	Aerospatiale AS-350-B2
Weight Class:	B (FAR 27)
Registration Number:	6100R
Conditions:	Wind speed 11 Knots. Assumed Sea State 3 based on wind speed.
Sequence of Events:	N6100R was destroyed following a loss of control while departing an oil platform. The helicopter rolled inverted and dropped into the ocean. Witnesses saw the floats deploy.
Damage:	Destroyed
Flotation System:	
Casualties:	The commercial pilot and one passenger sustained serious injuries, and two passengers were fatally injured.
Stage of Failure:	Stage 5: Craft remains upright
Relevant Modifications:	J

Report Number:	FTW00RA039
Date:	12/01/1999
City:	Cabinda, Republic of Angola
Make/Model:	Bell BHT-206-L1
Weight Class:	B (FAR 27)
Registration Number:	5005B
Conditions:	
Sequence of Events:	Following a loss of engine power during takeoff from an offshore oil platform the helicopter impacted the water.
Damage:	Substantial
Flotation System:	The emergency float system was not activated. Stowed floats capable of in flight inflation are available on this helicopter.
Casualties:	The pilot and one passenger were seriously injured. Another passenger was fatally injured.
Stage of Failure:	Stage 1: Flotation system activated
Relevant Modifications:	A, B

Report Number:	FTW00RA003
Date:	10/02/1999
City:	Dhahran, Saudi Arabia
Make/Model:	Bell BHT-214-ST
Weight Class:	D (FAR 29)
Registration Number:	704H
Conditions:	Wind Speed 8 Knots. Assumed Sea State 2 based on wind speed.
Sequence of Events:	The helicopter was substantially damaged upon impact with the water during take off from an offshore platform. The helicopters entry into the water was described as 'soft and gentle' by witnesses. The helicopter rolled and inverted in the water. It is assumed that some of the floats did not survive the impact and that is the reason for the craft inverting. The sea state is unlikely to produce a wave that would overturn the aircraft.
Damage:	Substantial
Flotation System:	The floats of the helicopter inflated during the accident sequence.
Casualties:	The 2 crew members and 10 passengers died. The other 8 passengers received minor injuries.
Stage of Failure:	Stage 4: Floats survive impact (Part)
Relevant Modifications:	G, J, I, H

Appendix E Cost Benefit Study – UK Accident Report Summaries

Report Number:	Aircraft Accident Report 10/82
Date:	08/12/1981
City:	Dunlin Alpha Platform
Make/Model:	Bell 212
Weight Class:	C (FAR 29)
Registration Number:	G-BIJF
Conditions:	Wind Speed 17 Knots. Assumed Sea State 4 based on wind speed.
Sequence of Events:	The helicopter was flying between the Brent Field and the Dunlin Platform when it encountered an area of reduced visibility and the decision was made to turn back. During the turn, control of the helicopter was lost. It began yawing rapidly to the right and descending and struck the sea.
Damage:	Substantial damage from impact and immersion. Aircraft considered beyond economical repair.
Flotation System:	Four inflatable floats were fitted to the fuselage. The emergency flotation bags were deployed from their stowages. The floats on the right side were deflated. The front left was fully inflated. The flexible pipe on the right hand side was ruptured.
Casualties:	1 Fatality, 2 serious injuries, 11 minor/none Assumed causes of fatalities: 0 – Due to primary impact. 1 – Died outside the helicopter due to exposure. 0 – Assumed to be due to not having sufficient time to escape from the helicopter.
Stage of Failure:	Stage 3: Gas enters some floats.
Relevant Modifications:	F

Report Number:	Aircraft Accident Report 2/93
Date:	03/14/1992
City:	Cormorant 'A' Platform, East Shetland Basin
Make/Model:	AS 332L Super Puma
Weight Class:	D (FAR 29)
Registration Number:	G-TIGH
Conditions:	Wind Speed 54-64 Knots. Assumed Sea State 8
Sequence of Events:	The helicopter was shuttling personnel from an oil production platform to a nearby accommodation 'Flotel'. Following takeoff from the platform the helicopter climbed to a height of 250 feet and began a right turn. The pilot reduced power and raised the nose of the aircraft. This reduced the airspeed to zero and a rate of descent built up. This could not be arrested and the helicopter struck the sea. It rolled onto its right side before inverting and sinking within a minute or two.
Damage:	Destroyed
Flotation System:	The helicopter was fitted with an emergency flotation system. Two inflatable bags on the nose of the aircraft and one on each sponson. The system was armed and available but was not activated.
Casualties:	11 fatalities, 1 serious injury, 5 minor/none Assumed causes of fatalities: 0 – Due to primary impact. 6 – Died outside the helicopter due to exposure. 5 – Assumed to be due to not having sufficient time to escape from the helicopter.
Stage of Failure:	Stage 1: Flotation system activated.
Relevant Modifications:	A+B

Report Number:	Aircraft Accident Report 8/84
Date:	07/16/1983
City:	St Mary's Aerodrome, Isles of Scilly
Make/Model:	Sikorsky S-61N
Weight Class:	D (FAR 29)
Registration Number:	G-BEON
Conditions:	Wind Speed 2-5 Knots. Assumed Sea State 1 based on wind speed.
Sequence of Events:	The helicopter was on a scheduled flight from Penzance to the Isles of Scilly. Whilst on the approach to St Mary's Aerodrome the helicopter gradually descended from its intended height of 250 feet without either pilot being aware of this and flew into the water.
Damage:	Destroyed
Flotation System:	The inflatable flotation gear was attached to the sponsons. The sponsons broke off making the emergency flotation gear unavailable.
Casualties:	20 fatalities, 2 serious injuries, 4 minor/none Assumed causes of fatalities: 0 – Due to primary impact. 3 – Died outside the helicopter due to exposure. 17 – Assumed to be due to not having sufficient time to escape from the helicopter.
Stage of Failure:	Stage 4: Floats survive impact.
Relevant Modifications:	G, I, J, H

Report Number:	Aircraft Accident Report 2/91
Date:	07/25/1990
City:	Brent Spar, East Shetland Basin
Make/Model:	Sikorsky S61N
Weight Class:	D (FAR 29)
Registration Number:	G-BEWL
Conditions:	Wind Speed 5 Knots or less. Assumed Sea State 1 based on wind speed.
Sequence of Events:	The helicopter was manoeuvring to land on the Brent Spar offshore platform. The tail rotor blade contacted a handrail on the installation crane 'A' frame. The helicopter crashed onto the helideck before falling into the sea and sinking.
Damage:	Destroyed
Flotation System:	Attached to damaged sponsons, not deployed
Casualties:	6 fatalities, 7 survivors. Assumed causes of fatalities: 2 – Due to primary impact. 0 – Died outside the helicopter due to exposure. 4 – Assumed to be due to not having sufficient time to escape from the helicopter.
Stage of Failure:	Stage 4: Floats survive impact
Relevant Modifications:	G, J, I, H

Appendix F Cost Benefit Study – Worked Example

1. Introduction

Cost benefit study, worked example for "Modification A+B: Automatic arming and activation".

2. Determine System Functional Effectiveness With No Modifications

Determine base-line probabilities with no modifications from the EFS deployment Tree (Figure 36)

$$Psink_0 := 0.5 + (0.5 \cdot 0) + (0.5 \cdot 1 \cdot 0) + (0.5 \cdot 1 \cdot 1 \cdot 0.17 \cdot 0) + (0.5 \cdot 1 \cdot 1 \cdot 0.83 \cdot 0.4) \quad Psink_0 = 0.67$$

$$Pinvert_0 := 0.5 \cdot 1 \cdot 1 \cdot 0.17 \cdot 1 + (0.5 \cdot 1 \cdot 1 \cdot 0.83 \cdot 0.6 \cdot 0.33) + (0.5 \cdot 1 \cdot 1 \cdot 0.83 \cdot 0.6 \cdot 0.67 \cdot 1) \quad Pinvert_0 = 0.33$$

$$Pairpocket_0 := 0.5 \cdot 1 \cdot 1 \cdot 0.83 \cdot 0.6 \cdot 0.67 \cdot 0 \quad Pairpocket_0 = 0$$

3. Determine Functional Effectiveness With Modification A+B In Place

$$Psink_{AB} := 0 + (1 \cdot 0) + (1 \cdot 1 \cdot 0) + (1 \cdot 1 \cdot 1 \cdot 0.17 \cdot 0) + (1 \cdot 1 \cdot 1 \cdot 0.83 \cdot 0.4) \quad Psink_{AB} = 0.33$$

$$Pinvert_{AB} := 1 \cdot 1 \cdot 1 \cdot 0.17 \cdot 1 + (1 \cdot 1 \cdot 1 \cdot 0.83 \cdot 0.6 \cdot 0.33) + (1 \cdot 1 \cdot 1 \cdot 0.83 \cdot 0.6 \cdot 0.67 \cdot 1) \quad Pinvert_{AB} = 0.67$$

$$Pairpocket_{AB} := 1 \cdot 1 \cdot 1 \cdot 0.83 \cdot 0.6 \cdot 0.67 \cdot 0 \quad Pairpocket_{AB} = 0$$

4. Determine Change in Functional Effectiveness Due to Modification A+B

$$\Delta Psink_{AB} := Psink_{AB} - Psink_0 \quad \Delta Psink_{AB} = -0.33$$

$$\Delta Pinvert_{AB} := Pinvert_{AB} - Pinvert_0 \quad \Delta Pinvert_{AB} = 0.33$$

$$\Delta Pairpocket_{AB} := Pairpocket_{AB} - Pairpocket_0 \quad \Delta Pairpocket_{AB} = 0$$

5. Calculate "Occupant Survival Number" For Modification A+B

Modifications which result in reduced sinkings are assumed to be 50% effective at saving occupants who would have drowned if no modifications were used.

Modifications which result in increased chances of an air pocket in the cabin with an overwater escape route are assumed to be 90% effective at saving occupants who would have drowned if no modifications were used.

$$Occupant_{AB} := (0.5 \cdot \Delta Pinvert_{AB}) + (0.9 \cdot \Delta Pairpocket_{AB}) \quad Occupant_{AB} = 0.17$$

6. Calculate Fatality Rate Per Year From UK Accident History

Search period 1980 to 1999, 20 years

Period := 20

Number of relevant fatalities (26)

Fatalities_{UK} := 26

$$\text{FatalityRateUK} := \frac{\text{Fatalities}_{\text{UK}}}{\text{Period}}$$

FatalityRateUK = 1.3

7. Calculate Number of Estimated Fatalities For UK Fleets Remaining Service Life

Estimated remaining life of UK fleet is 20 years

Life_{RemainingUK} = 20

$$\text{TotalFatality}_{\text{FutureUK}} := \text{FatalityRateUK} \cdot \text{Life}_{\text{RemainingUK}}$$

TotalFatality_{FutureUK} = 26

8. Calculated Potential Lives Saved By Modification A+B

Modification A+B will save 17% of the occupants who can be expected to escape from the helicopter.

$$\text{LivesSaved}_{\text{AB}} := \text{TotalFatality}_{\text{FutureUK}} \cdot \text{Occupant}_{\text{AB}}$$

LivesSaved_{AB} = 4.34

9. Calculate Cost of Modification A+B

Number of Helicopters in UK fleet is 79

Fleet_{size} := 79

Cost of Modification (A+B). 7% of EFS

Mod_{AB} := 0.07 · 200000

Overall cost for fleet

$$\text{Cost}_{\text{TotalAB}} := \text{Fleet}_{\text{size}} \cdot \text{Mod}_{\text{AB}}$$

Cost_{TotalAB} = 1106000.00

10. Calculate Cost per Live Saved of Modification A+B

$$\text{CostPerLifeSaved}_{\text{AB}} := \frac{\text{Cost}_{\text{TotalAB}}}{\text{LivesSaved}_{\text{AB}}}$$

CostPerLifeSaved_{AB} = 254721.33

Study II (Supplementary Study)

Prepared by BMT Fluid Mechanics Ltd

Executive Summary

The main purpose of this investigation was to assess the range of impact loads experienced by typical emergency flotation systems, installed within the sponsons or beneath fuselage panels of helicopters, during controlled ditchings and impacts onto water. The calculations were performed using a Monte Carlo simulation procedure, based on simplified empirical and theoretical formulae for estimating the impact force. Failure of the flotation system was deemed to occur whenever the load on the sponson or fuselage panel exceeded its design value. Four different types of incident were considered: a controlled ditching, vertical descent (low horizontal speed), loss of control (intermediate horizontal and vertical speeds) and fly-in (low vertical speed). The calculations were performed in representative central North Sea wave conditions and in calm water.

The results showed, as expected, that there is a very low probability of exceeding the design load in a controlled ditching incident. Flotation equipment is designed to survive a normal ditching. The base case investigation showed a relatively high probability of exceeding design loads on both the sponson and fuselage panel during vertical descent and loss of control crash scenarios. This result suggested that substantial increases in design loads would be required in order to avoid major structural damage to flotation systems in these two types of incident. A follow-up sensitivity study confirmed that a 100% increase in design loads would result in only a modest improvement in crashworthiness.

Major structural failures have occurred during actual fly-in accidents in the past. The simulations nonetheless predicted that the risks of exceeding design loads on both the sponson and fuselage panel during a fly-in are relatively low. There are two likely reasons for this unexpected result. Firstly, drag and planing forces make major contributions to the total predicted load during a fly-in. These forces are poorly understood, and the simplified formulae used in the present analysis may not be reliable. Secondly, the model considers loads on an individual sponson or panel in isolation, and does not consider failure of the surrounding hull structure. The design of flotation equipment should in practice consider the design and strength of the supporting hull structure.

Sea state conditions had little effect on the results obtained from the investigation as a whole. They had a significant effect on results obtained in severe sea conditions, however, and increased the range of loads substantially during controlled ditching and fly-in incidents.

The impact force proved to be sensitive to variations in several different parameters. It may therefore be difficult to characterise helicopter impact incidents in terms of a small number of deterministic scenarios.

Impact loads were sensitive to variations in the helicopter's mean speed and descent angle at the moment of impact. The drag force coefficient was also an important parameter. The helicopter's mean pitch angle and the planing force coefficient only affected loads experienced during ditching and fly-in incidents.

Investigations into float redundancy demonstrated that there are clear benefits, in terms of crashworthiness, from having additional floats on the upper cabin walls. Benefits emerged regardless of whether they were measured in terms of reducing the number of occasions when the helicopter sank, making it float on its side, or providing a satisfactory air space in the cabin. The largest improvement came when the first upper cabin float was added. There are possible advantages in this asymmetric float configuration, because it gives the

helicopter a preferred stable attitude in the water, eliminating the risk of a second rotation while the occupants are trying to escape.

Alternative methods for improving crashworthiness might also be considered, such as designing a 'crumple zone' or other energy-absorbing device into the support structure. Whatever solution is adopted, however, the structure must retain sufficient integrity to serve its primary function of providing buoyancy.

There may be potential for reducing impact loads during a fly-in incident by modifying the shape of the hull or sponson, and avoiding large flat areas.

The present investigations considered all-year wave conditions in the central area of the North Sea. It is likely that selecting a more severe wave climate (e.g. West of Shetland) would significantly increase the loads predicted during controlled ditching and fly-in incidents. Suitable design procedures would be needed to take account of increases in water impact loading due to waves.

BMT recommends that further work should be done to investigate the importance of drag and planing type forces in the water impact loading process, and the feasibility of representing these loads better in the calculations. These forces turned out to be more significant than originally anticipated, and simplifications in existing calculation procedures may have resulted in unrealistically low predicted forces during fly-in incidents.

Contents

	<i>Page</i>
1	INTRODUCTION 1
1.1	Terms of Reference 2
2	BACKGROUND AND KEY STAGES 2
2.1	Analysis of Loads on Flotation Systems 2
2.2	Key Stages 3
3	KEY RESULTS FROM THE LITERATURE REVIEW 4
3.1	Procedures for Estimating Loads on Seaplanes and Helicopters 4
3.2	General Considerations 5
3.3	Impact Loads on Circular Cylinders 7
3.4	Impact Loads on Wedge Sections 9
4	THEORETICAL BASIS 11
4.1	Assumptions 11
4.2	Monte-Carlo Simulation Procedure 12
4.3	Input Parameters 12
4.4	Initial Water Impact Forces 13
4.4.1	Maximum Impact Force on the Sponson 14
4.4.2	Maximum Impact Force on the Fuselage Panel 15
4.5	Structure Loads 16
4.6	Drag and Planing Forces 17
4.6.1	Drag Forces on the Sponson 18
4.6.2	Planing Forces on the Fuselage Panel 18
5	MAIN STUDY 19
5.1	Helicopter Details 20
5.2	Impact Loading Scenarios 20
5.3	Conditions Represented 21
5.3.1	Sea Conditions 21
5.3.2	Impact Force on the Sponson 22
5.3.3	Impact Force on the Fuselage Panel 23
5.3.4	Impact Scenarios 23
5.3.5	Modelling the Sponson 24
5.3.6	Modelling the Fuselage Panel 26
5.4	Results 27
5.4.1	Correlation Plots 27
5.4.2	Load Exceedance Distributions 28
6	SENSITIVITY STUDY 29
6.1	Scope of Work 29
6.2	Results from the Sensitivity Study 31
7	TWO-FLOAT REDUNDANCY STUDY 36
7.1	Scope of Work 36
7.2	Impact Loads on Sponsons 37
7.3	Impact Loads on Fuselage Panels 37
7.4	General Conclusions from Two-Float Redundancy Study 38

8	DATA INTERPRETATION AND APPRAISAL STUDY	39
8.1	Base Case Conditions	39
	8.1.1 Sponson Impact Loads	39
	8.1.2 Impact Severity Index Curves	40
	8.1.3 Fuselage Panel Impact Loads	41
8.2	Calm Water Conditions	41
	8.2.1 Failure Case Distributions	42
8.3	Increased Design Load	42
	8.3.1 Failure Case Distributions	42
8.4	Results from Two-Float Redundancy Study	43
	8.4.1 Failure Case Distributions	43
9	EH101 MULTI-FLOAT REDUNDANCY STUDY	44
9.1	Panel Definition	45
9.2	Hull and Flotation Unit Buoyancy	46
	9.2.1 Hull Buoyancy	46
	9.2.2 Float Buoyancy	48
9.3	Float Failure Consequences	48
9.4	Results	52
	9.4.1 Criteria for Floating or Sinking	52
	9.4.2 Probability of Sinking in a Severe Crash	53
	9.4.3 Criteria for Side-Floating	54
	9.4.4 Criteria for a Satisfactory Air Space	54
	9.4.5 Float Failure Combinations	55
9.5	Conclusions from EH101 Multi-Float Redundancy Study	57
10	OVERALL CONCLUSIONS	58
11	ACKNOWLEDGEMENTS	60
12	REFERENCES	60
	Key Nomenclature	63
	Figures	65
	Appendix A: Investigation Based on the Brent Spar and Cormorant Alpha Accidents	187

INTRODUCTION

BMT Fluid Mechanics Limited (BMT) was commissioned by the Civil Aviation Authority (CAA) to carry out an investigation into the crashworthiness of helicopter emergency flotation systems during a crash or ditching onto water. BMT's work formed part of a broader study, undertaken by WS Atkins Science and Technology (WSA), which included a literature review of past accidents, a finite element modelling study, a review of emergency flotation equipment design and its failure modes, a cost/benefit study on proposed modifications, and a review of current regulations. The results from this broader study are presented in a companion WSA report [1].¹

The main purpose of BMT's investigation was to estimate the range of water impact loads experienced by typical flotation systems, installed within the sponsons or beneath fuselage panels of helicopters, during controlled ditching, vertical descent, loss of control and fly-in incidents. The first phase of BMT's investigation [2] involved a literature review of model test results and impact force calculation methods, the development of a Monte Carlo simulation procedure based on simplified empirical and theoretical formulae for estimating the impact force, and a simulation study based on a number of agreed ditching and accident scenarios. Failure of the flotation system was deemed to occur whenever the load on the sponson or fuselage panel exceeded its design value. The calculations were performed in representative central North Sea wave conditions and in calm water.

During a second phase of work [3] BMT investigated sensitivity to changes in the parameters describing the helicopter and wave environment, alternative system failure modes, and water impact scenarios based on the *Brent Spar* [4] and *Cormorant Alpha* [5] accidents.

Input data parameters and design loads used during the initial investigation and subsequent sensitivity study were based on information for the *Sea King* helicopter, supplied by GKN Westland Helicopters Limited (GKN WHL). The *Cormorant Alpha* and *Brent Spar* investigations were based on input parameters and models agreed with WSA, which were ultimately derived from information contained in relevant reports of the Air Accidents Investigation Branch (of the UK Department of Transport).

The final phase of work involved a redundancy study on a multi-float system, based on the *EH101* helicopter with additional upper cabin flotation units.

It is assumed that the flotation system remains uninflated until after contact with the water, and will fail to deploy if the relevant sponson or cover panel suffers structural damage on impact. The loading range is characterised in terms of the exceedance probability distribution of maximum water impact forces on the sponson or panel.

These calculations were based on a simplified water impact loading model, which treats each flotation component in isolation, ignoring the effects of the surrounding hull structure. This type of model should be sufficient to demonstrate trends and sensitivity levels, but it is not easy to estimate the absolute accuracy of the predicted forces. Comparisons with results from the WSA finite element model-based analysis

¹ A full list of references may be found in Section 12 on page 60.

(reported separately by WSA [1]) have nonetheless shown an encouraging level of agreement.

The following report summarises results from the literature review, outlines the theoretical basis for BMT's Monte Carlo simulation procedure, and presents key results and conclusions from the project as a whole. Further details and additional results may be found in references [2] and [3].

1.1 **Terms of Reference**

BMT's scope of work and terms of reference for this investigation are defined in reference [6].

2 **BACKGROUND AND KEY STAGES**

Previous work on the analysis of helicopter crashes onto water [7, 8, 9, 10, 11] concluded that the primary cause of loss of life following water impact is drowning, and that improvements in the capability of helicopters to remain afloat after impact, long enough for occupants to escape, is the major factor in increasing occupant survivability. The CAA therefore commissioned a research project aimed at establishing the feasibility of improving the crashworthiness of helicopter emergency flotation systems. This project was undertaken by WS Atkins Science and Technology (WSA), with support from the BMT investigation reported in this document.

2.1 **Analysis of Loads on Flotation Systems**

GKN WHL had previously carried out an analysis [8] of the accelerations and loads sustained by the main helicopter fuselage during impact onto water using the *MSC/DYNA* program. *DYNA* is essentially a structural analysis program, and the water surface was modelled in an idealised manner (i.e. as a material with a given density and a specified relationship between its pressure and volume). This type of model is likely to predict the peak impact pressure occurring immediately after a vertical impact onto a smooth and still water surface quite well, when the forces are largely determined by the inertia of the fluid and by acoustic pressures. It is not obvious how to model the effects of free surface waves, water surface roughness and aeration, however, and it is difficult to model quasi-steady processes, such as viscous drag and planing forces, which are likely to become important during impacts at high forward speeds.

WSA have now undertaken a further numerical finite element modelling study, based around three actual accident scenarios. These three accidents occurred near the *Cormorant Alpha* platform in 1992, at the *Brent Spar* platform in 1990, and near the *Scilly Isles* in 1983. The results from WSA's investigations are presented in a separate companion report [1]. WSA's analysis aimed to predict detailed structural loads within the helicopter's hull during a small number of specific water impact events.

BMT have adopted a more pragmatic approach, which aims to define the range of loads occurring during many such impact events, but using a simplified water impact loading model to describe each such event. BMT's investigations were therefore intended to complement WSA's analysis by establishing trends and levels of sensitivity, and thus help to place WSA's results within a broader context.

BMT's approach is based on an empirical description of the impact loading process, rather than on a purely theoretical model. Experimental work has repeatedly demonstrated that water impact loads are extremely variable and sensitive to the shape and roughness of the structure and water surfaces, to the amount of air entrapment, and to the entry angle and velocity on impact. BMT have therefore adopted a probabilistic approach which recognises the highly random nature of the impact loading process, and its sensitivity to fairly small changes in the impact conditions. The loading model has also been adapted to represent simplified drag and planing forces as well as the initial impact.

The simplifications and assumption within this model have to be borne in mind when assessing the results. The main purpose of this investigation was to identify trends and the sensitivity of impact loads to variations in the helicopter's condition and sea state at the instant of impact, rather than to obtain high absolute accuracy in the predicted impact loads, or to identify the structural consequences.

Appendix A describes results from an investigation which allowed direct comparisons to be made between impact loads estimated by BMT and WSA. This investigation was based on the *Brent Spar* and *Cormorant Alpha* accident scenarios, and was intended to provide guidance on the accuracy, reliability and limitations of both types of model. The results from this comparison study are described in the accompanying WSA report [1].

2.2 Key Stages

The key stages of this investigation were as follows:

- a literature search and review aimed at identifying suitable procedures for estimating water impact loads on a sponson or fuselage panel during each of the four specified types of incident (Section 3);
- development of a Monte Carlo simulation procedure, based on selected load calculation methods, to establish probability distributions of water impact loads in each type of incident (Section 4);
- calculations based on *Brent Spar* and *Cormorant Alpha* accident scenarios, which enabled comparisons to be made with WSA's results (Appendix A);
- the definition of four base case scenarios describing ranges of ditching, vertical descent, loss of control and fly-in incidents, and an analysis based on those scenarios (Section 5);
- a sensitivity study to investigate the effects of varying the helicopter's condition and the sea state at the instant of impact (Section 6);
- an initial two-float redundancy study to investigate the effects of making alternative assumptions about the number of flotation units required to keep the helicopter afloat (Section 7);
- an interpretation and assessment study to help draw appropriate conclusions about prospects for enhancing the crashworthiness of emergency flotation equipment (Section 8);

- a multi-float redundancy study, based on the *EH101* helicopter with additional upper cabin flotation units (Section 9).

3 KEY RESULTS FROM THE LITERATURE REVIEW

3.1 Procedures for Estimating Loads on Seaplanes and Helicopters

Early procedures for predicting water impact forces on seaplanes and helicopters were based on a theoretical model developed by von Karman [12] to describe forces on a wedge descending vertically onto smooth water. Von Karman's theory was subsequently extended by Wagner [13], who took account of the rise in the water surface on either side of the descending wedge. Models of this type effectively assume that the velocity on impact is normal to the keel, and ignore the forward speed of the hull through the water.

Later investigators recognised that any significant forward motion of the hull through the water causes a loss of momentum in the downwash, and in the sheet of water that is thrown forwards and away from the craft. These momentum changes result in 'planing' forces, which are not represented in simple vertical impact models. Various empirical or intuitive modifications were made to the theory during the late 1940s and 1950s in order to take account of forces associated with forward motion.

Some of the earliest references considered during this review were three NACA reports [14, 15, 16] relating to the landing of seaplanes and helicopters on water. These are part of an extensive series of NACA papers and reports which investigated both impulsive slam-type loads and planing loads on cylindrical and V-shaped hull-sections, using empirical formulae and intuitive modifications to theoretical solutions. Theoretical predictions were also compared with results from extensive programmes of model tests.

NACA Technical Note 1008 [14] reviewed the von Karman and Wagner models, and considered a number of proposed improvements to the theory. It then proposed an intuitive modification to the theory to take account of forward speed and planing forces. Maximum forces predicted using this modified theory agreed favourably with measured forces on a V-shaped hull model.

NACA Report 1103 [15] developed a 'strip theory' procedure for estimating forces and moments on seaplane hulls, based on the force prediction formula proposed in [14]. The flow was assumed to be two-dimensional in each transverse flow plane, and an aspect ratio correction was applied to take account of three-dimensional flow effects. The loads were characterised in terms of a so-called 'approach' parameter, which depended on the craft's trim angle and flight path angle on impact. Predicted moments on seaplane hulls and the resulting motions agreed favourably with measurements.

NACA Technical Note 2889 [16] presented a theoretical procedure for estimating water impact loads on helicopters, which were modelled as elliptical cylinders. The theoretical model was based on the Wagner wedge impact theory, and forward speed was taken into account using the approach proposed in [15]. Predicted pressures agreed reasonably well with measurements on a dropped circular cylinder. These measurements have now been largely superseded by the more extensive Campbell data set discussed in Section 3.3.

A more recent Aeronautical Research Council report [17] reviewed these and other prediction procedures for seaplane impact, and compared predicted results with experimental data. Once again, an important distinction was made between impact forces and planing forces. The impact force was associated with the component of flow normal to the aircraft keel, whereas planing forces were associated with the component of flow parallel to the keel. Both types of forces were found to be important in cases where the aircraft had a significant forward speed and descent speed on contact with the water. Section 3 of [17] presented various alternative theoretical procedures for estimating the effects of planing and impact forces on seaplanes. Comparisons with experimental measurements on a *Sunderland* flying boat were somewhat inconclusive, however, and none of the theoretical solutions convincingly fitted both the model and full-scale experimental evidence. Certain discrepancies were attributed to experimental error, but the paper concluded that it might be necessary to determine three-dimensional planing forces and pressures experimentally on models of individual hull forms.

3.2 General Considerations

The initial objective of this study was to assess the range of possible impact loads occurring when the helicopter sponson or fuselage first contacts the water. At that stage the problem was seen as one of impact loading, rather than one of gradual immersion and the development of planing and drag forces. During the course of the project, however, it became clear that different physical processes are involved, depending on whether the helicopter falls vertically onto the water surface, or flies into the water at a high forward speed. In the latter case, planing and drag-type forces seem to be at least as important as the initial impact force and the physical processes are highly complex, three-dimensional in character, and not amenable to a straightforward theoretical analysis.

BMT was discouraged from adopting any of the seaplane impact models described in Section 3.1, partly by the apparent complexity of implementing such a model within a Monte Carlo simulation procedure, and partly by comments in [17] about the uncertain level of correlation between theoretical models of this type and experimental data.

With the initial goal of predicting water impact loads only, BMT therefore decided to develop a theoretical model based on conventional design procedures for estimating slam loading on objects impacted by sea waves. Such models are well established in engineering design, are relatively straightforward to implement, and have been validated against measurements.

As in most other water impact loading studies, it was assumed that the peak water impact load on a typical sponson or fuselage panel may be characterised using a slam force equation of the form:

$$F_{\max imp} = \frac{1}{2} C_s \rho A u_p |u_s| \quad (1)$$

where $F_{\max imp}$ is the peak impact force, C_s is the impact force coefficient, ρ is the water density, A is the presented area across which the impact occurs, u_p is the relative velocity of water particles resolved normal to the component, and u_s is the relative velocity of the water surface resolved normal to the component.

An equation of the same general form as (1) is recommended in the Health and Safety Executive's (HSE) Guidance Notes [18] for calculating wave slam loading on members of offshore structures, and similar formulae are widely used in other water impact loading problems, such as slamming on ships' hulls.

The background report to the HSE's Guidance Notes [19] contains extensive guidance on the selection of slam force coefficients for particular applications, and on the use of this formula in design. It also points out, however, that there is considerable variability in values of the slam force coefficient, C_s , that have been obtained from measurements. It is important to take this variability in C_s into account in the design process, together with the variability in other parameters, such as the impact velocities, u_p and u_s , and the impact angle ξ .

The slam force coefficient C_s in equation (1) has several sources of variability, associated with:

- variations in the angle between the structural component and water surface on impact,
- effects of the sea state and water surface roughness,
- inherent variability between different samples from nominally identical conditions.

BMT therefore undertook an extensive literature review [2] to find appropriate information on values of the slam force coefficient, its variability and dependence on the angle of impact and sea state conditions. This review included an initial literature search to identify papers and reports relating to impact forces on cylinders and other objects dropped onto the water surface, forces on fixed cylinders impacted by waves, breaking wave impact loads and slamming on ship hulls. The results contained in many of these papers and reports were considered to be of limited value for this investigation because of:

- the generally high levels of scatter in the results,
- evidence of severe contamination by natural period oscillations of the measurement equipment,
- little information that could be regarded as sufficiently systematic, extensive and reliable,
- and little data that had been analysed sufficiently to allow prediction formulae to be developed.

A small number of reports were investigated in detail, and key results are summarised in Sections 3.3 and 3.4. These particular papers and reports relate to water impact loads on circular cylinders and wedge sections. Further information about papers considered during this review study may be found in Appendix A of reference [2].

Impact Loads on Circular Cylinders

The procedure adopted here (see Section 4.4.1) for estimating water impact loads on the sponson was based primarily on an empirical equation proposed by Ridley [20] for estimating water impact forces on a circular cylinder. Ridley's formula was in turn based on results from an unusually extensive, thorough and systematic series of experiments on circular cylinders dropped onto still water. These experiments were performed by Campbell and colleagues [21, 22] at the Wolfson Unit (Southampton University).

These experiments measured both total forces and pressure distributions. Special care was taken to make the model very stiff (with a high natural frequency of 550 Hz), and to minimise (and correct for) effects of the model's dynamic response. Systematic tests covered cylinders of various diameters, horizontal and oblique water entry, smooth and disturbed water surfaces, smooth and fouled cylinder surfaces, and aerated water.

Campbell [21, 22] proposed an empirical formula for predicting the force time history during a horizontal impact with a smooth water surface, and an associated procedure for estimating impact loads during an inclined impact. This procedure took the form of a 'strip theory', in which the cylinder was treated as many short cylindrical segments, entering the water in succession.

Ridley [20] proposed an alternative formula for predicting the impact force time history, which also fitted the measured data well (see Figure 1). Ridley's formula has since become the basis of a widely-used procedure [19] for estimating wave slamming forces on tubular members of offshore structures. This formula is therefore well-established in offshore design, and seemed to offer a reasonable basis for estimating water impact loads on a helicopter sponson. BMT therefore developed a procedure for estimating loads on the sponson based on Ridley's impact force formula combined with Campbell's 'strip theory' approach.

Key results from Campbell's investigations were as follows:

- (a) When a perfectly horizontal cylinder impacted onto perfectly still water the measured impact force time histories could all be collapsed onto a single curve, as illustrated in Figure 1. The vertical bars in this Figure show the low level of variability between different tests, and represent one standard deviation either side of the mean value at each point in the time-history.
- (b) The maximum value of C_s was found to be very sensitive to small changes in the angle between the cylinder axis and water surface on impact. The peak value of C_s reduced from 5.3 to 2.6 as the cylinder inclination angle changed from 0° to only 1° . Small variations in the angle of impact are likely to be responsible for much of the observed variability in results obtained from slamming experiments in waves.
- (c) Measured values of C_s for inclined cylinder impacts and with a disturbed water surface could be predicted quite well from the time-history of force for horizontal impacts together with 'strip theory'.
- (d) The peak value of C_s for aerated water, and the time at which the peak occurred, were almost identical to those measured in still water, except when the angle of

impact was less than 0.5°. (Campbell's reports do not make it clear whether C_s was calculated using the density of aerated or unaerated water.) The effects of aerated water were ignored during the present study.

Campbell's experiments gave no indication of the effects of wave steepness and breaking. Measurements of slamming loads made by other researchers in very steep and breaking waves (e.g. reference [23]) have generally produced very variable results, which were difficult to interpret and use. The unsystematic nature of test programmes and questionable data quality made it generally difficult to see how to convert published measured data into suitable prediction formulae.

There was nonetheless evidence that the impact force coefficient C_s is more variable when impacts occur in rough water. BMT therefore decided to make the pragmatic assumption that Ridley's formula applies in rough sea conditions, but that the standard deviation of C_s should simply be increased to 1.0.

It was assumed that the sea state could be described as 'rough' or 'smooth', depending on whether the significant wave steepness, S_s , lay above or below a certain threshold value, S_{lim} . The significant wave steepness is defined as:

$$S_s = \frac{2\pi H_s}{g T_z^2} \quad (2)$$

where H_s is the significant wave height, and T_z is the mean zero up-crossing wave period.

Model tests have shown that the effects of entrained air and compressibility become very significant when the water and structure surfaces are smooth and almost parallel at the moment of impact [24]. The impact force varies substantially, depending on the amount of air entrapment, water surface roughness, and the precise angle of impact. It is assumed that the surfaces have sufficient curvature to allow circular cylinder data and formulae to be used.

Results from a numerical study [25] lent support to the assumption that the impact force would be proportional to the local radius of curvature of the structure surface. Forces on cylinders of circular and parabolic section had been predicted using a numerical finite difference model. Maximum forces on the two parabolic models were lower than the maximum force on the circular model, almost exactly in proportion to the radius of curvature of the section at its lowest point.

Figure 1 shows the time history of the force on a smooth horizontal circular cylinder, of diameter D , falling with velocity u onto still water of density ρ . The Figure compares Ridley's [20] empirical formula with Campbell's measured data [21]. Ridley expressed the force per unit length of the cylinder, $F(t)$, in terms of a non-dimensional quantity, $\Phi_s(t)$, and as a function of time t :

$$F(t) = \frac{1}{2} \rho u^2 D \Phi_s(t) \quad (3)$$

where:

$$\Phi_s(t) = C_s \left\{ a_0 + a_1 \exp\left(-b_1 \frac{ut}{D}\right) + a_2 \exp\left(-b_2 \frac{ut}{D}\right) \right\} \quad (4)$$

with the following fitted parameters: mean $C_s = 5.3$, $a_0 = 0.14$, $a_1 = 0.59$, $a_2 = 0.27$, $b_1 = 9.9$ and $b_2 = 54.9$. The first term in equation (4) represents the steady drag force, and $C_s a_0$ is effectively the drag force coefficient. The two exponentially decaying terms in equation (4) represent the effects of the initial impact.

Campbell's experiments considered the vertical drop scenario only, and did not consider the effects of forward speed. BMT therefore made simple intuitive adjustments to the theoretical model to allow for forward speed, based on physical arguments about the nature of the initial impact and drag forces, and about relationships between these forces and the relative velocity between the water and structure surfaces.

Details of procedures used to estimate both the initial impact force and quasi-steady drag force on the sponson are presented in Sections 4.4.1 and 4.6.

3.4 Impact Loads on Wedge Sections

The procedure adopted here for estimating the maximum impact load on a fuselage panel was based on Wagner's [13] wedge impact theory. Wagner's theory is based on a simple expanding flat plate model, and has been applied to a variety of water entry problems. Wagner's theory tends to over-predict maximum impact forces and pressures, when compared with measurements, and there is generally also significant scatter in the measured data, especially when the impact angle between the body and water surface is very small.

Chuang [26] reported results from an extensive and systematic programme of local impact pressure measurements on wedges and cones dropped onto both calm water and regular waves. The results from the tests in waves are of particular interest because wave slamming forces are known to be very sensitive to the shape of the water surface, its roughness and the amount of air entrapment. Figure 22 of Chuang's report [26], reproduced as Figure 2, summarises the results obtained from all of Chuang's tests in regular waves, and compares the results with his own empirical prediction formula (shown as a dashed line). The experimental data show considerable scatter (as is usual in experiments of this type in waves), but the empirical curve lies above the majority of the data.

The coefficient k , shown in Figure 2, is in an unconventional set of units, and is not the same as the usual maximum pressure coefficient, $C_{p \max}$, which may be obtained by setting:

$$C_{p \max} = \frac{p_{\max}}{\frac{1}{2} \rho u^2} = 288 k \quad (5)$$

where p_{\max} is the maximum measured pressure, ρ is the water density, and u is the relevant impact velocity. The angle ξ in Chuang's figure represents the effective impact angle between the structure surface and water surface, taking account of the vessel's trim and heel and the local slope of the water surface.

Entrapped air has a pronounced 'cushioning' effect at small angles of impact, and the impact pressure is very sensitive to small changes in the angle between the structure and water surfaces, to local changes in the surface shape and roughness, and to the degree of aeration. This is the reason why Chuang's empirical curve, shown in Figure 2, falls when the impact angle is small, whereas Wagner's theoretical model

predicts a very steep rise. It is also the reason for the much-increased level of scatter seen in the measured data at small impact angles.

Figure 3 compares maximum pressure coefficients predicted using Wagner's theoretical model [13] with those predicted using Chuang's empirical formula. The pressure coefficient, C_{pmax} , has been plotted against the impact angle, ξ . The two curves approach each other when ξ is greater than 15° , but behave in a very different manner when the impact angle is small. This Figure also shows the highest values of C_{pmax} obtained during Chuang's experiments. These highest values are very scattered, and are up to twice the values predicted by Chuang's formula.

Chuang's experiments measured local impact pressures rather than the impact force acting over the entire wedge surface. Impact pressures vary very rapidly with time, and vary spatially across the wedge face. This means that measurements of maximum local impact pressures give little indication of the magnitude of the impact force. The impact force on the panel as a whole cannot therefore be estimated reliably from Chuang's formulae and data, although it is possible to infer trends and draw some general conclusions.

It seems likely, in fact, that Wagner's theory will predict maximum total impact forces better than maximum local pressures, with less scatter. Chuang's data indicated that Wagner's model should predict maximum impact pressures satisfactorily when the impact angles is greater than about 10° to 15° . Maximum forces will probably be predicted satisfactorily down to lower impact angles.

Wagner's theory predicts that the force will tend to infinity as the impact angle tends to zero. The predicted behaviour is clearly unrealistic, and the force must be limited in practice by physical effects such as water compressibility. The force is therefore likely to level off at small impact angles. The calculation procedure used here was therefore based on Wagner's theoretical model [13], with a constant upper limit value at small impact angles.

The maximum impact force on the fuselage panel, $F_{max imp}$, was expressed in the form:

$$F_{max imp} = \frac{1}{2} C_o \rho u_p u_s W L \Phi_w(\xi) \quad (6)$$

where the non-dimensional quantity, Φ_w , has the form:

$$\Phi_w(\xi) = F_w(\xi) \quad \text{for } \xi \geq \xi_{min} \quad (7)$$

$$\Phi_w(\xi) = F_w(\xi_{min}) \quad \text{for } \xi < \xi_{min} \quad (8)$$

and $F_w(\xi)$ is the corresponding expression given by Wagner's theory. The minimum angle ξ_{min} was set equal to 2 degrees, which is the limit at which the Chuang formula starts to fall to zero.

The mean value of C_o in equations (7) and (8) was set equal to 1.0. C_o was then allowed to vary at each step in the simulation process, by use of a random sampling procedure, in order to represent random variability in the impact loading process.

Figure 4 compares values of $\Phi_w(\xi)$, defined using equations (7), (8) and (15), with the equivalent values obtained using the original Wagner theory.

Wagner's theory represents the initial impact force in vertical drop conditions only, and does not consider the effects of forward speed. Mayo [14] and Arlotte et al. [17] reviewed some of the many attempts made to enhance Wagner's theory and take account of forward speed. None of these enhancements seem to have been entirely satisfactory when compared with measured data. BMT therefore made simple intuitive adjustments to the theoretical model to allow for forward speed, based on physical arguments about relationships between the impact force and the relative velocity between the water and structure surfaces.

Mayo's and Arlotte's reviews indicated that planing forces are likely to become important when the helicopter has a high forward speed on contact with the water. A planing force term was therefore added, based on a simple theoretical model of a planing flat plate (equation 6.13.20 of [27]).

Procedures used to estimate both the initial impact force and quasi-steady planing force on the fuselage panel are described in Sections 4.4.2 and 4.6.

4 THEORETICAL BASIS

4.1 Assumptions

As in most other studies on wave slamming, such as [20], it is assumed that the surface of the water is an inclined flat plane, and that the water surface velocity is effectively uniform over the area spanned by the relevant structural component (i.e. the sponson or fuselage panel). These assumptions effectively mean that the dimensions of this component are small compared with distances over which the water surface slope varies. Local variations in water surface conditions, such as surface roughness and broken water, will be taken into account by varying the slam coefficient, C_s , rather than by varying the flow conditions.

The helicopter hull, sponson and water surface have complex three-dimensional surfaces, and it is impractical to model these in detail. The structure and water surfaces were therefore simplified in order to make the problem manageable:

- the water surface was assumed to be flat, but inclined to the horizontal,
- the sponson was modelled using 'strip theory' as a number of circular cylinder and cone segments with a common axis,
- the fuselage panel was modelled as an inclined flat plate.

The dynamic behaviour of the helicopter as a whole was ignored. The impact duration was assumed to be short enough for changes in helicopter speed, descent angle and attitude to be ignored, at least up to the instant when the maximum impact load occurs.

The maximum total impact force, $F_{max\ tot}$, was assumed to be the sum of a maximum initial impact force, $F_{max\ imp}$, and a quasi-static drag or planing force, F_d :

$$F_{max\ tot} = F_{max\ imp} + F_d \quad (9)$$

The analysis considered scalar force magnitudes only, and took no account of the vector directions in which the forces act.

Effects of hull shielding are treated in a very simplified manner. The sponsons are assumed to be far enough from the hull to experience no benefits from shielding whatsoever. The panels are assumed to be part of the hull, however, and are assumed to be totally protected by the helicopter's hull if impact occurs while they are inclined upwards, away from the water surface. In these circumstances the impact force is set to zero. No other shielding effects are represented, because the model knows nothing about the remainder of the hull. Clearly this is a highly simplified way in which to treat what is really a very complex hydrodynamic phenomenon.

It is difficult to know what the real effects of shielding are likely to be, and the present model may either overstate or understate the benefits of shielding, depending on where the panels and sponsons are located, and how the hull hits the water. In one respect BMT's model overstates the benefits, because it assumes that an upward-facing panel will survive a high speed impact, whereas the hull itself would fail in these circumstances.

4.2 **Monte-Carlo Simulation Procedure**

A Monte Carlo simulation procedure was used to develop probability distributions of maximum water impact loads on the sponson and fuselage panel. This procedure involved calculating maximum impact loads based on random samples from probability distributions of the various input parameters. The impact force corresponding to a given set of input parameters was calculated in a deterministic manner.

The main steps in the Monte Carlo simulation procedure were as follows:

- (a) sample randomly from each of the relevant distributions of input parameters,
- (b) calculate (deterministically) the maximum hydrodynamic impact force and structural force corresponding to this particular random combination of selected parameters,
- (c) repeat this sampling process a large number (20,000) of times,
- (d) derive probability distributions of the resulting maximum forces, and the probability of exceeding a specified design value.

4.3 **Input Parameters**

The maximum impact force depends on a range of parameters describing the speed, descent angle and attitude of the helicopter at the instant of impact, and local water surface conditions. Random variations in each of the following input parameters were considered:

- the impact force coefficient,
- the forward speed of the helicopter,

- its angle of descent,
- its roll, pitch and yaw angles on entry into the water,
- its heading angle relative to waves,
- the joint distribution of significant wave heights and periods, representing all sea states in which the impact may occur,
- individual values of wave steepness and phase angle in each sea state.

Most of these parameters were assumed to be normally distributed, and the distributions were defined in terms of mean values and standard deviations. Random samples from each of these distributions were obtained by standard numerical sampling procedures. There is no particular evidence to suggest that many of these parameters are normally distributed in practice, and one might in fact expect some of them (such as the helicopter's forward speed) to be skewed. Normal distributions were nonetheless assumed for reasons of convenience and consistency, and in the absence of an obvious alternative model. The main aim was to achieve a representative amount of variability, and a representative mean value of each parameter.

4.4 Initial Water Impact Forces

Details of the formulae and procedures used to calculate maximum impact loads on the sponson and fuselage panel may be found in Appendices B to H of reference [2]. Key equations only are reproduced here.

The maximum initial impact force was calculated using an approach recommended by the UK Health and Safety Executive (HSE) for calculating wave slamming loads on members of offshore structures [18, 19]. The peak hydrodynamic impact force, $F_{\max imp}$, on a typical sponson or fuselage panel was represented by a slam force equation of the form:

$$F_{\max imp} = \frac{1}{2} C_s \rho A u_p |u_s| \quad (10)$$

where C_s is the slam force coefficient, ρ is the water density, A is the presented area across which the impact occurs, u_p is the relative velocity of water particles resolved normal to the component, and u_s is the relative velocity of the water surface resolved normal to the component.

Figure 5 illustrates typical relationships between the helicopter velocity, \underline{u}_h , the water surface velocity, \underline{u}_w , the relative particle velocity, \underline{u}_p , the relative surface velocity, \underline{u}_s , and the resolved components, u_p and u_s . The formulae used to calculate these parameters may be found in Appendices B and C of [2].

The two velocities u_p and u_s have similar magnitudes in circumstances where the helicopter descends almost vertically into the water, but have very different magnitudes when the helicopter has a high forward speed and low rate of descent at the instant of impact. It is therefore important to distinguish clearly between u_p and u_s , and appropriate adjustments were made to various empirical formulae in order to represent these two velocities correctly.

The initial impact force depends on the rate of change of fluid added mass as the helicopter enters the water. The rate of entry into the water depends on the relative velocity between the structure surface and water surface, and therefore depends on u_s . The added mass at any given immersion depth depends on the relative velocity between water particles and the structure surface, and therefore depends on u_p . The rate of change of added mass (and therefore the impact force) therefore depends on the product of these velocities, $u_p u_s$.

Extending this intuitive argument further, it is reasonable to assume that the immersion time and impact duration will depend on the rate of entry into the water, and therefore on u_s alone. The impulse (defined as the force integrated over time, and representing the change of fluid momentum on impact) will depend on the total change in fluid added mass, and therefore on u_p alone.

4.4.1 *Maximum Impact Force on the Sponson*

The maximum impact force on the sponson was calculated using empirical equations describing the slam force on a horizontal circular cylinder dropped onto smooth water. As discussed in Section 3.3, these equations were proposed by Ridley [20], and were based on experimental measurements by Campbell and colleagues [21, 22]. These equations, (3) and (4), contain both constant and impulsive terms. The constant term, involving a_0 , represents the drag force, which develops as the cylinder becomes fully immersed. The two exponentially decaying terms, involving a_1 and a_2 , represent the initial impact force. The quasi-steady and impulsive terms are considered separately in the analysis.

Campbell [21] found that measured peak impact forces on inclined cylinders agreed very well with predictions based on a 'strip-theory' procedure combined with force coefficients for horizontal impacts. A similar approach has therefore been adopted here. The total force on a cylinder inclined to the water surface was calculated as the sum of contributions from short longitudinal segments or 'strips' of the cylinder. The force on each short segment was calculated as if its axis was parallel to the water surface on impact.

The impact force on a short segment of the cylinder was therefore calculated using equations (3) and (4). The force on the complete cylinder was then calculated by adding contributions from all the short segments, taking account of the fact that they enter the water in succession. The impact force on a horizontal cylinder is at a maximum when it first makes contact with the water, whereas the impact force on an inclined cylinder rises initially, then approaches a constant value until it becomes fully immersed. The maximum impact force in this second case occurs when the cylinder is just fully immersed.

Using equation (3) and (4), it may be shown (see Appendix D of [2]) that the maximum initial impact force, $F_{\max imp}$, on a cylindrical component of length L and diameter D inclined with its axis at an angle β to the water surface, is given by the formula:

$$F_{\max imp} = \frac{1}{2} C_s \rho u_s u_p D \Phi_c(L, \beta) \quad (11)$$

where:

$$\Phi_c(L, \beta) = \left[\frac{a_1 D}{b_1 \tan \beta} \left\{ 1 - \exp\left(-b_1 \frac{L \tan \beta}{D}\right) \right\} + \frac{a_2 D}{b_2 \tan \beta} \left\{ 1 - \exp\left(-b_2 \frac{L \tan \beta}{D}\right) \right\} \right] \quad (12)$$

Special limiting forms of this equation have to be considered when β approaches 0 or 90 degrees.

The impulse associated with immersing a length L of the cylinder is:

$$J = \frac{1}{2} C_s \rho u_p D^2 L \left\{ \frac{a_1}{b_1} + \frac{a_2}{b_2} \right\} \quad (13)$$

The sponson was modelled as a parallel-sided cylinder, together with a 'nose cone'. The force on the nose cone was calculated in the same manner as on the circular cylinder but using velocity components, u_s and u_p , normal to the cone's surface at the point of first impact, rather than velocity components normal to the cylinder axis.

The impact force coefficient, C_s , was assumed to have the mean value proposed by Ridley [20], but was allowed to vary in a random manner about that mean in order to allow for the variability observed in practice. Greater variability was assumed to occur in steeper wave conditions.

4.4.2 *Maximum Impact Force on the Fuselage Panel*

As noted in Section 3.4, the Wagner theoretical model [13] seemed to be a reasonable basis from which to calculate impact forces on the fuselage panel. The theory was nonetheless modified, as shown in equations (7) and (8), by imposing a minimum impact angle, $\xi = \xi_{\min}$, below which the impact force coefficient was assumed to remain constant. Intuitive arguments were then used to extend Wagner's theory from vertical impacts onto a horizontal surface to non-vertical impacts with forward speed onto an inclined water surface.

In accordance with equations (6), (7) and (8), the maximum impact force, $F_{\max imp}$, on a panel of width W and length L , inclined at an angle ξ to the water surface, was expressed in the form:

$$F_{\max imp} = \frac{1}{2} C_o \rho u_p u_s W L \Phi_w(\xi) \quad (14)$$

where (see Appendix E of [2]):

$$\Phi_w(\xi) = \frac{\pi^2}{2 sz cz} \quad (15)$$

$$\begin{aligned} sz &= \sin \xi \quad \text{when } |\sin \xi| \geq sz_{\min} \\ sz &= sz_{\min} \quad \text{when } |\sin \xi| < sz_{\min} \end{aligned} \quad (16)$$

$$\begin{aligned} cz &= \cos \xi \quad \text{when } |\cos \xi| \geq sz_{\min} \\ cz &= sz_{\min} \quad \text{when } |\cos \xi| < sz_{\min} \end{aligned} \quad (17)$$

$$sz_{\min} = \sin \xi_{\min} \quad (18)$$

The impulse, J , is given by:

$$J = \frac{\pi \rho u_p W^2 L}{4} \quad (19)$$

The purpose of the parameter C_o in equation (14) was to allow the impact force to vary in a random manner. C_o was sampled from a normal distribution with a mean value of 1.0. The standard deviation of the distribution was chosen to represent the level of variability observed in practice. Greater variability was assumed to occur in steeper wave conditions.

4.5 Structure Loads

Equations (11) and (14) describe hydrodynamic forces acting externally on the sponson and panel surfaces. The maximum force experienced within the structure depends on the duration of the external force, and on the way in which the structure responds. These in turn depend on the helicopter's structural properties.

The relationship between the impact force and the structure's response is complex, even when the structure is a simple single-degree-of-freedom, linear, spring/ mass/ damper system. The maximum response depends on the time-history of the impact force as well as on the characteristics of the structure. BMT therefore undertook an initial feasibility study to find a practical and justifiable procedure for estimating the maximum structure force analytically, without having to calculate the full response time history, and bearing in mind the necessary structural simplicity of the model. Initial attempts were based on use of the Laplace transform of the impact force history, and an assumed delay time between the initial impact and the maximum response. It quickly became clear, however, that the relationship between the force history and maximum response is complex, involving various different time scales, and simple assumptions about the delay time proved to be unsatisfactory.

A more straightforward and approximate approach was therefore adopted, based on considering both ends of the range of impact loading types. The structural loading process was assumed to be either impulsive or quasi-static in character, depending on whether the impact duration was short or long compared with the structure's natural response period.

The impact duration was estimated from the maximum impact force and the impulse (change in fluid momentum) associated with the impact. The response was assumed to be quasi-static in character if the impact duration was less than the natural response period divided by π , and impulsive in character if greater than the natural response period divided by π . The factor π was introduced simply in order to avoid discontinuities where the two load type ranges meet. If the response was considered to be quasi-static in character, then the structure force was set equal to the impact force. If it was impulsive in character, the maximum deflection of the structure was estimated, assuming a delta-function (i.e. an instantaneous 'spike') type of loading, and a linear spring/ mass/ damper system with low damping.

According to equation (2.63) of Bartrop and Adams [28], the response $x(t)$ of a single-degree-of-freedom linear system, which has mass m and damping ratio ζ , to an impulse J is:

$$x(t) = \left(\frac{J}{m\omega_d} \sin(\omega_d t) \right) \exp(-\zeta \omega_n t) \quad (20)$$

where ω_n and ω_d are the undamped and damped natural frequencies respectively. If the response is lightly damped, ζ is small and $\omega_d \approx \omega_n$. The maximum deflection is then:

$$x_{\max} = \frac{J}{m\omega_n} = \frac{\omega_n J}{c} \quad (21)$$

and the maximum structural force is:

$$F_{r \max} = c x_{\max} = \omega_n J \quad (22)$$

These equations apply only when the duration of the impact force, T_{imp} is short compared with the structure's natural response period, T_n . If T_{imp} is long compared with T_n , the response is quasi-static and a better approximation to the maximum structure force is:

$$F_{r \max} = F_{\max imp} \quad (23)$$

The impact duration may be estimated assuming that the impact force history is triangular in form. In this case:

$$T_{imp} = \frac{2J}{F_{\max imp}} \quad (24)$$

It may then be shown (see Appendix F of [2]) that the maximum structure force is approximately:

$$F_{r \max} = \omega_n J \quad \text{when } T_n > \pi T_{imp} \quad (25)$$

$$F_{r \max} = F_{\max imp} \quad \text{when } T_n \leq \pi T_{imp} \quad (26)$$

These equations assume that the impact duration is either very short or very long, and that there is no possibility of structural resonance causing dynamic amplification of the structural load. They are intended to provide a simple means of estimating a typical magnitude (rather than the precise value) of the maximum structural force. These assumptions mean that the calculated maximum structure force, F_{\max} , is never greater than the maximum hydrodynamic impact force, $F_{\max imp}$.

The kinetic energy transferred to the water and the energy absorbed by the structure were calculated from the impulse, entry speed and structure response. The relevant equations may be found in Appendix F of [2].

4.6 Drag and Planing Forces

Drag and planing forces are likely to become important when the helicopter has a high horizontal speed on entry into the water. These forces have a quasi-steady character, and continue to act while the helicopter moves through the water.

The physical processes giving rise to drag and planing forces are very different from those associated with the initial impact force, despite the outwardly similar forms of the force formulae. Drag and planing forces depend on the instantaneous values of particle velocities around the structure, but are relatively insensitive to its rate of immersion. They are therefore likely to depend on the normal component of the particle velocity squared, u_p^2 , rather than on the product of the particle velocity and immersion velocity $u_p u_s$. Both types of forces were therefore assumed to have the form:

$$F = \frac{1}{2} C_F \rho A u_p^2 \quad (27)$$

where C_F is the relevant force coefficient, and A is the area presented to the flow.

The full importance of drag and planing forces was recognised at a fairly late stage in the development of BMT's simulation model. Available evidence suggested a fairly complex relationship between these forces and the helicopter's flight parameters, but the form of this relationship was not clear. A simple and intuitive relationship was therefore assumed in the simulation model, more to ensure that drag and planing forces were included than to represent them in an accurate quantitative manner. Thus drag forces alone were assumed to act on the sponson, and planing forces alone on the fuselage panel, on the grounds that these were considered likely to be the dominant components of quasi-steady loading in each case.

4.6.1 *Drag Forces on the Sponson*

The drag force on a cylindrical component of the sponson, of diameter D and length L , is assumed to have the form:

$$F_d = \frac{1}{2} C_d \rho D L u_p^2 \quad (28)$$

where the drag force coefficient, C_d , is related to the parameters C_s and a_0 in Ridley's formula (equations (3) and (4)) using $C_d = C_s a_0$. Ridley's proposed mean values of these two parameters ($C_s = 5.3$ and $a_0 = 0.14$) result in $C_d = 0.74$, which is a typical value of the drag force coefficient for a smooth cylinder.

The drag force is represented here as a quasi-steady component of the impact force. This means that the drag force coefficient, C_d , varies in the same random manner as the impact force coefficient, C_s . This is an artificial assumption but probably had relatively little effect on the end results, bearing in mind the model's relative insensitivity to variations in C_s (see Tables 6.2 and 6.3).

The drag force reaches a maximum value when the cylinder is just fully immersed, if speed losses during impact are ignored. Maximum impact and drag forces are therefore likely to occur at approximately the same time, justifying the simple addition of these two components so as to obtain an estimate of the 'total' impact force.

4.6.2 *Planing Forces on the Fuselage Panel*

Several alternative formulae have been proposed in the past [17] for estimating planing and combined impact-planing forces. The choice of appropriate formulae is complex, and was considered to be beyond the scope of the present project. The force was therefore assumed to have the same form as the drag force, and was

estimated using a theoretical solution (equation 6.13.20 of [27]) for the force on a planing plate of width W and length L , with a void behind it, inclined at an angle α to a steady flow with incident velocity u . This force is:

$$F_{pl} = \frac{\pi \sin^2 \alpha}{\pi \sin \alpha + 4} \rho u^2 L W \quad (29)$$

The normal component of the incident velocity, u_p , is effectively $u \sin \alpha$, and so the planing force may be written:

$$F_{pl} = \frac{\pi}{\pi \sin \alpha + 4} \rho u_p^2 L W \quad (30)$$

where:

$$\alpha = \sin^{-1} \frac{u_p}{|u_p|} \quad (31)$$

This formula for the planing force on a flat plate has a lift component, at right angles to the flow direction. Lift forces were otherwise ignored.

Wagner's theory shows that the impact force reaches a maximum value when the panel is just fully immersed. The planing force also reaches a maximum value when the panel becomes fully immersed, if speed losses during impact are ignored. The 'total' impact force was therefore calculated by simply adding the maximum impact and planing forces.

Equation (30) may be written in the same general form as equation (27):

$$F_{pl} = \frac{1}{2} C_{pl} \rho L W u_p^2 \quad (32)$$

where the planing force coefficient, C_{pl} , is defined as:

$$C_{pl} = \frac{2\pi}{\pi \sin \alpha + 4} \quad (33)$$

The planing force coefficient was therefore regarded as a fixed quantity during this investigation, with no random variations of any kind. Bearing in mind the comment made earlier about variability in C_d , however, it seems likely that ignoring the variability in C_{pl} probably had relatively little effect on the end results.

5 MAIN STUDY

The next stage of the investigation took the form of a case study, based on data for the *Sea King* helicopter. Sample calculations were performed to identify the range of water impact loading on a typical sponson and fuselage panel, covering a range of alternative water impact scenarios and types of incidents considered to be survivable. Four basic types of incident were considered, and the case study considered a range of helicopter speeds, descent angles, attitudes and sea states at the instant of impact.

These calculations were performed using a computer model to perform Monte Carlo simulations of many thousands of such impacts in order to develop probability distributions of the impact force, and to provide an understanding of relationships between the impact force, the helicopter's condition, sea state and other parameters. The theoretical basis of this simulation model is described in Section 4, and results from a simulation study performed using this model are presented in Section 5.4.

The main aims of this part of the investigation were to help identify:

- (a) which parameters are important and which are unimportant in each of the four incident scenarios,
- (b) the range of impact load variability,
- (c) whether the risks of exceeding design load values are large or small,
- (d) the likely cost-effectiveness of design modifications.

5.1 Helicopter Details

Information about the *Sea King* helicopter, and about a typical fuselage-mounted emergency flotation system, were supplied by GKN Westland Helicopters Limited (GKN WHL) [29]. GKN WHL also provided basic information about the sponsons of the civil Sikorsky *S61N* helicopter, stating that they believed the sponson system of the *Sea King* to be similar to that of the *S61N* in terms of structure strength and failure characteristics. GKN WHL noted, however, that the breadth of the sponson on the *S61N* is 1.31m, which is substantially wider than the 0.84m sponson breadth on the *Sea King*, and is therefore likely to attract higher impact loads.

Two types of emergency flotation equipment were considered during this investigation. Flotation equipment is typically located in two sponsons, which are part of the wheel support assembly, and under two panels, one on either side of the nose section of the fuselage. These two flotation unit locations are illustrated in Figure 6. Figure 7 shows plan and side views of the starboard sponson on the *Sea King*.

The flotation equipment was assumed to be uninflated when the craft impacted onto the water surface. Failure was therefore considered to be due to structural failure of the sponson support assembly, or failure of the fuselage panel cover.

5.2 Impact Loading Scenarios

Following discussions with the CAA it was agreed that four basic types of incident should be considered:

- (a) a controlled ditching,
- (b) a vertical descent incident, representing a helicopter falling off the helideck of an offshore platform,
- (c) a loss of control incident, where the helicopter descends into the water following mechanical failure or pilot error,
- (d) a fly-in incident, at a high forward speed and shallow descent angle.

These four scenarios, and the parameters used to describe them, were initially based on incident types and descriptions in a GKN WHL report [8]. The parameter ranges were adjusted following discussions with the CAA, and the values finally selected are described in Section 5.3. Parameter ranges for the last three incident types were adjusted to identify them more closely with actual events: the *Brent Spar* accident in July 1990, the *Cormorant Alpha* accident in March 1992, and the *Scilly Isles* accident in July 1983, which were considered representative of vertical descent, loss of control and fly-in types of incident respectively. These three incidents were also being used as the basis for the associated WS Atkins study [1].

Ranges of horizontal and vertical craft speeds, attitudes and angles of impact were considered in each of these cases. The analysis also considered variations in the significant wave height and period, the steepness of individual waves, the degree of water surface roughness, and the inherent variability of the impact force coefficient, C_s . Variations in each of these parameters resulted in a range of possible impact loads for each selected incident scenario.

A Monte Carlo simulation procedure was developed in order to sample randomly from probability distributions of each of these parameters, and thus obtain a large number of random samples of water impact loads. These samples were then analysed to obtain probability distributions of impact loads, together with the associated structure loads, impulses and kinetic energies. The predicted impact load distributions were then compared with structural design load values for the *Sea King* helicopter, supplied by GKN WHL. These design load values included maximum total forces that can be resisted by the main sponson support struts, and the maximum design pressure for the fuselage panel.

5.3 **Conditions Represented**

5.3.1 *Sea Conditions*

Two alternative sets of sea conditions were considered during this investigation in order to demonstrate the effects of waves on the impact loading process:

- (a) all-year conditions for the central area of the North Sea,
- (b) a completely calm sea with no waves.

The calculations for the central area of the North Sea were based on the all-year, all-directions scatter table of significant wave heights, H_s , and zero-crossing periods, T_z , obtained from BMT's *PC-Global Wave Statistics* database. It was assumed for present purposes that there are no weather restrictions on helicopter operations, and sea states were sampled randomly from the entire scatter table. The central North Sea scatter table used in this analysis is shown in Table 5.1.

Table 5.1: Scatter table of significant wave heights and zero-crossing periods: central North Sea, all-year, all-directions.

European Database

Sig. Hgt. (m)	AREA No.	12	36	161	293	272	153	60	18	5	1	0	1000
	ALL DIRECTIONS = 100.00% Obs.												
	-----+-----												
>14	0	0	0	0	0	0	0	0	0	0	0	0	1
13-14	0	0	0	0	0	0	0	0	0	0	0	0	0
12-13	0	0	0	0	0	0	0	0	0	0	0	0	1
11-12	0	0	0	0	0	0	0	0	0	0	0	0	1
10-11	0	0	0	0	1	1	1	1	0	0	0	0	2
9-10	0	0	0	0	1	1	1	1	0	0	0	0	4
8- 9	0	0	0	1	2	2	2	1	1	0	0	0	7
7- 8	0	0	0	2	4	4	4	2	1	0	0	0	13
6- 7	0	0	1	4	7	7	7	4	2	0	0	0	25
5- 6	0	0	2	8	14	12	12	7	2	1	0	0	45
4- 5	0	0	4	17	27	21	21	10	3	1	0	0	83
3- 4	0	1	10	36	48	32	32	13	4	1	0	0	144
2- 3	0	2	26	70	73	39	39	13	3	1	0	0	227
1- 2	0	8	57	103	75	29	29	7	1	0	0	0	281
0- 1	2	25	61	51	20	5	5	1	0	0	0	0	165
	-----+-----												
		4- 5	6- 7	8- 9	10-11	12-13							
		< 4	5- 6	7- 8	9-10	11-12	>13						
	Zero Crossing Period (s)												

5.3.2 Impact Force on the Sponson

The maximum initial impact and drag forces on the sponson elements were calculated using equations (11), (12) and (28). The parameters in these equations took the values: mean $C_s = 5.3$, $a_0 = 0.14$, $a_1 = 0.59$, $a_2 = 0.27$, $b_1 = 9.9$ and $b_2 = 54.9$. These equations and the parameter values were based on an empirical equation (3) proposed by Ridley [20]. Table 5.2 summarises the impact force equation parameters used in the simulations.

Very little information was available about the way in which the force coefficients vary when the water surface is broken. There was nonetheless evidence that the impact force coefficient C_s is more variable when impacts occur in rough water. Following results in [21, 20], the standard deviation of the force coefficient was assumed to be 0.15 when the water was reasonably 'smooth', and was increased to 1.0 in 'rough' water. There is no precise dividing line between smooth and rough water conditions, and a limiting upper bound value of the significant wave steepness, S_s , shown in equation (2), for 'smooth' water was assumed (somewhat subjectively) to be $S_{lim} = 0.07$. Sea states with S_s less than 0.07 were regarded as 'smooth', and sea states with S_s greater than 0.07 were regarded as 'rough'.

Table 5.2: Impact force equation parameters for the sponson		
	'Smooth' water	'Rough' water
Mean C_s	5.3	5.3
standard deviation	0.15	1.0
a_0	0.14	0.14
a_1	0.59	0.59
a_2	0.27	0.27
b_1	9.9	9.9
b_2	54.9	54.9
S_{lim}	0.07	

5.3.3 *Impact Force on the Fuselage Panel*

The maximum impact and planing forces on the fuselage panel were calculated using equations (14), (15) and (30). Table 5.3 summarises the impact force equation parameters used in the simulations. The Wagner theory applies only when the impact angle, ξ , is larger than a specified lower limit value, ξ_{min} . This lower limit value was set equal to 2 degrees, as discussed in Section 3.4.

The mean value of C_o in equation (14) was set equal to 1.0, in order to make the mean force equal to that obtained using the Wagner theoretical model. The standard deviation of C_o was set equal to 0.2 in 'smooth' water, and 0.4 in 'rough' water. Once again the limiting value of the significant wave steepness, shown in equation (2), for smooth water was assumed to be $S_{lim} = 0.07$.

Table 5.3: Impact force equation parameters for the fuselage panel		
	'Smooth' water	'Rough' water
Mean C_o	1.0	1.0
standard deviation	0.2	0.4
ξ_{min}	2.0°	2.0°
S_{lim}	0.07	

5.3.4 *Impact Scenarios*

Eight base case Monte Carlo simulation runs were performed in order to calculate the probability distributions of water impact loads on:

- the selected sponson and fuselage panel,
- in the four selected incident scenarios outlined in Section 5.2 (controlled ditching, vertical descent, loss of control, and fly-in),
- in central North Sea wave conditions.

Codes used to identify these eight base-case simulation runs are listed in Table 5.4.

Table 5.4: Simulation run identification codes: central North Sea conditions.				
	Controlled ditching	Vertical descent	Loss of control	Fly-in incident
Sponson	SPNDT1	SPNVD1	SPNLC1	SPNFL1
Fuselage panel	PANDT1	PANVD1	PANLC1	PANFL1

Table 5.5: Parameters used to describe impact scenarios				
Scenario	Controlled ditching	Vertical descent	Loss of control	Fly-in incident
Mean speed standard deviation	15 m/s 1 m/s	20 m/s 2.5 m/s	25 m/s 5 m/s	35 m/s 6 m/s
Mean descent angle standard deviation	5° 1°	90° 20°	25° 10°	3° 1°
Mean roll angle standard deviation	0° 1°	0° 20°	0° 20°	0° 1°
Mean pitch angle standard deviation	5° 1°	0° 10°	0° 10°	0° 1°
Mean yaw angle standard deviation	0° 5°	0° 20°	0° 10°	0° 5°
Mean angle to waves standard deviation	0° 5°	60° 60°	60° 60°	60° 60°

The simulations covered ranges of helicopter speeds, attitudes and descent angles considered to be representative of each of these four scenarios. Table 5.5 summarises key parameters used in the calculations. The actual value used at each step in the Monte Carlo simulation was obtained by sampling from a normal distribution with the specified mean value and standard deviation. 20,000 alternative combinations of the input parameters were considered during each simulation run. Exceedance probability distributions of water impact loads were then constructed for each incident scenario.

It was assumed that the helicopter pilot will normally attempt to land head into waves during a controlled ditching, but the heading relative to waves will be more random during vertical descent, loss of control or fly-in incidents.

5.3.5 *Modelling the Sponson*

The starboard sponson of the *Sea King* helicopter was modelled as a circular cylinder with a 'nose cone'. The total length and breadth of this model are the same as those of the actual *Sea King* sponson, which is illustrated in Figure 7. Key information about the sponson was supplied in two GKN WHL faxes [29], dated 6 February and 27 February 1997.

The total length of the sponson is 2.58m, and its breadth is 0.84m. It is modelled as two segments:

- (a) a cylinder with parallel sides representing the rear 2.12m of the sponson's length,
- (b) a 'nose-cone' representing the forward 0.46m of the sponson's length, with the nose cone sides inclined at an angle of 30° to the cylinder axis.

The sponson is attached to the helicopter fuselage through two struts. According to GKN WHL [29], these struts are designed for the following maximum failure loads: 207 kN in the vertical direction, 164 kN in the fore-aft direction, and 239 kN in the transverse direction.

The corresponding maximum deflections of the sponson under failure loading are: 6mm in the vertical direction, 46mm in the fore-aft direction, and 24mm in the transverse direction.

For the purpose of estimating stiffnesses and natural frequencies of the sponson mounting system it was assumed that the load/deflection relationships are linear, so that the stiffnesses are: 35.5 MN/m in the vertical direction, 3.6 MN/m in the fore-aft direction, and 9.9 MN/m in the transverse direction. Discussions with GKN WHL suggested that the design deflections include some plastic deformation, although the linear load/deflection assumption is likely to be sufficiently accurate for the purposes of this study.

The natural periods depend on the mass of the sponson system, including its added mass when in contact with the water. The added mass is likely to represent a large part of the total mass, and varies continuously as the sponson enters the water. For present purposes it is assumed that the total mass of the sponson system is half of its total displaced mass. If the sponson is an ellipsoid with principal axes of lengths 2.58m, 0.84m and 0.84m, half of its displacement mass in sea water is approximately 0.5 tonnes. The natural periods of the sponson are therefore approximately: 0.02s in the vertical direction, 0.07s in the fore-aft direction, and 0.04s in the transverse direction.

A single characteristic value of stiffness and natural period had to be selected for use in the calculations. It was not immediately obvious which values should be chosen, because the sponson is inclined at about 11° to the horizontal (upwards at the front), and the analysis took no account of force direction. It was decided to use the fore-aft component, however, on the grounds that the sponson supports are most flexible in this direction, and so dynamic effects are likely to be most apparent in this direction. Table 5.6 therefore summarises key sponson parameters used in the analysis.

Length	2.58m
Breadth	0.84m
Inclination to horizontal	11°
Design maximum load (fore-aft)	164 kN
Design maximum deflection	46 mm
Stiffness (fore-aft)	3.6 MN/m
Natural period (fore-aft)	0.07 s

5.3.6 *Modelling the Fuselage Panel*

Details of the fuselage panel were contained in two GKN WHL faxes, dated 6 February and 14 May 1997 [29]. A single panel on the starboard side of the helicopter's nose was modelled.

The area of the fuselage panel was approximately 0.165 m², and it was approximately 0.6m long. The effective panel width was therefore 0.275m. The panel was considered to have failed if the pressure exceeded 0.1288 N/mm². The failure force was therefore approximately 21.3 kN.

The attitude of the panel was described by three inclination angles, representing successive clockwise rotations of an initially vertical panel facing to starboard, about axes pointing forwards, to starboard, and downwards. The panel was inclined at an angle of 14° to starboard, 0° (level) in the fore-aft direction, and -10° relative to the forward direction.

Associated maximum displacements of the panel were not available. It was therefore assumed that the natural period of the panel and its supports was approximately 0.01s, and its effective mass was the added mass of a flat plate with the same area. The effective total mass was therefore approximately 0.02 tonnes, the panel's effective stiffness was approximately 7.2 MN/m, and the displacement associated with the failure load was 3mm. Discussions with GKN WHL suggested that these were reasonable order-of-magnitude estimates, and should be sufficient for the purposes of this study.

Table 5.7 summarises key panel parameters used in the calculations.

Length	0.6m
Width	0.275m
Inclination about roll axis	14°
Inclination about pitch axis	0°
Inclination relative to forward direction	-10°
Design maximum load	21.3 kN
Estimated maximum deflection	3 mm
Stiffness	7.2 MN/m
Natural period	0.01 s

5.4 Results

Results from each Monte Carlo simulation run were presented [2, 3] in two alternative ways:

- correlation plots illustrating relationships between the total impact force and other simulation parameters, based on the first 200 points from each simulation,
- exceedance probability distributions of the total hydrodynamic impact force, based on the full 20,000-point simulation.

5.4.1 Correlation Plots

Figures 8 to 15 illustrate relationships between simultaneous estimates of the maximum total hydrodynamic impact force on the sponson and corresponding estimates of the maximum structure force and drag force. These correlation plots are based on the first 200 samples from each 20,000-point simulation run. Each quantity is plotted against the corresponding value of the maximum total impact force.

Corresponding results for the fuselage panel are shown in Figures 16 to 23. These figures show relationships between estimates of the maximum total impact force and corresponding estimates of the structure force and planing force.

Figures 24 to 27 show sample results illustrating relationships between the maximum total impact force, impact duration, the impact velocities u_p and u_s , and the impact angle β for the sponson in a vertical descent incident. Corresponding results for the fuselage panel are shown in Figures 28 to 31.

Equation (24) suggests an approximately inverse relationship between the duration and severity of an impact. This seems intuitively reasonable. The maximum force on a panel or sponson tends to increase rapidly as its surface becomes more parallel to the water surface on impact, but at the same time it enters the water more quickly, reducing T_{imp} . Figures 24 and 28 therefore show the **inverse** of the impact duration, $1/T_{imp}$, plotted against the maximum impact force, $F_{max\ imp}$.

A number of conclusions were drawn from the correlation plots:

- The duration of each impact event was generally longer than the relevant natural period. The structural load predicted by the simple structural response model was therefore equal to the hydrodynamic impact load, suggesting that the loading would be essentially quasi-static in character.
- Drag forces on the sponson were found to represent a large proportion of the total impact force in all four types of incident. Planing forces represented only a small proportion of the total force on the fuselage panel in ditching, vertical descent and loss of control types of incident, but about half the total in a fly-in incident.
- The results confirm that there is an approximately inverse relationship between the impact duration and maximum impact force. Very high impact loads were associated with very short impact durations, thus keeping the impulse and energy within reasonable bounds.
- As expected, there was a fairly high level of correlation between the impact velocities, u_p and u_s , and the maximum total impact force, although the highest forces on the sponson were generally associated with moderate impact velocities. The highest forces on the panel were generally associated with high impact velocities.
- A very small number of impacts were much more severe than the remainder. Severe impacts on both the sponson and fuselage panel were generally associated with small impact angles. These very severe impacts may not be modelled satisfactorily by the present procedure because no attempt has been made to represent, in detail, the effects of air entrapment or acoustic pressure limits.
- The distribution of impact angles during ditching and fly-in incidents lay in a band about the panel inclination angle. The band of impact angles was much broader during vertical descent and loss of control incidents, reflecting the broader range of attitudes of the helicopter in these conditions.
- The degree of scatter in ditching and fly-in incidents was noticeably greater in central North Sea conditions, compared with calm water. Wave conditions had a less significant effect on results obtained from the vertical descent and loss of control incidents, as had been expected.

5.4.2 *Load Exceedance Distributions*

The maximum impact loads occurring in the 20,000 individual impact events represented in each simulation run were assembled together in the form of a load exceedance probability distribution. Each distribution shows the range of variability of total impact loads occurring in each incident scenario, and the probability of exceeding a given impact load level.

Load exceedance distributions obtained during this initial base case study were presented in reference [2]. A selection of these distributions will be compared in

Section 6.2 with corresponding results obtained during the sensitivity study. A number of conclusions were drawn during the initial base case study:

- Flotation equipment is designed to survive normal ditching incidents, and the simulation results confirmed that the risk of exceeding the design load in these circumstances is small. There are significant risks of exceeding design loads for both the sponson and fuselage panel, however, in vertical descent and loss of control incidents. These results confirmed initial expectations.
- The results obtained from the simulation model of fly-in incidents were more unexpected. The simulations suggested that there should be a relatively low risk of exceeding design load values for the sponson and fuselage panel in a fly-in incident. Considerable structural damage has occurred during such incidents in the past, however, and one must question whether the simulation represents forces occurring during a fly-in realistically.
- The simulation model represents drag and planing forces, as well as the initial impact force. The drag force represented almost all of the force acting on the sponson, and about half the total force acting on the fuselage panel in a large number of impact events. The present investigation was originally intended to consider impact loading only, however. Drag and planing forces were added almost as an after-thought, and are represented in a very simplified manner. The physical processes involved in the development of these forces during a fly-in incident are extremely complex, and are poorly understood. No fully established and validated theoretical model is known to exist. Predicted fly-in loads are therefore of very uncertain accuracy and reliability.
- There are further difficulties in modelling the fly-in scenario. BMT's simulation model considers loads on a single sponson or fuselage panel in isolation, and does not consider loads on the surrounding hull structure. A fuselage panel is in practice an integral part of the hull structure, however, and some parts of the helicopter's nose are likely to experience much higher loading than the fuselage panel. Failure of the fuselage panel in a fly-in incident is likely to occur as a result of over-loading the surrounding nose structure rather than over-loading the panel itself. Failure of the surrounding hull structure was specifically excluded from consideration during the present study.

6 SENSITIVITY STUDY

6.1 Scope of Work

The initial base case study, described in Section 5, assumed specific mean values and standard deviations of parameters describing the helicopter's condition at the instant of impact, and specific values of the impact force coefficients. There are large uncertainties in some of these assumed values, however, and the effects of varying these parameters were not obvious. A sensitivity study was therefore undertaken in order to discover how changes in these assumed parameter values would affect the impact load distributions and conclusions from the study.

Table 6.1 identifies parameters (marked with a ✓ symbol) that were varied during this investigation. Other parameters were left unchanged during this investigation, because they were considered to be of secondary importance or interest. These cases are identified by the symbol × in Table 6.1.

Table 6.1: Parameters varied during the sensitivity study				
Scenario	Controlled ditching	Vertical descent	Loss of control	Fly-in incident
Calm water conditions	✓	✓	✓	✓
Mean speed	✓	✓	✓	✓
standard deviation	✓	✓	✓	✓
Mean descent angle	✓	×	✓	✓
standard deviation	✓	✓	✓	✓
Mean roll angle	×	×	×	×
standard deviation	✓	✓	✓	✓
Mean pitch angle	✓	✓	✓	✓
standard deviation	✓	✓	✓	✓
Mean yaw angle	×	×	×	×
standard deviation	✓	✓	✓	✓
Beam waves	✓	×	×	×
Following waves	✓	×	×	×
standard deviation of heading	✓	×	×	×
Drag/ planing force coefficient	✓	✓	✓	✓
Impact force coefficient	×	×	×	×
Standard deviation	✓	✓	✓	✓

The following variations in parameter values were considered:

- Mean values of the helicopter speed and descent angle were increased by 20% above base case values.
- Mean pitch angles were increased by 2 degrees.
- Values of standard deviations are generally more uncertain than mean values, and these were all increased by 50%.
- There are also large uncertainties in the drag and planing force coefficients, C_d and C_{pl} , and these were both increased by 50%.

The effects of ditching the helicopter beam-on to waves (90° heading angle) and in following waves (180° heading angle) were also considered. A head-on (0° heading angle) condition was assumed during the base case ditching investigation.

The above calculations were performed on both the sponson-mounted and fuselage-mounted flotation systems, making 92 sets of calculations in total.

Eight base case conditions were considered during the main sensitivity study, and are listed in Table 5.4. Model details and values of key parameters assumed in these eight cases are summarised below, and are described more fully in reference [2]. Definitions of symbols and variable names may be found in the 'Nomenclature' section of reference [2].

Only one parameter at a time was varied during this sensitivity study, leaving all other parameters unchanged at their base case values. Base case values assumed during this investigation are defined in Section 5.3.

6.2 Results from the Sensitivity Study

The results from each simulation run were presented in the form of an exceedance probability distribution of 'total' impact loads. The full set of results obtained during the sensitivity study are presented in reference [3]. Only a small sample of key results are presented here.

Figures 32 to 55 show exceedance distributions of the total impact force on the sponson in each of the above incident scenarios. Figures 56 to 81 show corresponding results for the fuselage panel. The exceedance distribution shows the range of variability of the total impact load within each incident scenario.

In each case the result of varying each parameter in turn (shown as a dashed line) is overlaid on top of the corresponding distribution obtained from the base case simulation (shown as a solid line).

The simulation model assumes that the maximum 'total' impact force may be represented as the sum of the maximum initial impact force and the maximum quasi-steady drag or planing force. Drag forces are assumed to act on the sponson, and planing forces on the fuselage panel. The initial impact force has an impulsive character, and is likely to reach its maximum value approximately when the sponson or panel becomes fully immersed, and will then die away to zero. The drag and planing forces are likely to increase as the sponson or panel becomes more deeply immersed, and will continue to act while the helicopter moves through the water. The simulation model makes the conservative assumption that the maximum impact force and the maximum drag or planing force occur at the same instant of time, and that these forces act in the same direction.

The correlation study described in Section 5.4 indicated that loads on the sponson and panel were essentially quasi-static in character, thus justifying the decision to compare distributions of total (hydrodynamic) impact forces directly with (structural) design load values provided by GKN WHL. These comparisons may be used to assess the cost-effectiveness of possible design changes to improve crashworthiness.

Design loads for the sponson in the vertical, fore-aft and transverse directions were therefore superimposed on relevant distributions of maximum impact forces, and are shown in each figure as three vertical bars. No attempt was made to calculate the directions associated with individual impact forces, and all three design load values are therefore shown in the figures. The design load for the fuselage panel, based on maximum design pressures, was superimposed on corresponding panel force distributions.

Table 6.2 summarises results from all calculations on the sponson in the form of a single table. Table 6.3 summarises corresponding results for the fuselage panel. These tables show whether each individual parameter change resulted in a general increase (+) or decrease (-) in impact loading across the entire range of the distribution, or whether the changes in loading were insignificant or variable (~). One such symbol (+, - or ~) indicates a small change in impact loads, two symbols (++, -- or ~~) indicates a more substantial change, and three symbols (+++, --- or ~~~) indicates a large change. Three symbols therefore indicate high sensitivity to a change in the relevant parameter, whereas one symbol indicates little or no sensitivity.

These symbols were chosen on the basis of the visual appearance of the distribution, rather than on any calculated difference parameter. Differences occurring in the upper and lower tails of the distributions were generally ignored when making this assessment. A change of less than about 10% in maximum impact loads was generally regarded as insignificant, and a change of more than 20% was regarded as large in this context.

Bearing in mind the different formulations adopted for estimating impact loads on the sponson and fuselage panel, there is a remarkable level of consistency between the two sets of results.

Impact load distributions obtained from simulations in calm water were compared with those obtained in base case conditions (i.e. all-year central North Sea waves). Wave conditions had a significant effect on the load distributions obtained in ditching and fly-in incidents, but relatively little effect on distributions obtained in vertical descent and loss of control incidents. Ditching and fly-in generally involve relatively high forward speeds and shallow descent angles, and the sea state was expected to have a significant effect on maximum impact loads in these circumstances. As expected, waves tended to increase the range of possible loads. The vertical descent and loss of control scenarios typically involved lower forward speeds, higher vertical speeds and steeper angles of descent, and the sea state was expected to be less important in these circumstances.

Increasing the mean speed on impact caused a major increase in the impact load in all cases. This is because the maximum impact load depends on the square of the relative velocity at the instant of impact.

Increasing the drag coefficient resulted in a major increase in loads experienced by the sponson in all conditions. The same percentage increase in planing loads on the fuselage panel resulted in a somewhat smaller increase in total impact loads, mainly in the controlled ditching and fly-in scenarios. The importance of drag and planing forces was not anticipated at the start of the project, and the present model represents these in a highly simplified and approximate manner. This model is probably sufficient to show the relative importance of drag, planing and impact loads, but may not represent accurate numerical values.

Increasing the mean descent angle also resulted in increased impact loads. Increasing the mean pitch angle had a more variable effect. It increased loads on the sponson and fuselage panel during controlled ditching and fly-in incidents, but not during vertical descent or loss of control incidents.

As expected, an increase in the standard deviation of an input parameter generally broadened the resulting impact load distribution, resulting in a wider range of possible loads.

Changes in a single parameter often seemed to have relatively little effect on the shape of the probability distribution. Lack of sensitivity does not necessarily mean that this parameter is unimportant, because the variability in the load often comes from the combined effect of several such parameters. The results are generally insensitive to changes in the value of the standard deviation of any single parameter. This clearly does not mean that the same results will be obtained if all parameters are set at their fixed mean values. It merely shows that no single parameter dominates the spread of the distribution.

The effects of doubling the mean value and standard deviation of the wave heading angles (assumed during vertical descent, loss of control and fly-in incidents) were also considered, even though these cases were not part of the agreed scope of work, and are therefore not listed in Table 6.1. The resulting impact load probability distributions were almost indistinguishable from the base case distributions, confirming that the assumed base case parameters adequately represented randomly chosen wave headings.

The probability distributions often approach a limit less than 1.0 as the force tends to zero. This simply indicates that the sponson or panel in question sometimes fell 'upside down', or else the random sampling procedure sometimes resulted in a non-physical parameter value (e.g. a 'negative' impact force coefficient). The impact force on a fuselage panel would genuinely be zero if it fell 'upside down', because it would then be sheltered behind the hull. The situation is less clear for a sponson, although this too would probably experience a much reduced load if it were sheltered behind the hull on impact. In all such cases the impact force was set to zero, resulting in a step change in the exceedance probability distribution at this point. These zero values were included in the exceedance distribution analysis because they either represented events that genuinely resulted in zero or small impact loads, or else represented valid (though non-physical) samples from the specified distributions of input parameters.

**Table 6.2: Sensitivity to parameter variations:
impact loads on sponson**

Parameter variation	Controlled ditching	Vertical descent	Loss of control	Fly-in
1. Calm water	~~	~	~	~~~
2. Mean speed $\times 1.2$	+++	+++	+++	+++
3. St dev speed $\times 1.5$	~	~	~~	~~
4. Mean descent angle $\times 1.2$	+		++	+
5. St dev descent angle $\times 1.5$	~	-	~~	~
6. St dev roll $\times 1.5$	~	+	~	~
7. Mean pitch + 2 deg	+	-	~	++
8. St dev pitch $\times 1.5$	~	-	-	~
9. St dev yaw $\times 1.5$	~	~	~	-
10. 90 deg heading	~~			
11. 180 deg heading	~			
12. St dev heading $\times 1.5$	~			
13. Drag coeff $\times 1.5$	+++	+++	+++	+++
14. St dev $C_s \times 1.5$	~	~	~	~

Key: +++ large increase, ++ moderate increase, + small increase
 --- large decrease, -- moderate decrease, - small decrease
 ~~~ major variation,    ~~ moderate variation,    ~ little or no variation

**Table 6.3: Sensitivity to parameter variations:  
impact loads on fuselage panel**

| Parameter variation                  | Controlled ditching | Vertical descent | Loss of control | Fly-in |
|--------------------------------------|---------------------|------------------|-----------------|--------|
| 1. Calm water                        | ~~                  | ~                | ~               | ~~~    |
| 2. Mean speed $\times 1.2$           | +++                 | +++              | +++             | +++    |
| 3. St dev speed $\times 1.5$         | ~                   | ~                | ~               | ~      |
| 4. Mean descent angle $\times 1.2$   | +                   |                  | ++              | +      |
| 5. St dev descent angle $\times 1.5$ | ~                   | -                | ~               | ~      |
| 6. St dev roll $\times 1.5$          | ~                   | ~~~              | ~~              | ~      |
| 7. Mean pitch + 2 deg                | +                   | ~                | ~               | +      |
| 8. St dev pitch $\times 1.5$         | ~                   | ~                | ~               | ~      |
| 9. St dev yaw $\times 1.5$           | ~~                  | ~                | ~               | ~~     |
| 10. 90 deg heading                   | ~~                  |                  |                 |        |
| 11. 180 deg heading                  | ~                   |                  |                 |        |
| 12. St dev heading $\times 1.5$      | ~                   |                  |                 |        |
| 13. Planing coeff $\times 1.5$       | ++                  | +                | +               | ++     |
| 14. St dev $C_o \times 1.5$          | ~                   | ~                | ~               | ~      |

**Key:** +++ large increase,    ++ moderate increase,    + small increase  
 --- large decrease,    -- moderate decrease,    - small decrease  
 ~~~ major variation,    ~~ moderate variation,    ~ little or no variation

7 TWO-FLOAT REDUNDANCY STUDY

7.1 Scope of Work

The two main stages of this investigation, described in Sections 5 and 6, considered impact loads on a single fuselage panel or sponson in isolation, and were therefore concerned with risks to a particular item of flotation equipment, rather than risks to the helicopter and its occupants as a whole.

The risk to the helicopter as a whole depends on many additional factors, including levels of redundancy and independence between flotation units. The following calculations were performed to demonstrate the principles and potential benefits of having some degree of redundancy between flotation units. In this simplified example the helicopter was assumed to have only two flotation units: one on each side of the craft.

The 'no redundancy' scenario was assumed to represent the situation where both units have to remain intact, whereas the 'one unit redundant' scenario represented the situation where only one unit is needed to keep the craft afloat. The following calculations demonstrated that the risk of failure of both units simultaneously may be significantly lower than the risk of failure of a single unit in isolation, whereas the risk of failure of either one of two units may be correspondingly higher than the risk of failure of a single unit.

The main investigation (Section 5) considered impact loads on a starboard panel or sponson only. Impact load distributions for the port panel were expected to be identical to those obtained for the starboard panel, because the scenario itself is essentially symmetric. The mean yaw and roll angles of the helicopter were zero, and the forward and backward faces of the wave surface were symmetric. The calculations presented below did in fact confirm that impact loads on the port and starboard fuselage panels had identical probability distributions.

Impact loads occurring on port and starboard panels during any individual impact event are different, however, depending on the roll and yaw angles of the helicopter, and on the wave slope at the instant of impact. This means that the probability of system failure depends on whether it is based on failure of a single flotation unit alone, failure of either one of the two units, or failure of both units simultaneously.

In the 'no redundancy' scenario, the system fails if the load on either unit exceeds its design value. This scenario may therefore be characterised by constructing a probability distribution based on the maximum of the loads experienced by the two units during each individual impact event.

In the 'one unit redundant' scenario, however, the system fails only if the loads on both units exceed their design values. This scenario may therefore be characterised by constructing a probability distribution based on the minimum of the loads experienced by the two units during each individual impact event.

The following four exceedance probability distributions of maximum impact loads were therefore calculated and compared:

- impact loads on the starboard flotation unit alone;
- impact loads on the port flotation unit alone;
- maximum loads experienced by either of the two units (representing the 'no redundancy' scenario, where both units are necessary to keep the helicopter afloat);
- minimum loads experienced by either of the two units (representing the 'one unit redundant' scenario, where one unit alone is sufficient to keep the helicopter afloat).

7.2 **Impact Loads on Sponsons**

In BMT's simulation model the port and starboard sponsons are identical, and are symmetric about their centrelines. The simulation model therefore predicts identical impact loads on both the port and starboard sponsons during any individual impact event. This means that if one sponson fails during a particular impact event, then so too does the other. The risk of one sponson failing on its own is therefore the same as the risk of both sponsons failing simultaneously. According to this simplified model, there is no benefit from having redundancy in the system or avoiding common failure modes. The risks to the flotation system and to the helicopter as a whole are determined by the risk of failure of a single sponson.

These conclusions are a direct consequence of artificial assumptions made within the theoretical model. Different loads would be experienced by the two sponsons of a real helicopter, and this would in practice affect the probability of survival, depending on whether both sponsons have to remain intact, or one alone is sufficient. Some benefit is therefore to be expected in practice from having redundancy in the flotation system, and in avoiding common failure modes.

7.3 **Impact Loads on Fuselage Panels**

The simulation model predicts different loads on the port and starboard panels of a fuselage-mounted system, however, and the results show that there are significant differences between risks of failure, depending on whether both panels have to remain intact, or one alone is sufficient. Probability distributions of impact loads were calculated on the port and starboard panels individually, and also based on the maximum and minima of the two, using exactly the same sequence of impact events in all four cases. The sequence of impact events was identical to that already chosen for earlier base case and sensitivity studies.

Figure 82 compares the four resulting exceedance distributions of maximum impact loads in the controlled ditching scenario. The load distribution for the 'starboard panel' alone is identical to that obtained during the base case study. As expected, the results for the 'starboard panel' and 'port panel' alone are almost indistinguishable.

The distribution identified as the 'maximum of the two' always lies well above the first two curves, because it is based on the higher of the impact loads occurring on the port and starboard panels during each impact incident. This distribution is used to characterise the probability of system failure in circumstances where survival of the system as a whole depends on both panels remaining intact.

The distribution identified as the 'minimum of the two' always lies well below all the others, because it is based on the lower of the impact loads occurring on the port and starboard panels during each impact incident. This distribution is used to characterise the probability of system failure in circumstances where survival depends on only one panel remaining intact.

Figures 83, 84 and 85 show similar sets of results obtained in scenarios representing fly-in, loss of control and vertical descent incidents respectively.

7.4 **General Conclusions from Two-Float Redundancy Study**

The above calculations are based on results from an analysis where the flotation comes from two fuselage panels mounted on either side of the helicopter. They demonstrate that there is a significantly higher risk of helicopter loss if survival depends on both fuselage panels remaining intact, compared with a situation where a single intact panel is sufficient to keep the helicopter afloat. In the latter case the crashworthiness of the flotation equipment may be enhanced significantly by eliminating sources of common-mode failure between the two flotation units.

The simplifications implicit in this model should be borne in mind when interpreting these results. The effects of hull shielding are, in particular, treated in a very simplified manner. The sponsons are assumed to be far enough from the hull to experience no benefits from shielding. The model therefore predicts identical loads on both sponsons and no benefits from sponson redundancy. The loads on two sponsons of a real helicopter would be different in practice, and sponson redundancy should therefore provide some benefit. The fuselage panels in BMT's model are assumed to be part of the hull, and are assumed to be totally protected if impact occurs while they are inclined upwards, away from the water surface. Once again this represents a very simplified way in which to treat what is really a very complex hydrodynamic phenomenon. The results from this study should therefore be regarded as indicative, rather than being a precise quantitative measure of the benefits of redundancy.

The above results may be generalised further without running actual simulations. In cases where the helicopter has more than two flotation units, it should be possible to enhance crashworthiness by having more redundancy in the flotation system, and by avoiding common-mode failures between separate units. Compared with a situation where all four units out of four have to remain intact, for example, the chances of survival are better if the helicopter is able to remain afloat with three out of four units intact, and better still if two out of four units are sufficient. There is a law of diminishing returns, however, because it may be expensive to provide additional independent buoyancy units. A cost/benefit analysis would therefore be needed in order to decide on the most cost effective arrangement.

Results from a more realistic redundancy study, based on a helicopter with either four, five or six flotation units, may be found in Section 9.

8 DATA INTERPRETATION AND APPRAISAL STUDY

The earlier sensitivity study (Section 6) showed that the helicopter's forward speed and descent angle on impact were two of the most significant parameters determining the maximum impact load. Impact velocity scatter plots were therefore constructed, bringing together results from simulations based on ditching, vertical descent, loss of control and fly-in incidents, and showing the helicopter's vertical and horizontal velocities during each individual impact event along the vertical and horizontal axes respectively. These scatter plots showed which individual events caused loads less than and greater than the design value, and were used to identify relationships between the flotation unit failure rate (expressed as a percentage of the total number of impact events) and the helicopter's speed on impact. Once again, the impact forces were characterised by maximum loads on an individual sponson or fuselage panel, and the four incident scenarios were those considered during the main base case study (Section 5).

This analysis assumed implicitly that all four types of incident are of equal importance. Equal numbers of each type of incident (4,000) were included in the analysis.

8.1 Base Case Conditions

8.1.1 *Sponson Impact Loads*

Figure 86 shows the velocity scatter plot obtained from simulations of maximum impact loads on the sponson in the four base case scenarios defined in Section 5.3. This scatter plot shows the first 4,000 impact events from each of the four simulation runs, representing ditching, vertical descent, loss of control and fly-in incidents. These data points have been split into two groups:

- green points indicate impact events where the maximum load was less than the design value,
- red points indicate impact events where the maximum load was greater than the design value.

The design value in this case was chosen to be the lowest (164 kN) of the three (fore-aft, vertical and transverse) design forces specified by GKN WHL for the sponson support struts. These three values are discussed in Section 5.3.5.

Four clusters of points may be seen in Figure 86:

- a compact group with horizontal velocities less than about 20 m/s, and low vertical velocities, representing ditching events,
- a further well-defined group, covering a small range of vertical velocities less than about 5 m/s, and a broad range of horizontal velocities, representing fly-in events,
- a broad cluster of points, with high vertical velocities, and moderate horizontal velocities of less than about 10 m/s, representing vertical descent events,

- a scatter of points, covering a broad range of vertical and horizontal speeds, representing loss-of-control incidents.

Two further curves are shown on this figure:

- a blue rectangular boundary, representing the ditching velocity limits specified in reference [9], with maximum forward and vertical speeds equal to 15.2 m/s (50 ft/s) and 1.5 m/s (5 ft/s) respectively;
- an elliptical curve, outlined in paler blue, which represents a boundary proposed by the Federal Aviation Authority (FAA) in Figure 5 of reference [9], within which 95% of human occupants should survive a crash onto water, according to the FAA's accident statistics.

As noted in Section 5.4, very few ditching events caused impact loads above the design value.

Green points (impact loads below the design value) obtained during fly-in events tend to lie towards the bottom left side of the cluster, and red points (impact loads above the design value) tend to lie towards the top right side, but there is a broad area of overlap between these two distributions.

There is even more overlap between the distributions based on vertical descent and loss of control events, where the areas covered by red and green points are almost indistinguishable. This overlap occurs because impact loads depend on many parameters other than the helicopter's vertical and horizontal velocities. They depend in particular on the helicopter's attitude at the instant of impact, and this was highly variable during vertical descent and loss of control scenarios. Waves also caused some scatter in the distributions.

As noted earlier, the analysis was based on loads experienced by an individual sponson, and took no account of loads on the helicopter's hull as a whole. Points lying in the upper right hand area of the figure represent severe impact events, which would cause a major hull failure, even though the present model suggests that an individual sponson would survive. In many of these cases the sponson survived simply because it entered the water in an axial direction, and the simulation model does not represent axial loads.

Figures 87 and 88 show the same information as Figure 86, but separated into points lying below and above the design value. From a practical viewpoint, the only points of concern are those lying above the design value. These points are shown in Figure 88, and will be regarded as 'failure' cases in the discussion below.

8.1.2 *Impact Severity Index Curves*

Elliptical curves were drawn on Figure 88 to provide a simple means of classifying impact events according to their severity, based on the observation that impact severity and survivability tend to depend more on the helicopter's vertical velocity than on its horizontal velocity. The *Brent Spar* and *Scilly Isles* accidents were regarded as being two especially severe but survivable events. For present purposes these two events were regarded as being of comparable severity. Mean estimates of the vertical (22 m/s) and horizontal (46 m/s) impact speeds of the helicopters involved in the *Brent Spar* and *Scilly Isles* accidents were therefore used to define the

vertical and horizontal semi-axes, respectively, of a base case ellipse represented by the chain-dotted curve in Figure 88. A number of further concentric ellipses were then constructed (shown as dotted lines in Figure 88) by multiplying the semi-axes of the base case ellipse by factors ranging from 0.1 to 1.4. These factors were then used to define a simple 'impact severity index', with points around the boundary of each ellipse being regarded as being of comparable severity. Relationships between the number of float failures and the impact severity index were then investigated by counting up the number of failure cases within each of these elliptical boundaries.

The FAA's 95% survivability boundary lies between curves corresponding to impact severity index values 0.3 and 0.4. Very few failure cases lie within the FAA's 95% survivability boundary (significantly less than 5% of the total number of simulated impact events). Incidents occurring within the FAA's boundary may therefore be regarded as moderate impact events.

Impacts occurring beyond impact severity index 0.7 are considered to be severe, and impacts occurring beyond severity index 1.0 are generally likely to be unsurvivable. The greatest benefits in terms of crashworthiness are likely to come from increasing the survivability of floats when the impact severity index lies between 0.7 and 1.0.

8.1.3 *Fuselage Panel Impact Loads*

Figures 89 to 91 show corresponding results obtained from simulations of impact loads on the fuselage panel in the four base case impact scenarios. Once again the green points correspond to impacts where the load on the panel was less than the design value (21.3 kN) defined in Section 5.3.6, and the red points denote 'failure' cases where the impact load was greater than the design value.

The results are broadly similar to those obtained from simulations of loads on the sponson, although a smaller percentage of impact events resulted in failure of the fuselage panel. Once again, very few failures occurred during ditching events, and fly-in failures tended to occur at relatively high horizontal speeds. It is not clear, however, whether the model represents fly-in loads adequately, and the results from the fly-in simulation therefore have to be treated with caution.

Results obtained from simulations of vertical descent and loss of control scenarios again show a broad area of overlap between points corresponding to loads above and below the design value. A significant number of green points, corresponding to impact loads below the design value, occur at very high vertical and horizontal impact speeds. A number of these cases represent events where the panel was on the protected side of the hull (i.e. on the side away from the point of impact), and therefore experienced no loading. As noted earlier, the analysis considered loads on a single panel on one side of the helicopter's nose in isolation, ignoring loads on the remainder of the hull. In many of these cases the hull itself would fail, even though the analysis suggests that an individual panel will survive.

8.2 **Calm Water Conditions**

Figures 92 and 93 show corresponding impact velocity scatter plots for cases representing sponson and panel failure in calm water.

Comparing these two figures with those obtained in corresponding central North Sea wave conditions (Figures 88 and 91), the calm water results show very few failure cases in the lower left area of the scatter plots. Ditching caused no impact loads above the design value. Fly-in speeds less than 30 m/s also caused relatively few failures. As noted earlier, however, the procedures for calculating impact loads in high forward speed conditions may not be accurate or reliable, and the results should again be treated with caution.

Once again the results show considerable scatter in results obtained during vertical descent and loss-of-control scenarios, where the impact load generally depended on the helicopter's attitude at the moment of impact rather than on the sea state.

8.2.1 *Failure Case Distributions*

The number of failure cases within each impact severity index curve was then counted, in order to determine the percentage of failure cases (relative to the total number of incidents) as a function of the impact severity index. Figure 94 compares percentages of sponson failure cases in both base case and calm water conditions, and Figure 95 shows corresponding results for the fuselage panel.

The sponson / panel failed on less than 5% of occasions when the impact severity index was less than 0.6 / 0.7 respectively. The failure probability distributions level off at high values of the severity index, simply because the number of incidents at high levels is small. Only 47% / 30% of all incidents resulted in sponson / panel failures respectively.

The base case and calm water curves are almost indistinguishable in both Figures, showing that overall (i.e. considering all four types of incidents together, and incidents randomly distributed throughout the year) the sea state had little effect on the probability of failure. The waves are nonetheless likely to have a significant effect on the impact load occurring in certain types of incident scenario, and in severe wave conditions.

8.3 **Increased Design Load**

Figures 96 and 97 show the velocity scatter plots obtained when design loads on the sponson and fuselage panel were increased by 100%. A 100% increase in the design load would generally require major modifications to the design and operational capability of the helicopter, and would therefore have major cost implications. Any such increase in design loads would therefore only be justified if it resulted in a correspondingly large crashworthiness benefit for the emergency flotation system.

These two figures show no failures during ditching events, and very few failures during fly-in events. As noted above, however, the results obtained from the fly-in scenario should be treated with caution. The number of failures has also reduced significantly during loss of control and vertical descent incidents, although the number of failure cases remains large when the vertical velocity exceeds about 7 to 10 m/s.

8.3.1 *Failure Case Distributions*

Relationships between float failures and the impact severity index were again assessed by counting the number of failure cases within each impact severity index

curve. Figures 98 and 99 compare the distributions obtained using base case design loads with those obtained when these loads were increased by 100%. As expected the total number of failure cases fell significantly: from 47% to 30% of the total number of impacts for the sponson, and from 30% to 20% for the fuselage panels.

The simulation model predicts that the sponson or panel will often survive in high speed impact conditions. Many of these high speed impacts would not be survivable in practice by human occupants. It was therefore considered more meaningful to judge improvements in crashworthiness in terms of the change in the impact severity index at which 95% of panels and sponsons survived (i.e. with a 5% level of float failures). Figures 98 and 99 show that the relevant value of the impact severity index increased from about 0.65 to 0.75 for both the sponson and panel. This means that a 100% increase in design loads resulted in only about 15% increase in the impact severity index associated with 5% of failures. This represents a poor gain in crashworthiness when considered in relation to such a major increase in design loads.

8.4 **Results from Two-Float Redundancy Study**

Section 7 describes results from a preliminary investigation into redundancy between floats installed under two fuselage panels, on the port and starboard sides of the helicopter. This investigation suggested that there might be crashworthiness benefits if the flotation unit under a single panel were sufficient to keep the helicopter afloat, over the situation where both flotation units have to remain intact.

The results from this preliminary investigation have now been assembled together in the form of velocity scatter plots. In the 'no redundancy' scenario, both panels have to remain intact on impact if the helicopter is to remain afloat. In this case an impact results in a 'failure' if either of the two fuselage panels fails. In the 'one panel redundant' scenario, a single panel is sufficient to keep the helicopter afloat. In this case a 'failure' (shown as a red cross) only occurs if both panels fail.

The resulting failure case scatter plots are shown in Figures 100 and 101. There are very obvious differences between these two scatter plots, which show a very significant reduction in the number of failure cases when only one panel is necessary for survival, compared with the 'no redundancy' scenario. This is particularly true at low and moderate impact speeds, which are considered to be the most survivable.

8.4.1 *Failure Case Distributions*

The number of failure cases within each severity index curve was again counted. The results are presented, as previously, in the form of failure case percentages as a function of the impact severity index.

Results from the two-panel redundancy study are shown in Figure 102. As indicated by the scatter plots, there are major reductions in the number of failure cases if only one out of the two panels is sufficient to keep the helicopter afloat, compared with the situation where both panels must remain intact. There are also major reductions compared with the failure rate for a single panel on its own. This is because many impact events caused one panel or the other to fail, but not both.

This analysis took no account of structural failure of the hull as a whole, however, and inevitably overestimated the number of survivable events at high impact speeds.

The analysis nonetheless suggests that, at the more realistic velocities associated with a 5% failure level, the impact severity index increases from about 0.6 to about 0.9, representing a significant enhancement in the level of crashworthiness.

9 ***EH101* MULTI-FLOAT REDUNDANCY STUDY**

The main objective of this final stage of the investigation was to find out whether there are likely to be significant benefits, in terms of crashworthiness, from having redundancy between either four, five or six flotation units.

This phase of the work was originally envisaged as a simple extension of the two-float redundancy study described in Section 7, based simply on considering the number of floats remaining intact after impact, regardless of their location or size. After discussion, however, it was agreed that the study would be more realistic and would have greater practical value if:

- the model was based on the helicopter type (*WG34/EH101*) and flotation configuration previously tested in the HTC model basin [31];
- the analysis considered whether the floats remaining intact after an impact were sufficient to:
 - (a) allow the helicopter to remain floating at the surface, albeit inverted,
 - (b) enable the helicopter to float on its side,
 - (c) provide a satisfactory air space in the cabin.

A conventional four-float arrangement was considered first. The floats were arranged as on the *EH101*, with two floats at the nose and the other two (main) floats located in sponsons attached directly to the hull. It was assumed that a four-float helicopter would always capsize and become inverted after impact, leaving the floor level at or below the water surface, and the cabin totally submerged. In these circumstances the occupants have little time to re-orient themselves and escape, because there is little or no air space in the cabin.

There will only be a satisfactory air space in the cabin, sufficient to allow the occupants to take breath before escaping, if the helicopter floats on its side (see Section 9.3). The benefits of adding either one or two extra floats on the upper cabin walls were therefore investigated. These asymmetric (five-float) and symmetric (six-float) configurations not only provide redundancy but also enable the helicopter to float on its side after capsize, usually with a satisfactory air space in the cabin, thereby improving chances of escape and survival. The dimensions and locations of these extra floats were based on 'long units' which had been model-tested at HTC [31], and had shown some promise in terms of providing a side-floating attitude after capsize.

As in earlier stages of this investigation, it was assumed that the floats would only deploy after impact with the water surface. A float was deemed to 'fail' if the impact force on its covering panel exceeded the design load. Each float was treated as a single entity, ignoring any internal sub-compartmentation. Consequences of hull damage, failure of the float itself and associated equipment were not considered.

Panel Definition

Tables 9.1 to 9.3 summarise the dimensions of the cover panels on all three different types of float, together with their inclinations and failure loads.

| Table 9.1: Summary of forward panel parameters. | |
|--|---------|
| Length | 0.81m |
| Width | 0.41m |
| Inclination about roll axis | 10° |
| Inclination about pitch axis | 0° |
| Inclination relative to forward direction | -14° |
| Design maximum load | 42.8 kN |

| Table 9.2: Summary of main (sponson) panel parameters. | |
|---|---------|
| Length | 1.28m |
| Width | 0.52m |
| Inclination about roll axis | 0° |
| Inclination about pitch axis | 0° |
| Inclination relative to forward direction | 0° |
| Design maximum load | 85.7 kN |

| Table 9.3: Summary of upper cabin panel parameters. | |
|--|----------|
| Length | 3.1m |
| Width | 0.45m |
| Inclination about roll axis | -10° |
| Inclination about pitch axis | 0° |
| Inclination relative to forward direction | 0° |
| Design maximum load | 179.7 kN |

It was considered adequate to estimate the dimensions of the forward and main (sponson) panels from photographs of the *EH101* helicopter [30]. Upper cabin floats do not exist on present-day helicopters, and so the dimensions of the upper cabin panels had to be estimated from the dimensions of the 'long' inflated floats

considered during the HTC model tests [31]. The panel length and height were assumed to be equal to half the length and half the height of the inflated unit.²

The orientations of the panels were also estimated from photographs. The sponson panel was assumed to be exactly vertical and parallel to the helicopter's longitudinal axis. The forward panel was assumed to be inclined downwards and forwards, with angles similar to those assumed during the earlier *Sea King* study (see Section 5.3.6). It seemed reasonable to assume that the upper cabin panel would be parallel to the helicopter's longitudinal axis, and inclined slightly upwards by 10 degrees. This panel was assumed to be flat despite its considerable length (3.1m).

Each panel was assumed to fail if the impact pressure exceeded 0.1288 N/mm^2 . This failure pressure was the value supplied by GKN WHL in connection with the earlier *Sea King* study (see Section 5.3.6). The maximum design load on each panel was then equal to the failure pressure times the panel area.

9.2 **Hull and Flotation Unit Buoyancy**

9.2.1 *Hull Buoyancy*

The helicopter was assumed to float (or sink) depending on whether the total buoyancy from the hull and flotation units was greater than (or less than) the helicopter's weight. The main complication here was in deciding how much buoyancy should be attributed to the hull. Initial calculations showed that the buoyancy of the *EH101* hull was significant and could not be ignored, even when all internal air spaces were flooded. The buoyancy of the hull will depend in practice on the amount of damage sustained in a crash, but it was not practical to take such variations into account. The hull buoyancy was therefore assumed to remain constant throughout, and was estimated from the displacement of the airframe and fuel tanks, assuming that all other internal spaces would flood.

The aim here was to obtain a realistic estimate of hull buoyancy, but one that erred slightly on the low side so as to increase slightly the predicted probability of sinking.

Two further assumptions, that the fuel tanks were full and remained intact on impact, were considered to have the following effects:

- An empty (or partially full) intact tank provides the same buoyancy as a full tank, but weighs less. Assuming a full tank therefore overestimated its net weight, slightly increasing the predicted probability of sinking.
- A ruptured tank tends to lose weight and buoyancy at similar rates, because aviation fuel is only slightly less dense than water, and lost fuel is replaced by the same volume of water. Assuming an intact tank would therefore have little effect on the predicted probability of sinking.

Previous studies had suggested that tail booms of helicopters often fail on impact with water. Loss of the tail boom was not considered to be an important factor in this study, however, because of its relatively small effect on the helicopter's net weight in water.

² Based on the dimensions of existing panels and floats on the EH101, where this ratio varies between 0.36 and 0.53.

Four alternative estimates of hull buoyancy were made, designated as follows:

| | |
|--|-----------|
| <i>Naval estimate:</i> | 8,164 kg |
| <i>Weight estimate:</i> | 6,971 kg |
| <i>Commando light weight estimate:</i> | 6,421 kg |
| <i>Combination estimate:</i> | 5,474 kg. |

The *naval estimate* came directly from a GKN WHL report on the naval version of the *EH101* [32]. Certain parts of the helicopter were assumed to flood in GKN WHL's analysis, and were not included in their buoyancy estimate.

The *weight estimate* was based on two values of the helicopter's weight quoted in an EEL report [33] for the civilian version of the *EH101*: 14,290 kg with the fuel tanks full, and 12,839 kg with them half full. This means that the weight of the full fuel tanks was 2,902 kg, and their buoyancy was therefore 3,718 kg. The light weight of the *EH101* was estimated by subtracting the fuel weight and the weight of 25 people (each assumed to have an average weight of 100 kg) from the total helicopter weight (i.e. $14,290 - 2,902 - 2,500 = 8,888$ kg). This estimate is very close to the operating weight when empty (8,993 kg) quoted by the helicopter designers [30]. Assuming that the average density of the airframe was that of aluminium, the airframe buoyancy was estimated to be 3,253 kg. The combined buoyancy of the airframe and full fuel tanks was then 6,971 kg.

An average airframe density had to be assumed, because no weight breakdown was available. Certain items, such as the main rotor, gear box and engines, are made of steel and are therefore much denser than aluminium. On the other hand certain other items are made of plastic, which is a less dense material. On average it therefore seemed reasonable to assume that the average density of the airframe would be that of aluminium.

The *Commando light weight estimate* came from a report on model ditching tests on the *WG34* [34]. In this report the *Commando* version was stated to have a light weight of 16,281 lb. Assuming again that the airframe had the same average density as aluminium, and adding the buoyancy of the fuel tanks calculated using the method explained above, the total buoyancy was estimated to be 6,421 kg.

The *combination estimate* was based on a breakdown of buoyancy elements quoted in the naval *EH-101* report (see *naval estimate* above) and the fuel buoyancy estimate (from the *weight estimate* above). All items relating to the fuel tank were subtracted from the naval estimate, giving a buoyancy equal to 1,756 kg. The fuel tank buoyancy found by the second method (3,718 kg) was then added, giving a total buoyancy equal to 5,474 kg.

There are substantial differences between the above four buoyancy estimates, but some are likely to be more reliable and relevant than others. The *naval*, *Commando light weight* and *combination estimates* are all based on military versions of the *EH101*, and may therefore represent variants with different weights and buoyancy. The *weight estimate* is probably the most relevant and reliable because it is based on documented all-up and fuel weights for the civilian version of the *EH101*. After discussion, however, it was agreed that a lower value should be assumed: making the combined buoyancy of the airframe and full fuel tanks equal to 6,000 kg. This value lies towards the lower end of the above range of estimates, and was considered to provide a conservative (i.e. pessimistic) view of flotation system requirements. The

aim of choosing a low value of hull buoyancy was to increase the relative importance of the floats, and increase the number of failure cases obtained from the analysis.

9.2.2 *Float Buoyancy*

The buoyancy provided by each float was assumed to be identical to the value stated in the HTC model test report [31]. The buoyancy of each forward float was 1,630 kg. That of each main float was 3,864 kg, and that of each upper cabin float was 4,038 kg.

9.3 **Float Failure Consequences**

A 'consequence table' was constructed, in order to describe the outcome of each combination of float failures. There are 64 ($= 2^6$) possible float failure combinations when six floats are installed, although symmetry reduces the number of different possibilities to 32. When only five or four floats are installed, the consequence table is a simple subset of the six-float table.

With only four conventional flotation units the helicopter cannot float on its side. There are only two possible outcomes in this case: the helicopter may either float or sink after impact.

Additional 'consequence classes' have to be considered, however, when five or six floats are installed. These classes distinguish between whether the floats remaining intact after each simulated crash event either:

- (i) provide insufficient buoyancy, causing the helicopter to sink,
- (ii) allow the helicopter to remain floating at the surface, albeit inverted,
- (iii) enable the helicopter to float on its side,
- (iv) provide a satisfactory air space in the cabin.

It was not always easy to predict the attitude of the helicopter after a crash, or to decide which attitudes represent side-floating conditions. The helicopter's attitude in the water could have been assessed by carrying out a hydrostatics analysis, but this option was rejected partly on grounds of cost, and partly because of the uncertain effects of internal flooding. It was therefore agreed that it would be adequate to assess the outcome of each panel failure scenario in a subjective manner. Most scenarios have a fairly obvious outcome, but six scenarios with less obvious outcomes are identified below.

Table 9.4 represents BMT's best subjective assessment of the consequences of panel failure, and Figure 103 shows the float numbering system used during this analysis. This table should be interpreted as follows:

- When a cell below a *Bag x* column is red, it means that the relevant float has failed. A green cell means that the float is intact.
- 'Sys. Buoyancy' represents the total available buoyancy of the helicopter's hull plus remaining intact floats.

- The next three columns of the table represent the helicopter's attitude with the particular combination of float failures indicated. If the cell in the first of these columns, labelled '*sink*', is red, then the helicopter will sink. The helicopter will stay afloat if this cell is green.
- If the cell in the second of these three columns is green, then the helicopter will float on its side. It will invert if it is red.
- If the cell in the third column is green, there will be a satisfactory air space within the cabin.
- Note that if the helicopter sinks (first cell red) then the second and third cells will automatically be red (the helicopter cannot float on its side or provide a satisfactory air space in the cabin). Similarly, if the helicopter does not float on its side, it cannot provide a satisfactory air space.

Assuming that the earlier estimates of helicopter buoyancy and weight are realistic, then it is straightforward to decide whether the helicopter will float or sink. Confidence in this particular outcome is therefore high.

The system buoyancy in Table 9.4 represents the total amount available from the hull and all intact floats. This total is often greater than the weight of the helicopter. This simply means that part of the available flotation lies above the water surface. It is nonetheless fair to include this excess buoyancy in the calculation, because all floats have to sink below the surface, providing their full buoyancy, before the helicopter itself can sink.

There was generally little doubt in deciding whether the helicopter would float on its side. If the helicopter floated at all (this required at least three floats to be intact), then in general only one intact upper cabin float was needed to ensure side flotation. The only exceptions to this rule were cases 25 and 26, which are discussed below.

Most of the uncertainties lay in deciding whether there would be a satisfactory air space. After discussion, however, it was agreed that if an upper cabin float on one side, and a main float situated on the other side of the helicopter, are both intact, then there should generally be a satisfactory air space within the cabin.

Table 9.4: Consequence table based on the six-float configuration. ³

| 44134/20 | | Buoyancy helicopter | | | 6000 kg | | Helicopter Weight | | | 14290 kg | |
|----------|-------|---------------------|-------|-------|---------|-------|-------------------|------|-------------|----------|--|
| | | Buoyancy bag 1 & 2 | | | 1630 kg | each | | | | | |
| | | Buoyancy bag 3 & 4 | | | 3864 kg | each | | | | | |
| | | Buoyancy bag 5 & 6 | | | 4038 kg | each | | | | | |
| Sequence | bag 1 | bag 2 | bag 3 | bag 4 | bag 5 | bag 6 | Sys. buoyancy | Sink | Side floats | air gap | |
| 1 | Red | Red | Red | Red | Red | Red | 6000 | Red | Red | Red | |
| 2 | Red | Red | Red | Red | Red | Red | 10038 | Red | Red | Red | |
| 3 | Red | Red | Red | Red | Red | Red | 10038 | Red | Red | Red | |
| 4 | Red | Red | Red | Red | Red | Red | 9864 | Red | Red | Red | |
| 5 | Red | Red | Red | Red | Red | Red | 9864 | Red | Red | Red | |
| 6 | Red | Red | Red | Red | Red | Red | 7630 | Red | Red | Red | |
| 7 | Red | Red | Red | Red | Red | Red | 7630 | Red | Red | Red | |
| 8 | Red | Red | Red | Red | Red | Red | 14076 | Red | Red | Red | |
| 9 | Red | Red | Red | Red | Red | Red | 13902 | Red | Red | Red | |
| 10 | Red | Red | Red | Red | Red | Red | 13902 | Red | Red | Red | |
| 11 | Red | Red | Red | Red | Red | Red | 11668 | Red | Red | Red | |
| 12 | Red | Red | Red | Red | Red | Red | 11668 | Red | Red | Red | |
| 13 | Red | Red | Red | Red | Red | Red | 13902 | Red | Red | Red | |
| 14 | Red | Red | Red | Red | Red | Red | 13902 | Red | Red | Red | |
| 15 | Red | Red | Red | Red | Red | Red | 11668 | Red | Red | Red | |
| 16 | Red | Red | Red | Red | Red | Red | 11668 | Red | Red | Red | |
| 17 | Red | Red | Red | Red | Red | Red | 13728 | Red | Red | Red | |
| 18 | Red | Red | Red | Red | Red | Red | 11494 | Red | Red | Red | |
| 19 | Red | Red | Red | Red | Red | Red | 11494 | Red | Red | Red | |
| 20 | Red | Red | Red | Red | Red | Red | 11494 | Red | Red | Red | |
| 21 | Red | Red | Red | Red | Red | Red | 11494 | Red | Red | Red | |
| 22 | Red | Red | Red | Red | Red | Red | 9260 | Red | Red | Red | |
| 23 | Red | Red | Red | Red | Red | Red | 17940 | Red | Red | Red | |
| 24 | Red | Red | Red | Red | Red | Red | 17940 | Red | Red | Red | |
| 25 | Red | Red | Red | Red | Red | Red | 15706 | Red | Red | Red | |
| 26 | Red | Red | Red | Red | Red | Red | 15706 | Red | Red | Red | |
| 27 | Red | Red | Red | Red | Red | Red | 17766 | Red | Red | Red | |
| 28 | Red | Red | Red | Red | Red | Red | 15532 | Red | Red | Red | |
| 29 | Red | Red | Red | Red | Red | Red | 15532 | Red | Red | Red | |
| 30 | Red | Red | Red | Red | Red | Red | 15532 | Red | Red | Red | |
| 31 | Red | Red | Red | Red | Red | Red | 15532 | Red | Red | Red | |
| 32 | Red | Red | Red | Red | Red | Red | 13298 | Red | Red | Red | |
| 33 | Red | Red | Red | Red | Red | Red | 17766 | Red | Red | Red | |
| 34 | Red | Red | Red | Red | Red | Red | 15532 | Red | Red | Red | |
| 35 | Red | Red | Red | Red | Red | Red | 15532 | Red | Red | Red | |
| 36 | Red | Red | Red | Red | Red | Red | 15532 | Red | Red | Red | |
| 37 | Red | Red | Red | Red | Red | Red | 15532 | Red | Red | Red | |
| 38 | Red | Red | Red | Red | Red | Red | 13298 | Red | Red | Red | |
| 39 | Red | Red | Red | Red | Red | Red | 15358 | Red | Red | Red | |
| 40 | Red | Red | Red | Red | Red | Red | 15358 | Red | Red | Red | |
| 41 | Red | Red | Red | Red | Red | Red | 13124 | Red | Red | Red | |
| 42 | Red | Red | Red | Red | Red | Red | 13124 | Red | Red | Red | |
| 43 | Red | Red | Red | Red | Red | Red | 21804 | Red | Red | Red | |
| 44 | Red | Red | Red | Red | Red | Red | 19570 | Red | Red | Red | |
| 45 | Red | Red | Red | Red | Red | Red | 19570 | Red | Red | Red | |
| 46 | Red | Red | Red | Red | Red | Red | 19570 | Red | Red | Red | |
| 47 | Red | Red | Red | Red | Red | Red | 19570 | Red | Red | Red | |
| 48 | Red | Red | Red | Red | Red | Red | 17336 | Red | Red | Red | |
| 49 | Red | Red | Red | Red | Red | Red | 19396 | Red | Red | Red | |
| 50 | Red | Red | Red | Red | Red | Red | 19396 | Red | Red | Red | |
| 51 | Red | Red | Red | Red | Red | Red | 17162 | Red | Red | Red | |
| 52 | Red | Red | Red | Red | Red | Red | 17162 | Red | Red | Red | |
| 53 | Red | Red | Red | Red | Red | Red | 19396 | Red | Red | Red | |
| 54 | Red | Red | Red | Red | Red | Red | 19396 | Red | Red | Red | |
| 55 | Red | Red | Red | Red | Red | Red | 17162 | Red | Red | Red | |
| 56 | Red | Red | Red | Red | Red | Red | 17162 | Red | Red | Red | |
| 57 | Red | Red | Red | Red | Red | Red | 16988 | Red | Red | Red | |
| 58 | Red | Red | Red | Red | Red | Red | 23434 | Red | Red | Red | |
| 59 | Red | Red | Red | Red | Red | Red | 23434 | Red | Red | Red | |
| 60 | Red | Red | Red | Red | Red | Red | 21200 | Red | Red | Red | |
| 61 | Red | Red | Red | Red | Red | Red | 21200 | Red | Red | Red | |
| 62 | Red | Red | Red | Red | Red | Red | 21026 | Red | Red | Red | |
| 63 | Red | Red | Red | Red | Red | Red | 21026 | Red | Red | Red | |
| 64 | Red | Red | Red | Red | Red | Red | 25064 | Red | Red | Red | |

³ Green cell denotes 'float intact' / 'success'. Red cell denotes 'failure'.

The outcomes of six scenarios were nonetheless considered to be especially uncertain and subjective, and are discussed in detail below:

- **Cases 25 and 26:** There was some doubt in these two cases about both the size of the air space and whether the helicopter would float on its side. With two upper cabin floats intact, together with one forward float, the final waterline is likely to be at mid-height through the two cabin floats, and most of the cabin would be under water. The forward float would probably provide enough buoyancy either to raise the nose of the helicopter, or to make it incline towards one side. If the helicopter has much of its buoyancy low down, in the area of the fuel tanks, then this too would tend to raise the nose or make the helicopter incline. Having little quantitative information on which to base a decision, however, a pessimistic outcome was assumed: that the helicopter would not float on its side, and in consequence would not provide a satisfactory air space.
- **Case 28, 29, 36 and 37:** In these cases one upper cabin float and the main float on the same side are intact, together with any one of the forward floats. In these four cases it was clear that the helicopter would float on its side, with the final waterline going through the main and cabin floats, with most of the helicopter under water. The question was then whether the forward float would have enough buoyancy to raise the nose, and thereby create a satisfactory air space. Although the cabin floats are likely to provide buoyancy fairly centrally, the main float would provide buoyancy in the aft part of the helicopter. Again, a pessimistic outcome was assumed: that the helicopter would lie on its side, with its nose inclined downwards.

A further conservative assumption was also made: that the helicopter would always capsize after impact, regardless of the type of incident. Past accident statistics [9] show that helicopters have capsized in the majority (80%) of survivable and partially survivable accidents on water. It therefore seemed reasonable to assume that the helicopter would always capsize after a crash. This assumption seemed more questionable in ditching conditions, however, because helicopters are designed to remain upright after ditching in a moderate sea. Whether they do in fact remain upright depends on a number of factors, including the severity of the sea state, the helicopter's attitude as it enters the water and any damage sustained. Representing all these factors would have added to the complexity of the model, without necessarily reducing key uncertainties. Bearing in mind that this investigation was concerned primarily with crashworthiness, and that ditchings represent only a quarter of the incidents in the simulation, accurate modelling of ditching events was considered to be of lesser importance.

The above assumption gives a pessimistic view of the helicopter's crashworthiness in the four-float base line condition, but may as a result give a slightly optimistic view of the benefits of adding extra floats.

A further element of pessimism lies in the fact that a helicopter takes time to fill with water after a crash, and may remain afloat long enough for survivors to escape, even though simple static buoyancy and weight calculations show that it will eventually sink.

9.4 Results

The results from this investigation were analysed and presented in much the same way as in Section 8. As previously, four different types of water impact scenarios were simulated: controlled ditchings, vertical descent, loss of control and fly-in incidents. Four thousand individual impact events of each type were simulated, using the Monte Carlo simulation and sampling procedures described in Sections 4 and 5. The central North Sea wave scatter table was used, together with distributions of helicopter speed, descent angle, roll, pitch and yaw angles, wave incidence angle and impact force coefficients identical to those assumed in the earlier *Sea King* study. These distributions are defined in Tables 5.1, 5.3 and 5.5.

Results from these 4,000 simulations of four different types of impact events were then combined together into scatter plots showing the vertical and horizontal components of velocity corresponding to each impact event, and percentage probabilities of 'failure' within elliptical impact severity index curves, as described in Section 8. Three different types of 'failure' were considered in the analysis: when the helicopter failed to provide a satisfactory air space, failed to float on its side, or failed to float at all.

9.4.1 *Criteria for Floating or Sinking*

The first aspect investigated was whether the helicopter would float or sink after a water impact. The criterion used here was simply whether the total buoyancy from the hull and intact floats was greater than, or less than the total weight.

The analysis was performed first with a conventional configuration of four floats (two forward and two sponson floats). Figure 104 shows 'failure' cases (ie. where the helicopter sank after impact) from four simulation runs, representing 4,000 separate ditching, vertical descent, loss of control and fly-in events. The red crosses in this figure show the vertical and horizontal components of the helicopter's velocity at the instant of impact, presented in the same form as in Section 8.

As previously there are four separate clusters of points:

- The broad spread of points around the vertical velocity axis corresponds to vertical descent incidents. The majority of these impacts resulted in float failures sufficient to make the helicopter sink.
- A second broad spread of points, near the centre of the figure, corresponds to loss of control incidents. Again, many of these incidents resulted in the helicopter sinking.
- The third cluster, just above the horizontal velocity axis (horizontal velocities between about 30 m/s and 50 m/s), correspond to fly-in incidents. Only a small proportion of these incidents resulted in the helicopter sinking. As previously, however, it should be noted that:
 - (i) drag and planing loads were modelled in a simplified manner, and may not be represented satisfactorily in fly-in conditions;
 - (ii) the analysis only considered direct loads on the flotation panel, and took no account of surrounding hull damage.

- Very few ditching incidents resulted in the helicopter sinking. Failures during ditching are represented by only four crosses at low vertical speeds, with horizontal velocities close to 15 m/s.

The analysis was then repeated with a single upper cabin float added on the starboard side (float 5 in Figure 103). Figure 105 shows incidents in which the helicopter sank with this five-float configuration. Adding one upper cabin float resulted in a substantial reduction in the number of failure cases. All four different types of incident (ditching, vertical descent, loss of control and fly in) benefited from having the additional float, but in varying proportions:

- the helicopter floated after every ditching incident;
- only a small number of fly-in incidents caused sinking;
- sinking occurred less often after vertical descent and loss of control incidents, although a significant number of failure cases remained.

No scatter plot is presented for the six-float configuration, because no 'failures' were recorded during any of the simulation runs. At least one main float, one upper cabin float and one other float remained intact on every occasion, providing sufficient buoyancy to keep the helicopter afloat.

Figure 106 shows the percentage of failure cases lying within each impact severity index curve for each float configuration. The solid line represents results obtained with the conventional four-float arrangement. The dashed line represents the five-float system, and the dotted line (along the horizontal axis) a six-float combination. Adding an upper cabin float significantly increased the probability of remaining afloat after a moderate to severe impact. In cases where the impact severity index was less than 0.8, the percentage of impact events in which the helicopter sank reduced from 12% for a conventional four-float system to 3% for the five-float system, and to zero for the six-float combination. Expressed in another way: the impact severity index below which there was a 5% probability of sinking increased from 0.7 to 0.9 when the first upper cabin float was added, and to a point well above the survivability limit when all six floats were present.

9.4.2 *Probability of Sinking in a Severe Crash*

In their accompanying cost-benefit study [1] WSA estimated that the probability of sinking in a severe (but otherwise partially survivable) water impact accident is about 0.65. This figure was based on accident statistics from the NTSB accident database between 1982 and 1989. Many assumptions had to be made when interpreting the NTSB data, and it was difficult to make a comparison with the results of the present study. An attempt was nonetheless made to find out whether WSA's estimate was at all similar to the value obtained from the present model by considering the proportion of severe but partially survivable incidents which resulted in sinking with a conventional four-float system. In this context a severe but partially survivable incident was considered to be one where the impact severity index lay between 0.8 and 1.2. The total number of such incidents, from Figure 104, was 5,364, and the helicopter sank on 3,299 of these occasions. Sinking therefore occurred on 61% of occasions. Lowering the upper limit to 1.0 reduced the proportion to 58%, showing that the end result was not unduly sensitive to where the upper limit was set.

The similarity between WSA's estimate (65%) and that obtained here (61%) is partly fortuitous, bearing in mind the very different underlying assumptions, but obtaining values which were even remotely similar gave some confidence that both estimates might be realistic.

9.4.3 *Criteria for Side-Floating*

It was assumed, for the purposes of this study, that a helicopter with a conventional four-float system would always capsize on impact. Because the helicopter could never float on its side, every impact event resulted in a 'failure'.

Adding one upper cabin float gave a significant improvement in the 'success' rate, but also gave the somewhat surprising result that if the helicopter floated at all, it always floated on its side. This meant that the 'failure' scatter plot for side-floating ability was identical to that for floating ability (Figure 105). Another way of looking at this result is to say that any impact severe enough to damage the (relatively unexposed) upper cabin float also damaged enough other floats to make the helicopter sink.

There is also no difference between results based on floating and side-floating criteria with a six-float system. In this case the helicopter always floated on its side, regardless of the severity or type of impact. No impact caused both upper cabin floats to fail simultaneously, one float always remaining intact to make the helicopter float on its side.

Figure 107 shows the percentage of occasions when the helicopter failed to float on its side within each impact severity index curve. The curves corresponding to the five-float and six-float systems are identical to those shown in Figure 106, but the curve for the conventional four-float system has moved up to 100%.

9.4.4 *Criteria for a Satisfactory Air Space*

It was assumed, for the purposes of this study, that a helicopter with a conventional four-float system would always capsize and invert on impact. As a result there would never be a satisfactory air space in the cabin, and every impact event resulted in a 'failure'.

Figure 108 shows incidents in which the helicopter, with a five-float system, failed to provide a satisfactory air space. Most of the results shown in this plot correspond to vertical descent and loss of control incidents, with very few fly-in cases. Figure 109 shows similar results for the six-float system.

Figure 110 shows the percentage of occasions when there was an unsatisfactory air space in the cabin, as the impact severity index varied. The solid line represents results obtained with a conventional four-float system. The dashed line represents a five-float system, and the dotted line a six-float combination. Adding a single upper cabin float greatly increased the probability of having a satisfactory air space in the cabin after a moderate to severe impact. When the impact severity index was less than 0.8, the air space was always unsatisfactory with a conventional four-float system, but on only 7% of occasions with the five-float system, and on 5% of occasions with the six-float combination. Expressed in another way, the impact severity index below which there was 5% probability of having an unsatisfactory air space increased from 0.75 to 0.85 when the second upper cabin float was added.

Measured in these terms, most of the gain in crashworthiness occurred when the first upper cabin float was added. The second upper cabin float resulted in only a small further improvement.

9.4.5 *Float Failure Combinations*

Tables 9.5 to 9.7 show how many times each panel failure combination occurred during each simulation run, broken down according to the type of impact incident (ditching, vertical descent, loss of control or fly-in). Cells in the first six columns of each table show (in red) the panels that failed and (in green) those that remained intact. Hatched cells indicate that the relevant float was not present (eg. there were no upper cabin floats in the four-float system). The float numbering system used in these tables is the same as is shown in Figure 103.

Ten out of 16 possible float failure combinations occurred with the four-float system, but only 12 out of a possible 32 occurred with the five-float system, and 13 out of a possible 64 with the six-float system. Other failure combinations did not occur for one or another of the following reasons:

- (a) the analysis only considered loading on an individual panel, and did not take account of damage to the surrounding hull and neighbouring panels;
- (b) one or other of the two main sponson panels always faced away from the water surface on impact, and it was impossible to fail both simultaneously;
- (c) their orientations were such that no more than three panels could face towards the water surface, and therefore fail, during any given impact event;
- (d) the two upper cabin panels could only fail simultaneously if the helicopter were to fall onto the water surface upside down at high speed, and this very rare event never occurred.

The next four columns in each table show the number of times each failure combination occurred in 4,000 impact events representing each of the four types of incident. The last column shows the total number of times each failure combination occurred (out of a total of 16,000 impact events) when results from all four types of incident were combined.

Many of the numbers are repeated between one table and another without change. These repeated numbers generally correspond to combinations where an upper cabin float remained intact. Incidents in which an upper cabin float was damaged were not common, and only occurred when the helicopter landed on one side at a steep angle of inclination, leaving the floats on the other side intact.

**Table 9.5: Number of occurrences for each failure combination:
four-float configuration.**

| Failure combination ⁴ | | | | | | Ditching | Vertical descent | Loss of control | Fly in | Total |
|----------------------------------|-------|-------|-------|--|--|----------|------------------|-----------------|--------|-------|
| Bag 1 | Bag 2 | Bag 3 | Bag 4 | | | | | | | |
| | | | | | | 0 | 18 | 31 | 3 | 52 |
| | | | | | | 0 | 15 | 37 | 2 | 54 |
| | | | | | | 4 | 341 | 487 | 344 | 1176 |
| | | | | | | 0 | 1322 | 642 | 8 | 1972 |
| | | | | | | 0 | 1278 | 631 | 10 | 1919 |
| | | | | | | 19 | 334 | 772 | 721 | 1846 |
| | | | | | | 14 | 364 | 818 | 707 | 1903 |
| | | | | | | 0 | 7 | 0 | 0 | 7 |
| | | | | | | 0 | 3 | 0 | 0 | 3 |
| | | | | | | 3963 | 318 | 582 | 2205 | 7068 |
| Total | | | | | | 4000 | 4000 | 4000 | 4000 | 16000 |

**Table 9.6: Number of occurrences for each failure combination:
five-float configuration.**

| Failure combination ⁴ | | | | | | Ditching | Vertical descent | Loss of control | Fly in | Total |
|----------------------------------|-------|-------|-------|-------|--|----------|------------------|-----------------|--------|-------|
| Bag 1 | Bag 2 | Bag 3 | Bag 4 | Bag 5 | | | | | | |
| | | | | | | 0 | 18 | 31 | 3 | 52 |
| | | | | | | 0 | 15 | 37 | 2 | 54 |
| | | | | | | 0 | 722 | 357 | 1 | 1080 |
| | | | | | | 4 | 341 | 487 | 344 | 1176 |
| | | | | | | 0 | 600 | 285 | 7 | 892 |
| | | | | | | 0 | 1278 | 631 | 10 | 1919 |
| | | | | | | 0 | 1 | 0 | 0 | 1 |
| | | | | | | 19 | 334 | 772 | 721 | 1846 |
| | | | | | | 14 | 364 | 818 | 707 | 1903 |
| | | | | | | 0 | 6 | 0 | 0 | 6 |
| | | | | | | 0 | 3 | 0 | 0 | 3 |
| | | | | | | 3963 | 318 | 582 | 2205 | 7068 |
| Total | | | | | | 4000 | 4000 | 4000 | 4000 | 16000 |

⁴ Green cell denotes 'float intact'. Red cell denotes 'failure'.

| Table 9.7: Number of occurrences for each failure combination: six-float configuration. | | | | | | | | | | |
|---|-------|-------|-------|-------|-------|----------|------------------|-----------------|--------|-------|
| Failure combination ⁴ | | | | | | Ditching | Vertical descent | Loss of control | Fly in | Total |
| Bag 1 | Bag 2 | Bag 3 | Bag 4 | Bag 5 | Bag 6 | | | | | |
| | | | | | | 0 | 18 | 31 | 3 | 52 |
| | | | | | | 0 | 15 | 37 | 2 | 54 |
| | | | | | | 0 | 722 | 357 | 1 | 1080 |
| | | | | | | 0 | 748 | 372 | 4 | 1124 |
| | | | | | | 4 | 341 | 487 | 344 | 1176 |
| | | | | | | 0 | 600 | 285 | 7 | 892 |
| | | | | | | 0 | 530 | 259 | 6 | 795 |
| | | | | | | 0 | 1 | 0 | 0 | 1 |
| | | | | | | 19 | 334 | 772 | 721 | 1846 |
| | | | | | | 14 | 364 | 818 | 707 | 1903 |
| | | | | | | 0 | 6 | 0 | 0 | 6 |
| | | | | | | 0 | 3 | 0 | 0 | 3 |
| | | | | | | 3963 | 318 | 582 | 2205 | 7068 |
| Total | | | | | | 4000 | 4000 | 4000 | 4000 | 16000 |

9.5 Conclusions from EH101 Multi-Float Redundancy Study

The objective of this investigation was to find out whether there are likely to be significant benefits, in terms of crashworthiness, from having additional redundant emergency flotation units installed. The benefits were judged in terms of whether the extra units would improve the helicopter's ability to float (inverted), float on its side, or provide a satisfactory air space in the cabin after water impact.

Adding one upper cabin float significantly improved the helicopter's crashworthiness, compared with a conventional four float system. An upper cabin float increased the probability that the helicopter would float, and enabled the helicopter to float on its side, which in most cases also provided a satisfactory air space in the cabin.

Adding a second cabin float improved crashworthiness further. It prevented sinking and inversion completely, at least in the circumstances considered during this study (where the possibility of hull damage was not taken into account). It also increased to some extent the number of occasions when there was a satisfactory air space.

Only a small proportion of the 64 possible float failure combinations occurred during this study. No more than three floats failed in any impact event. It was also rare for an upper cabin float to be damaged, because of its relatively protected location on the cabin wall. An upper cabin float only failed when the helicopter fell onto that side, leaving all floats on the opposite side intact.

Although this study made many simplifying assumptions, the general principles and conclusions seem intuitively to be valid. The study demonstrated that there are clear benefits, in terms of crashworthiness, from having additional floats on the upper cabin walls. Benefits emerged regardless of whether they were measured in terms of reducing the number of occasions when the helicopter sank, making it float on its side, or providing a satisfactory air space in the cabin. The largest improvement came when the first upper cabin float was added.

There are possible advantages in this asymmetric float configuration, because it gives the helicopter a preferred orientation in the water. Model tests at HTC [31] had shown that the six-float arrangement allowed two possible stable orientations of the hull after capsizing. With a five-float arrangement, however, there was only one stable attitude, eliminating the risk of a second rotation while the occupants are trying to escape.

10 OVERALL CONCLUSIONS

Detailed conclusions from BMT's initial investigations have already been presented in reference [2]. Conclusions from BMT's subsequent sensitivity study, together with investigations based on the *Brent Spar* and *Cormorant Alpha* accident scenarios, were presented in reference [3]. The following overall conclusions are based on results from these initial investigations together with follow-up data assessment and float redundancy studies.

Each of the flotation units considered during this investigation was assumed to be mounted within either a sponson or fuselage panel, and was assumed to be uninflated at the moment of impact. The flotation unit was deemed to fail if the impact load on the sponson or fuselage panel exceeded its design value.

Impact, planing and drag forces on the sponson and panel were estimated by combining simple theoretical and empirical load calculation procedures. Exceedance probability distributions of water impact loads were then estimated using a Monte Carlo simulation procedure. This procedure took account of the randomness and variability in the impact scenario and in the loading process. Predicted exceedance distributions of maximum total impact loads were compared with typical design loads for the sponson and panel.

Key conclusions from this investigation were as follows:

- The probability of exceeding design loads in a controlled ditching incident was found to be very low, as had been expected. Flotation equipment is designed to survive a normal ditching.
- The base case investigation showed a relatively high probability of exceeding design loads on both the sponson and fuselage panel during vertical descent and loss of control incidents. This result suggested that substantial increases in design loads would be required in order to avoid major structural damage to flotation systems in these two types of incident.
- A follow-up sensitivity study confirmed that a 100% increase in design loads would result in only a modest improvement in crashworthiness.

- Major structural failures have occurred during actual fly-in accidents in the past. The simulations nonetheless predicted that the risks of exceeding design loads on both the sponson and fuselage panel during a fly-in are relatively low. There are two likely reasons for this unexpected result. Firstly, drag and planing forces make major contributions to the total predicted load during a fly-in. These forces are poorly understood, and the simplified formulae used in the present analysis may not be reliable. Secondly, the model considers loads on an individual sponson or panel in isolation, and does not consider failure of the surrounding hull structure. The design of flotation equipment should in practice consider the design and strength of the supporting hull structure.
- Severe impacts on the fuselage panel were typically associated with small angles of impact between the hull and water surfaces. These very severe impacts may not be modelled satisfactorily by the present procedure, because no attempt was made to represent in detail the effects of air entrapment or acoustic pressure limits.
- Sea state conditions had little effect on the results obtained from the investigation as a whole. They had a significant effect on results obtained in severe sea conditions, however, and increased the range of loads substantially during controlled ditching and fly-in incidents.
- The impact force proved to be sensitive to variations in several different parameters. It may therefore be difficult to characterise helicopter impact incidents in terms of a small number of deterministic scenarios.
- Impact loads were sensitive to variations in the helicopter's mean speed and descent angle at the moment of impact. The drag force coefficient was also an important parameter. The helicopter's mean pitch angle and the planing force coefficient only affected loads experienced during ditching and fly-in incidents.
- Investigations into float redundancy demonstrated that there are clear benefits, in terms of crashworthiness, from having additional floats on the upper cabin walls. Benefits emerged regardless of whether they were measured in terms of reducing the number of occasions when the helicopter sank, making it float on its side, or providing a satisfactory air space in the cabin. The largest improvement came when the first upper cabin float was added. There are possible advantages in this asymmetric float configuration, because it gives the helicopter a preferred stable attitude in the water, eliminating the risk of a second rotation while the occupants are trying to escape.

The results from this study suggested a number of further possible conclusions, although these issues were not considered in detail:

- Alternative methods for improving crashworthiness might also be considered, such as designing a 'crumple zone' or other energy-absorbing device into the support structure. Whatever solution is adopted, however, the structure must retain sufficient integrity to serve its primary function of providing buoyancy.
- There may be potential for reducing impact loads during a fly-in incident by modifying the shape of the hull or sponson, and avoiding large flat areas.

- The present investigations considered all-year wave conditions in the central area of the North Sea. It is likely that selecting a more severe wave climate (e.g. West of Shetland) would significantly increase the loads predicted during controlled ditching and fly-in incidents. Suitable design criteria would be needed to take account of increases in water impact loading due to waves.
- BMT recommends that further work should be done to investigate the importance of drag and planing type forces in the water impact loading process, and the feasibility of representing these loads better in the calculations. These forces turned out to be more significant than originally anticipated, and simplifications in existing calculation procedures may have resulted in unexpectedly low predicted forces during fly-in incidents.

11 ACKNOWLEDGEMENTS

BMT gratefully acknowledges assistance provided by GKN Westland Helicopters Limited, who supplied design information on the *Sea King* helicopter, and provided valuable advice and comments during the course of this project. BMT also gratefully acknowledges information provided by WS Atkins Science and Technology for the investigations based on the *Brent Spar* and *Cormorant Alpha* accident scenarios.

12 REFERENCES

- [1] WS Atkins Science and Technology, 'Crashworthiness of helicopter emergency flotation systems' report ref. AM3504/R006, 2000.
- [2] BMT Fluid Mechanics Limited, 'Crashworthiness of Helicopter Emergency Flotation Systems: Main Report and Results', Report no. 44134r23, 1998.
- [3] BMT Fluid Mechanics Limited, 'Crashworthiness of Helicopter Emergency Flotation Systems: Results from Supplementary Investigations', Report no. 44134r33, 1999.
- [4] Air Accidents Investigation Branch, 'Report on the accident to Sikorsky S61N, G-BEWL, at Brent Spar, East Shetland Basin on 25 July 1990', AAIB report no. 2/91, 1991.
- [5] Air Accidents Investigation Branch, 'Report on the accident to AS332L Super Puma, G-TIGH, near Cormorant 'A' Platform, East Shetland Basin on 14 March 1992', AAIB report no. 2/93, 1993.
- [6] CAA contract no. 084/SRG/R&AD/1, dated 4 September 1996 and re-issued 21 October 1996, together with Amendments.
- [7] Westland Helicopters Limited, 'A review of UK military and world civil helicopter water impacts over the period 1971-1992', Stress Department report no. SDR 146, November 1993, published in CAA Paper no. 96005.
- [8] Westland Helicopters Limited, 'An analysis of the response of helicopter structures to water impact', Stress Department report no. SDR 156, March 1995, published in CAA Paper no. 96005.
- [9] Federal Aviation Administration, 'Survey and analysis of rotorcraft flotation systems', US Department of Transportation, Office of Aviation Research, report no. DOT/FAA/AR-95/53, 1996.

- [10] Federal Aviation Administration, 'Rotorcraft ditchings and water related impacts that occurred from 1982 to 1989 - phase I', US Department of Transportation, Federal Aviation Administration Technical Center report no. DOT/FAA/CT-92/13, 1993.
- [11] Federal Aviation Administration, 'Rotorcraft ditchings and water related impacts that occurred from 1982 to 1989 - phase II', US Department of Transportation, Federal Aviation Administration Technical Center report no. DOT/FAA/CT-92/14, 1993.
- [12] Von Karman, T., 'The impact of seaplane floats during landing', NACA Technical Note 321, Washington, 1929.
- [13] Wagner, H., 'Über Stoss- und Gleitvorgänge an der Oberfläche von Flüssigkeiten', Zeitschrift für Angewandte Mathematik und Mechanik, vol. 12, part 4, pp. 193-235, 1932.
- [14] Mayo, W.L., 'Analysis and modification of theory for impact of seaplanes on water', National Advisory Committee for Aeronautics, Technical Note no. 1008, 1945.
- [15] Milwitzky, B., 'Generalised theory for seaplane impact', National Advisory Committee for Aeronautics, Report no. 1103, 1952.
- [16] Schnitzer, E., and Hathaway, M.E., 'Estimation of hydrodynamic impact loads and pressure distributions on bodies approximating elliptical cylinders with special reference to water landing of helicopters', National Advisory Committee for Aeronautics, Technical Note no. 2889, 1953.
- [17] Arlotte, T., Ward Brown, P., and Crewe, P.R., 'Seaplane impact - a review of theoretical and experimental results', ed. A.G. Smith, Aero. Res. Council R.& M. no. 3285, 1958.
- [18] The Health and Safety Executive, 'Offshore Installations: Guidance on Design, Construction and Certification, 4th edition with amendments, 1993.
- [19] Department of Energy, 'Fluid Loading on Fixed Offshore Structures', Volume 1, Offshore Technology Report no. OTH 90 322, HMSO, 1990.
- [20] Ridley, J.A., 'A study of some theoretical aspects of slamming', National Maritime Institute Report no. NMI R158, Department of Energy Offshore Technology report no. OT-R-82113, 1982.
- [21] Campbell, I.M.C., and Weynberg, P.A., 'Measurement of parameters affecting slamming', Wolfson Unit for Marine Technology, University of Southampton, Report no. 440, Department of Energy report no. OT-R-8042, 1980.
- [22] Campbell, I.M.C., 'Response of a tubular beam to an inclined slam impact', Wolfson Unit for Marine Technology, University of Southampton, Report no. 488/1, 1982.
- [23] Prasad, S., Chan, E-S., and Isaacson, M., 'Breaking wave impact on a slender horizontal cylinder', Proc. 4th Intl. Offshore and Polar Engineering. Conf., Osaka, Vol. III, pp. 225-232, 1994.
- [24] Chuang, S.L., 'Experiments on flat bottom slamming', J. Ship Res., pp. 10-17, March 1966.

- [25] Arai, M., Cheng, L.Y., and Inoue, Y., 'Hydrodynamic impact loads on horizontal members of offshore structures', Proc. Offshore Mechanics and Arctic Engineering Conf., Vol. 1-A, pp. 199-206, 1995.
- [26] Chuang, S-L., 'Slamming tests of three-dimensional models in calm water and waves', Naval Ship Research and Development Center report no. 4095, Bethesda, 1973.
- [27] Batchelor, G.K., 'An Introduction to Fluid Dynamics', Cambridge University Press, 1967.
- [28] Barltrop, N.D.P., and Adams, A.J., 'Dynamics of Fixed Structures', third edition, Butterworth-Heinemann, 1991.
- [29] GKN Westland Helicopters Limited: drawings received 2 January 1997; fax dated 14 January 1997; fax dated 6 February 1997; fax ref. E/WSC/4245 dated 27 February 1997; fax ref. E/WSC/4296 dated 14 May 1997.
- [30] E.H. Industries Ltd., 'EH101 The New Generation', Brochure No. EB0001, undated.
- [31] Civil Aviation Authority, 'Devices to Prevent Helicopter Total Inversion Following a Ditching', CAA paper no. 97010, December 1997.
- [32] Westland Helicopters Ltd., 'Definition of emergency flotation system for EH101 "ASW 299D" basic naval variant (AUW = 15,000kg)', Power System Note no. 315, February 1995.
- [33] EEL Limited, 'Model flotation tests on the EH101 helicopter (civil version)', report no. EEL/ED/414 Issue A, February 1987.
- [34] EEL Limited, 'Model ditching tests on the WG-34 helicopter', report no. X/0/2639, August 1979.
- [35] WS Atkins, facsimile addressed to BMT Fluid Mechanics Limited, ref. AM3504/03/34, dated 6 March 1998.
- [36] WS Atkins, facsimile addressed to BMT Fluid Mechanics Limited, ref. AM3504/03/47, dated 23 July 1998.
- [37] WS Atkins, facsimile addressed to BMT Fluid Mechanics Limited, ref. AM3504/03/53, dated 21 December 1998..
- [38] WS Atkins, facsimile addressed to BMT Fluid Mechanics Limited, ref. AM3504/03/25/egc, dated 30 October 1997.
- [39] BMT Fluid Mechanics Limited, facsimile addressed to WS Atlins, ref. 44134/sjr/f21, dated 4 February 1998.

KEY NOMENCLATURE

| | |
|------------------------|--|
| A | area presented to the flow |
| a_0, a_1, a_2 | coefficients in cylinder impact force equations (4) and (12) |
| b_1, b_2 | coefficients in cylinder impact force equations (4) and (12) |
| c | structure stiffness |
| C_d | drag force coefficient |
| C_{pl} | planing force coefficient |
| $C_{p \max}$ | maximum pressure coefficient (equation (5)) |
| C_s | impact force coefficient (equation (1)) |
| C_o | variability parameter in panel impact force equation (14) |
| F_d | drag force on the sponson (equation (28)) |
| $F_{\max \text{ imp}}$ | maximum impact force on the sponson or fuselage panel (equations (11) and (14)) |
| F_{pl} | planing force on the fuselage panel (equation (30)) |
| $F_{r \max}$ | maximum structure force in the sponson or fuselage panel assembly (equations (25) and (26)) |
| F_w | maximum non-dimensional panel force calculated using Wagner's theory (equations (7) and (8)) |
| D | mean diameter of cylinder or cone segment |
| g | acceleration due to gravity |
| H_s | significant wave height |
| J | impulse on the sponson segment or fuselage panel |
| L | length of the sponson segment or fuselage panel |
| S_{lim} | limiting value of significant wave steepness |
| S_s | significant wave steepness (equation (2)) |
| t | time |
| T_{imp} | impact duration |
| T_n | natural response period of the sponson or fuselage panel assembly |
| T_z | mean zero up-crossing wave period |
| \underline{u}_b | helicopter velocity vector |
| \underline{u}_p | relative water particle velocity vector |
| u_p | relative water particle velocity, resolved normal to structure surface |
| \underline{u}_s | relative water surface velocity vector |
| u_s | relative water surface velocity, resolved normal to structure surface |
| \underline{u}_w | water surface velocity vector |
| W | fuselage panel width |
| α | inclination of plate to flow (in planing force equation (30)) |

| | |
|--------------|---|
| β | angle between the sponson segment axis and water surface on impact |
| Φ_c | inclined cylinder impact force coefficient (equation (12)) |
| Φ_s | non-dimensional cylinder impact force coefficient (equation (4)) |
| Φ_w | non-dimensional panel impact force coefficient (equation (15)) |
| ρ | water density |
| ξ | impact angle between the fuselage panel and water surface |
| ξ_{\min} | minimum value of ξ , used in panel impact force equation (15) |
| ω_n | angular natural frequency of the sponson or fuselage panel assembly |

ABBREVIATIONS

| | |
|---------|---|
| AAIB | Air Accidents Investigation Branch |
| BMT | BMT Fluid Mechanics Limited |
| CAA | Civil Aviation Authority |
| FAA | Federal Aviation Authority |
| GKN WHL | GKN Westland Helicopters Limited |
| HSE | The Health and Safety Executive |
| HTC | Hydrodynamic Test Centre |
| NACA | National Advisory Committee for Aeronautics |
| NTSB | National Transportation Safety Board |
| UK | United Kingdom |
| WSA | WS Atkins Science and Technology |

Figures

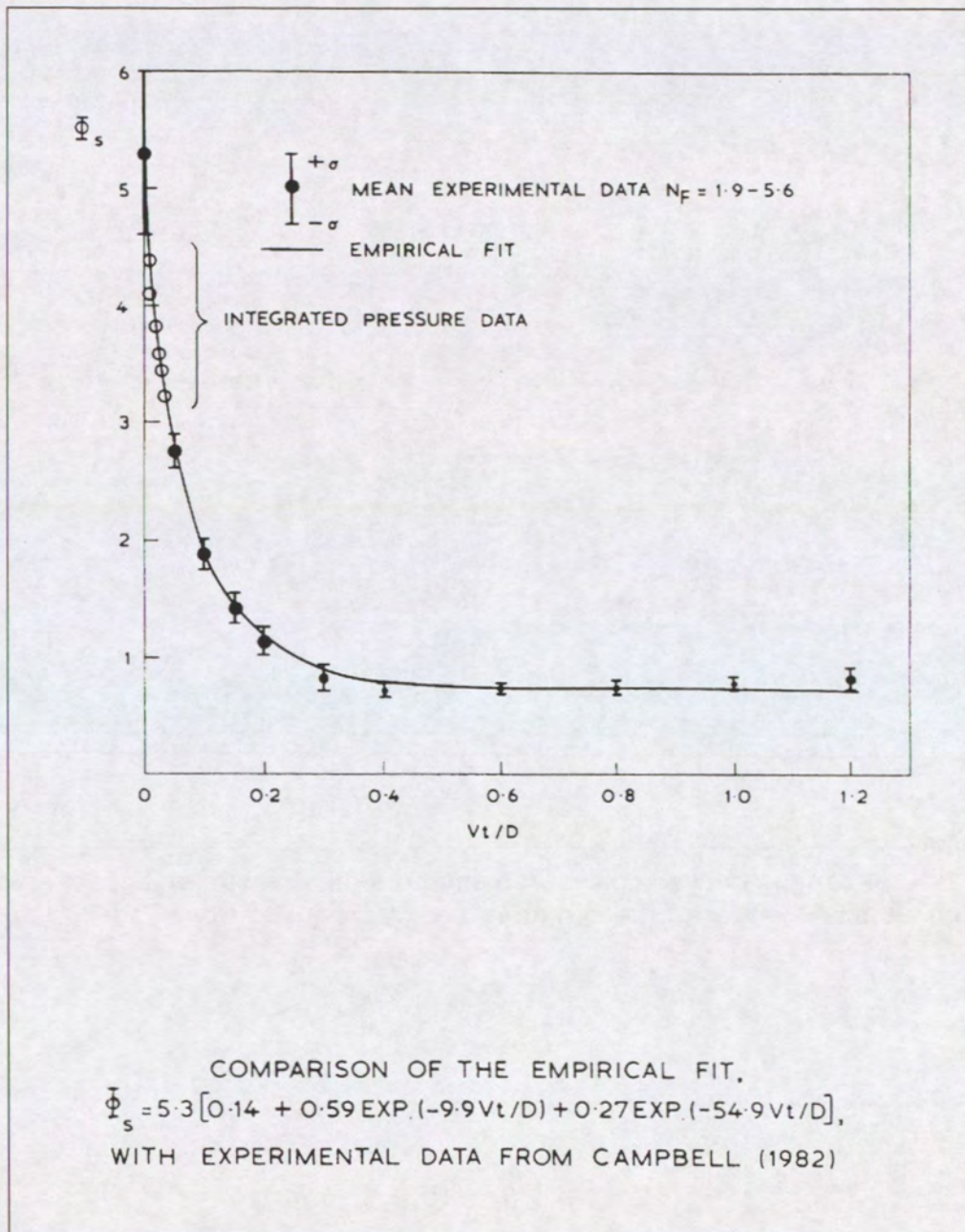


Figure 1: Comparison between the theoretical force history and measured data for horizontal cylinder impacts on smooth water (reproduced from Ridley [20]).

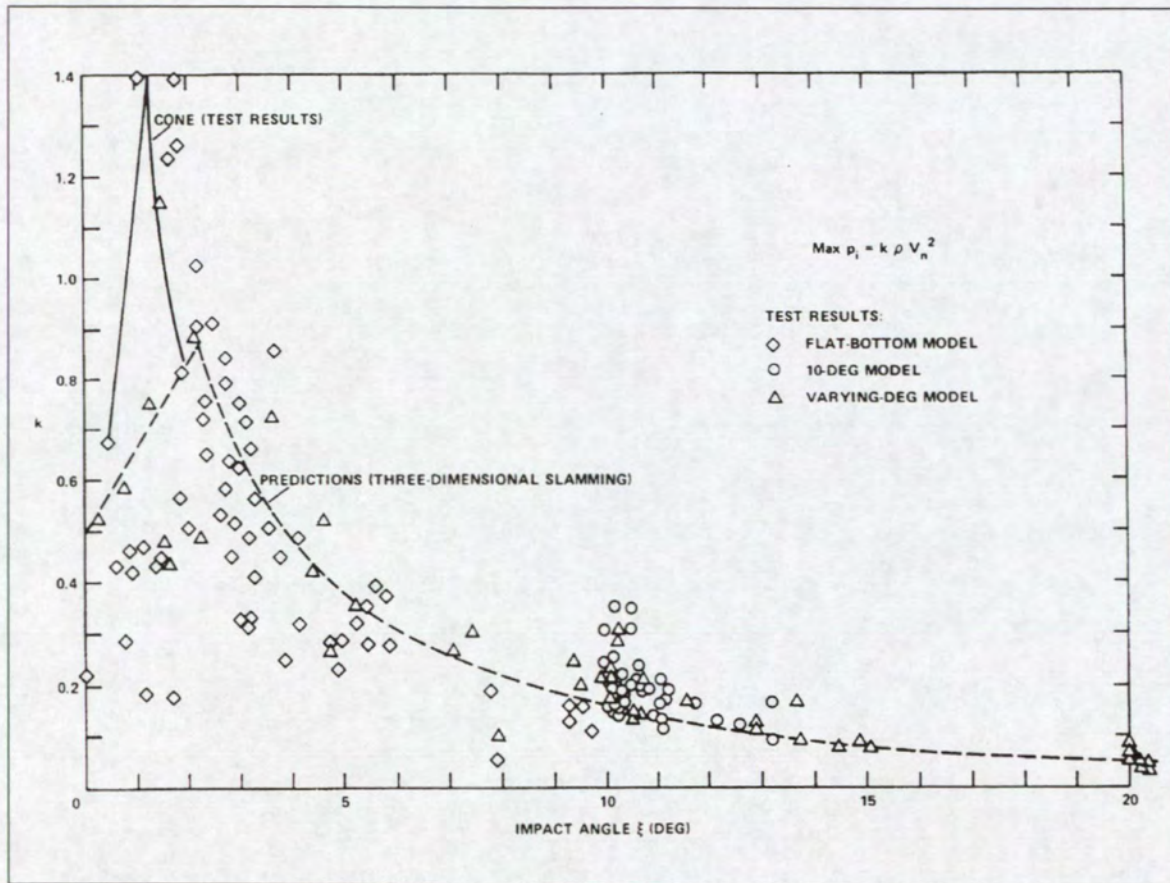


Figure 2: Comparison between measured and predicted maximum impact pressures from tests on wedges dropped onto waves (reproduced from Chuang [26]).

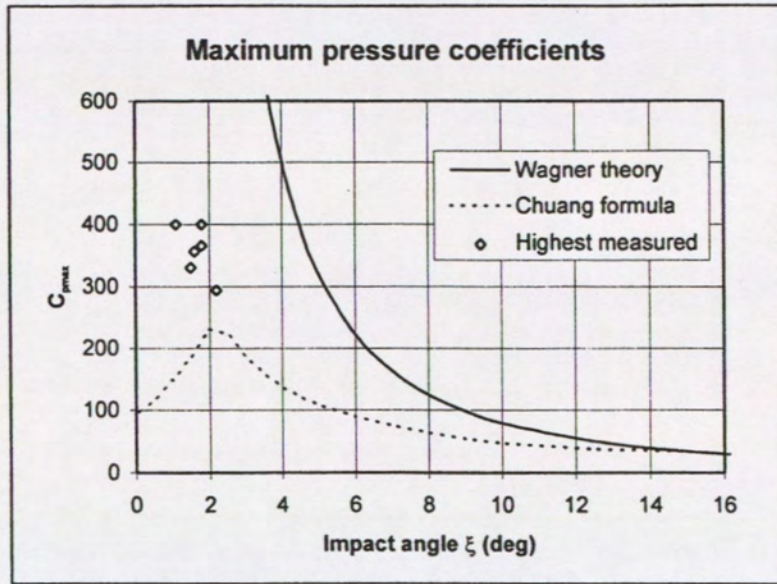


Figure 3: Comparison between Wagner and Chuang formulae for the maximum pressure coefficient.

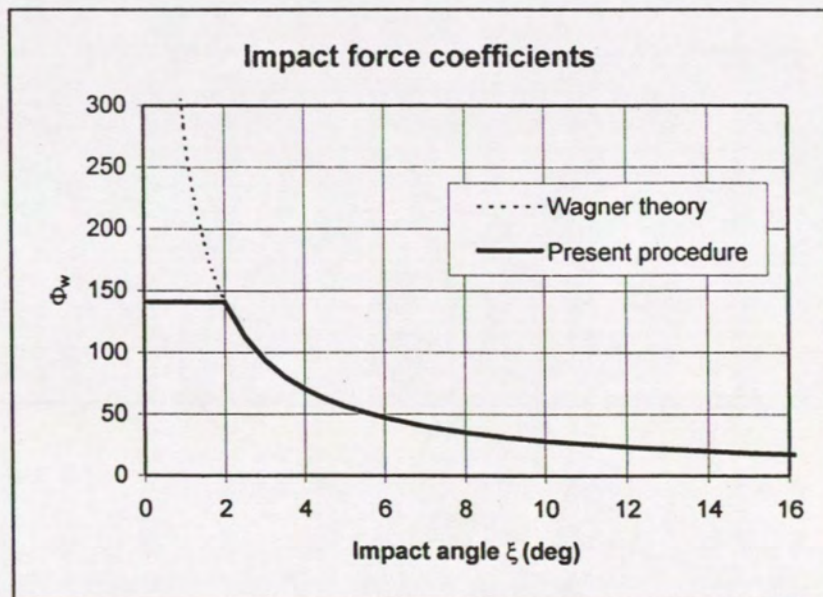


Figure 4: Comparison between the impact force coefficient $\Phi_w(\xi)$ used in the present analysis with that predicted by Wagner's theory.

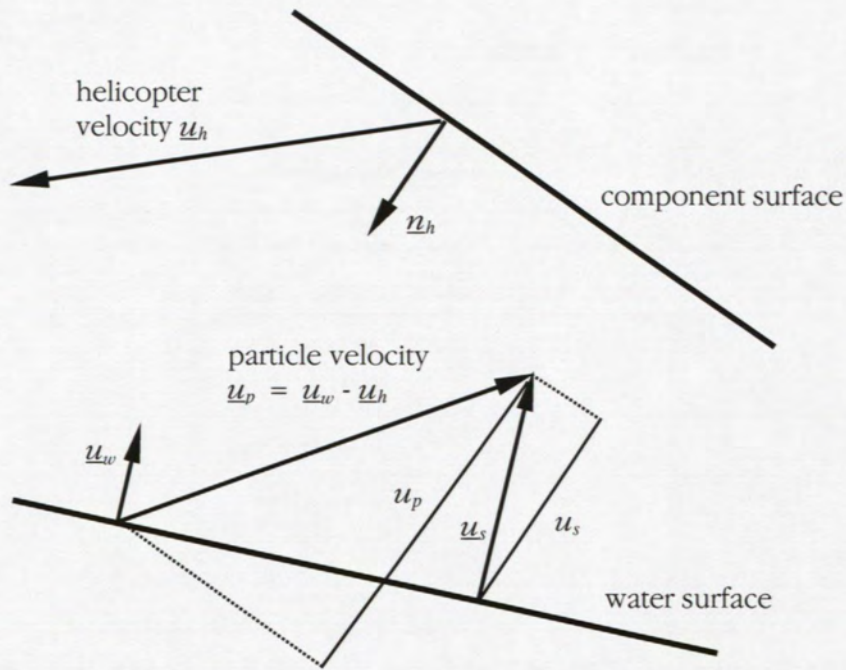


Figure 5: Typical relationships between helicopter, water surface and relative water particle velocities.

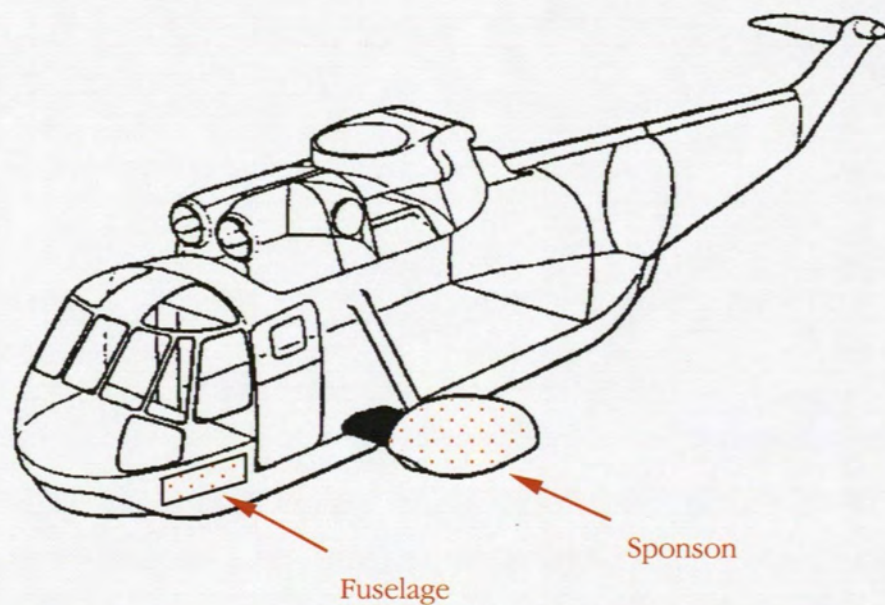


Figure 6: Typical sponson and fuselage panel locations assumed in base case and sensitivity studies.

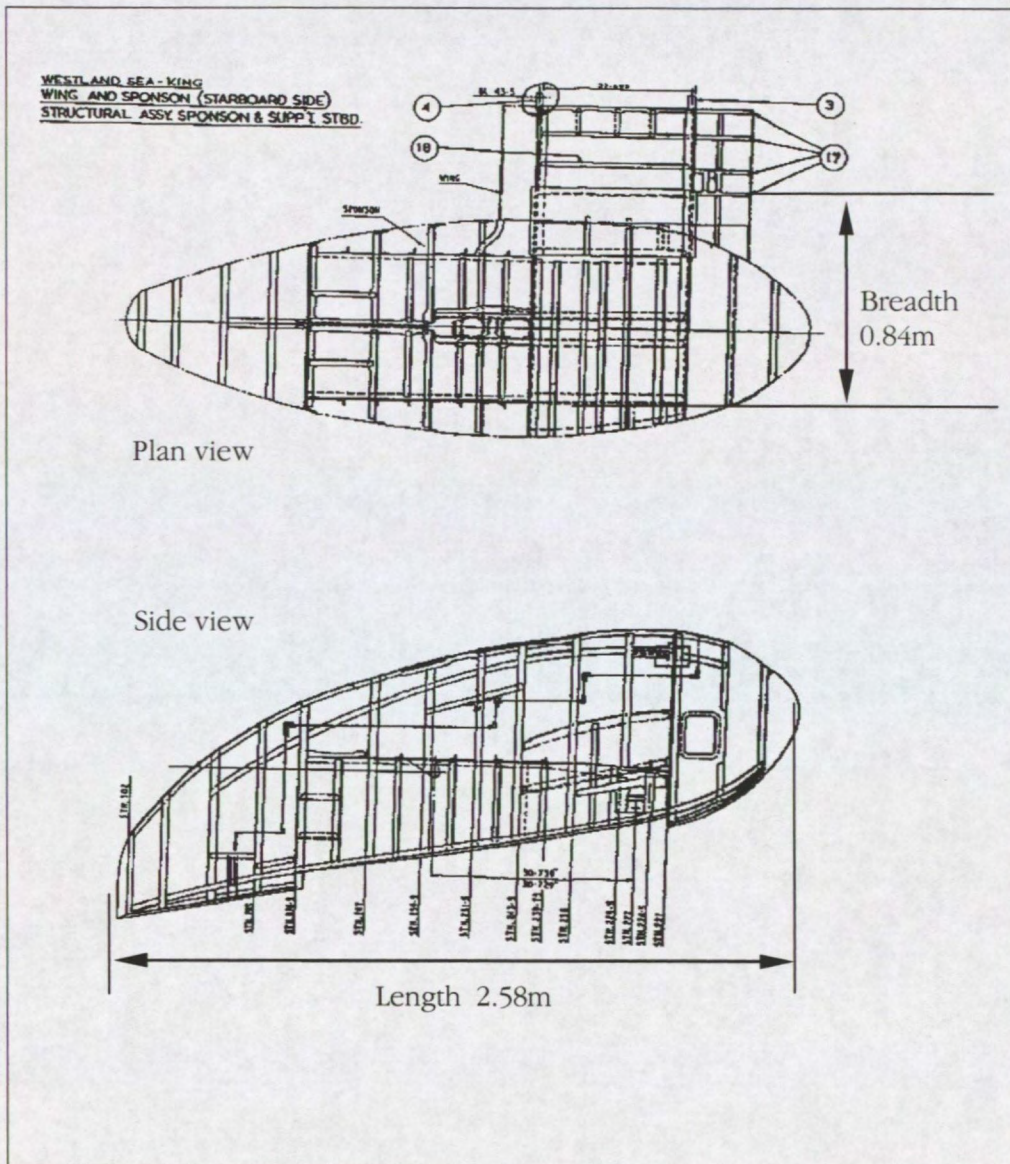


Figure 7: Plan and side views of the *Sea King* sponson.

**Correlation plots: maximum structure and drag forces
against the total impact force on the sponson;
all incident scenarios, base case conditions.**

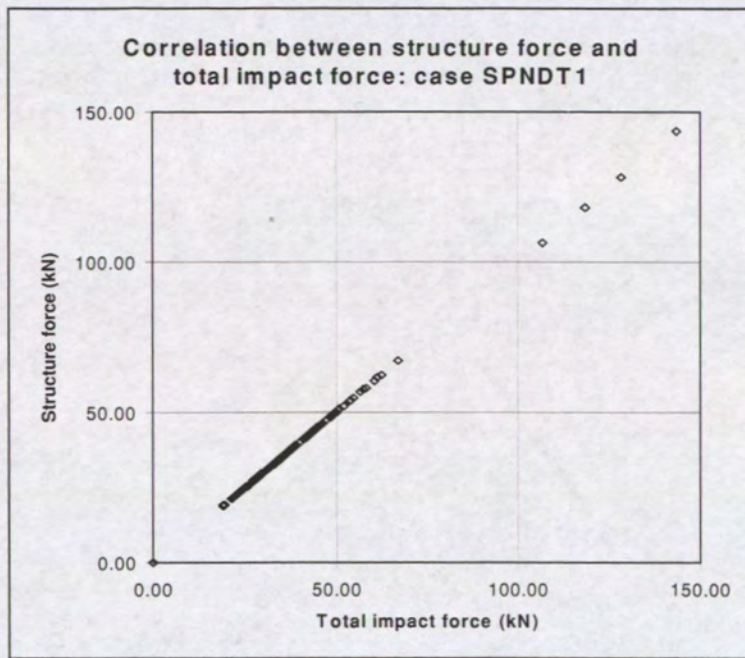


Figure 8: Correlation between maximum structure force and total impact force: sponson in controlled ditching incident, central North Sea waves.

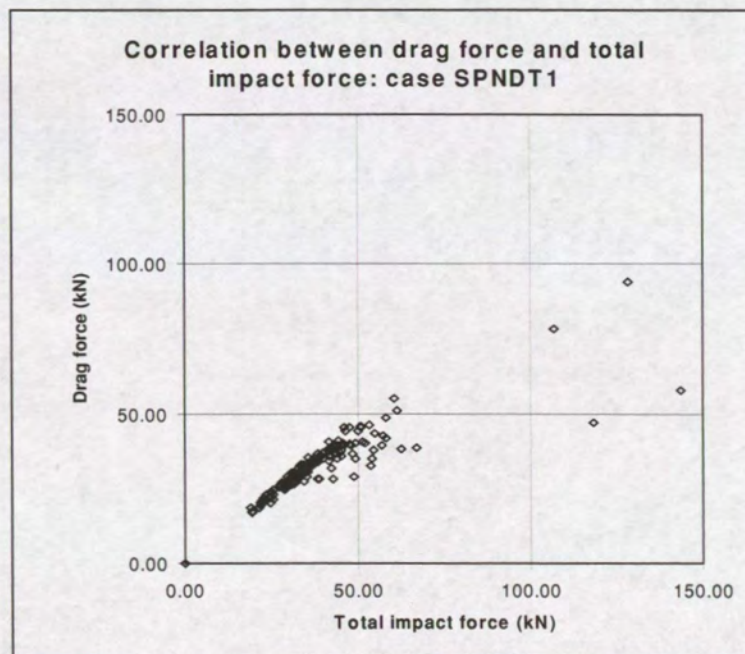


Figure 9: Correlation between the drag force and maximum total impact force: sponson in controlled ditching incident, central North Sea waves.

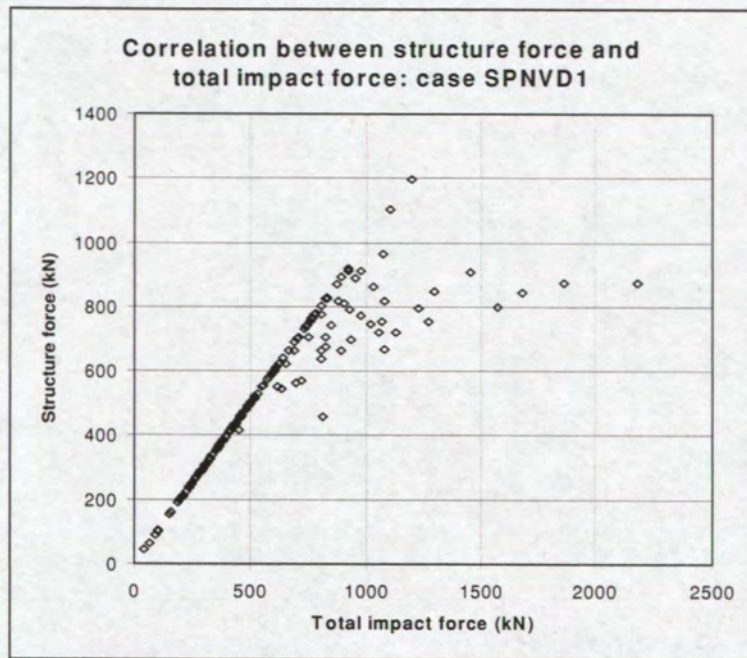


Figure 10: Correlation between maximum structure force and total impact force: sponson in vertical descent incident, central North Sea waves.

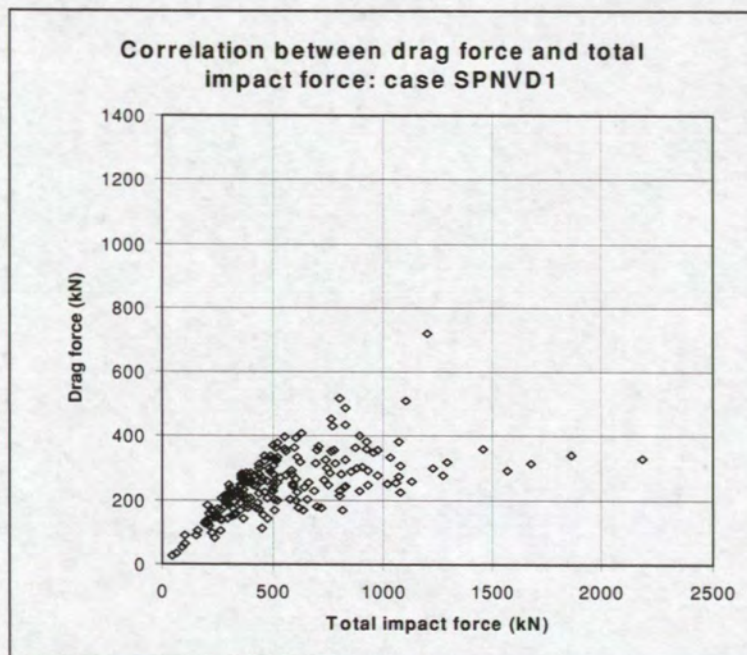


Figure 11: Correlation between the drag force and maximum total impact force: sponson in vertical descent incident, central North Sea waves.

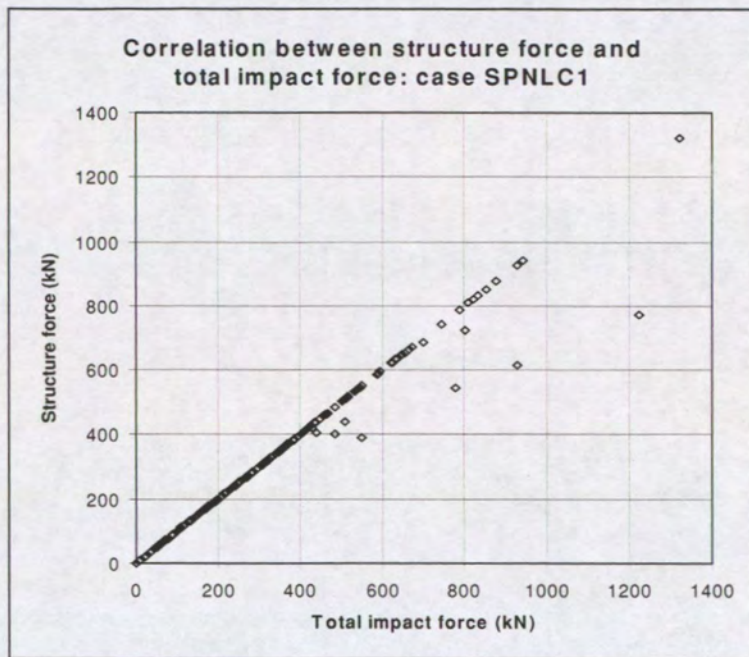


Figure 12: Correlation between maximum structure force and total impact force: sponson in loss of control incident, central North Sea waves.

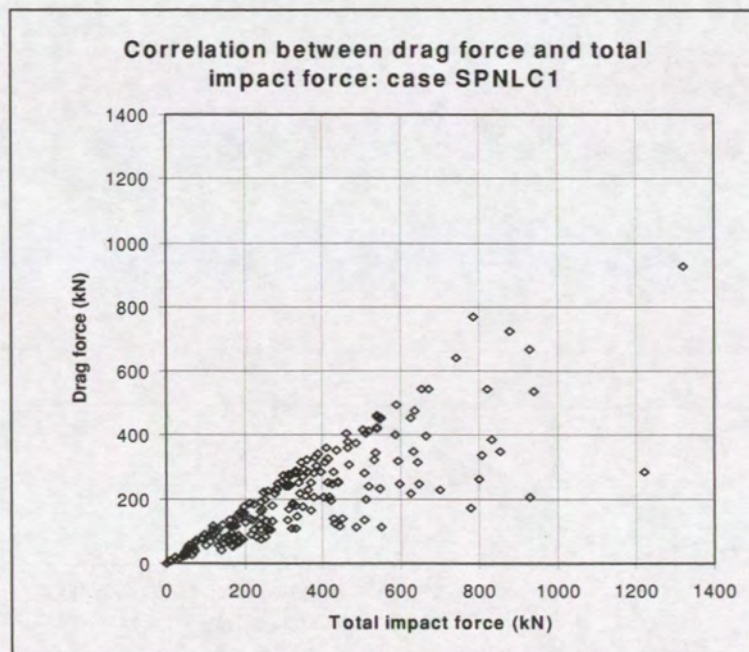


Figure 13: Correlation between the drag force and maximum total impact force: sponson in loss of control incident, central North Sea waves.

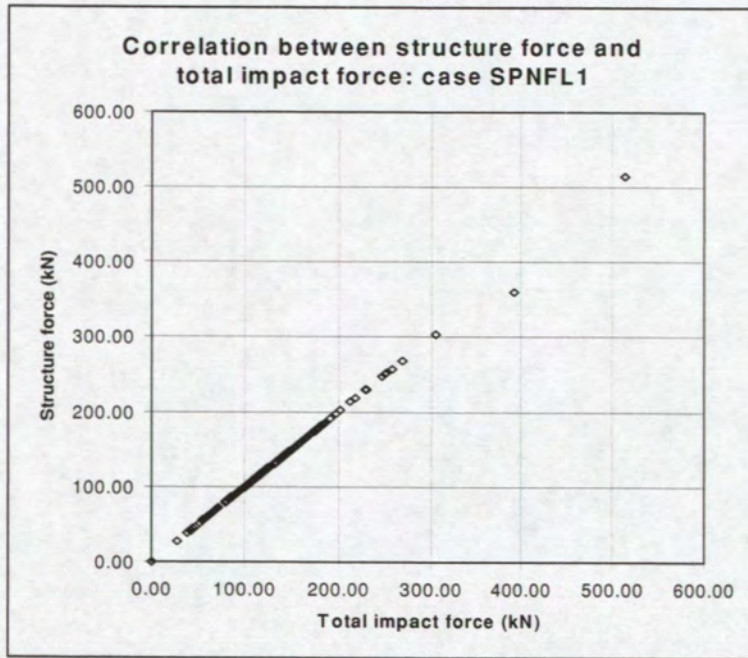


Figure 14: Correlation between maximum structure force and total impact force: sponson in fly-in incident, central North Sea waves.

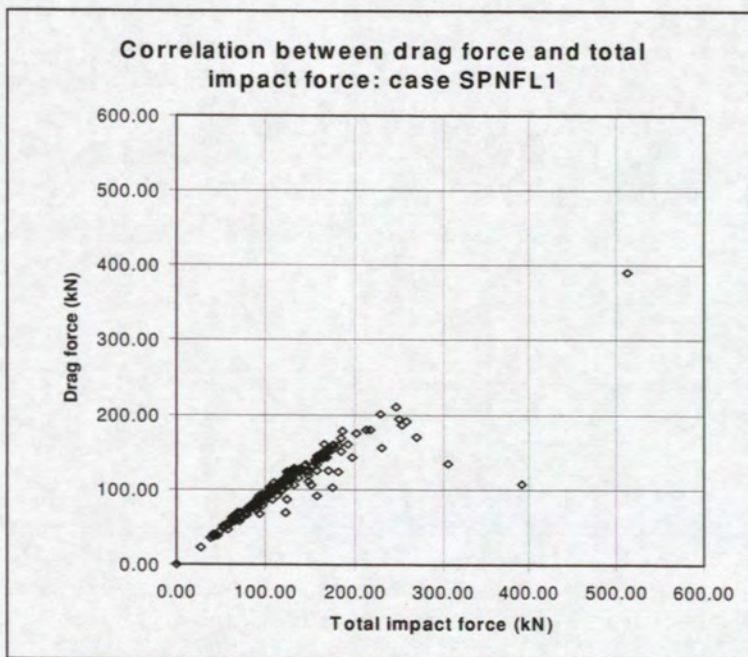


Figure 15: Correlation between the drag force and maximum total impact force: sponson in fly-in incident, central North Sea waves.

**Correlation plots: maximum structure and planing forces
against the total impact force on the fuselage panel;
all incident scenarios, base case conditions.**

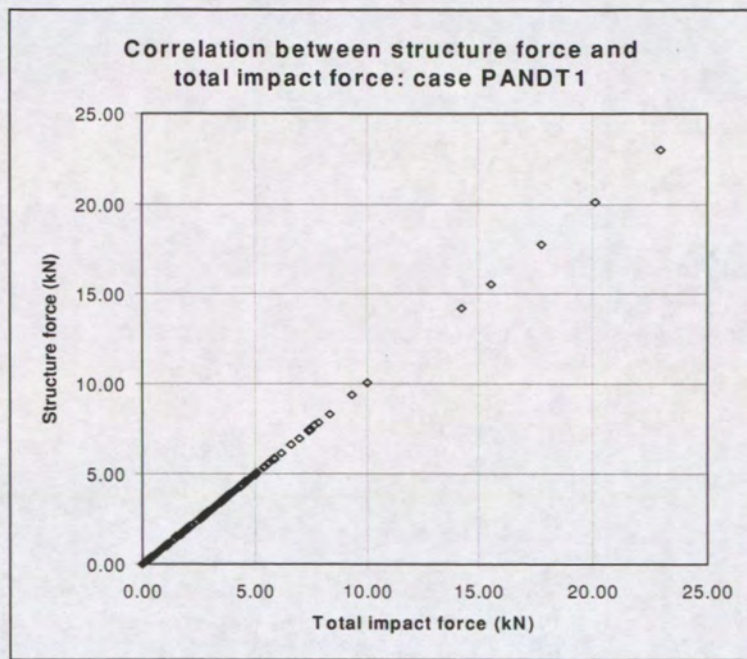


Figure 16: Correlation between maximum structure force and total impact force: panel in controlled ditching incident, central North Sea waves.

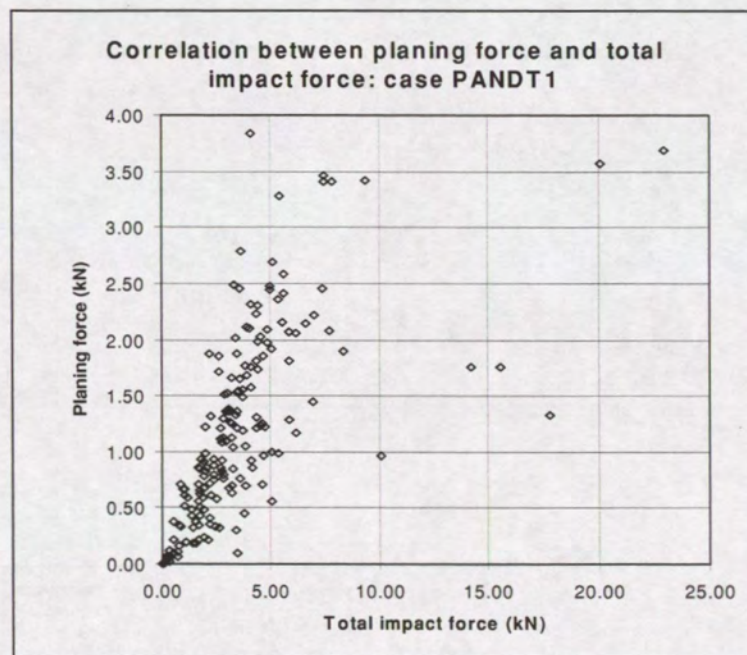


Figure 17: Correlation between the planing force and maximum total impact force: panel in controlled ditching incident, central North Sea waves.

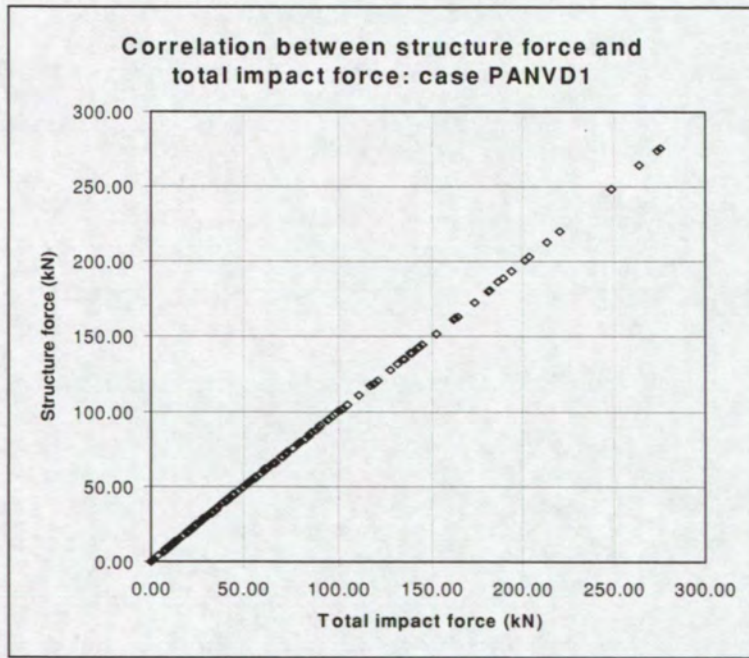


Figure 18: Correlation between maximum structure force and total impact force: panel in vertical descent incident, central North Sea waves.

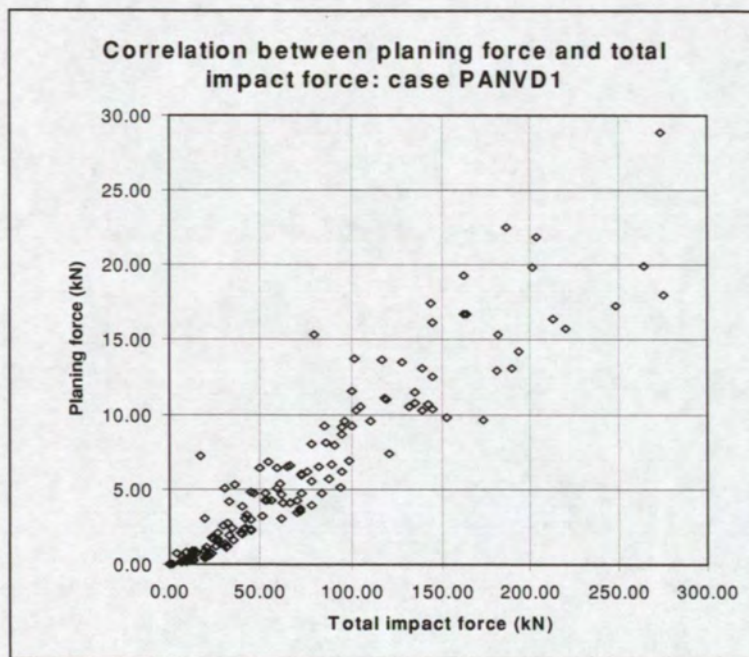


Figure 19: Correlation between the planing force and maximum total impact force: panel in vertical descent incident, central North Sea waves.

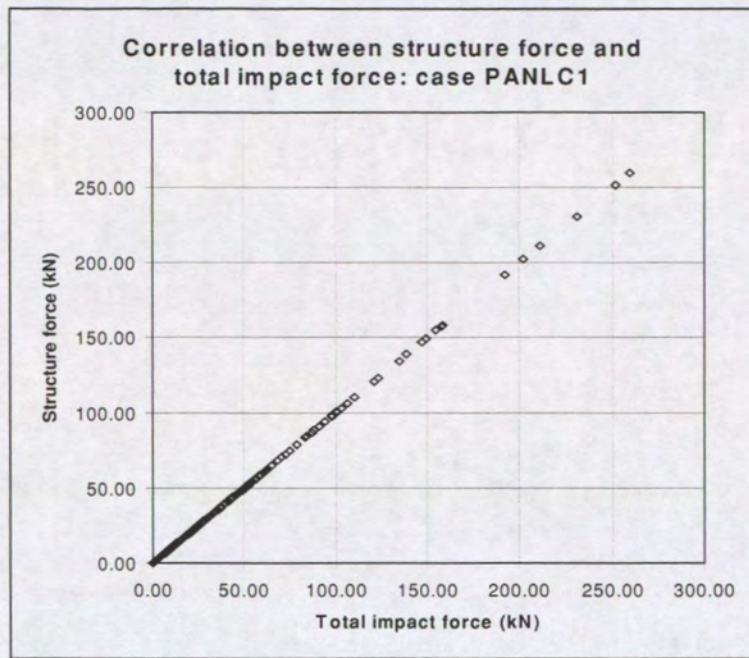


Figure 20: Correlation between maximum structure force and total impact force: panel in loss of control incident, central North Sea waves.

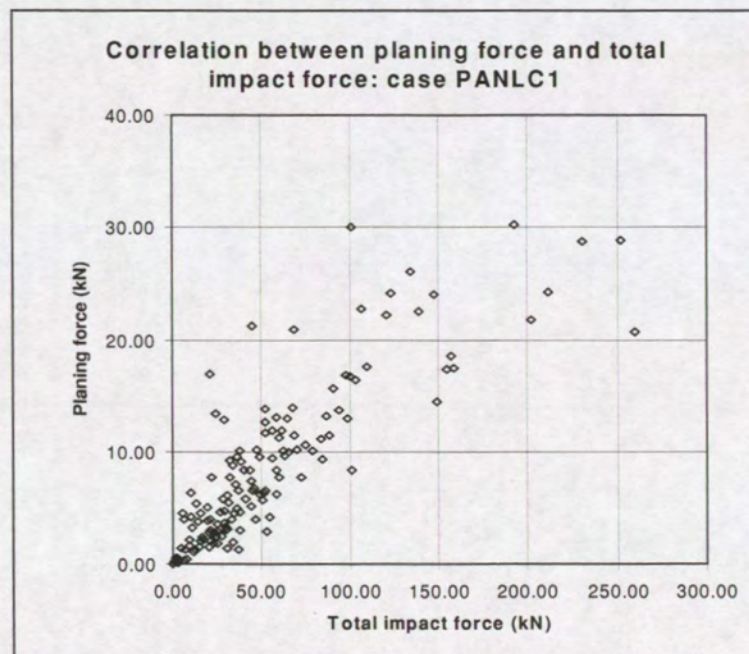


Figure 21: Correlation between the planing force and maximum total impact force: panel in loss of control incident, central North Sea waves.

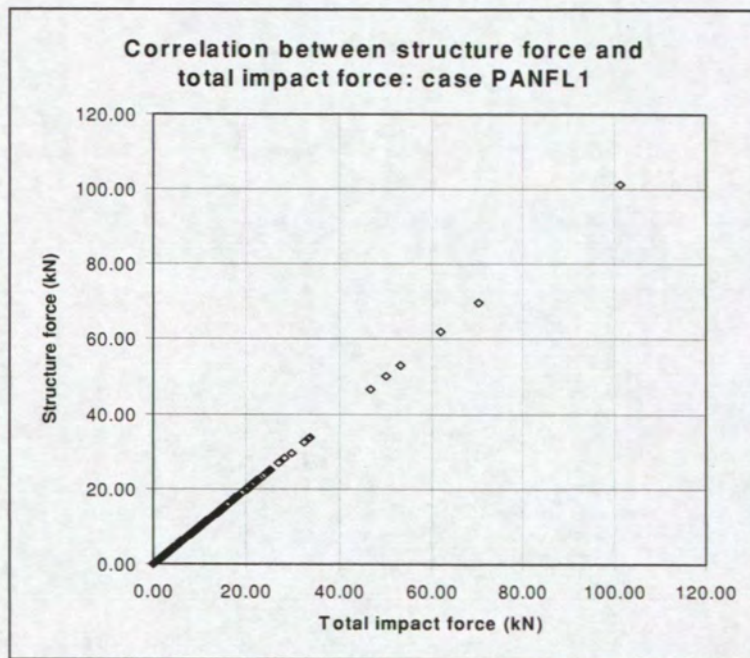


Figure 22: Correlation between maximum structure force and total impact force: panel in fly-in incident, central North Sea waves.

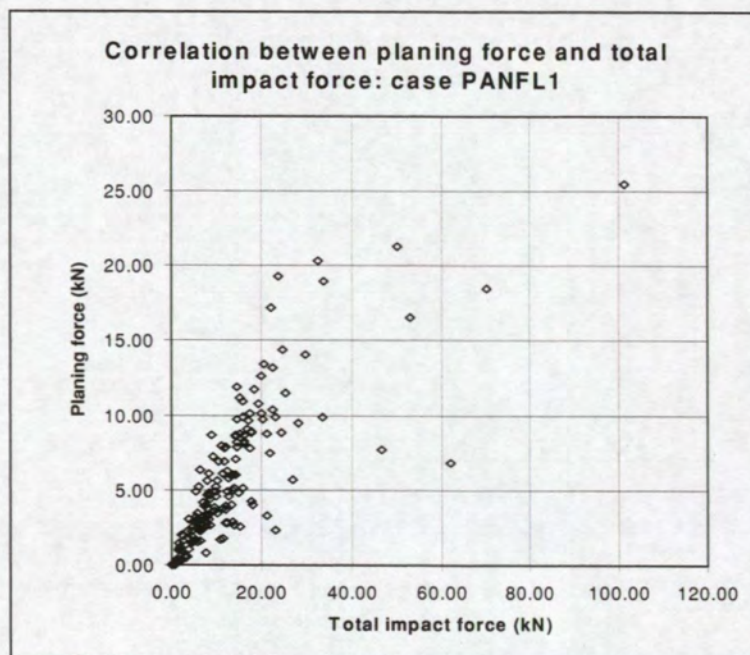


Figure 23: Correlation between the planing force and maximum total impact force: panel in fly-in incident, central North Sea waves.

**Correlation plots: impact duration, velocities and angle
against the total impact force on the sponson;
vertical descent scenario, base case conditions.**

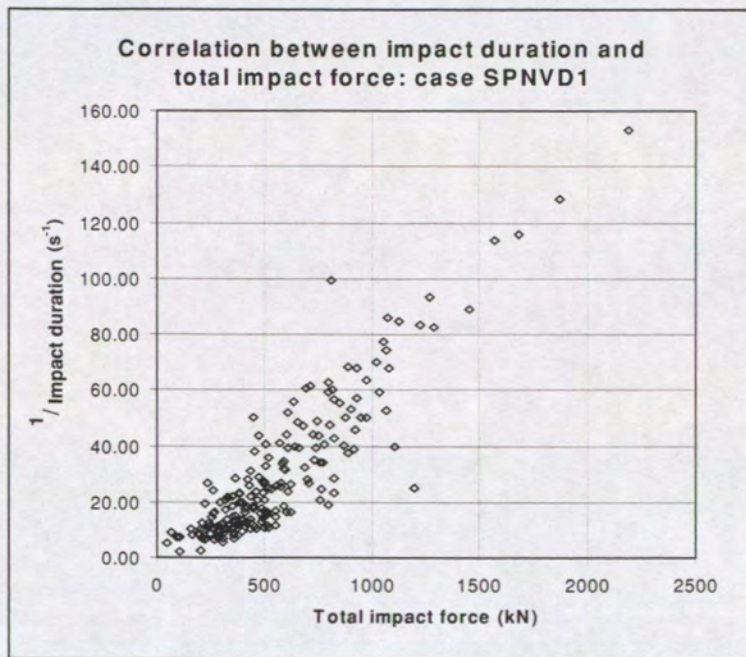


Figure 24: Correlation between the impact duration and maximum total impact force: sponson in vertical descent incident, central North Sea waves.

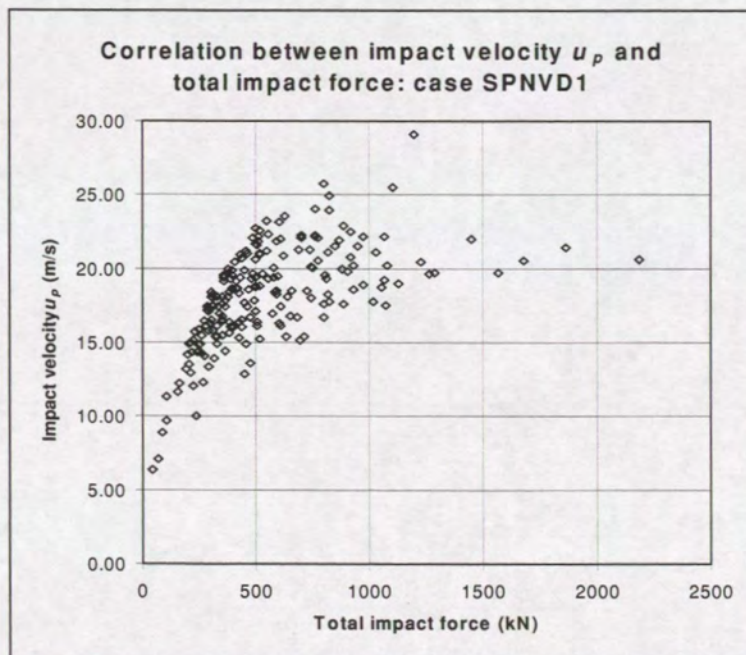


Figure 25: Correlation between the impact velocity u_p and maximum total impact force: sponson in vertical descent incident, central North Sea waves.

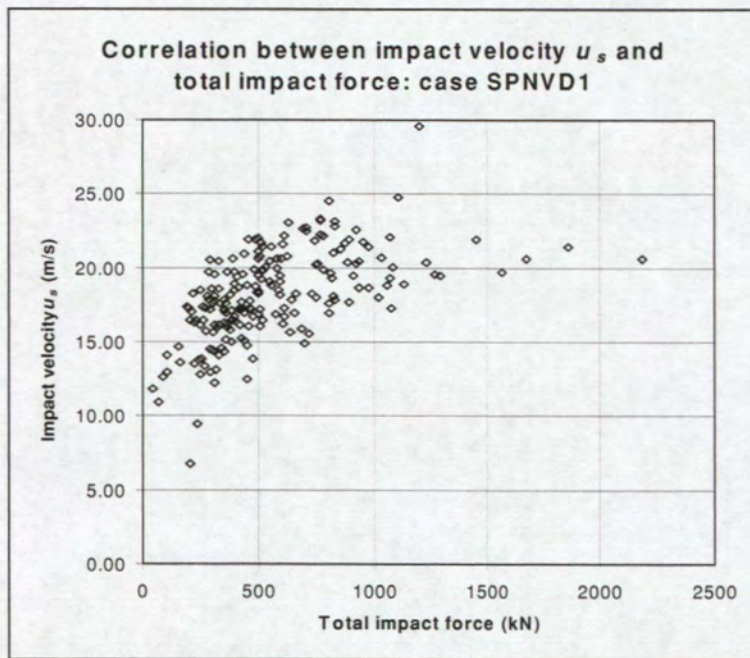


Figure 26: Correlation between the impact velocity u_s and maximum total impact force: sponson in vertical descent incident, central North Sea waves.

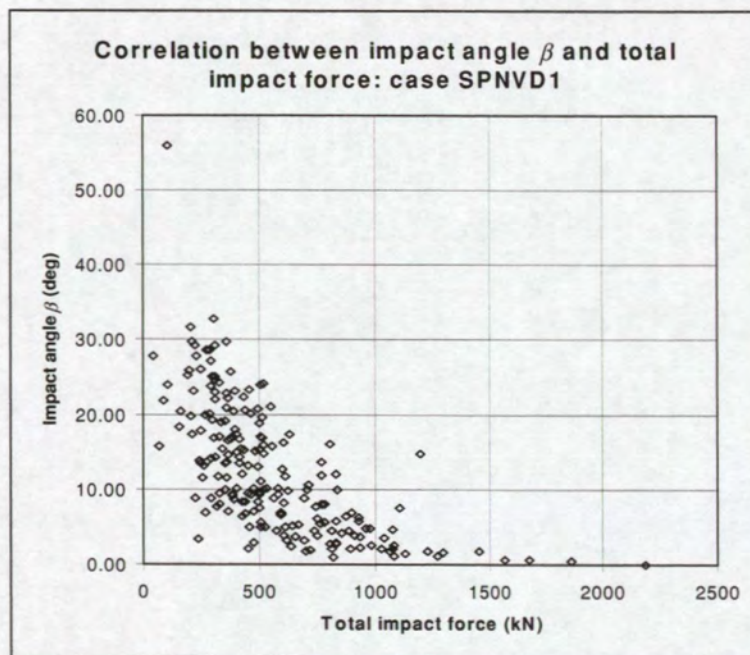


Figure 27: Correlation between the impact angle β and maximum total impact force: sponson in vertical descent incident, central North Sea waves.

**Correlation plots: impact duration, velocities and angle
against the total impact force on the fuselage panel;
vertical descent scenario, base case conditions.**

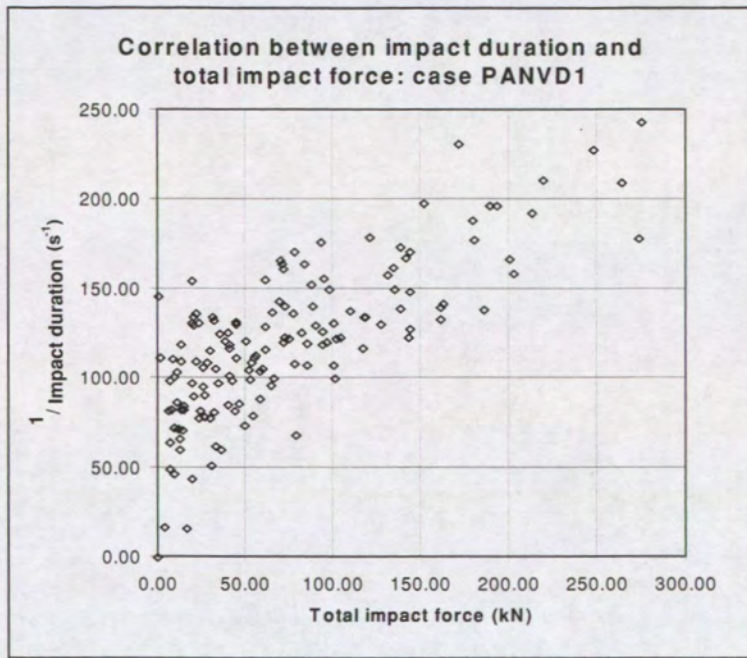


Figure 28: Correlation between the impact duration and maximum total impact force: panel in vertical descent incident, central North Sea waves.

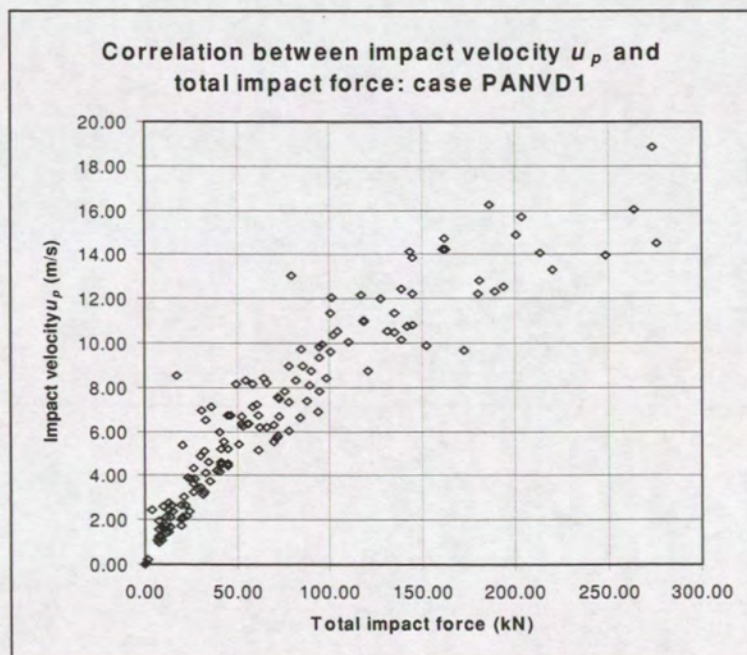


Figure 29: Correlation between the impact velocity u_p and maximum total impact force: panel in vertical descent incident, central North Sea waves.

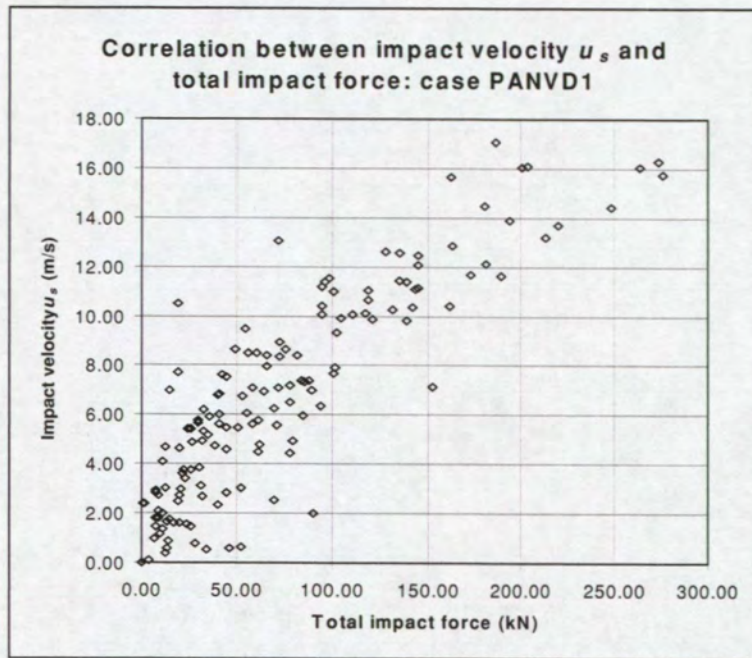


Figure 30: Correlation between the impact velocity u_s and maximum total impact force: panel in vertical descent incident, central North Sea waves.

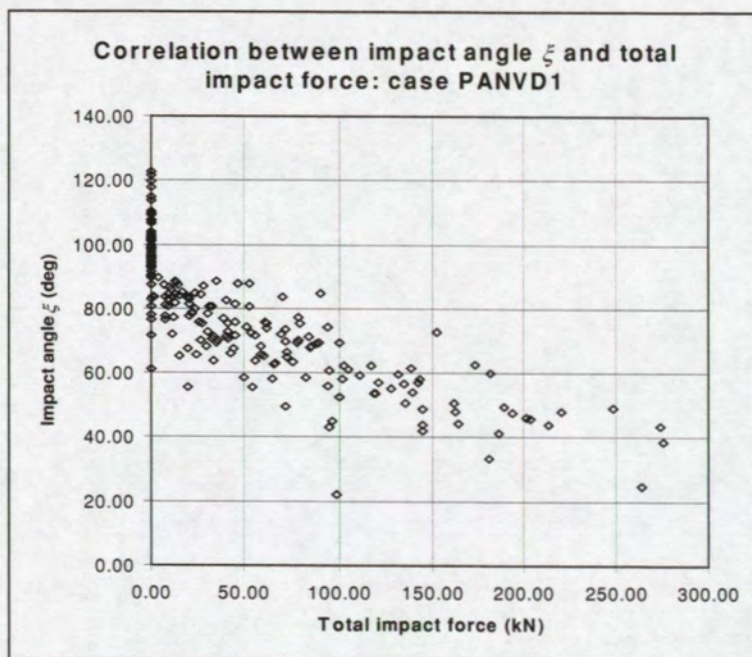


Figure 31: Correlation between the impact angle ξ and maximum total impact force: panel in vertical descent incident, central North Sea waves.

Results from Sensitivity Study

**Exceedance distributions of the maximum
total impact force on the sponson:**

1. Controlled ditching incident

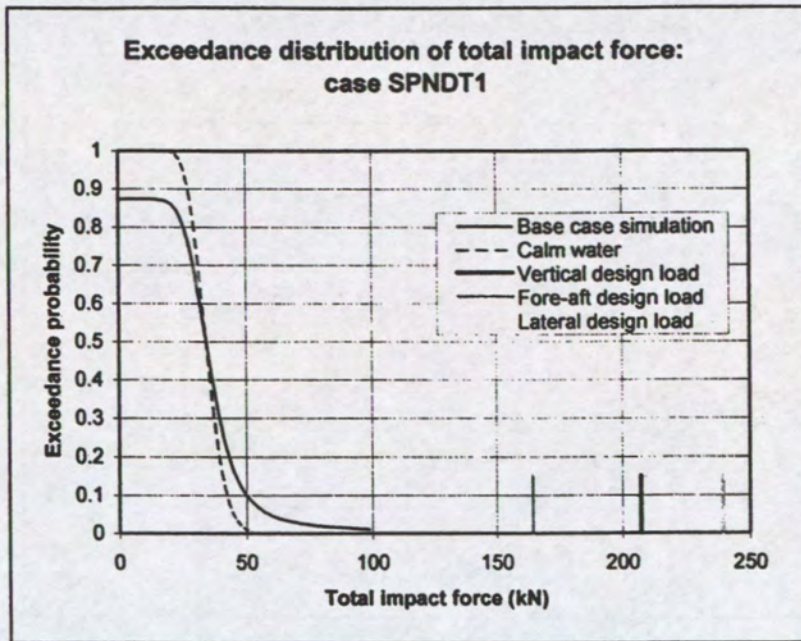


Figure 32: Exceedance distribution of the maximum total impact force: sponson in controlled ditching incident, effect of calm water.

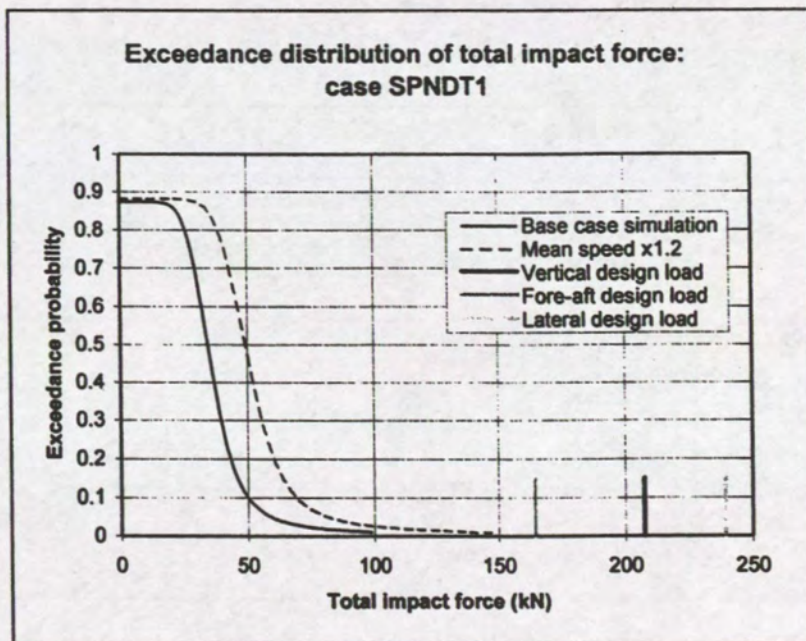


Figure 33: Exceedance distribution of the maximum total impact force: sponson in controlled ditching incident, effect of increased mean speed.

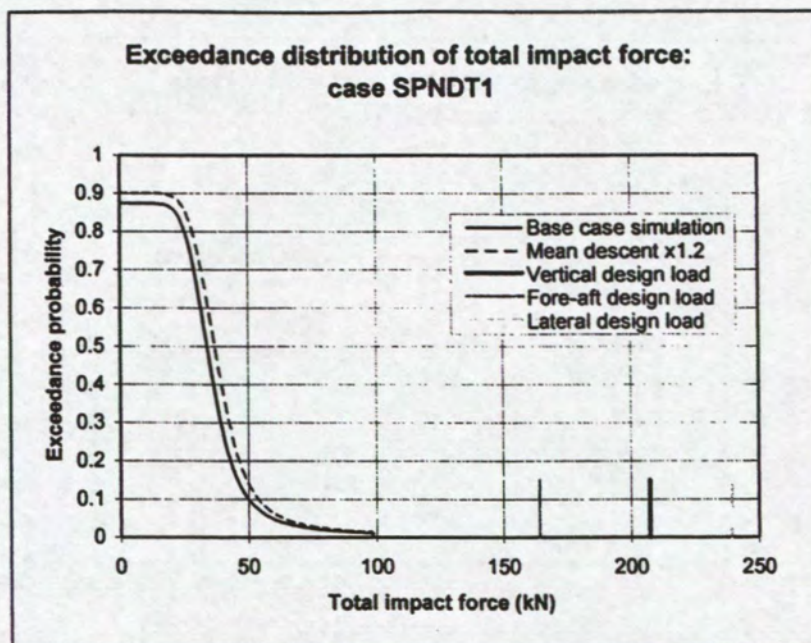


Figure 34: Exceedance distribution of the maximum total impact force: sponson in controlled ditching incident, effect of increased mean descent angle.

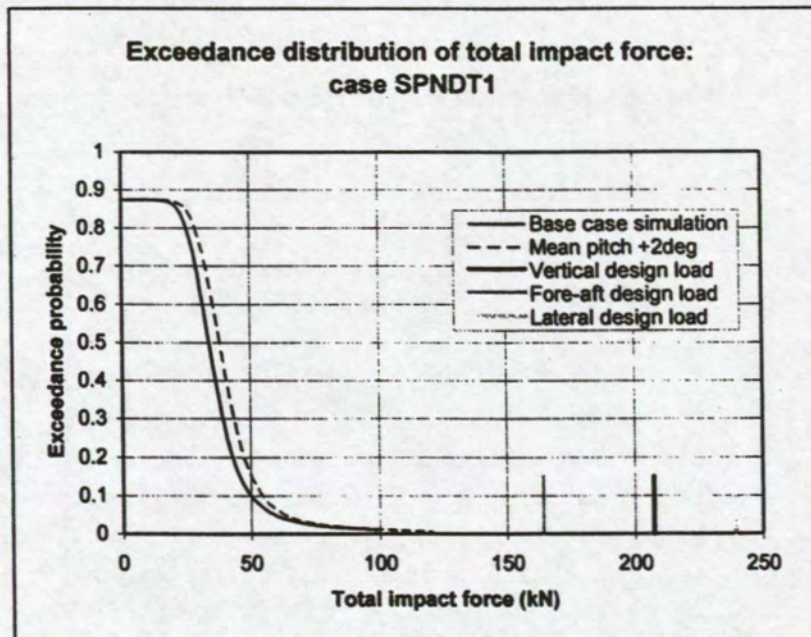


Figure 35: Exceedance distribution of the maximum total impact force: sponson in controlled ditching incident, effect of increased mean pitch angle.

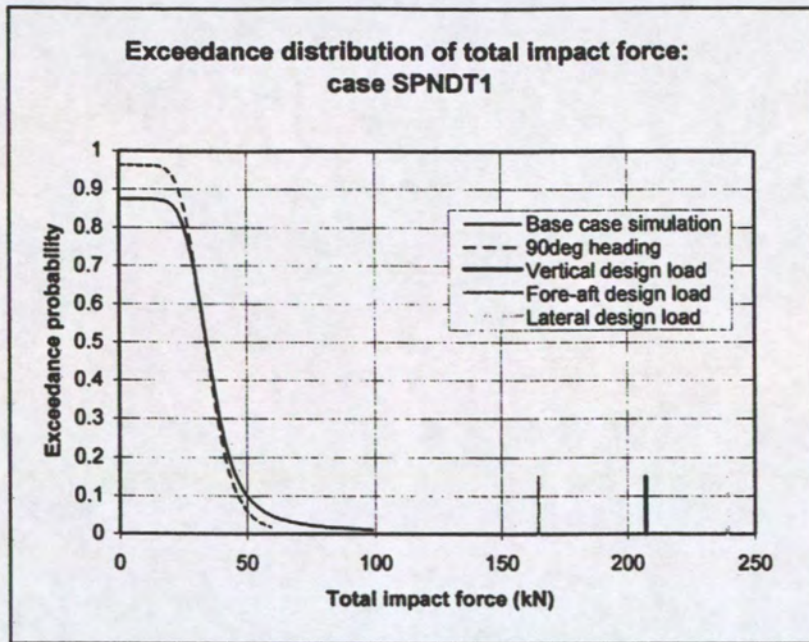


Figure 36: Exceedance distribution of the maximum total impact force: sponson in controlled ditching incident, effect of landing beam-on to waves.

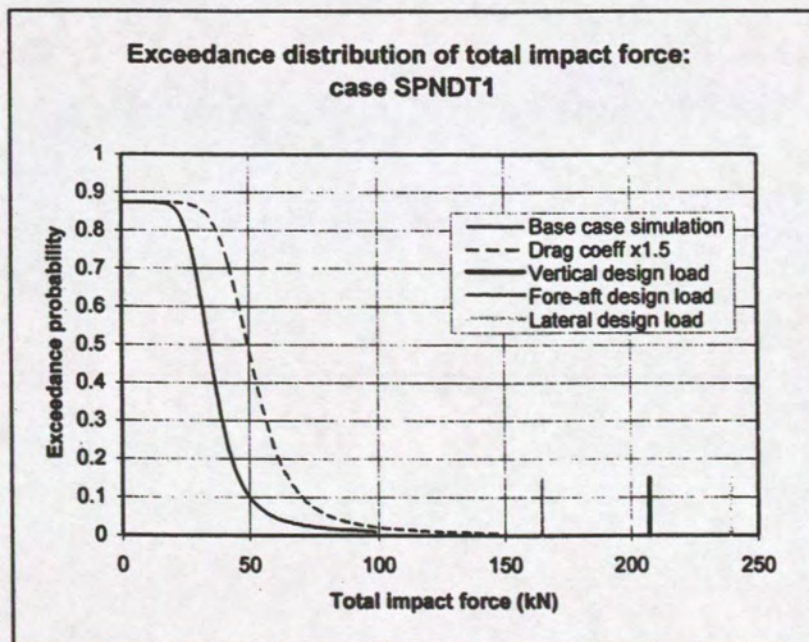


Figure 37: Exceedance distribution of the maximum total impact force: sponson in controlled ditching incident, effect of increased drag coefficient.

Results from Sensitivity Study

**Exceedance distributions of the maximum
total impact force on the sponson:**

2. Vertical descent incident

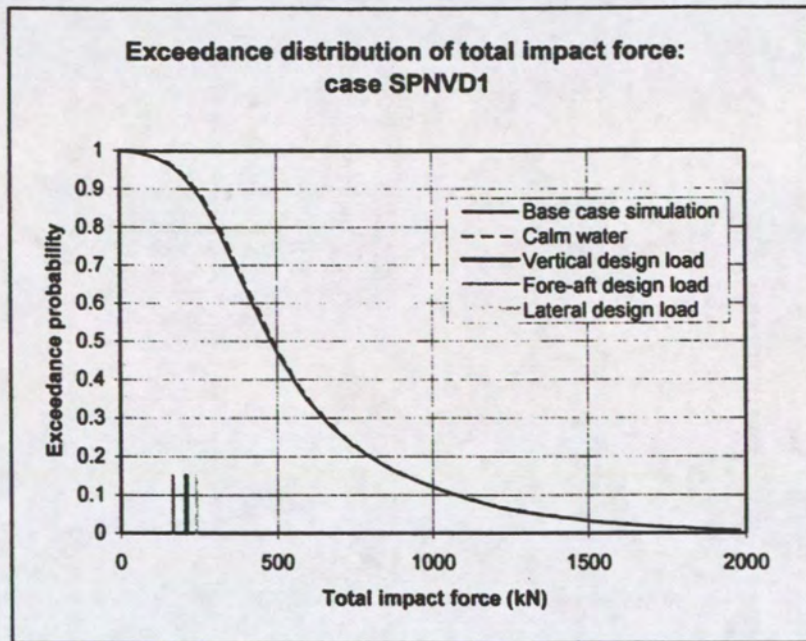


Figure 38: Exceedance distribution of the maximum total impact force: sponson in vertical descent incident, effect of calm water.

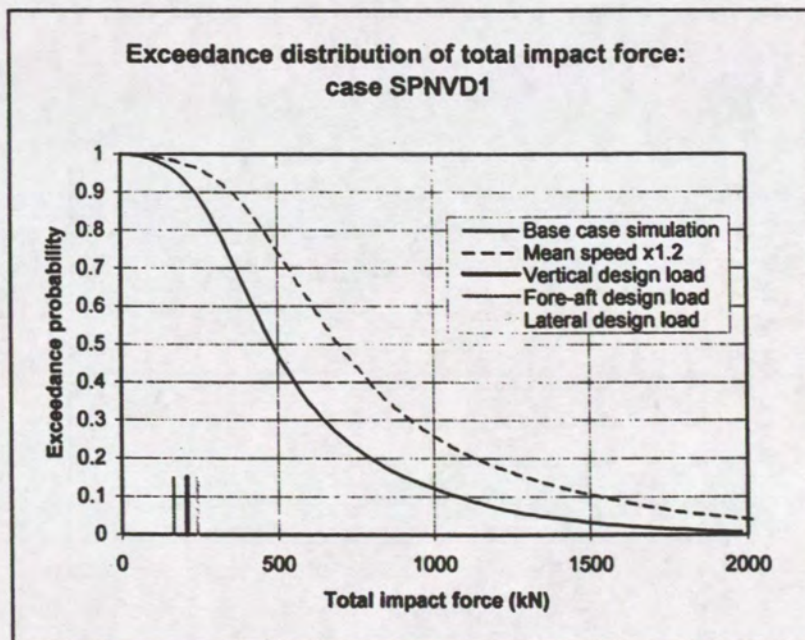


Figure 39: Exceedance distribution of the maximum total impact force: sponson in vertical descent incident, effect of increased mean speed.

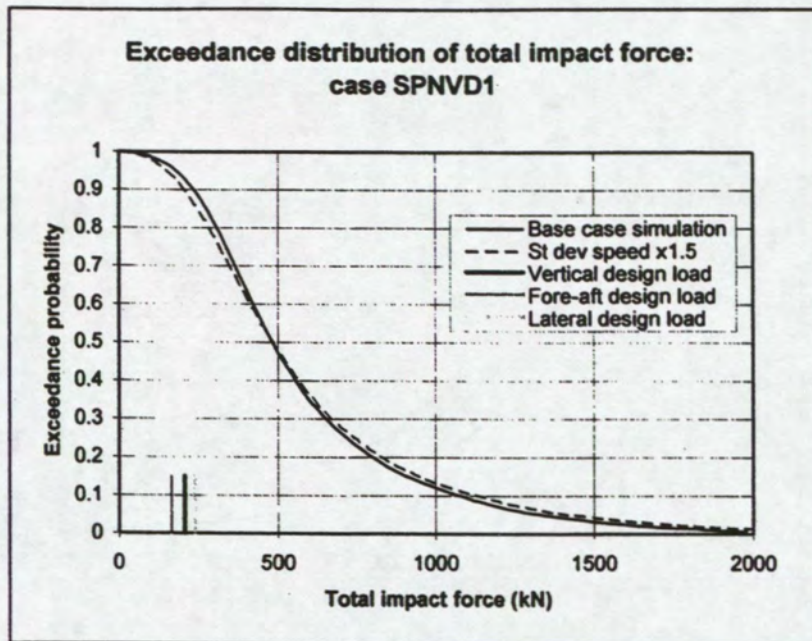


Figure 40: Exceedance distribution of the maximum total impact force: sponson in vertical descent incident, effect of increased speed range.

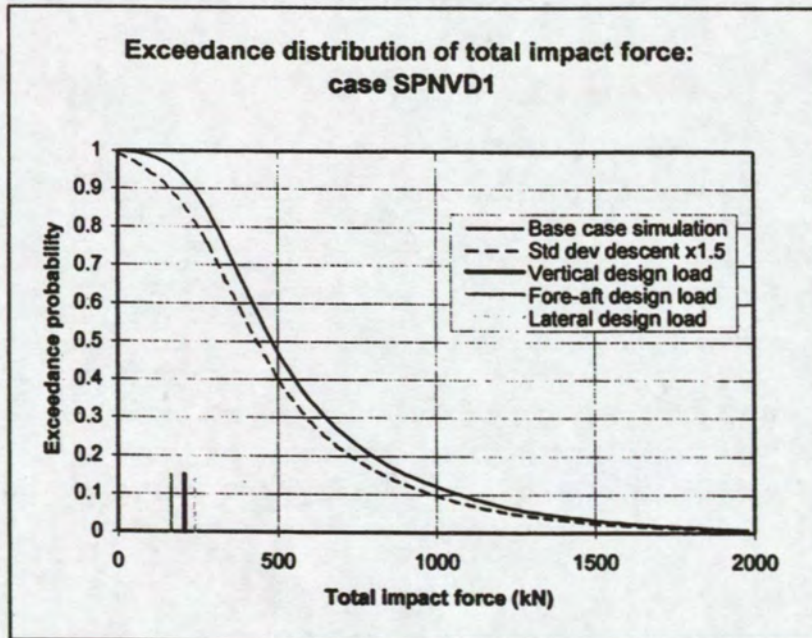


Figure 41: Exceedance distribution of the maximum total impact force: sponson in vertical descent incident, effect of increased descent angle range.

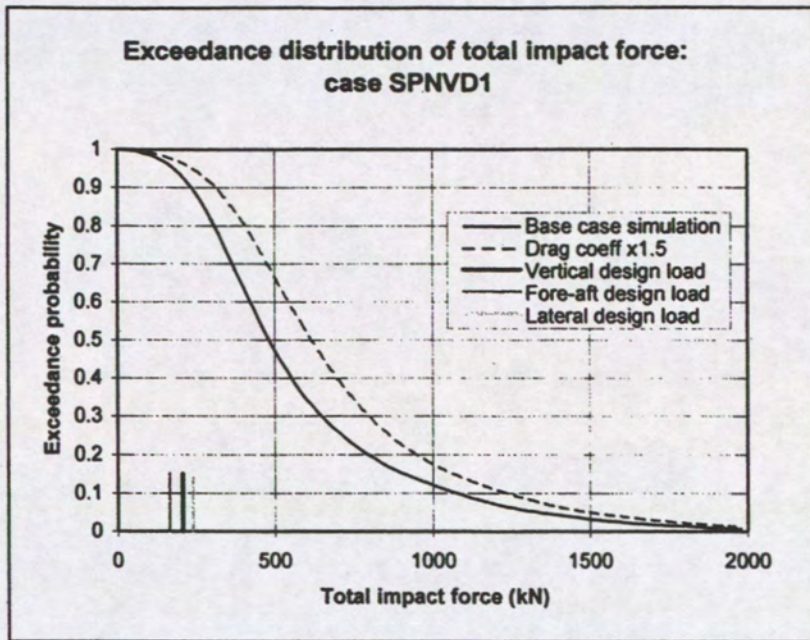


Figure 42: Exceedance distribution of the maximum total impact force: sponson in vertical descent incident, effect of increased drag coefficient.

Results from Sensitivity Study

**Exceedance distributions of the maximum
total impact force on the sponson:**

3. Loss of control incident

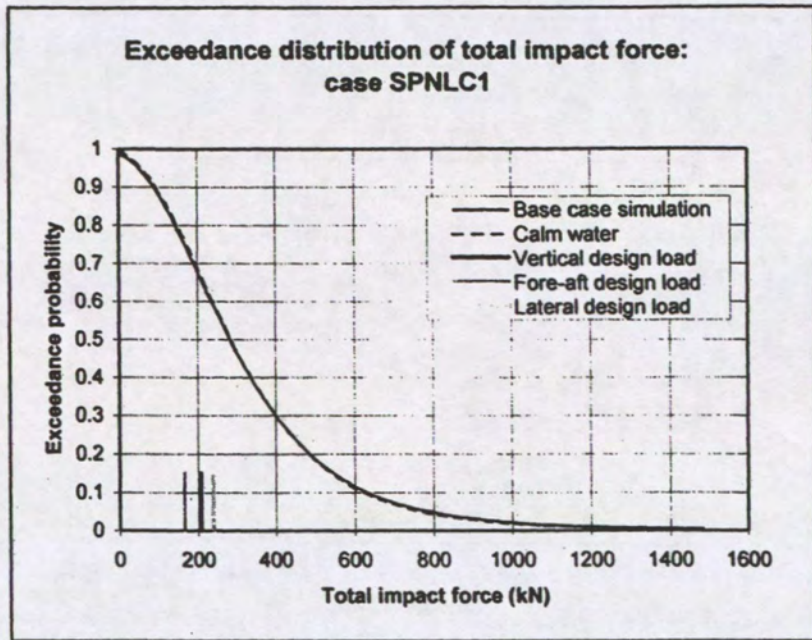


Figure 43: Exceedance distribution of the maximum total impact force: sponson in loss of control incident, effect of calm water.

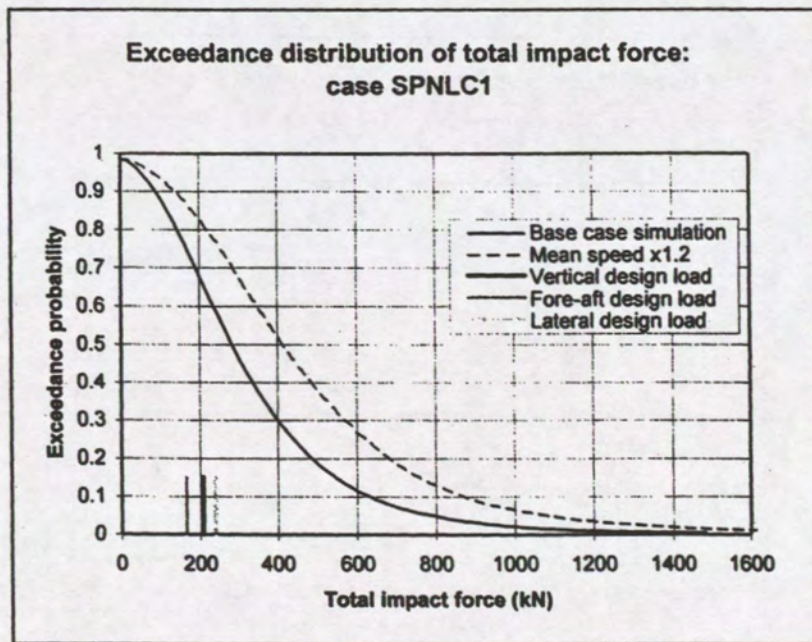


Figure 44: Exceedance distribution of the maximum total impact force: sponson in loss of control incident, effect of increased mean speed.

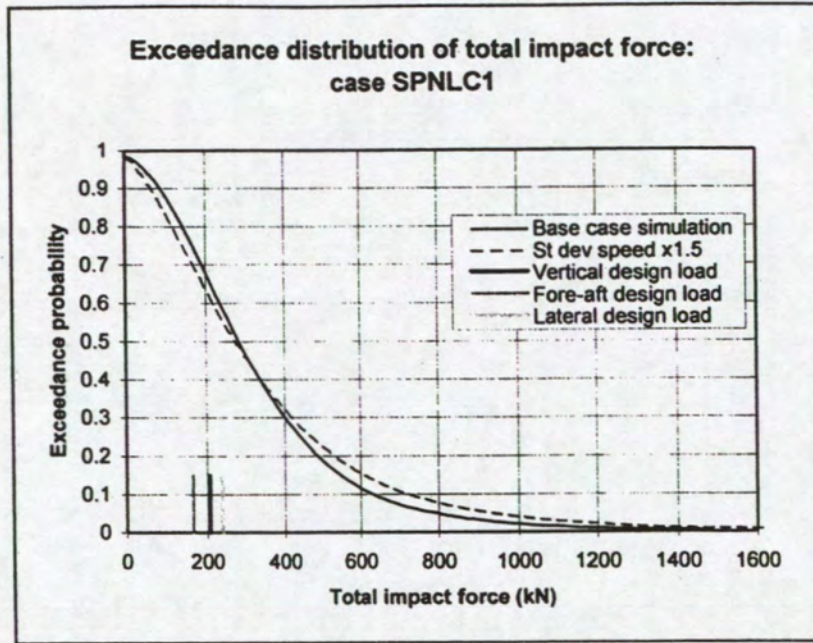


Figure 45: Exceedance distribution of the maximum total impact force: sponson in loss of control incident, effect of increased speed range.

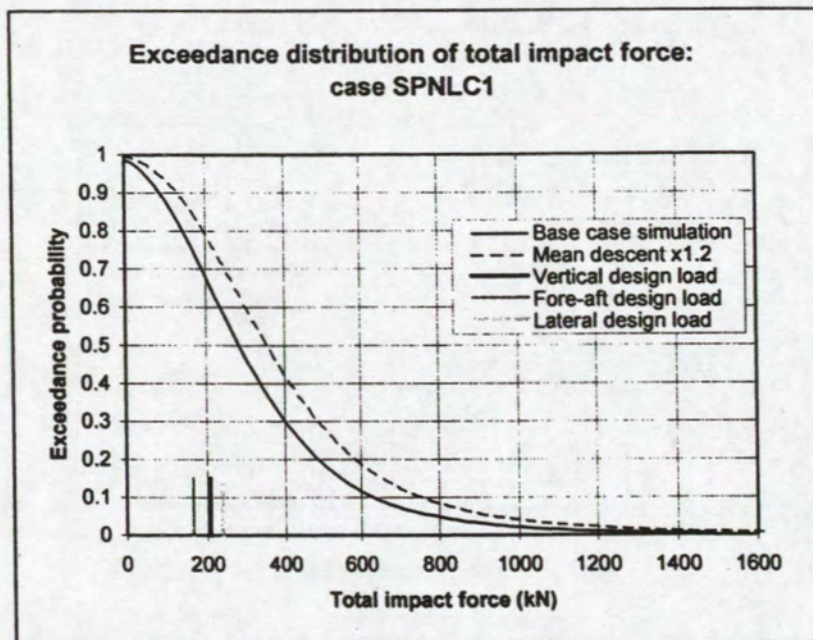


Figure 46: Exceedance distribution of the maximum total impact force: sponson in loss of control incident, effect of increased mean descent angle.

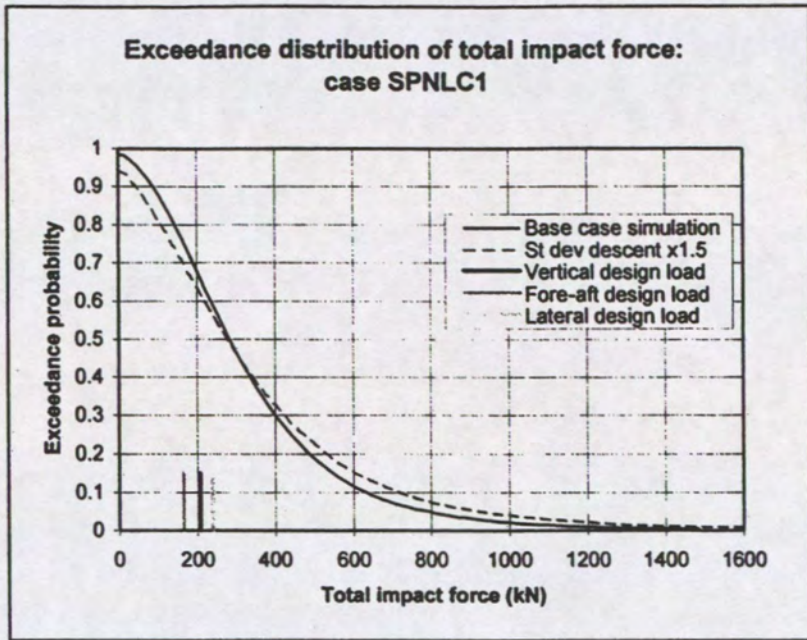


Figure 47: Exceedance distribution of the maximum total impact force: sponson in loss of control incident, effect of increased descent angle range.

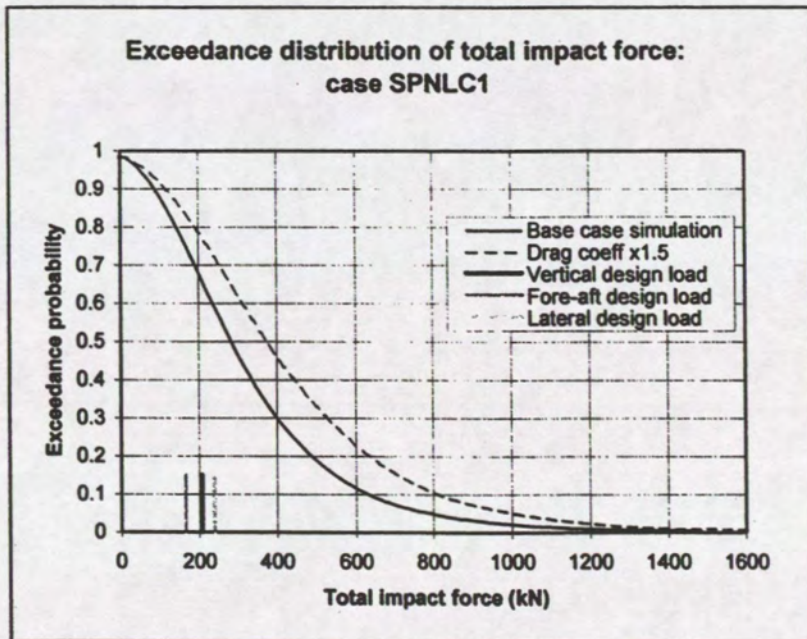


Figure 48: Exceedance distribution of the maximum total impact force: sponson in loss of control incident, effect of increased drag coefficient.

Results from Sensitivity Study

**Exceedance distributions of the maximum
total impact force on the sponson:**

4. Fly-in incident

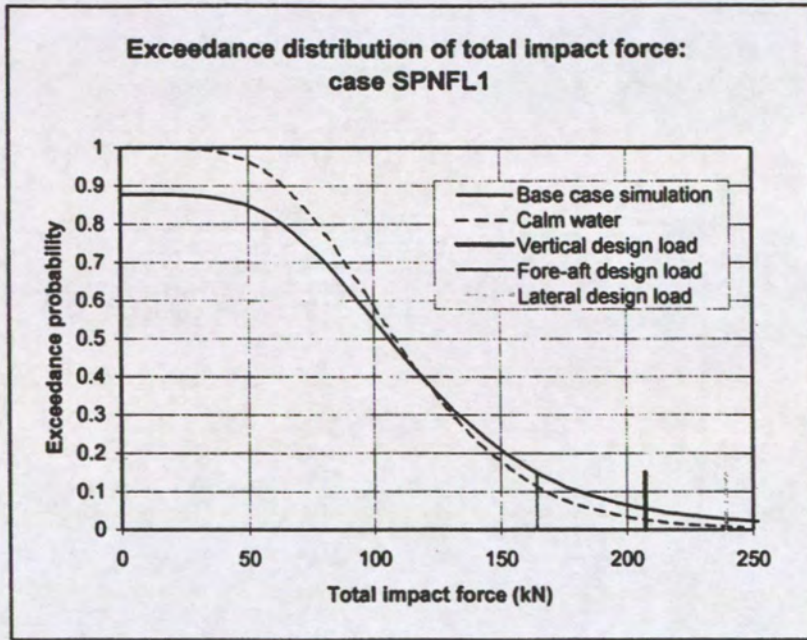


Figure 49: Exceedance distribution of the maximum total impact force: sponson in fly-in incident, effect of calm water.

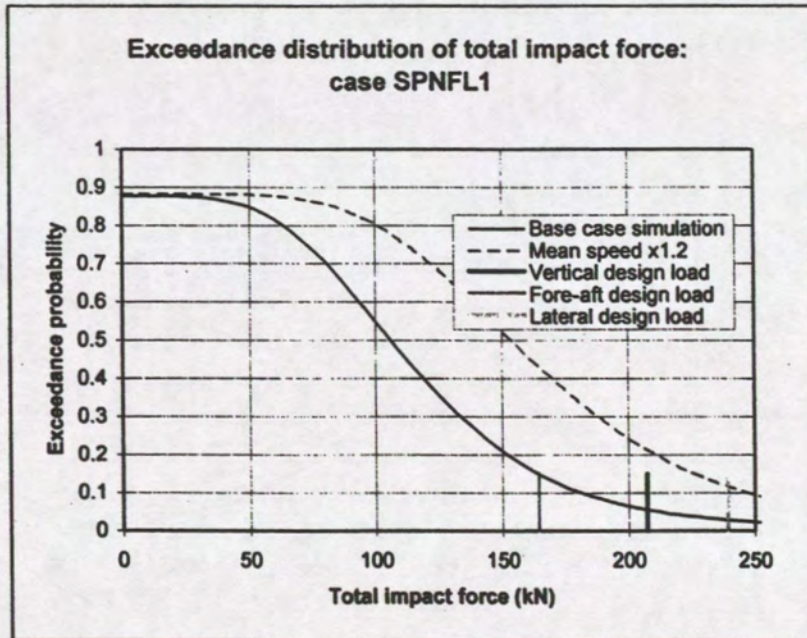


Figure 50: Exceedance distribution of the maximum total impact force: sponson in fly-in incident, effect of increased mean speed.

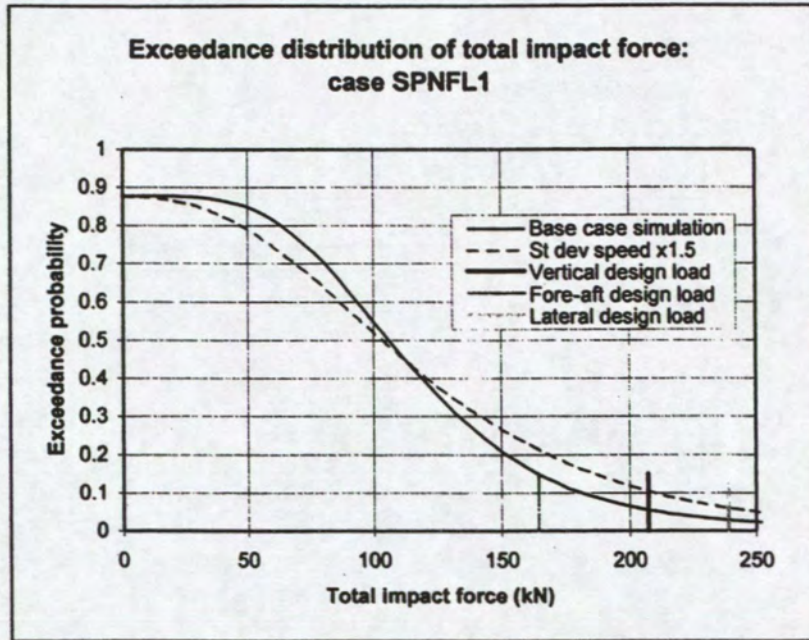


Figure 51: Exceedance distribution of the maximum total impact force: sponson in fly-in incident, effect of increased speed range.

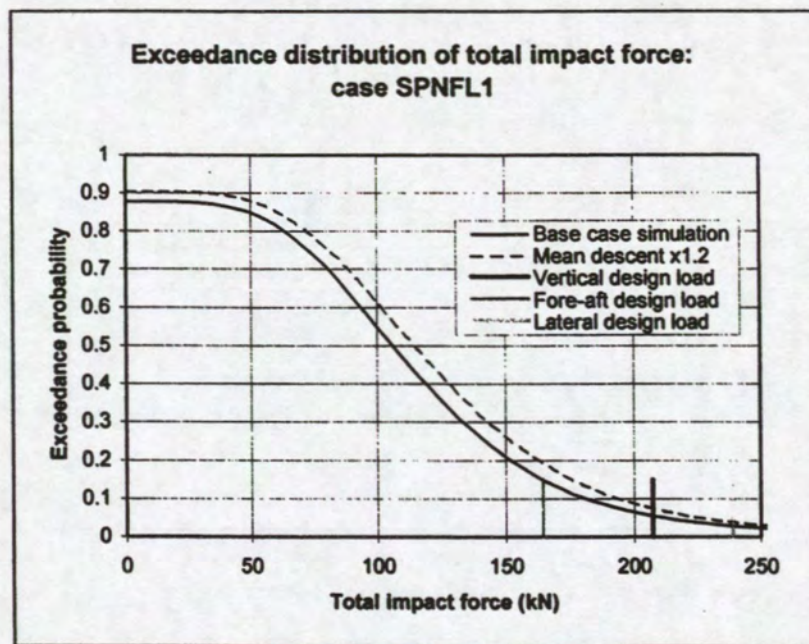


Figure 52: Exceedance distribution of the maximum total impact force: sponson in fly-in incident, effect of increased mean descent angle.

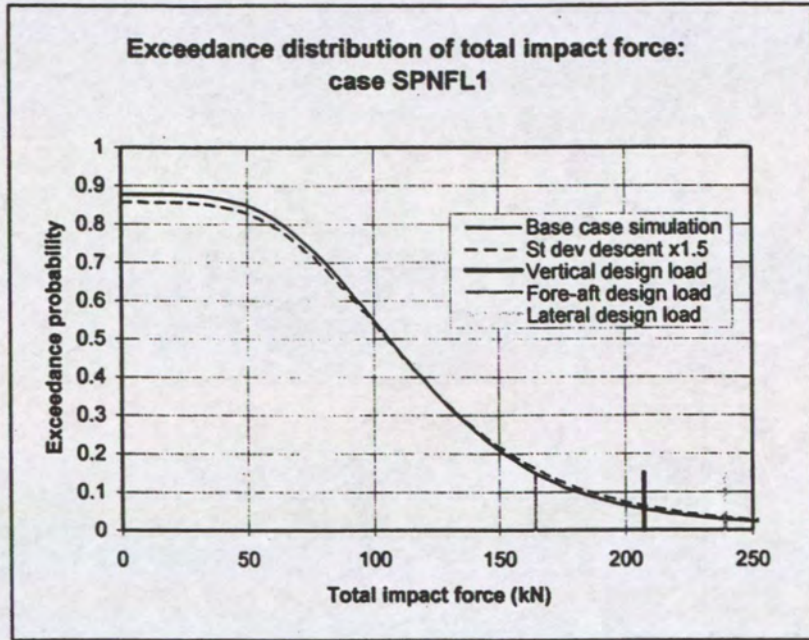


Figure 53: Exceedance distribution of the maximum total impact force: sponson in fly-in incident, effect of increased descent angle range.

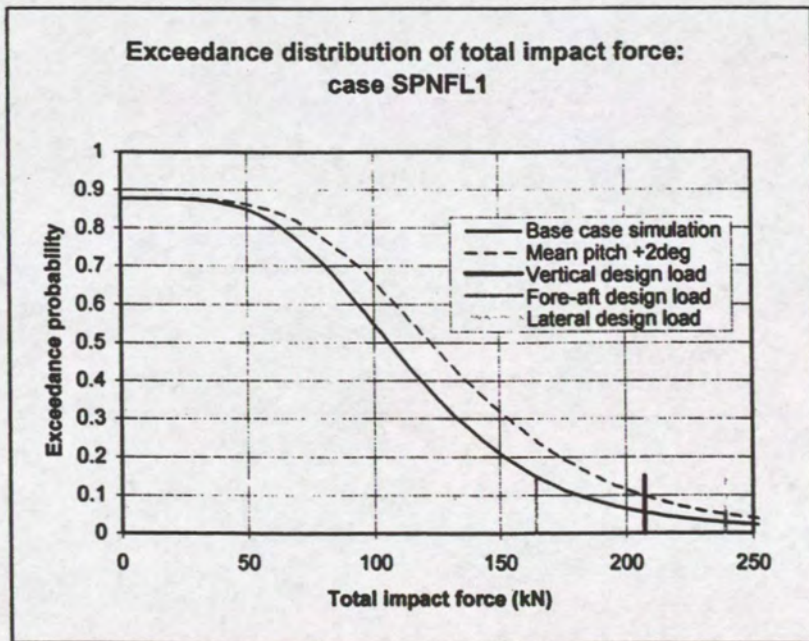


Figure 54: Exceedance distribution of the maximum total impact force: sponson in fly-in incident, effect of increased mean pitch angle.

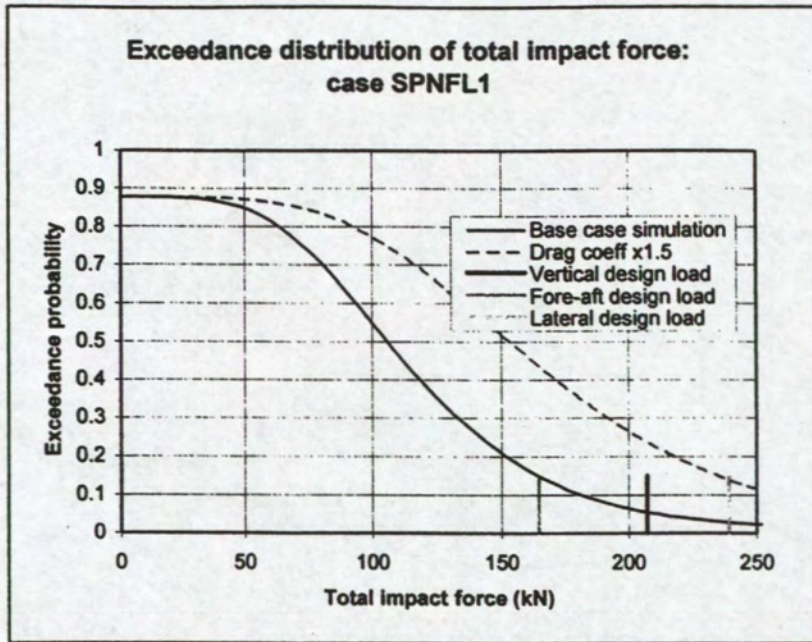


Figure 55: Exceedance distribution of the maximum total impact force: sponson in fly-in incident, effect of increased drag coefficient.

Results from Sensitivity Study

**Exceedance distributions of the maximum
total impact force on the fuselage panel:**

1. Controlled ditching incident

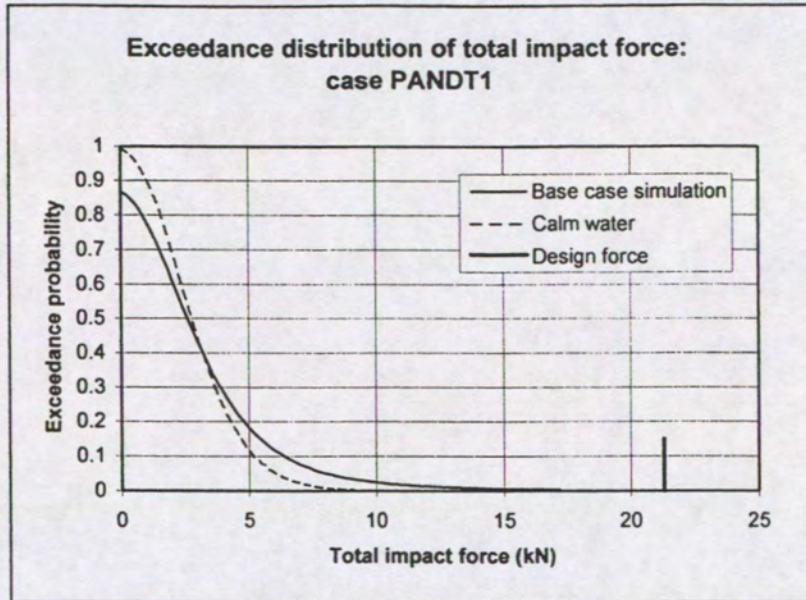


Figure 56: Exceedance distribution of the maximum total impact force: panel in controlled ditching incident, effect of calm water.

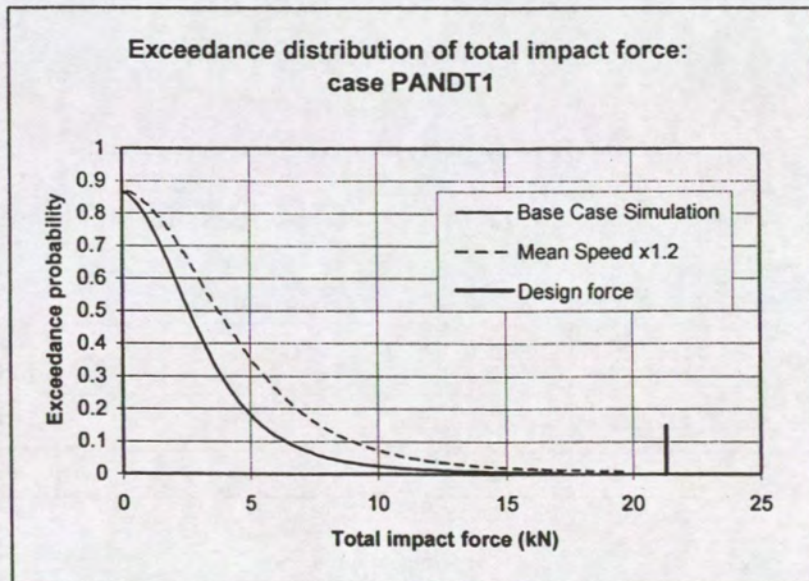


Figure 57: Exceedance distribution of the maximum total impact force: panel in controlled ditching incident, effect of increased mean speed.

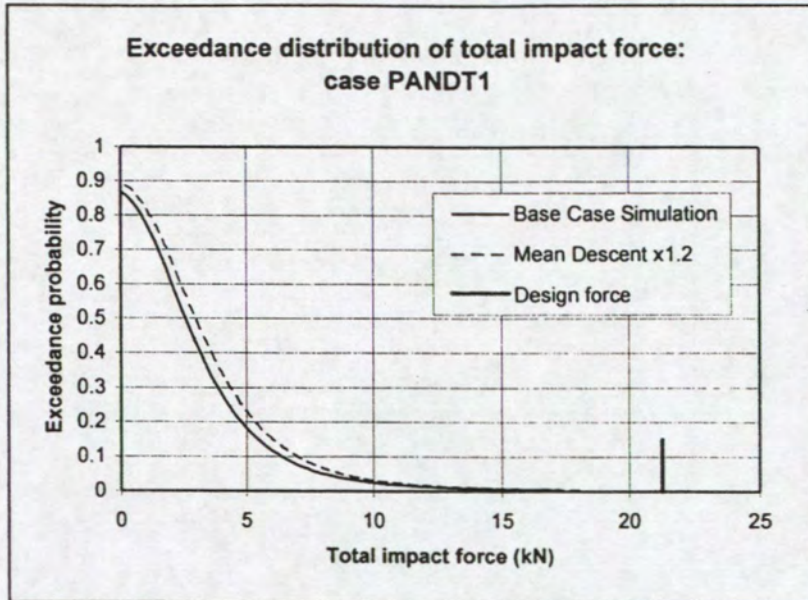


Figure 58: Exceedance distribution of the maximum total impact force: panel in controlled ditching incident, effect of increased mean descent angle.

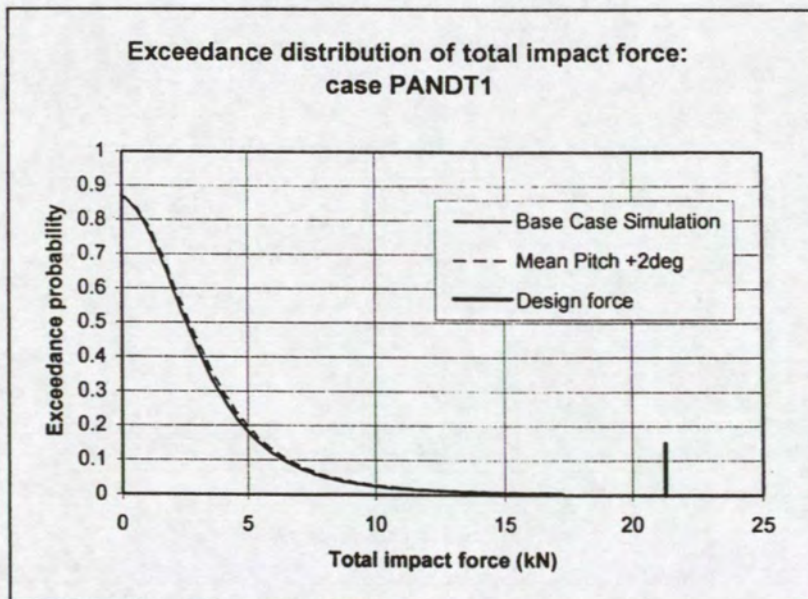


Figure 59: Exceedance distribution of the maximum total impact force: panel in controlled ditching incident, effect of increased mean pitch angle.

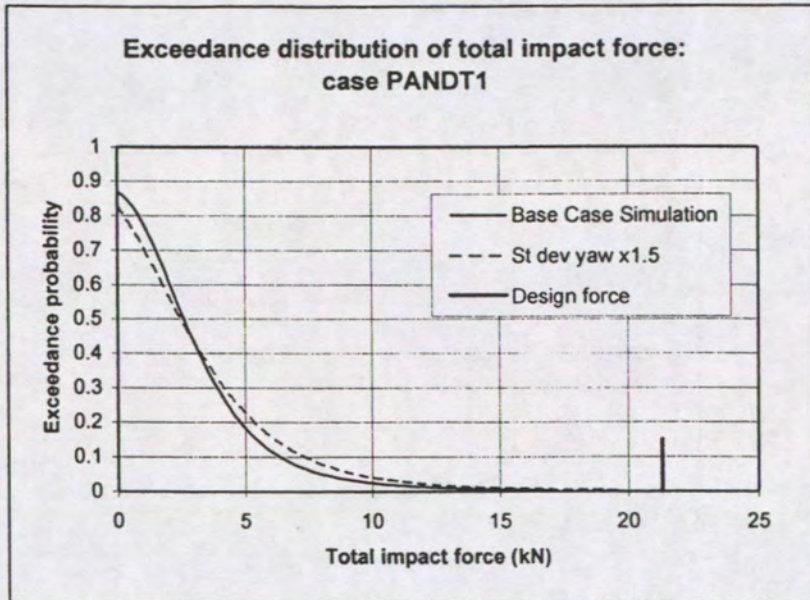


Figure 60: Exceedance distribution of the maximum total impact force: panel in controlled ditching incident, effect of increased yaw angle range.

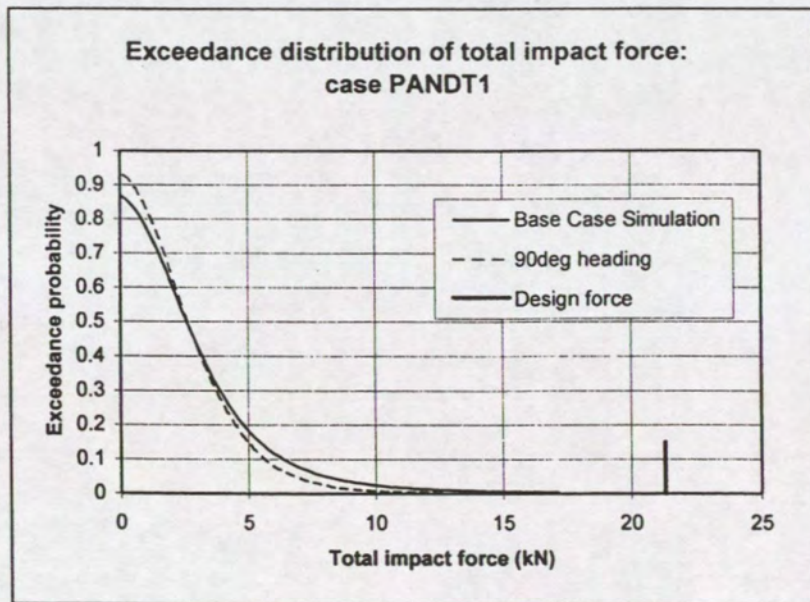


Figure 61: Exceedance distribution of the maximum total impact force: panel in controlled ditching incident, effect of landing beam-on to waves.

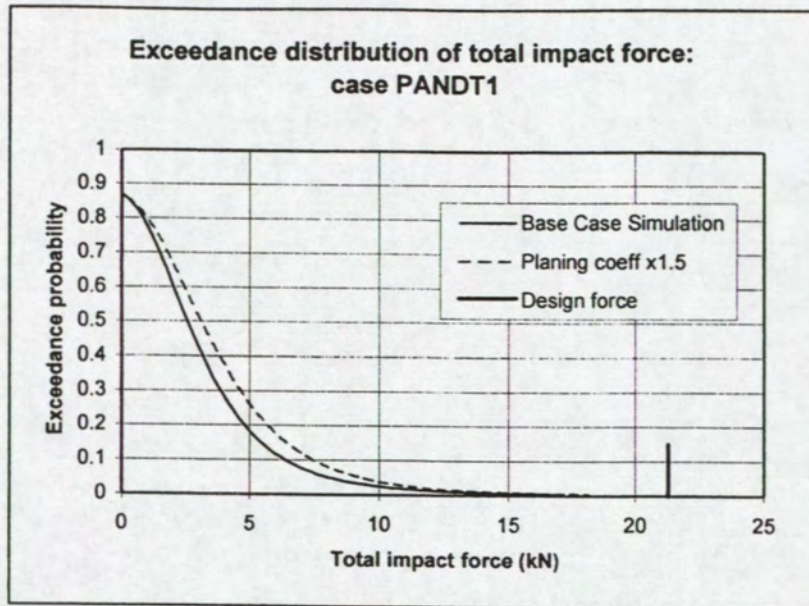


Figure 62: Exceedance distribution of the maximum total impact force: panel in controlled ditching incident, effect of increased planing force coefficient.

Results from Sensitivity Study

**Exceedance distributions of the maximum
total impact force on the fuselage panel:**

2. Vertical descent incident

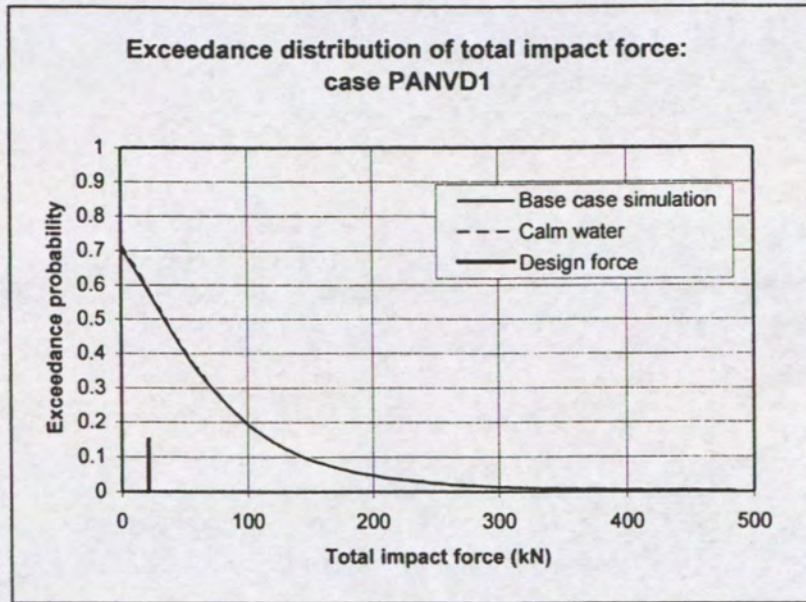


Figure 63: Exceedance distribution of the maximum total impact force: panel in vertical descent incident, effect of calm water.

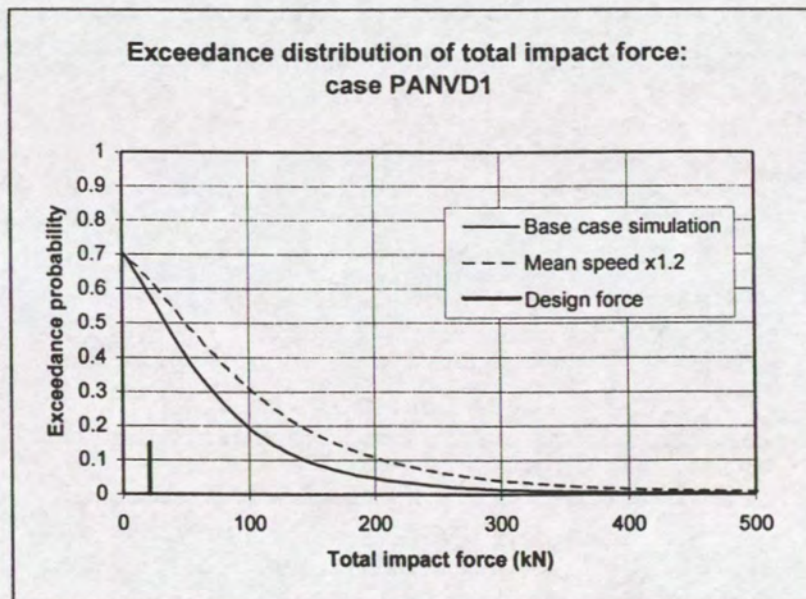


Figure 64: Exceedance distribution of the maximum total impact force: panel in vertical descent incident, effect of increased mean speed.

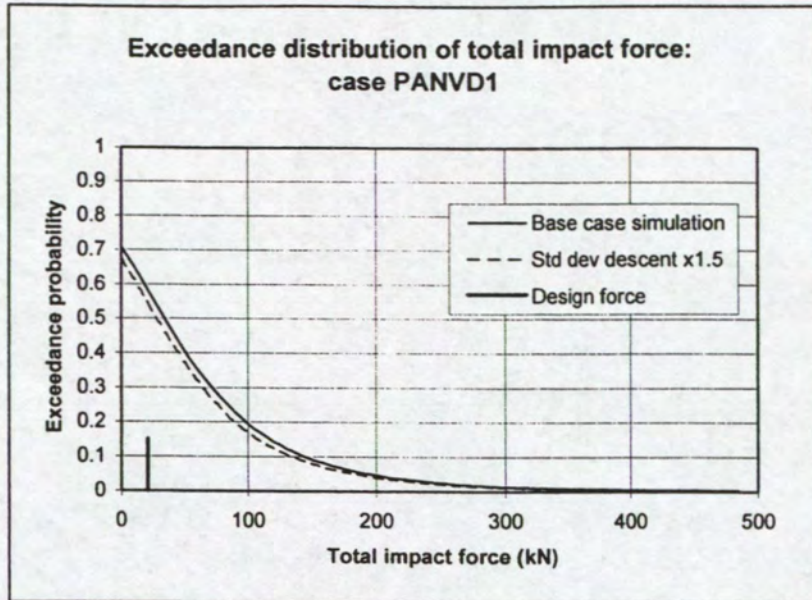


Figure 65: Exceedance distribution of the maximum total impact force: panel in vertical descent incident, effect of increased descent angle range.

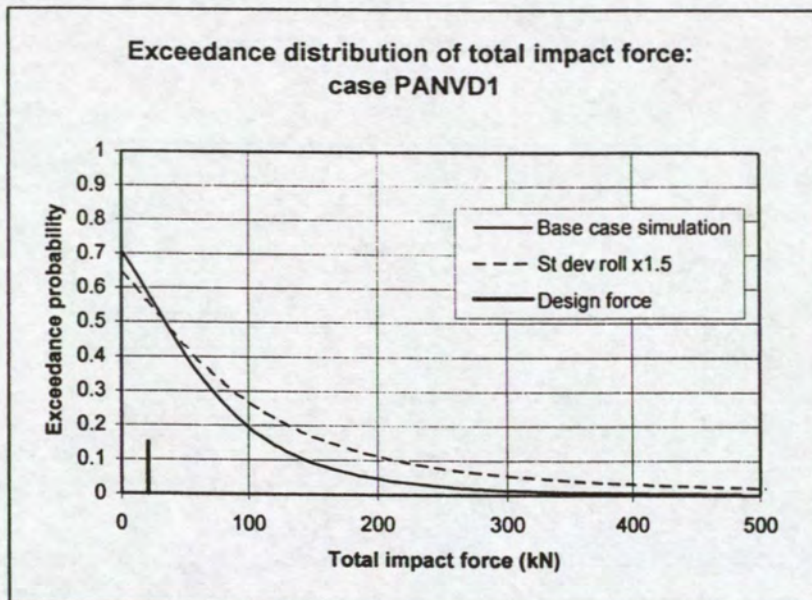


Figure 66: Exceedance distribution of the maximum total impact force: panel in vertical descent incident, effect of increased roll angle range.

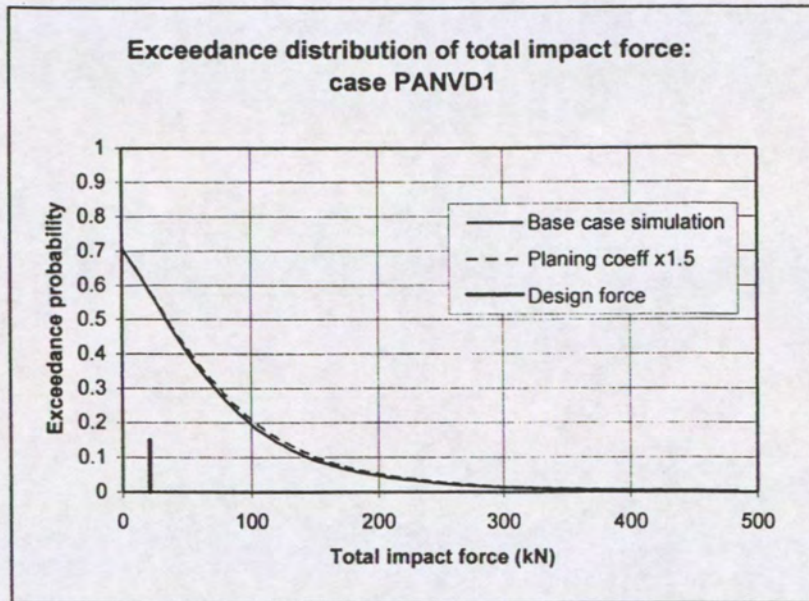


Figure 67: Exceedance distribution of the maximum total impact force: panel in vertical descent incident, effect of increased planing force coefficient.

Results from Sensitivity Study

**Exceedance distributions of the maximum
total impact force on the fuselage panel:**

3. Loss of control incident

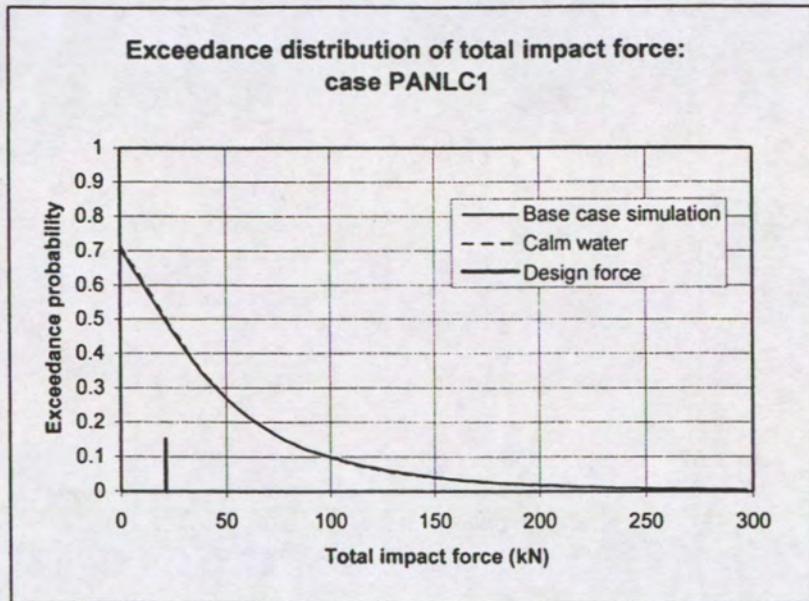


Figure 68: Exceedance distribution of the maximum total impact force: panel in loss of control incident, effect of calm water.

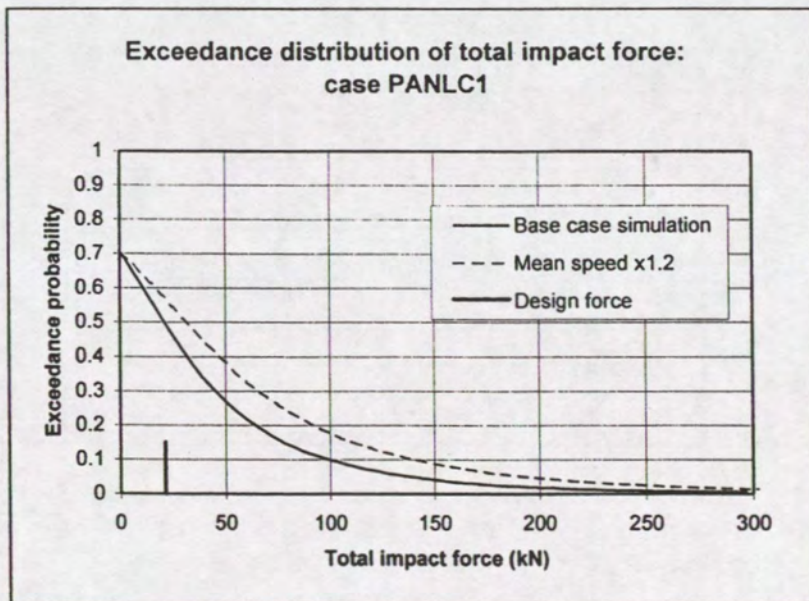


Figure 69: Exceedance distribution of the maximum total impact force: panel in loss of control incident, effect of increased mean speed.

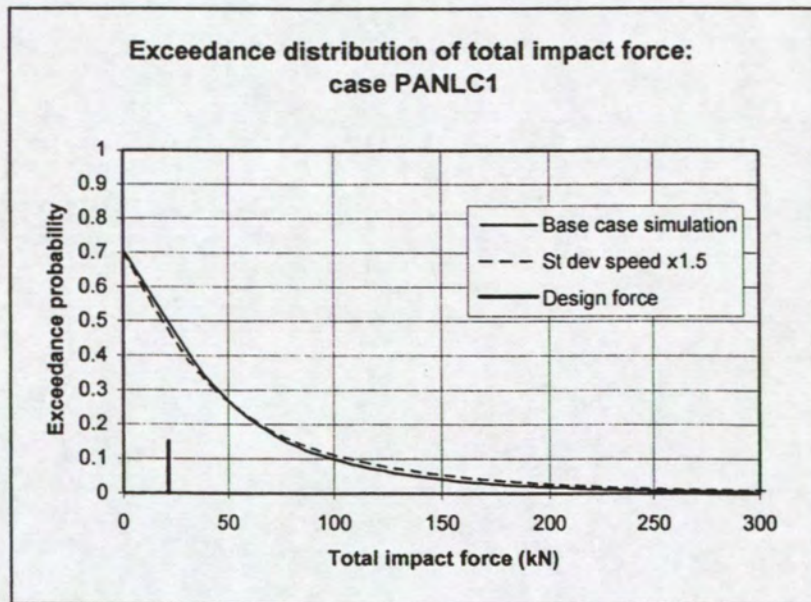


Figure 70: Exceedance distribution of the maximum total impact force: panel in loss of control incident, effect of increased speed range.

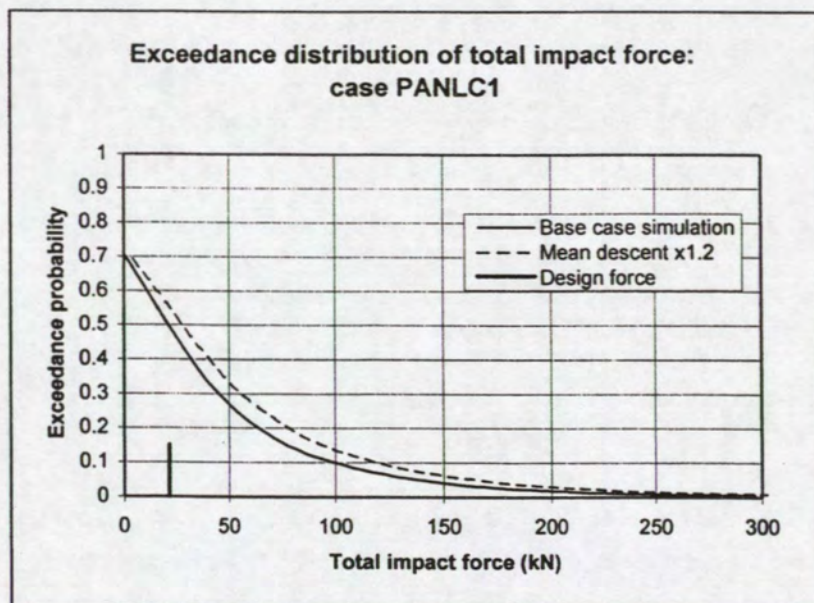


Figure 71: Exceedance distribution of the maximum total impact force: panel in loss of control incident, effect of increased mean descent angle.

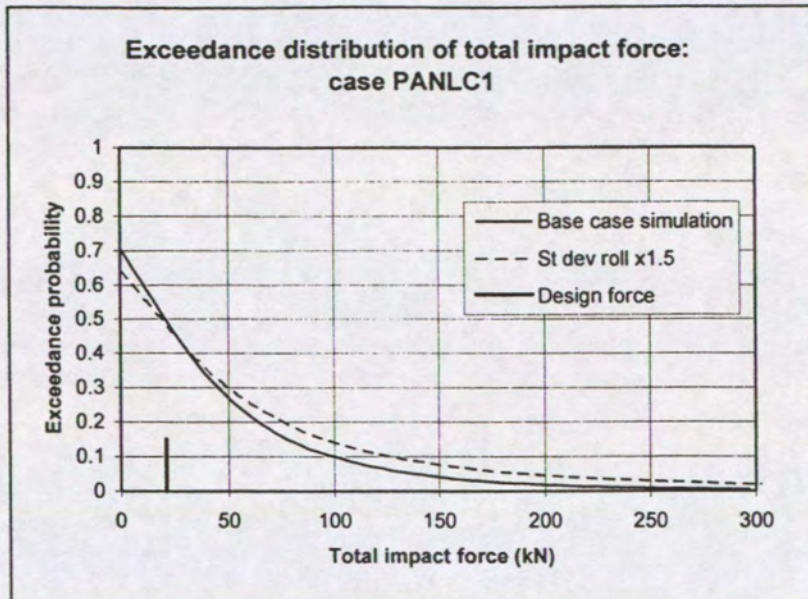


Figure 72: Exceedance distribution of the maximum total impact force: panel in loss of control incident, effect of increased roll angle range.

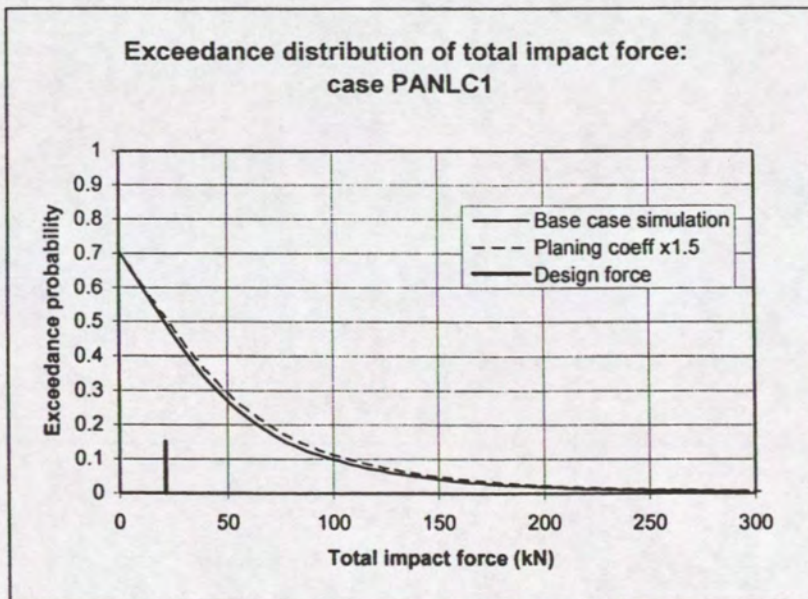


Figure 73: Exceedance distribution of the maximum total impact force: panel in loss of control incident, effect of increased planing force coefficient.

Results from Sensitivity Study

**Exceedance distributions of the maximum
total impact force on the fuselage panel:**

4. Fly-in incident

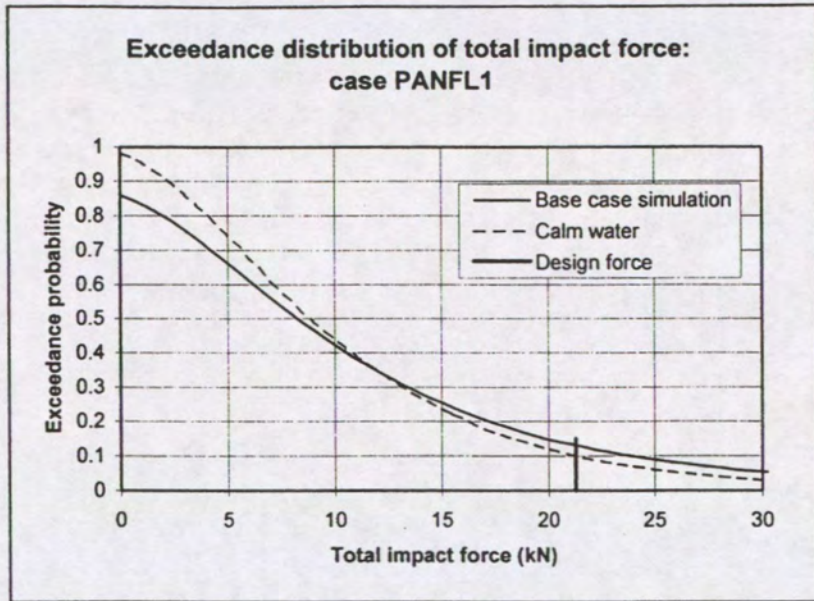


Figure 74: Exceedance distribution of the maximum total impact force: panel in fly-in incident, effect of calm water.

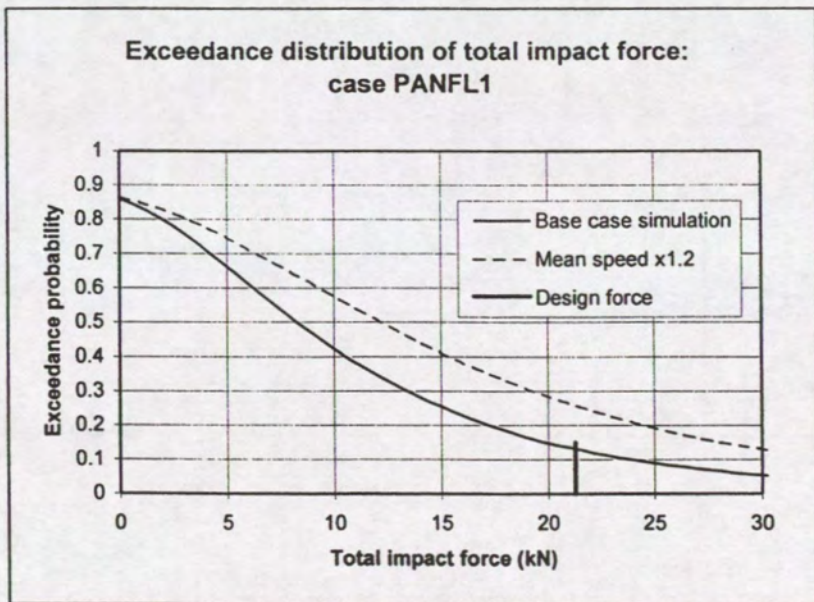


Figure 75: Exceedance distribution of the maximum total impact force: panel in fly-in incident, effect of increased mean speed.

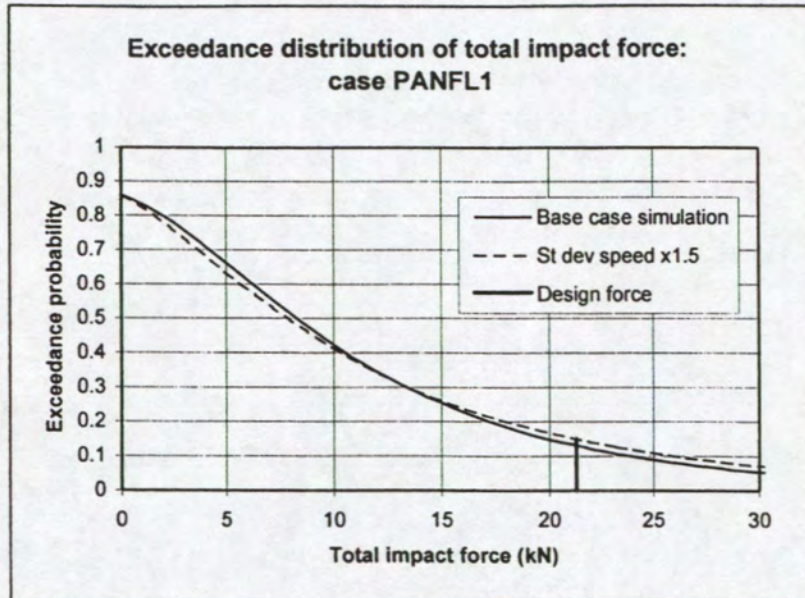


Figure 76: Exceedance distribution of the maximum total impact force: panel in fly-in incident, effect of increased speed range.

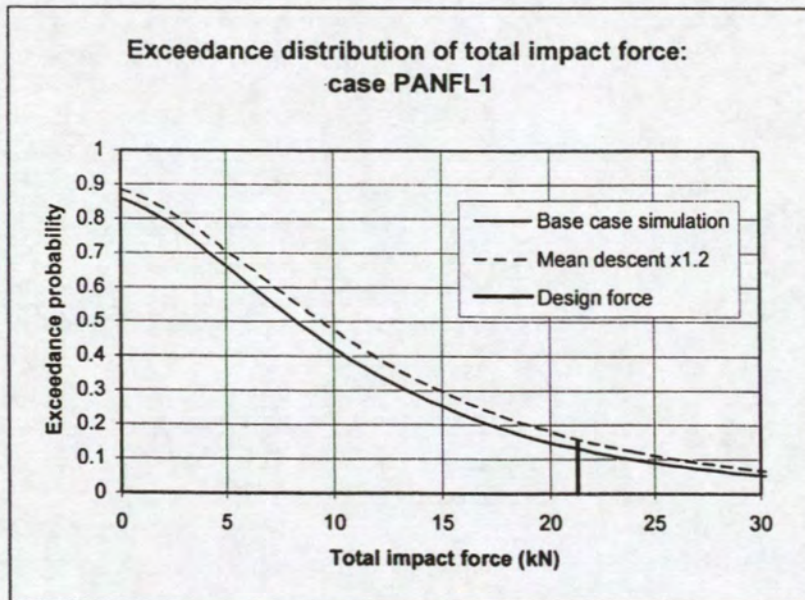


Figure 77: Exceedance distribution of the maximum total impact force: panel in fly-in incident, effect of increased mean descent angle.

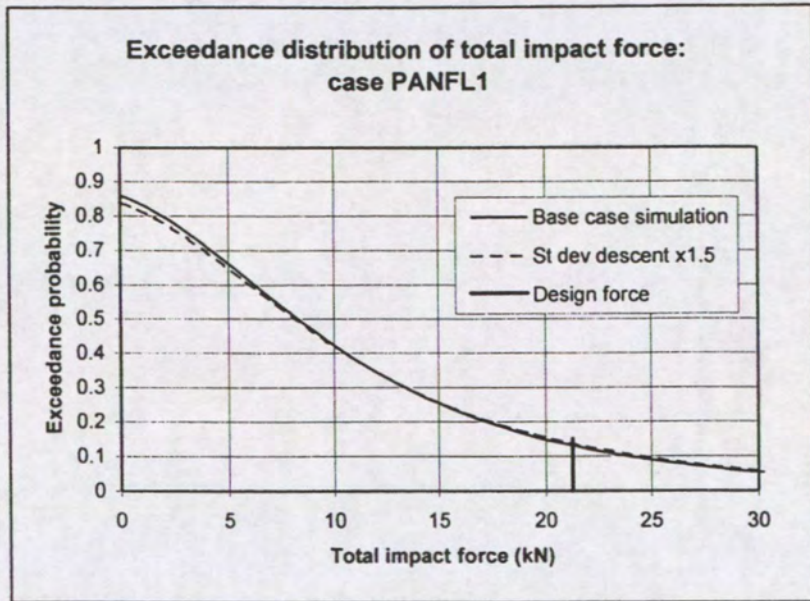


Figure 78: Exceedance distribution of the maximum total impact force: panel in fly-in incident, effect of increased descent angle range.

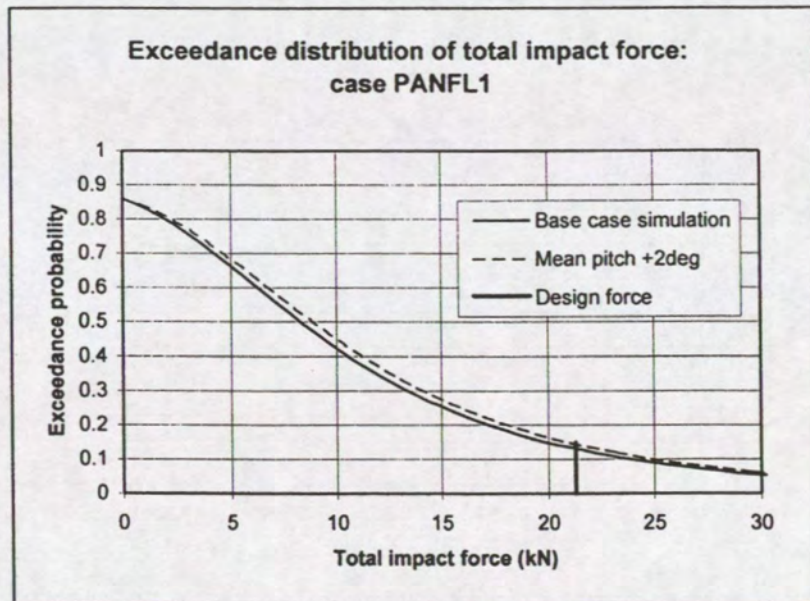


Figure 79: Exceedance distribution of the maximum total impact force: panel in fly-in incident, effect of increased mean pitch angle.

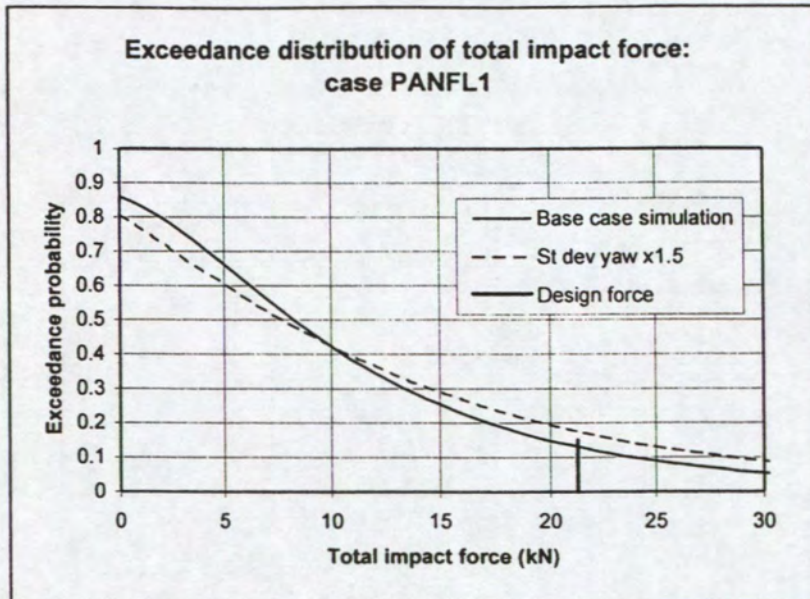


Figure 80: Exceedance distribution of the maximum total impact force: panel in fly-in incident, effect of increased yaw angle range.

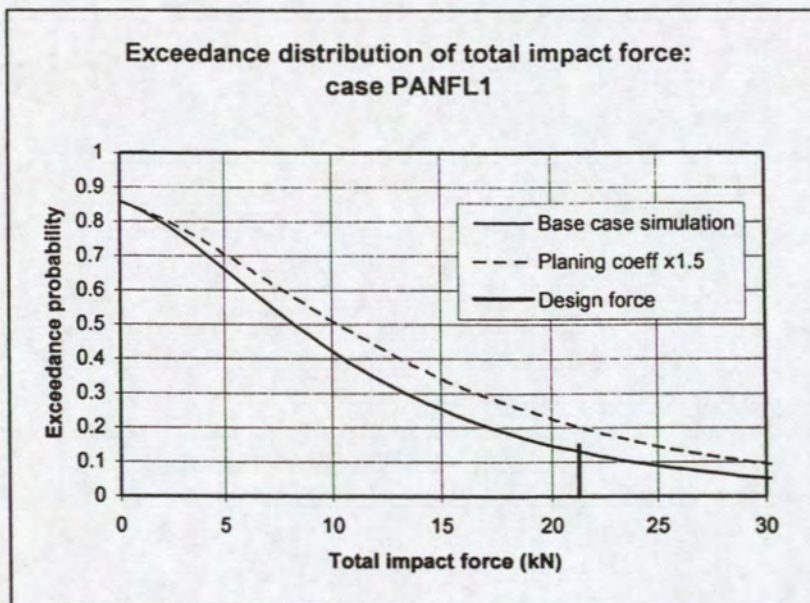


Figure 81: Exceedance distribution of the maximum total impact force: panel in fly-in incident, effect of increased planing force coefficient.

Results from Panel Redundancy Study

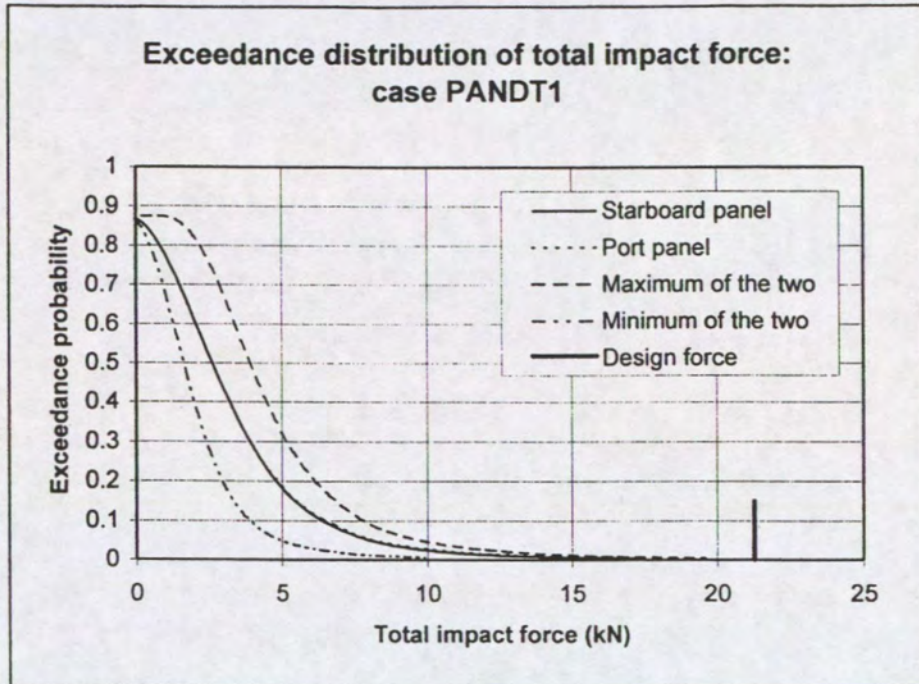


Figure 82: Exceedance distribution of the maximum total impact force on fuselage panels in a controlled ditching incident; individually and together.

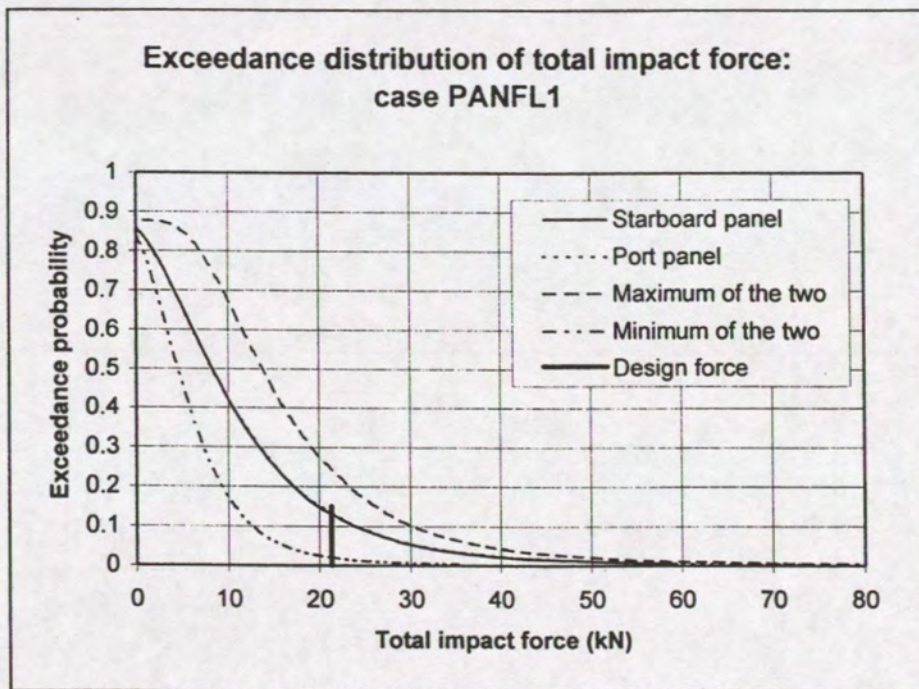


Figure 83: Exceedance distribution of the maximum total impact force on fuselage panels in a fly-in incident; individually and together.

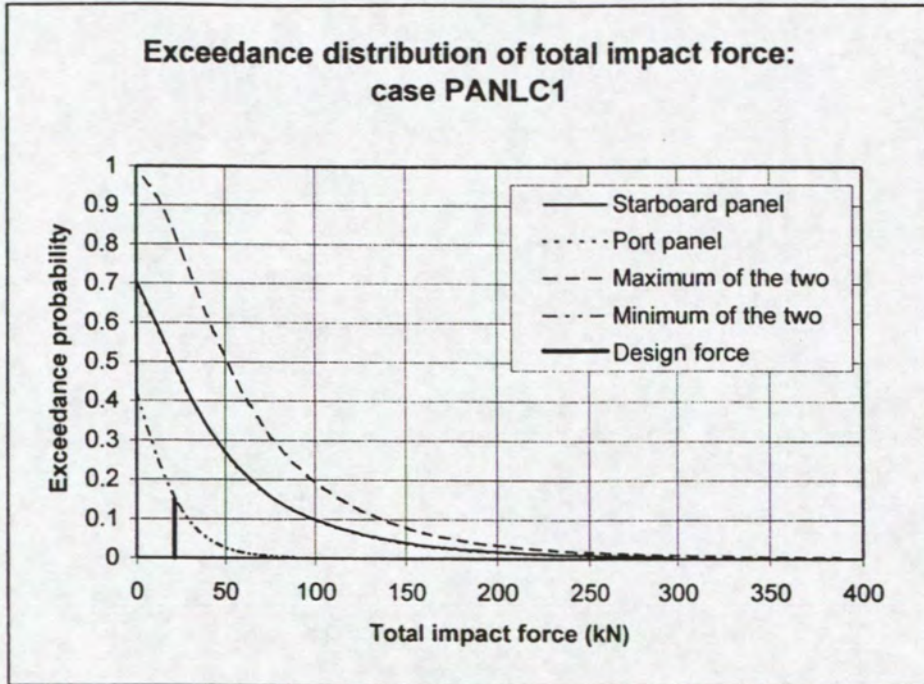


Figure 84: Exceedance distribution of the maximum total impact force on fuselage panels in a loss of control incident; individually and together.

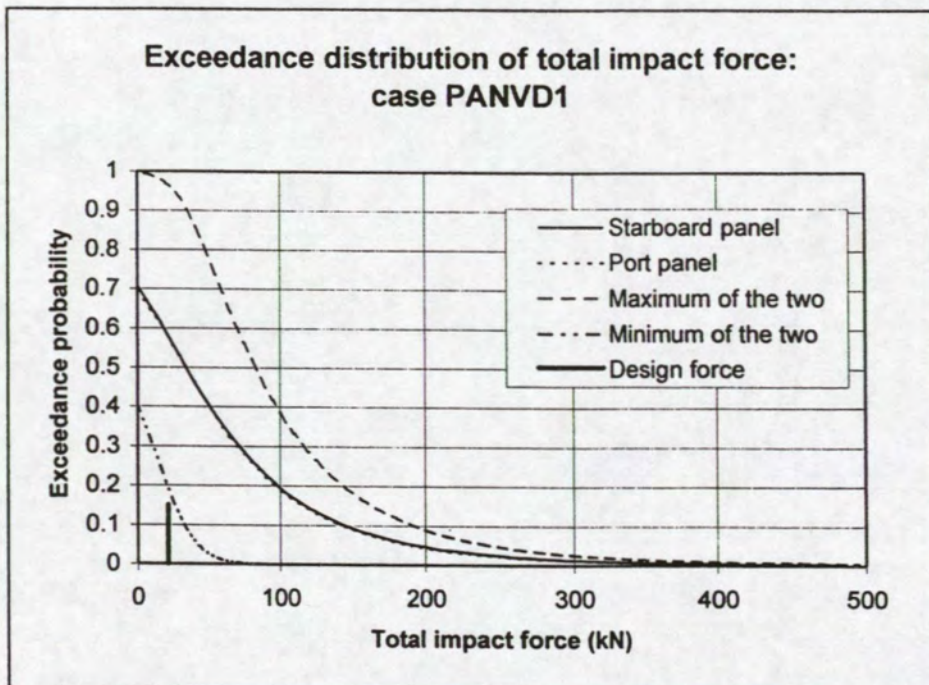


Figure 85: Exceedance distribution of the maximum total impact force on fuselage panels in a vertical descent incident; individually and together.

Helicopter Velocity Scatter Plots

Sponson and fuselage panel: base case conditions

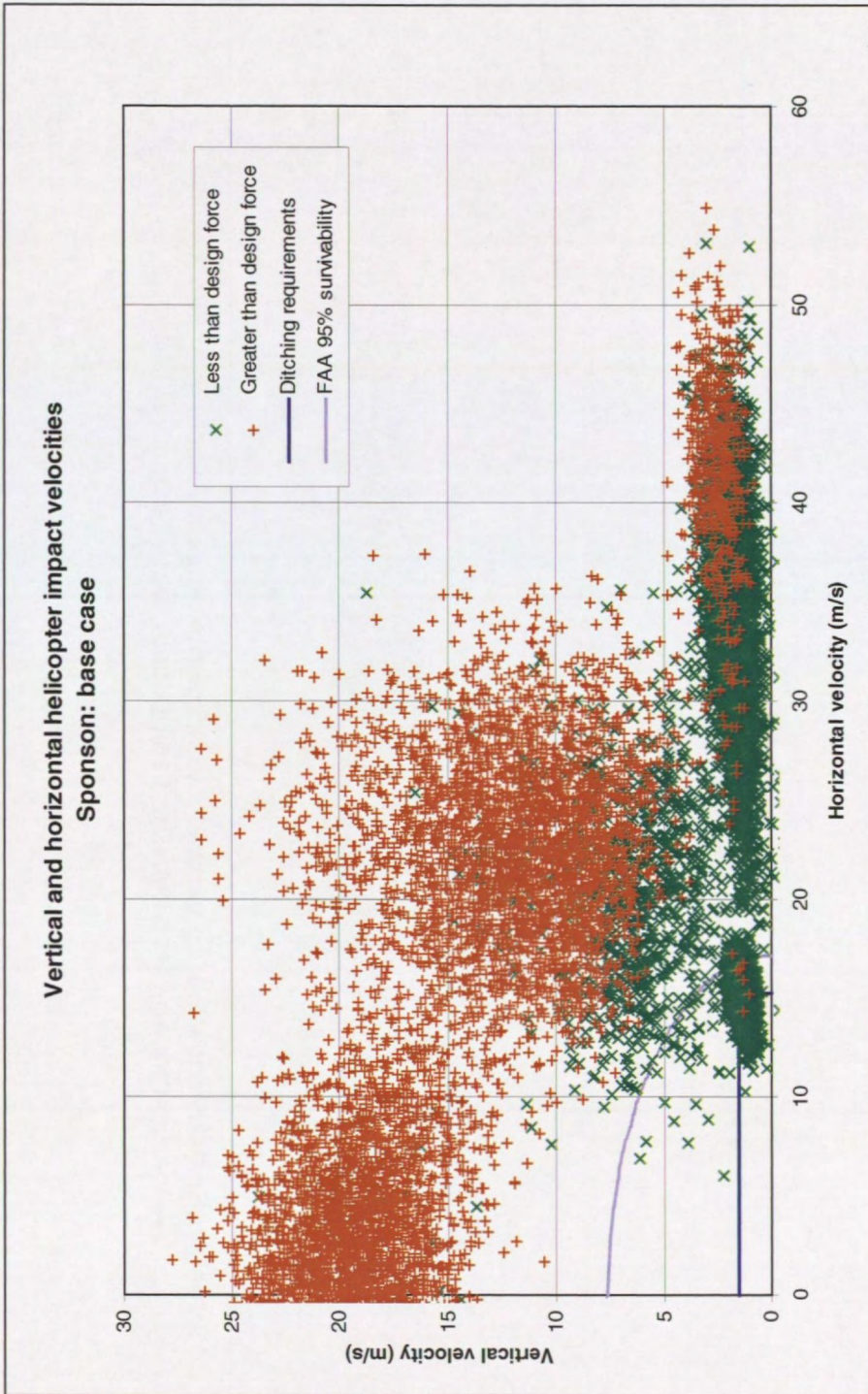


Figure 86: Scatter plot showing vertical and horizontal impact velocities of helicopter: loads on sponson greater than and less than the design load: base case conditions.

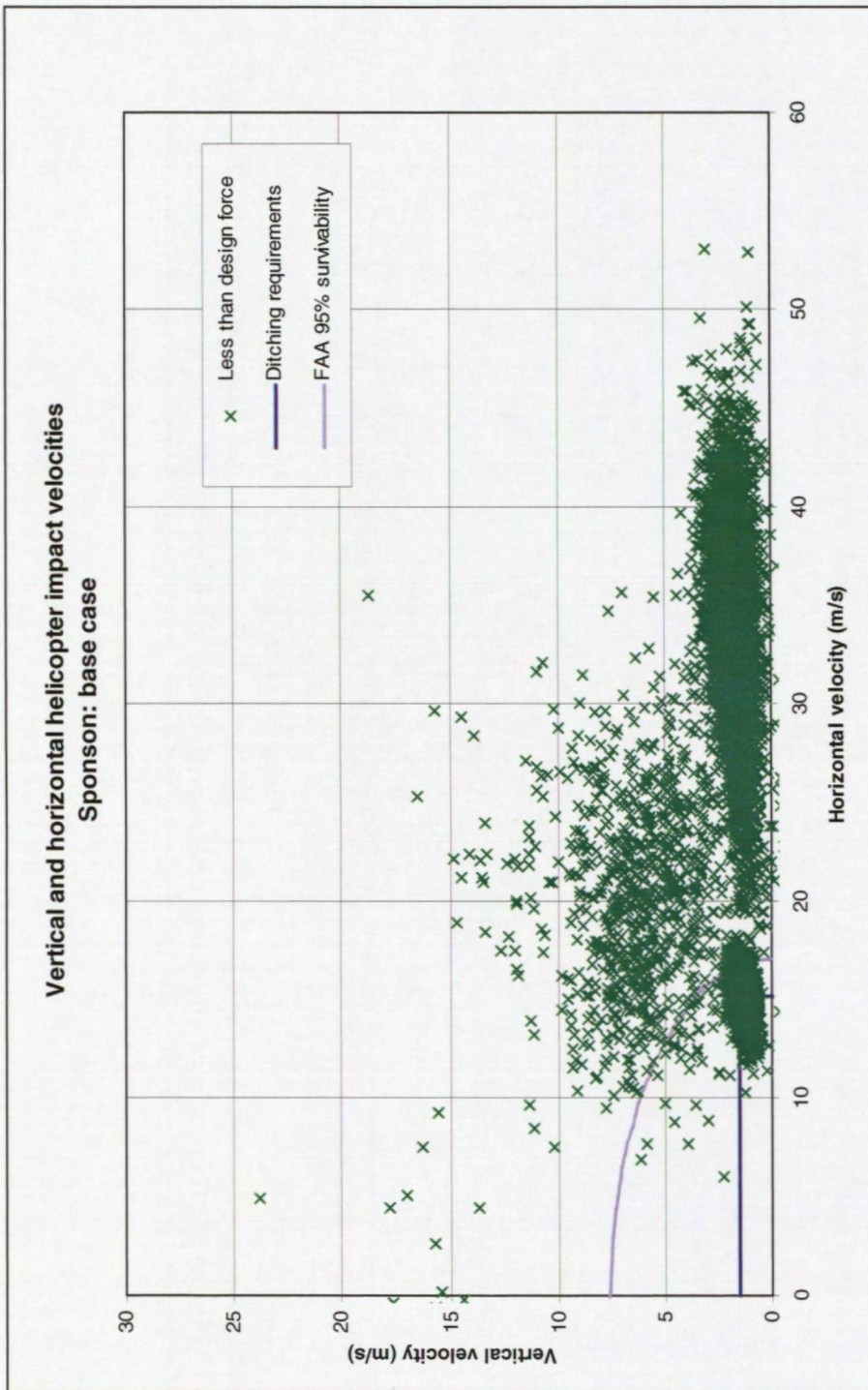


Figure 87: Scatter plot showing vertical and horizontal impact velocities of helicopter: loads on sponson less than the design load: base case conditions.

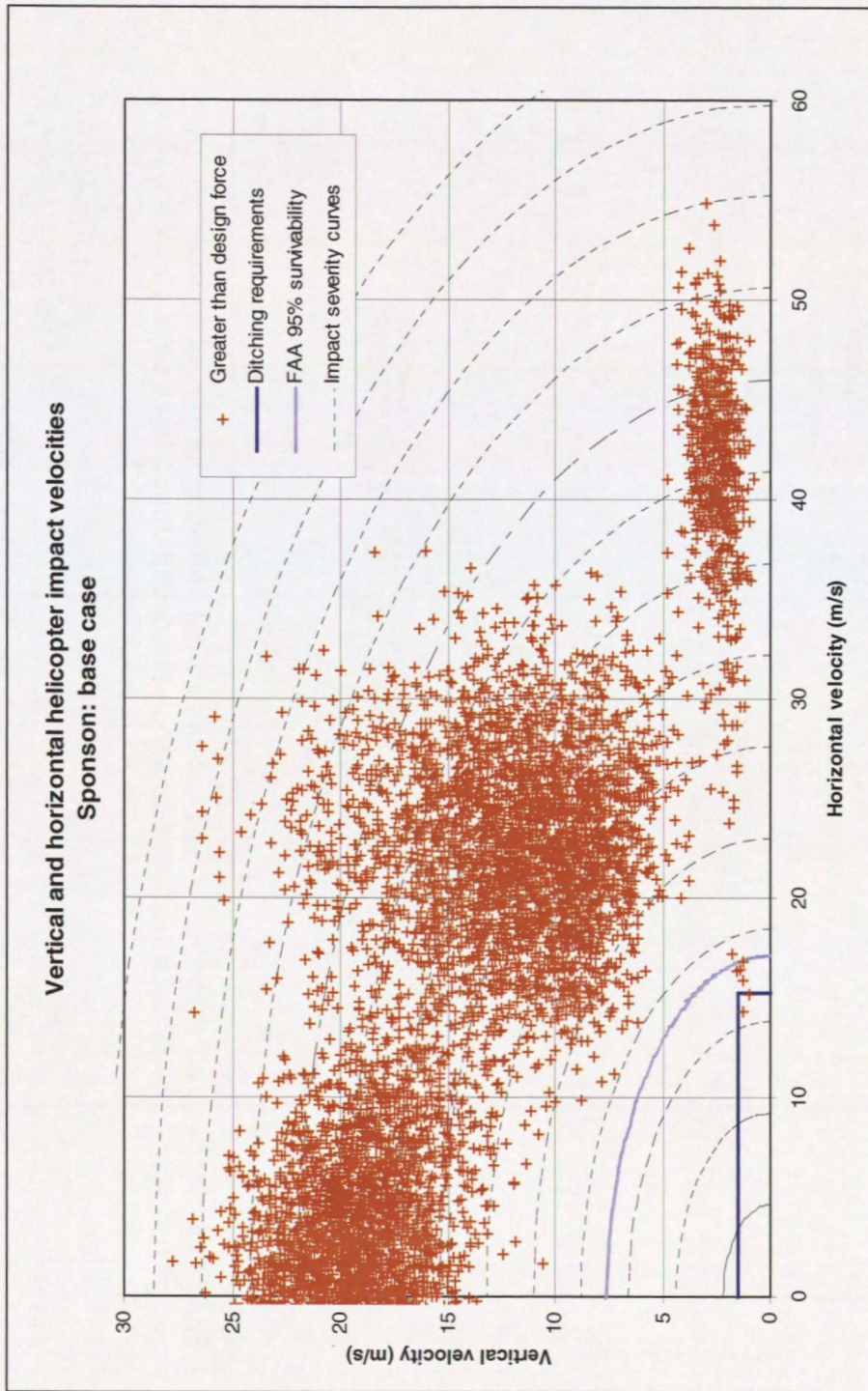


Figure 88: Scatter plot showing vertical and horizontal impact velocities of helicopter: loads on sponson greater than the design load: base case conditions.

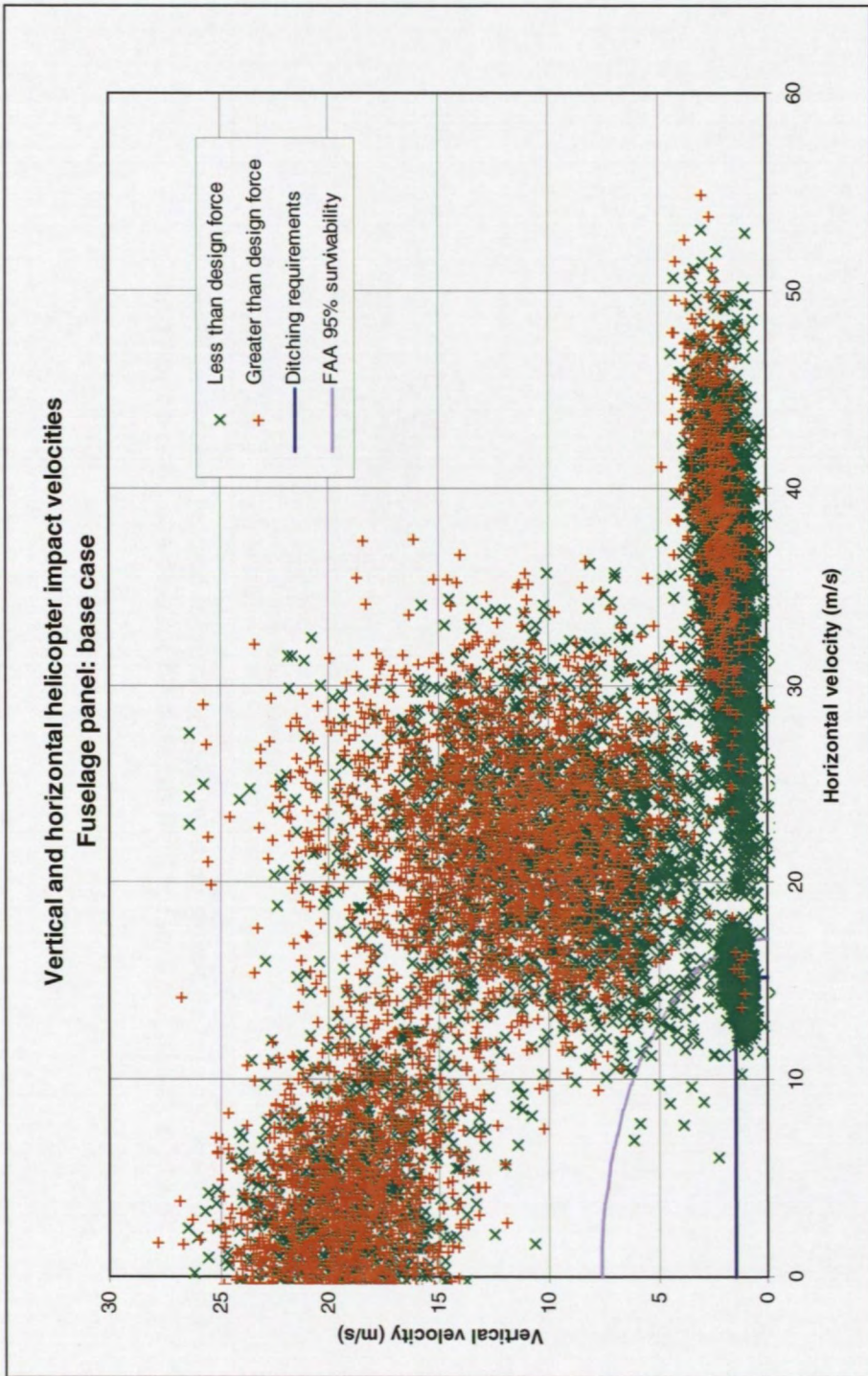


Figure 89: Scatter plot showing vertical and horizontal impact velocities of helicopter: loads on fuselage panel greater than and less than the design load: base case conditions.

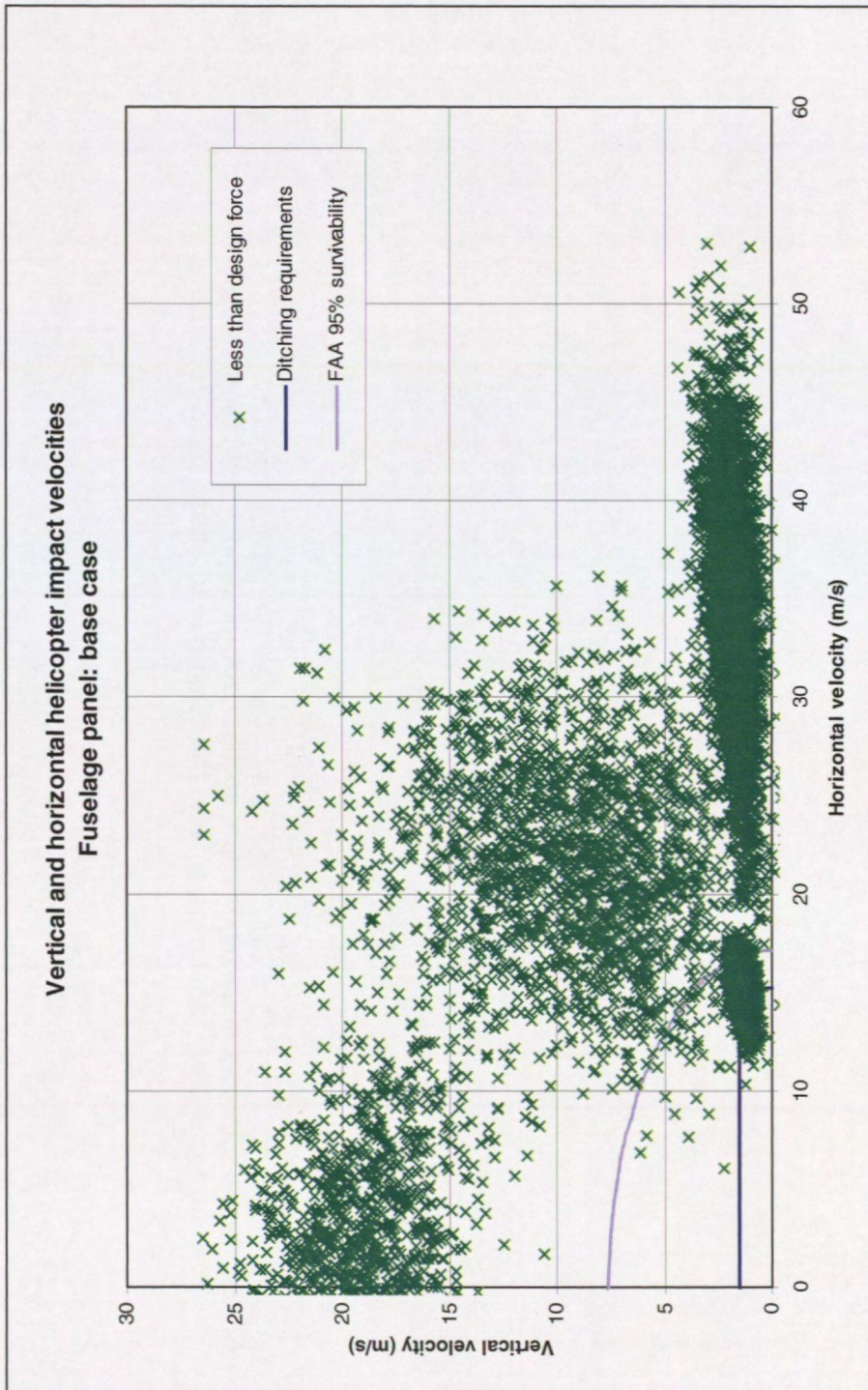


Figure 90: Scatter plot showing vertical and horizontal impact velocities of helicopter: loads on fuselage panel less than the design load: base case conditions.

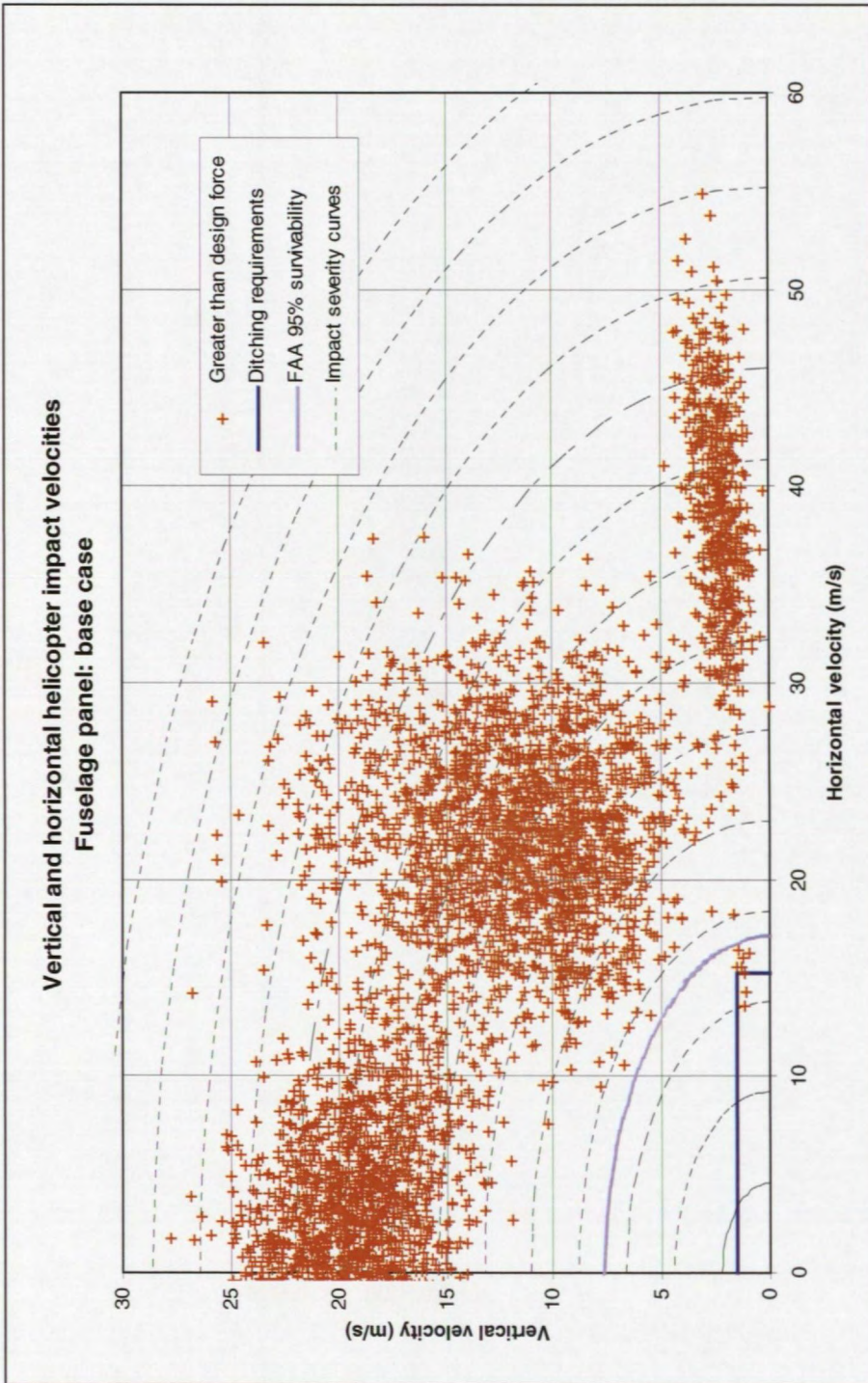


Figure 91: Scatter plot showing vertical and horizontal impact velocities of helicopter: loads on fuselage panel greater than the design load: base case conditions.

Helicopter Velocity Scatter Plots

Sponson and fuselage panel: calm water conditions

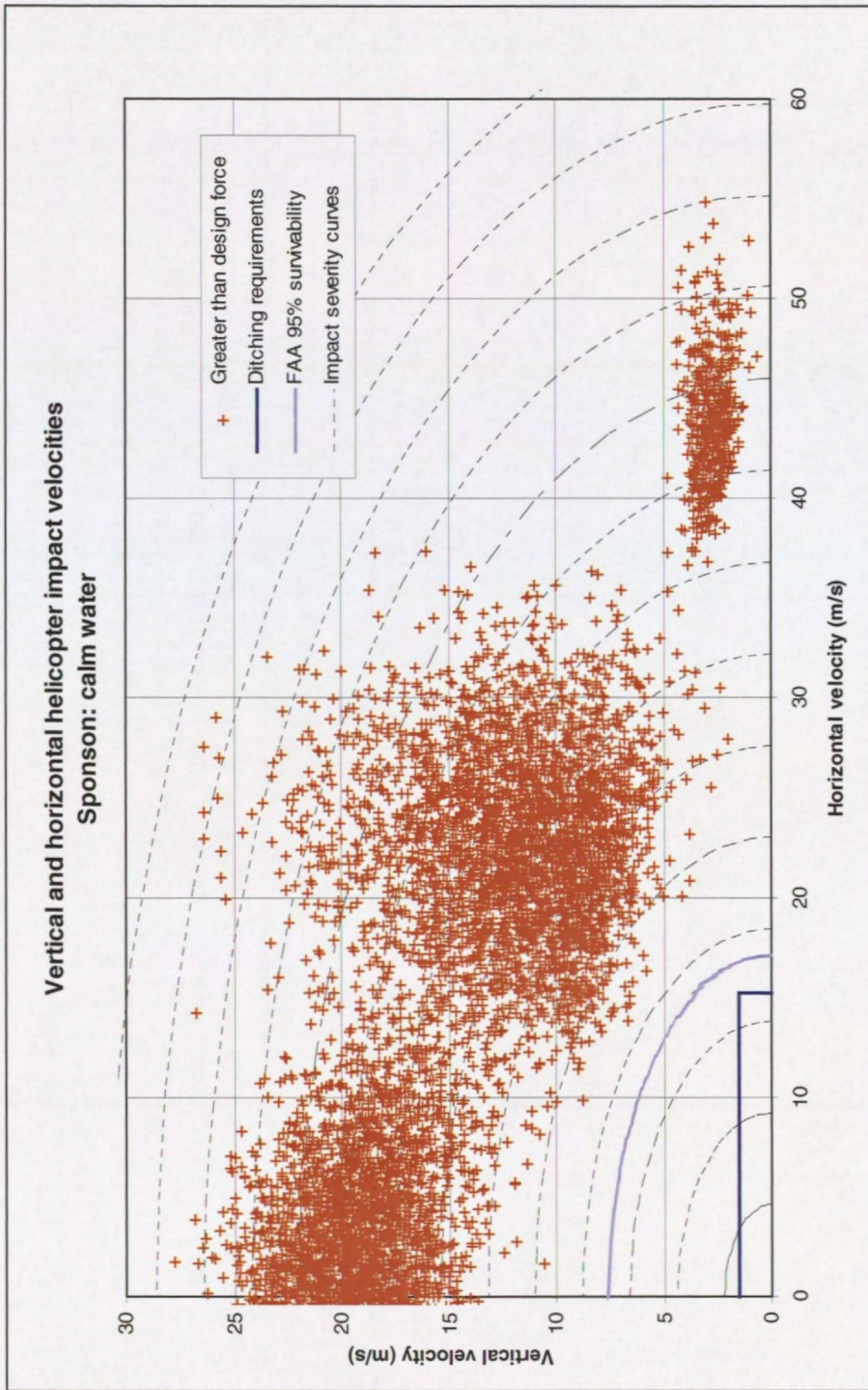


Figure 92: Scatter plot showing vertical and horizontal impact velocities of helicopter: loads on sponson greater than the design load: calm water conditions.

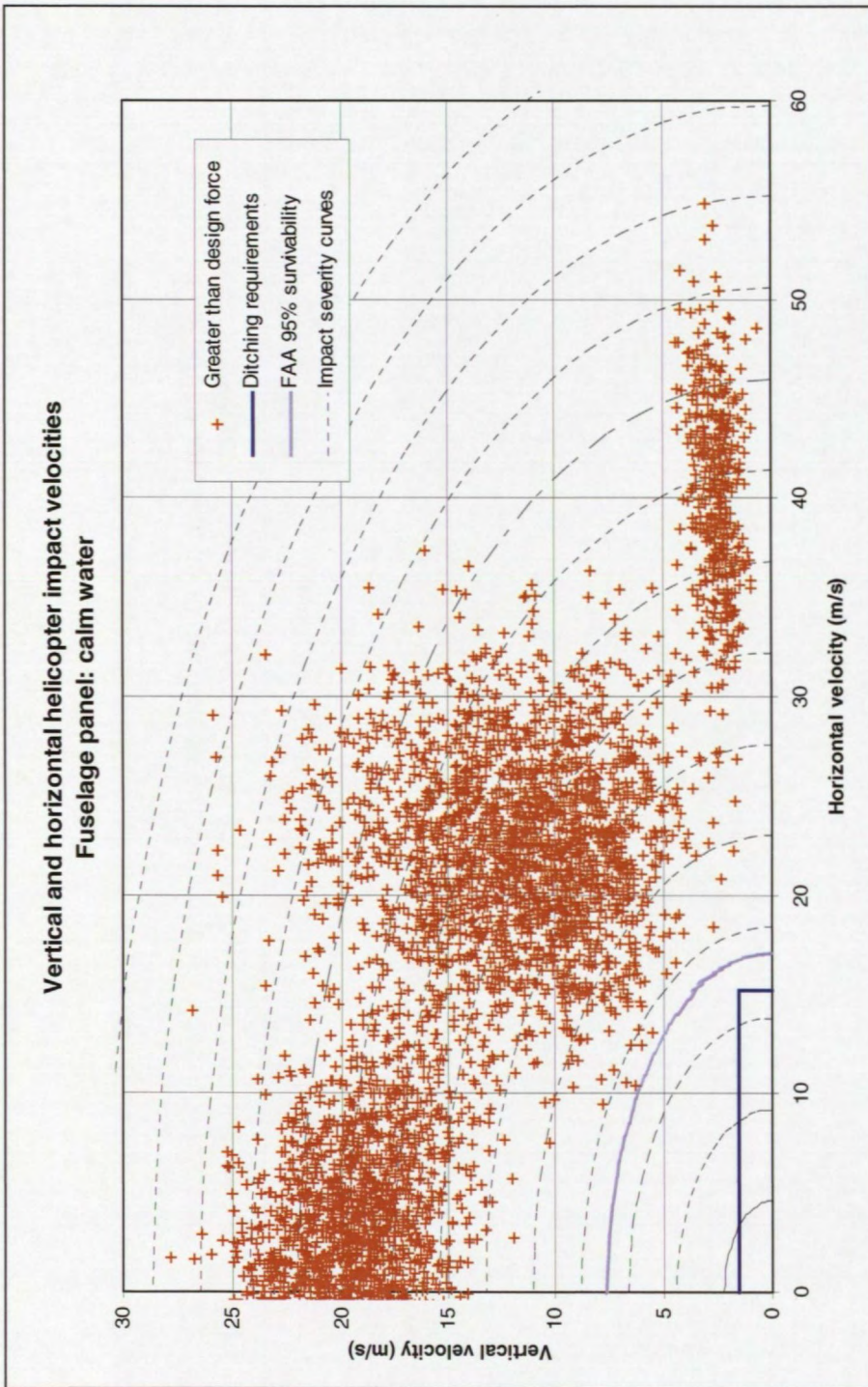


Figure 93: Scatter plot showing vertical and horizontal impact velocities of helicopter: loads on fuselage panel greater than the design load: calm water conditions.

**Percentage of Impact Events Exceeding the Design Load
within each Impact Severity Index Curve**

Sponson and fuselage panel: base case and calm water conditions

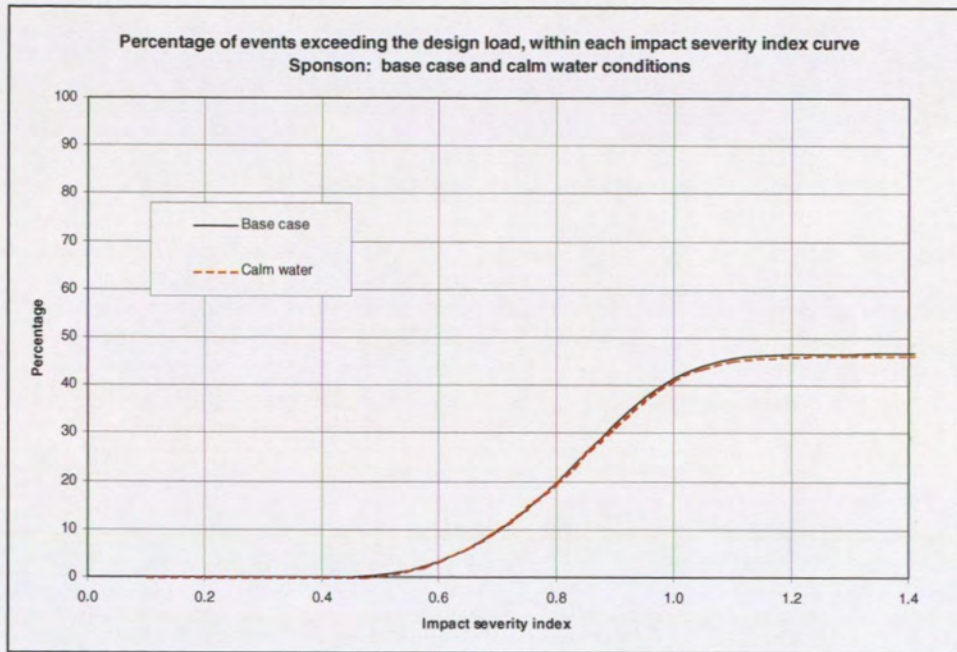


Figure 94: Percentage of impact events exceeding the design load within each impact severity index curve: sponson in base case & calm water conditions.

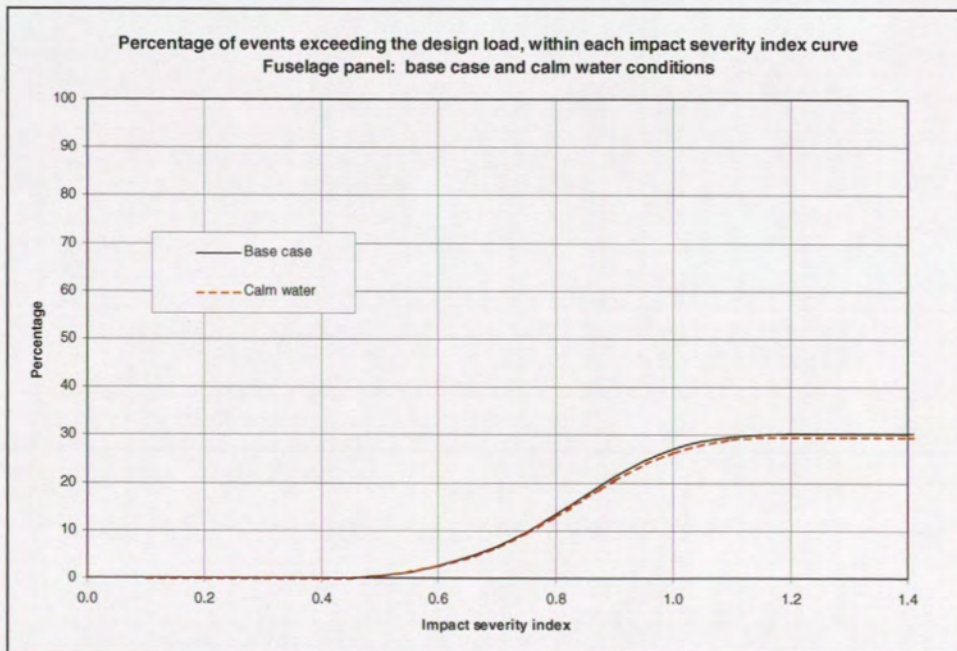


Figure 95: Percentage of impact events exceeding the design load within each impact severity index curve: fuselage panel in base case & calm water conditions.

Helicopter Velocity Scatter Plots

Sponson and fuselage panel: 100% increase in design loads

Vertical and horizontal helicopter impact velocities
Sponson: 100% increase in design force

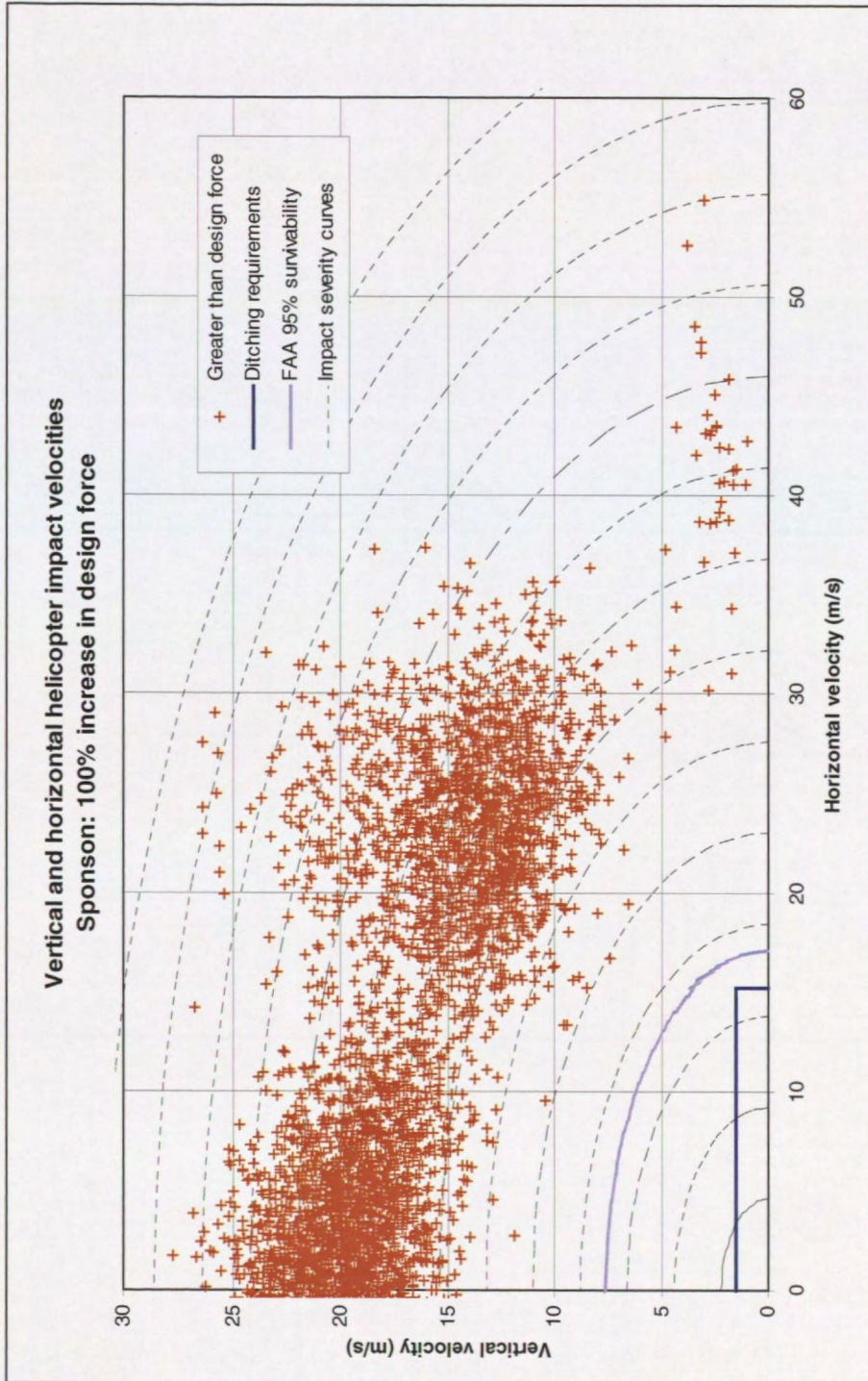


Figure 96: Scatter plot showing vertical and horizontal impact velocities of helicopter: loads on sponson greater than the design load: 100% increase in design load.

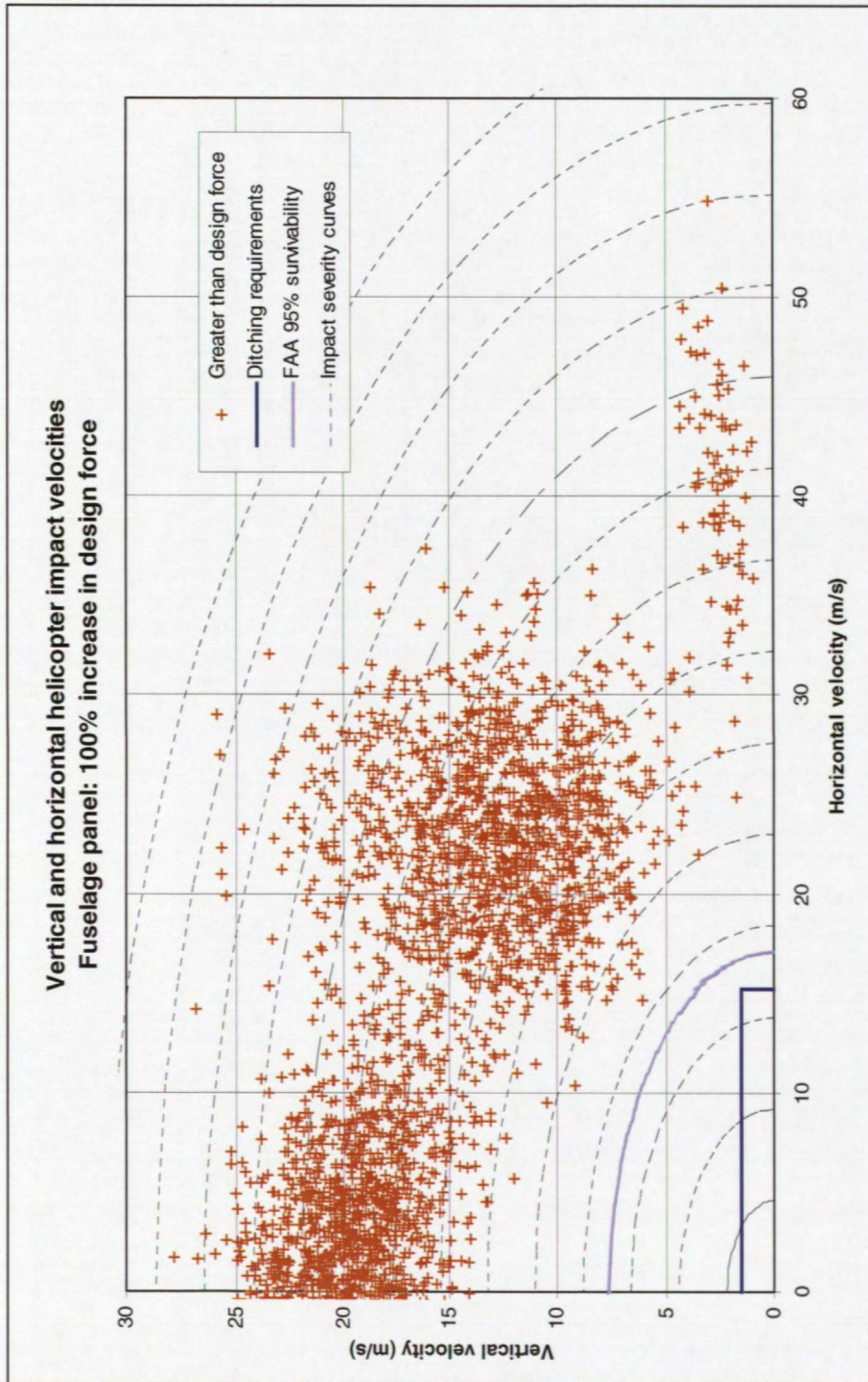


Figure 97: Scatter plot showing vertical and horizontal impact velocities of helicopter: loads on fuselage panel greater than the design load: 100% increase in design load.

**Percentage of Impact Events Exceeding the Design Load
within each Impact Severity Index Curve**

**Sponson and fuselage panel: base case,
and with 100% increase in the design load**

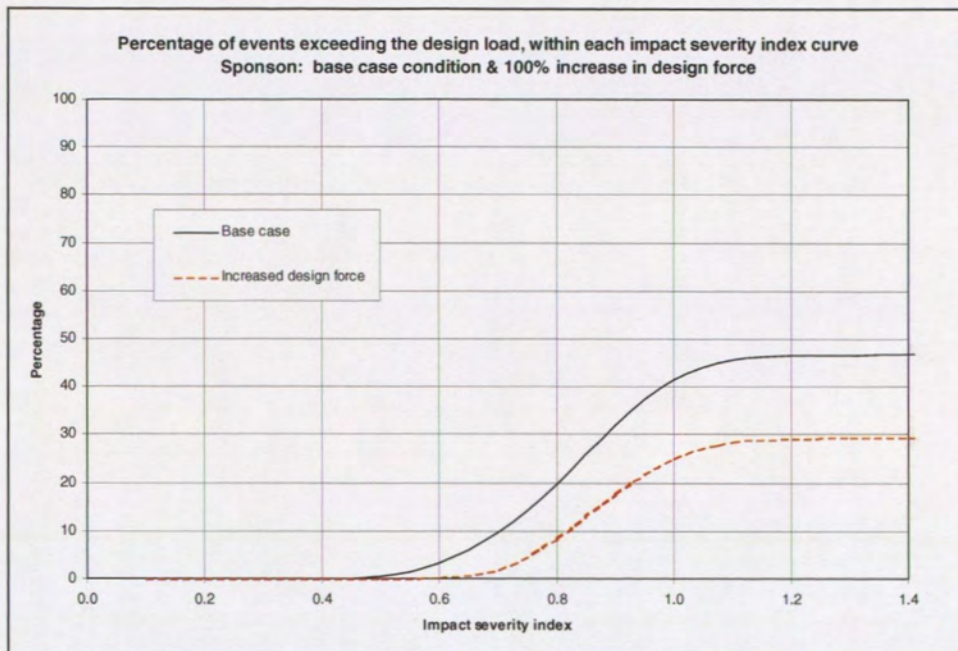


Figure 98: Percentage of impact events exceeding the design load within each impact severity index curve: sponson in base case conditions, and with 100% increase in the design load.

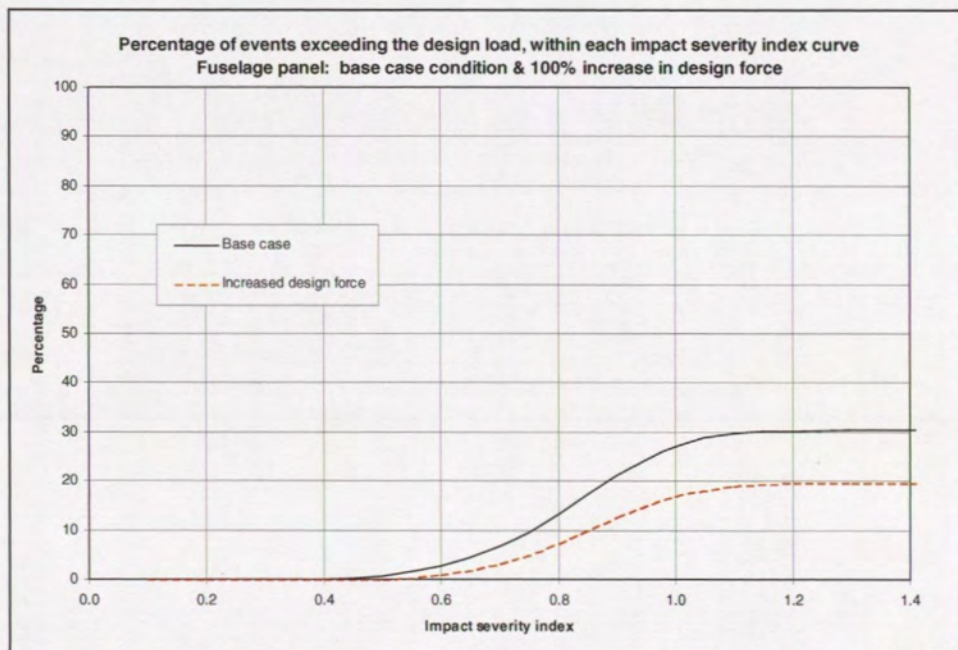


Figure 99: Percentage of impact events exceeding the design load within each impact severity index curve: fuselage panel in base case conditions, and with 100% increase in the design load.

Helicopter Velocity Scatter Plots
Two-panel redundancy study

Vertical and horizontal helicopter impact velocities
Two fuselage panels: no redundancy

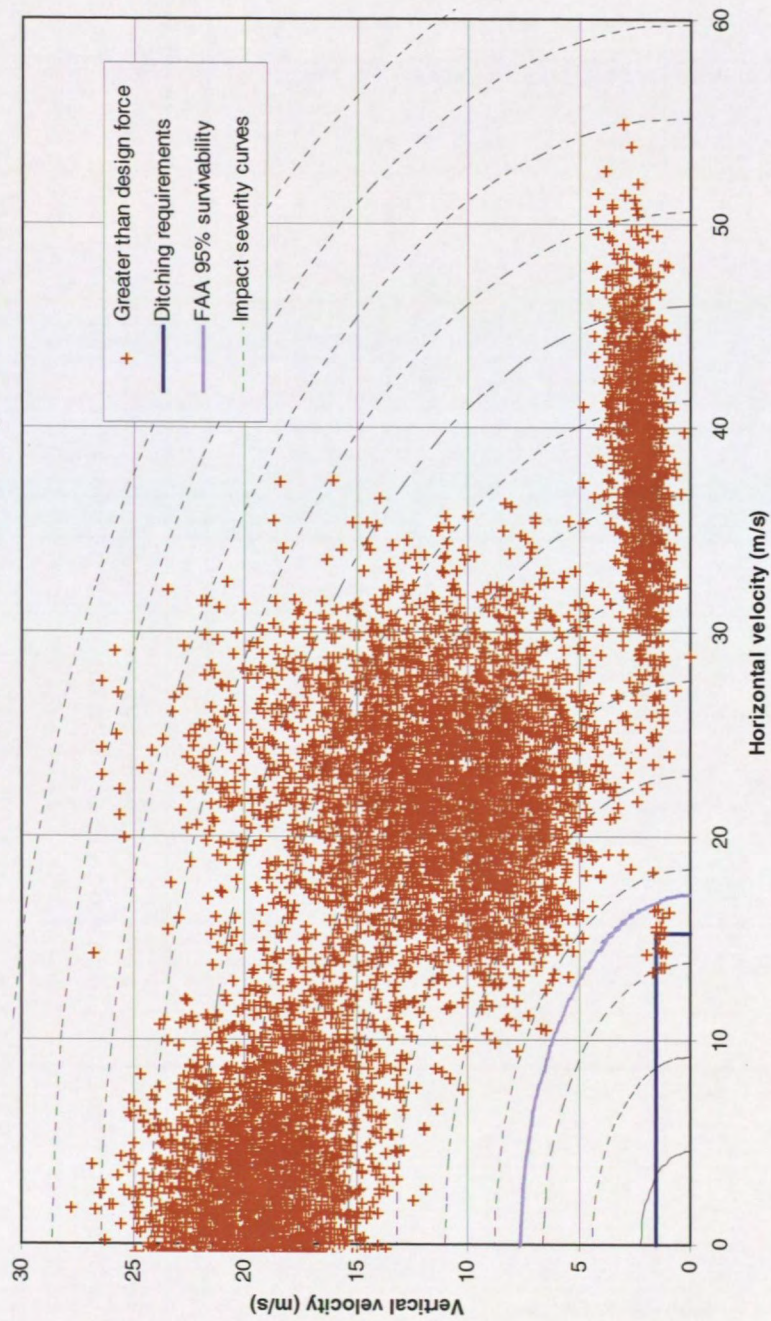


Figure 100: Scatter plot showing vertical and horizontal impact velocities of helicopter loads greater than the design load: two fuselage panels, no redundancy.

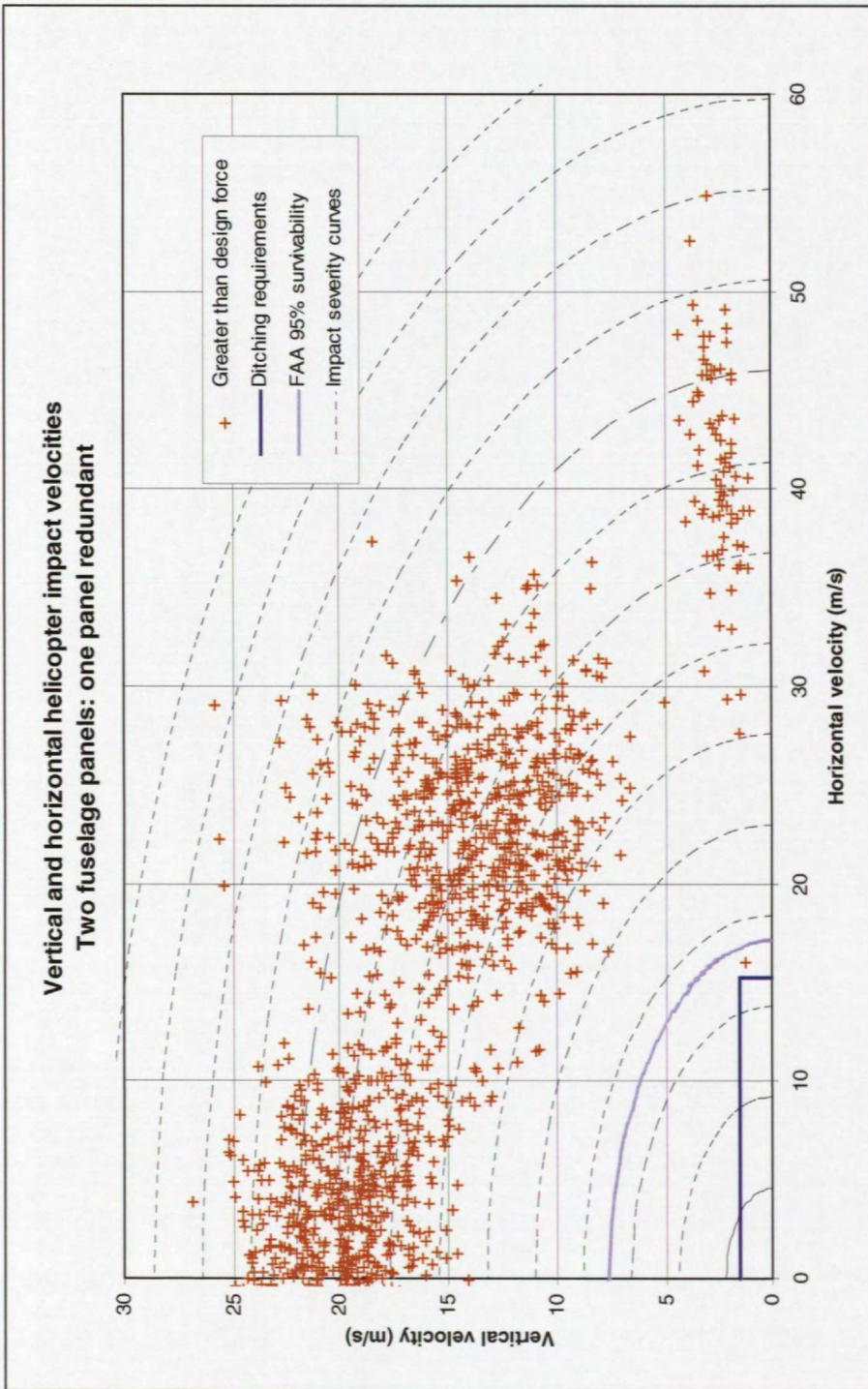


Figure 101: Scatter plot showing vertical and horizontal impact velocities of helicopter: loads greater than the design load: two fuselage panels, one panel redundant.

**Percentage of Impact Events Exceeding the Design Load
within each Impact Severity Index Curve**

Two-panel redundancy study

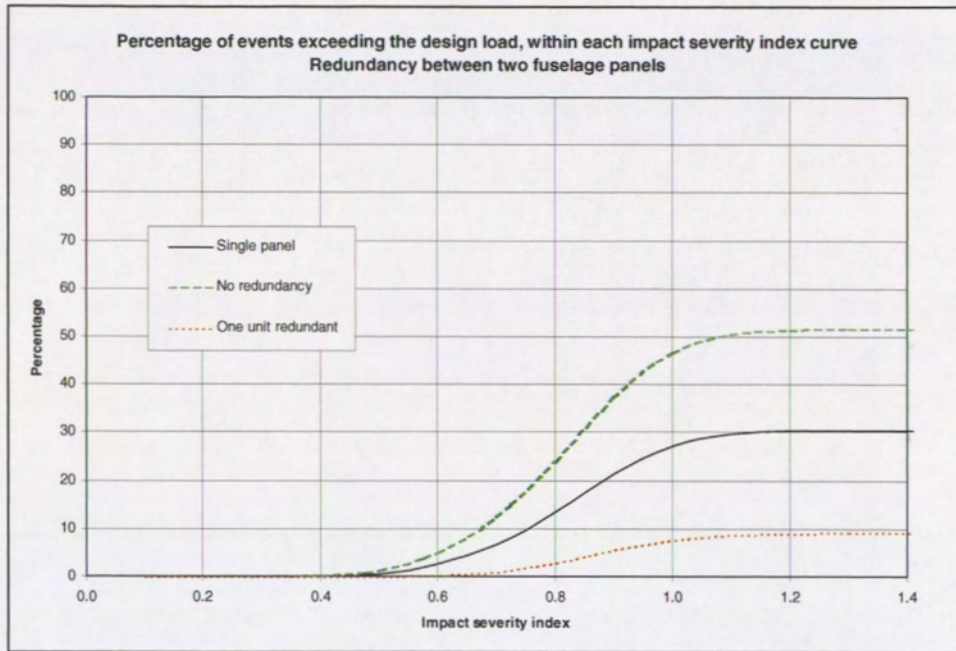


Figure 102: Percentage of impact events exceeding the design load within each impact severity index curve: redundancy between two fuselage panels.

Results from *EH101* Float Redundancy Study

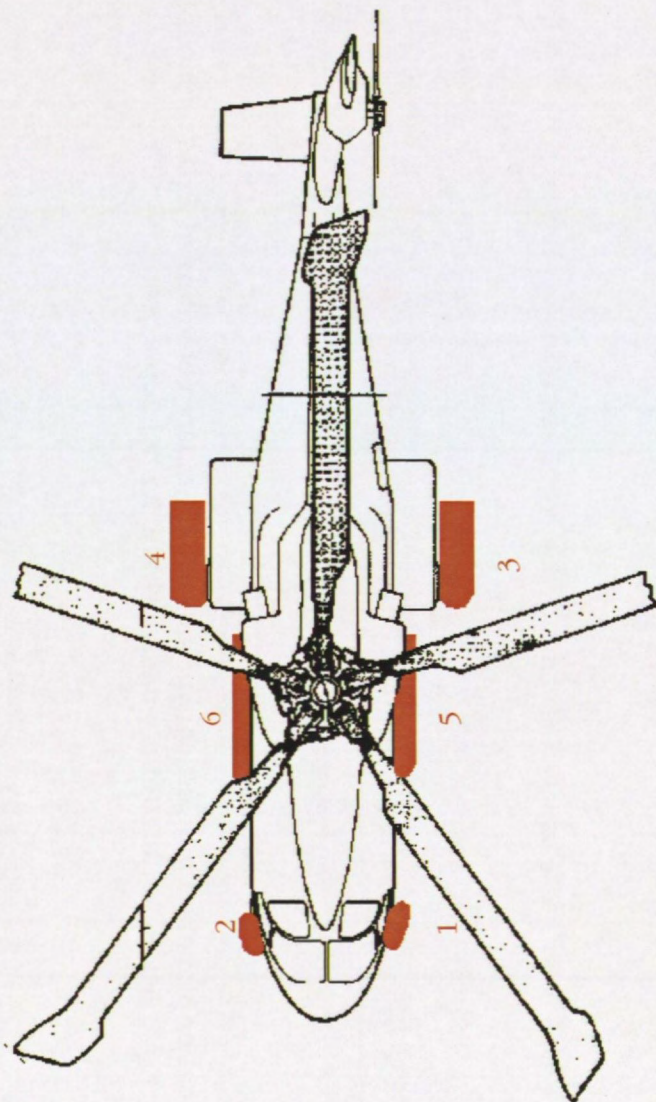


Figure 103: EH101 float numbering scheme.

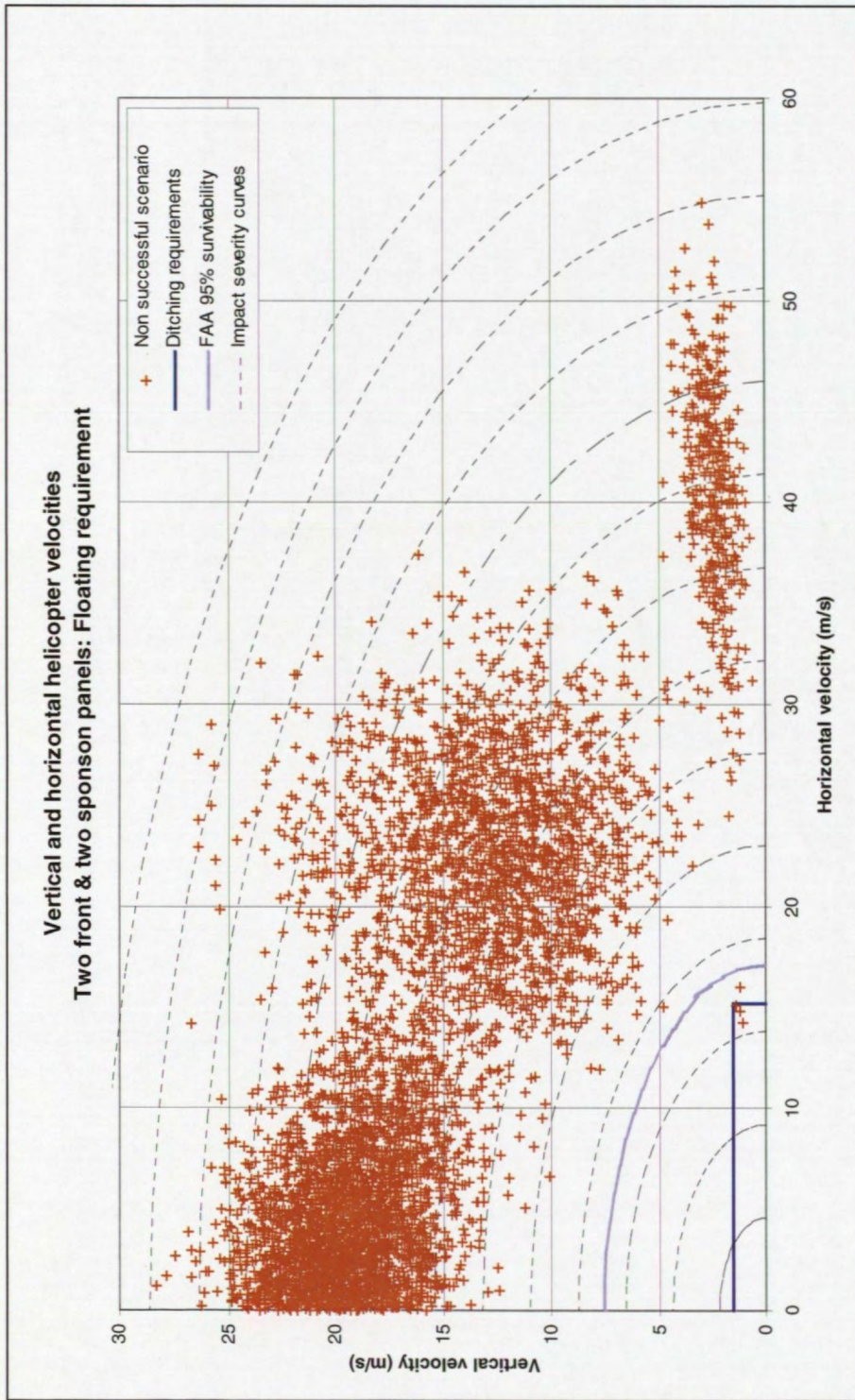


Figure 104: Scatter plot showing vertical and horizontal impact velocities of EH101 helicopter: 4-float configuration; cases where the helicopter sank.

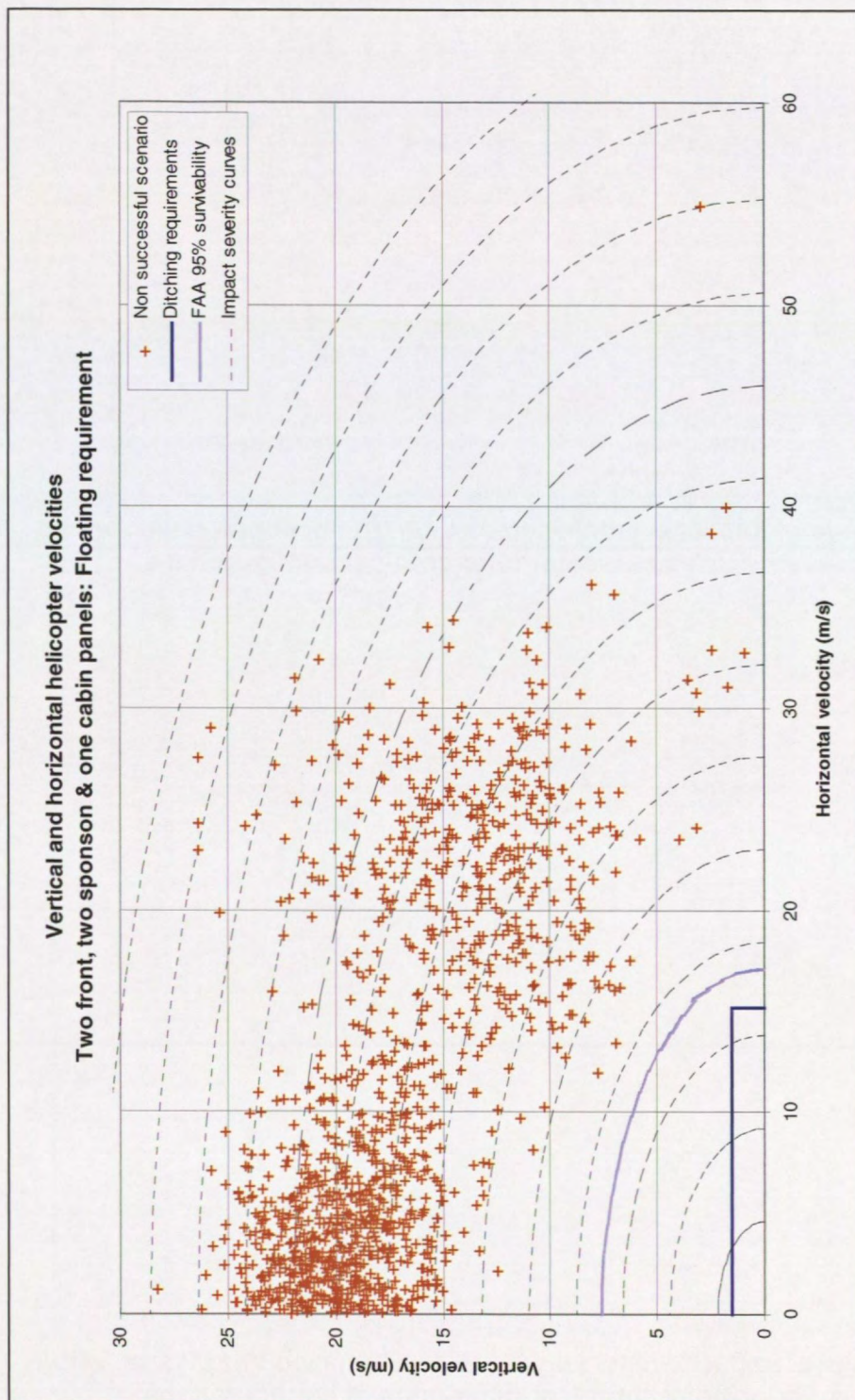


Figure 105: Scatter plot showing vertical and horizontal impact velocities of EH101 helicopter: 5-float configuration; cases where the helicopter sank.

Figure 107: Percentage of impact events where the EH101 helicopter inverts, within each impact severity index curve, for different float configurations.

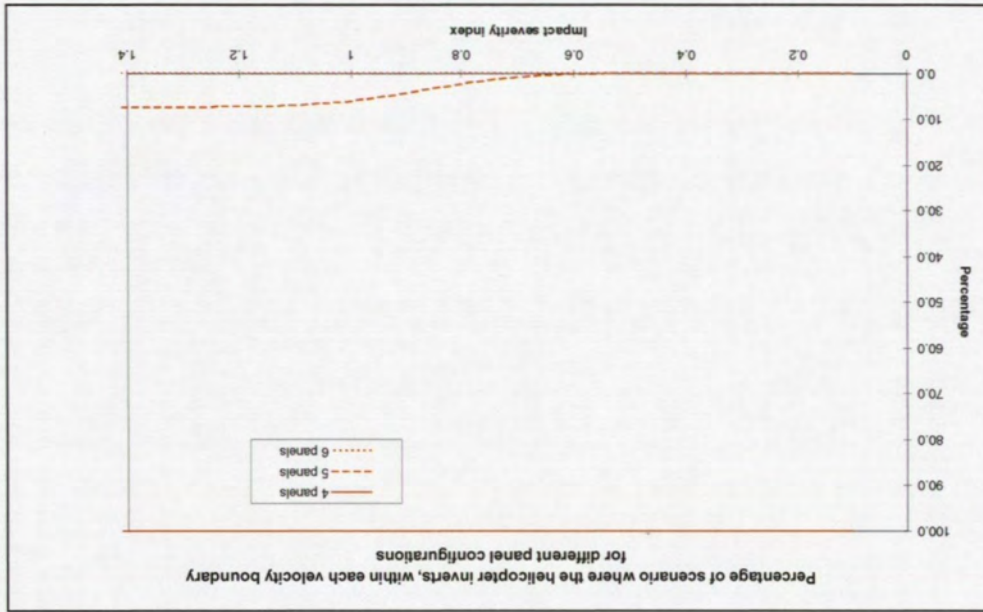
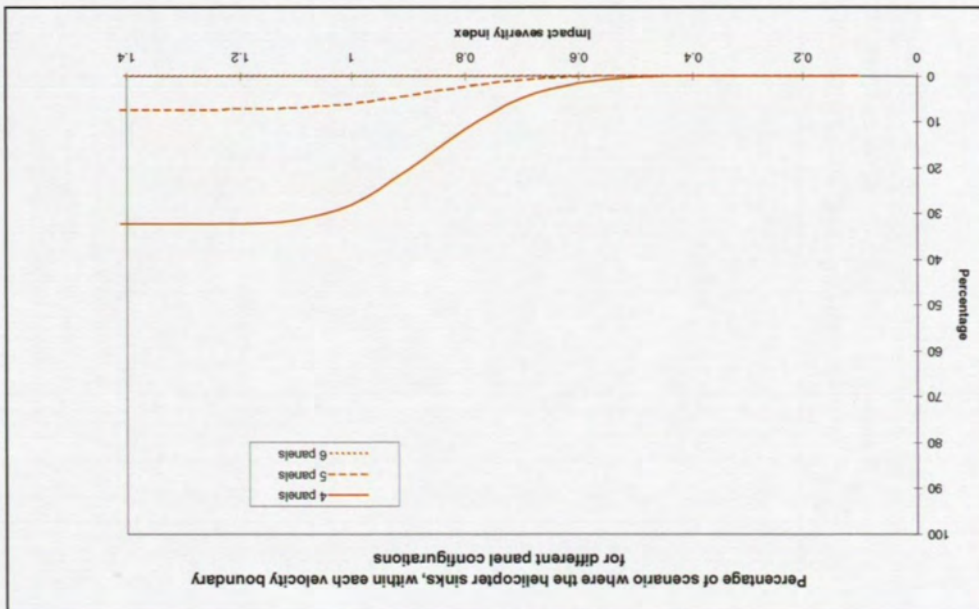


Figure 106: Percentage of impact events where the EH101 helicopter sinks, within each impact severity index curve, for different float configurations.



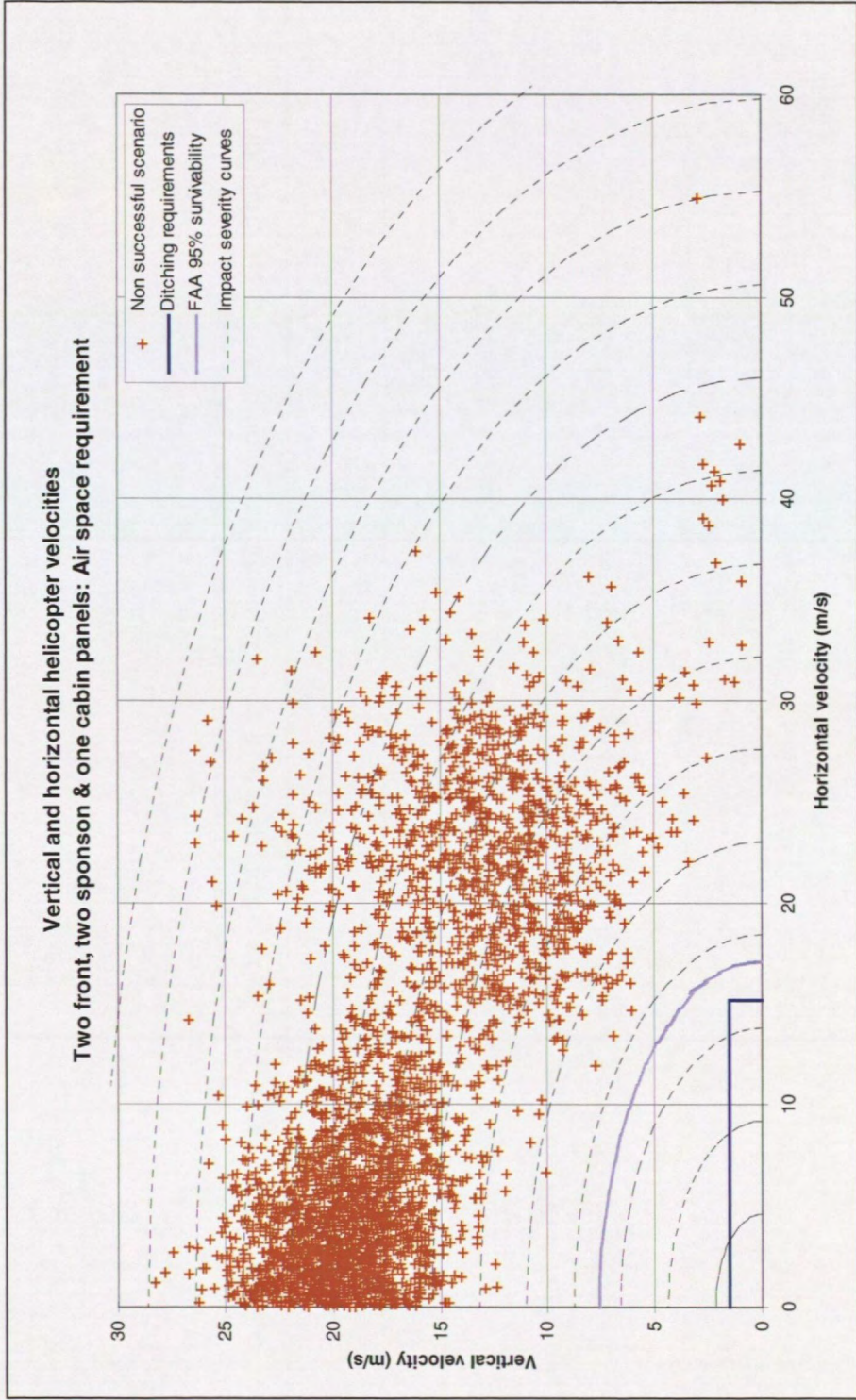


Figure 108: Scatter plot showing vertical and horizontal impact velocities of EH101 helicopter: 5-float configuration; cases with an unsatisfactory air space.

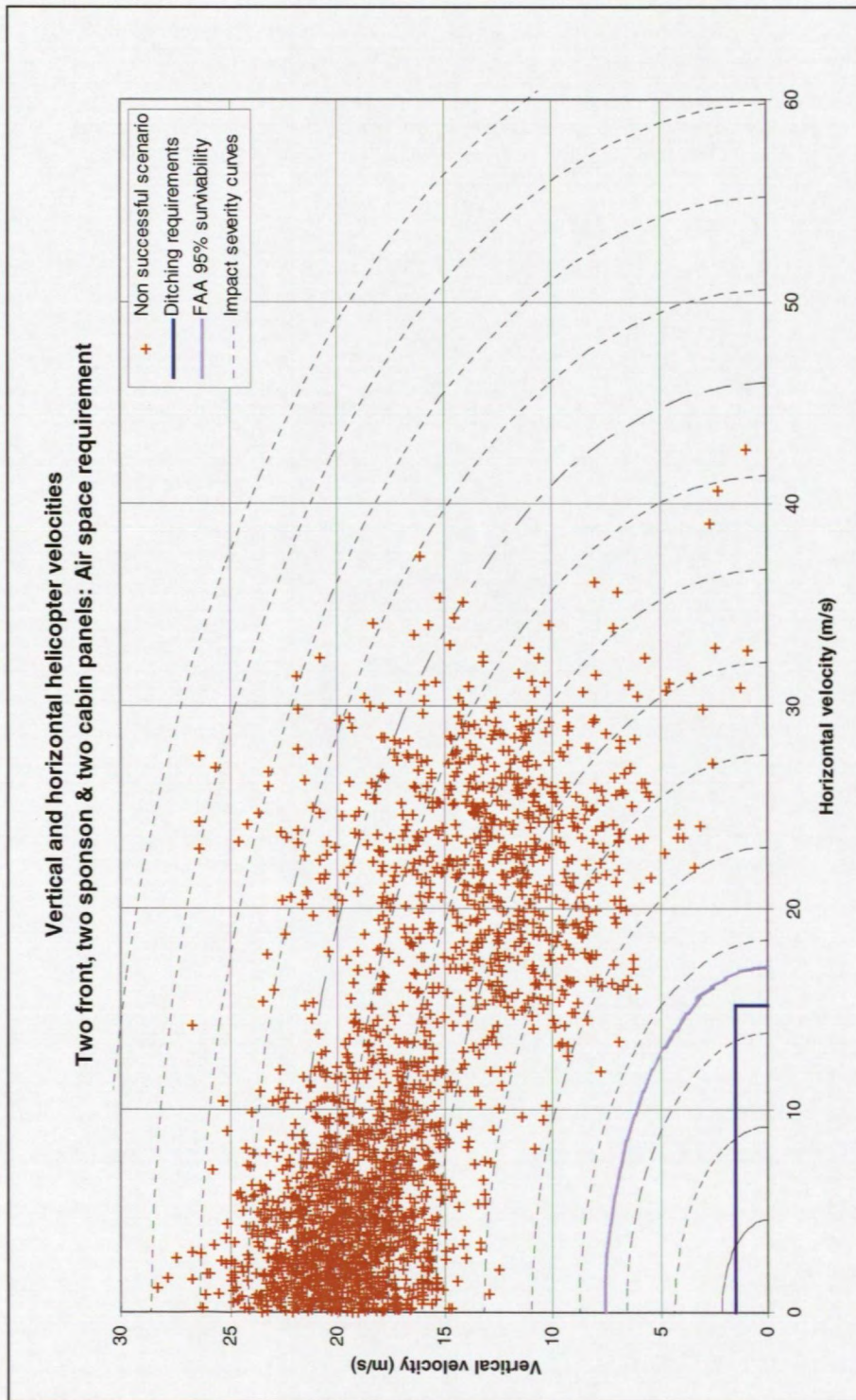


Figure 109: Scatter plot showing vertical and horizontal impact velocities of EH101 helicopter: 6-float configuration; cases with an unsatisfactory air space.

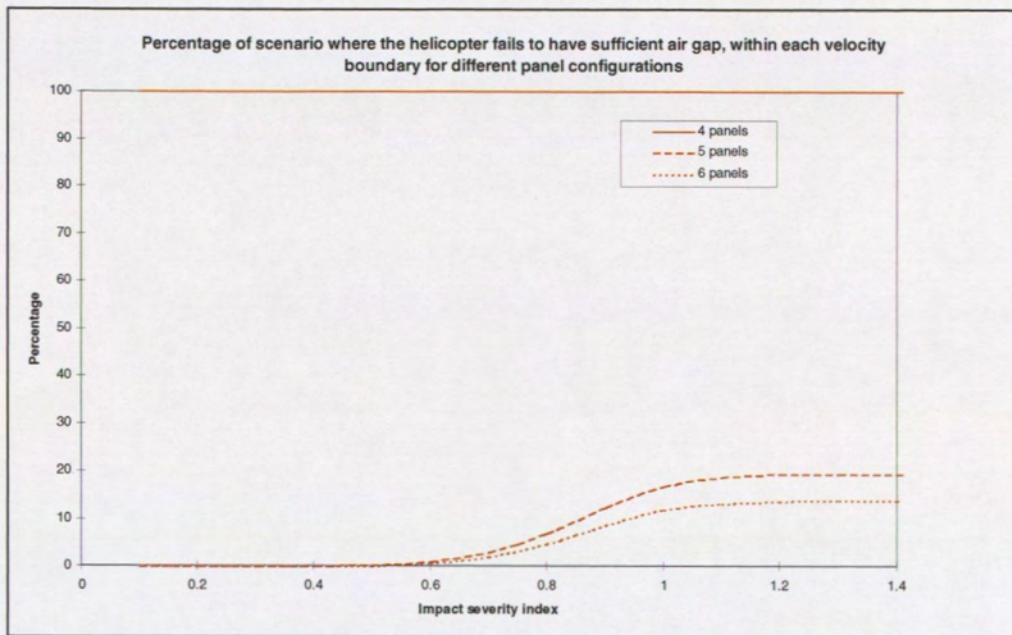


Figure 110: Percentage of impact events where the *EH101* helicopter provided an unsatisfactory air space, within each impact severity index curve, for different float configurations.

Appendix A: Investigation Based on the Brent Spar and Cormorant Alpha Accidents

WS Atkins Science and Technology (WSA) carried out a parallel investigation for the CAA based on three actual helicopter accident scenarios. These three accidents occurred near the *Cormorant Alpha* platform in 1992, at the *Brent Spar* platform in 1990, and near the *Scilly Isles* in 1983. Further information about these three accidents may be found in WSA's literature review [1] and in the relevant Air Accidents Investigation Branch (AAIB) reports.

WSA's investigation was 'generic' to the extent that it was based on a single helicopter type, the *WG30*, rather than the specific helicopter type involved in each of these three accidents. WSA set up a full structural model of the *WG30*, and then investigated a small number of 'deterministic' models of each accident scenario. Each deterministic scenario was based on a single set of parameters to describe the helicopter's speed, descent angle and orientation, and the wave surface at the time of each accident. Because of the complexity of their structural and fluid models, however, WSA were only able to consider the consequences of limited variations in modelling parameters.

BMT's investigations were intended to complement WSA's deterministic analysis. They were based on a highly simplified impact loading model, but were intended to show in a probabilistic manner how the impact loads are likely to vary with changes in the modelling parameters and assumptions.

The models developed by BMT and WSA represented the water impact loading process in very different ways, and it was not easy to predict in advance how the results from the two models would compare. BMT therefore undertook additional calculations, based on WSA's deterministic models of the *Cormorant Alpha* and *Brent Spar* accidents, which would enable results from the two models to be compared directly. These comparisons are described in the accompanying WSA report [1].

BMT therefore calculated water impact loads on two fuselage panels near the nose of the *WG30* helicopter, based on two agreed accident scenarios. Mean values of parameters describing the helicopter and wave conditions were chosen to be identical to those used in WSA's own deterministic analysis, and were in turn based on information contained in the two relevant accident reports [4, 5]. The standard deviation of each parameter was chosen to be representative of the uncertainty in the chosen mean value. A single sea state was modelled in each case, but realistic levels of uncertainty in the significant wave height and zero-crossing period in each sea state were represented. Mean values of each parameter, and the uncertainty in each parameter value, were agreed with WSA before the study commenced [35, 36].

The procedures used in this investigation were identical to those used during BMT's base case and sensitivity studies (see Sections 5 and 6), and were based on the formulation described in Section 4. Results from BMT's Monte Carlo simulation were compared with results obtained by running the program in a 'deterministic' manner, using mean values of each parameter which were identical with those used during WSA's analysis.

A1 Panel Models

A1.1 *Brent Spar*

The helicopter involved in the *Brent Spar* accident suffered structural damage in a number of different areas [1]. WSA's investigations indicated severe water impact loading on the starboard side of the nose. The panels defined in Figure 111 and Figure 112 were therefore agreed to be of particular interest [36]. The attitude of the helicopter in these diagrams is shown at the instant of impact onto the water surface, with the same heel and trim angles as the helicopter involved in the *Brent Spar* accident.

The calculations were based on a simplified model of the starboard panels identified in Figure 112. They were modelled as two separate rectangular panels: a 'base panel' facing downwards, and a 'side panel' facing to starboard. Impact loads on these two panels were calculated as if they were in isolation. Panel dimensions and orientations were based on information supplied by WSA [36], and are described in Table A1-1. The length and breadth of each rectangular panel were chosen to give the same length and area as the equivalent group of WSA panels.

The orientation of the panel was described by three inclination angles, representing successive clockwise rotations of an initially vertical panel facing to starboard, about axes pointing forwards, to starboard, and downwards respectively. These three angles are shown in Table A1-1.

| Table A1-1: Panel parameters considered during the <i>Brent Spar</i> investigation. | | |
|--|-------------------|-------------------|
| | Side panel | Base panel |
| Inclination about roll axis | 41° | 74° |
| Inclination about pitch axis | 0° | 0° |
| Inclination relative to forward direction | -20° | 0° |
| Panel length | 0.82 m | 0.82 m |
| Panel width | 0.18 m | 0.16 m |

A1.2 *Cormorant Alpha*

The helicopter involved in the *Cormorant Alpha* accident also suffered structural damage on the starboard side of the nose [1]. It was therefore agreed [37] that BMT's calculations should be based on the same fuselage panels that had been considered during the *Brent Spar* investigation. Panel dimensions and orientations were based on information supplied by WSA [37], and are described in Table A1-2.

| | Side panel | Base panel |
|---|-------------------|-------------------|
| Inclination about roll axis | 24° | 73.5° |
| Inclination about pitch axis | 0° | 8.6° |
| Inclination relative to forward direction | -23.8° | -10.0° |
| Panel length | 0.82 m | 0.82 m |
| Panel width | 0.18 m | 0.16 m |

A2 **Impact Parameters**

A2.1 *Brent Spar*

Impact parameters representing the *Brent Spar* scenario were also agreed with WSA, and are summarised in Table A2-1. The impact speed represents the resultant speed of the helicopter in its direction of travel at the instant of impact, and the mean direction of fall was vertically downwards. Two impact speed scenarios were considered: a 'full-speed' scenario, representing a helicopter falling vertically under gravity off the deck of a representative offshore platform 25m high, and a 'half-speed' scenario representing a lower drop height.

WSA's fax [36] listed the co-ordinates of each panel relative to earth-based axes at the instant of impact. The panel angles used in BMT's simulations therefore already took account of the helicopter's orientation, and the mean roll, pitch and yaw angles of the helicopter itself were set equal to zero.

WSA [36] stated that the uncertainty in the vertical impact speed was ± 2 m/s in the full-speed case and ± 1 m/s in the half-speed case, and the uncertainty in the horizontal impact speed was ± 2 m/s in both cases. The uncertainty in the horizontal velocity, relative to the mean vertical velocity, was treated as an uncertainty in the descent angle. WSA stated that the uncertainties in the angles of orientation of the panels were $\pm 1.5^\circ$, and these were treated as uncertainties in the roll, pitch and yaw angles of the helicopter itself. As agreed with WSA, the 'uncertainty' was considered to be a maximum value, and was assumed to represent three standard deviations of a normal distribution.

The mean value and standard deviation of the helicopter's heading angle relative to waves were chosen to be consistent with BMT's earlier simulations of vertical drop incidents, and represent a fairly broad spread of angles. The range of wave heading angles chosen has no particular significance, however, because the results proved to be insensitive to wave conditions.

| Table A2-1: Impact parameters based on the <i>Brent Spar</i> accident scenario. | | |
|--|--|---|
| | Mean | Standard deviation |
| Impact speed | 22.0 m/s full-speed
11.0 m/s half-speed | 0.7 m/s full-speed
0.35 m/s half-speed |
| Descent angle | 90.0° (vertical descent) | 2.0° full-speed
4.0° half-speed |
| Helicopter roll, pitch and yaw angles | 0.0° | 0.5° in all cases |
| Heading angle to waves | 60.0° | 60.0° |

The sea conditions at the time of the *Brent Spar* accident were stated to be 'calm'. This description has been interpreted as a sea state with a significant wave height of 1.0m or less. Sea states were sampled from a wave scatter table constructed as follows. The significant wave height was assumed to be between 0.0m and 1.0m, at 0.2m intervals, all such heights having equal probability. The distribution of wave periods was assumed to be identical to that used during BMT's main sensitivity study (see Section 6.1 of [2]), for wave heights between 0.0m and 1.0m, and was based on all-year, all-directions 'PC-Global Wave Statistics' data for the Central North Sea area.

A2.2 *Cormorant Alpha*

Impact parameters representing the *Cormorant Alpha* scenario were also agreed with WSA, and are summarised in Table A2-2. The helicopter's assumed mean heading and wave direction at the instant of impact are illustrated in Figure 117. These parameters are based on conditions defined in references [38] and [39].

WSA's fax [37] quoted the co-ordinates of each panel relative to earth-based axes at the instant of impact. Once again the panel angles used in BMT's simulations already took account of the helicopter's orientation, and the mean roll, pitch and yaw angles of the helicopter itself were set equal to zero.

WSA had defined the helicopter and sea state conditions at the time of the *Cormorant Alpha* accident [37], stating that the uncertainty in the helicopter's resultant speed on impact was ± 5 m/s, and the uncertainty in its descent angle was ± 1.5 degrees. The uncertainties in the roll and pitch angles were stated to be ± 1.5 degrees. The helicopter's yaw angle at the time of the actual incident was not known. It was agreed, therefore, that the mean yaw angle should be set to zero, and a fairly large uncertainty in the yaw angle (± 15 degrees) should be assumed. Once again the 'uncertainty' was considered to be a maximum value, and was assumed to represent three standard deviations of a normal distribution.

| | Mean | Standard deviation |
|------------------------|-------------|---------------------------|
| Impact speed | 23.4 m/s | 2.0 m/s |
| Descent angle | 19.0° | 0.5° |
| Helicopter roll angle | 0.0° | 0.5° |
| Helicopter pitch angle | 0.0° | 0.5° |
| Helicopter yaw angle | 0.0° | 5.0° |
| Heading angle to waves | -120° | 5.0° |

Conditions at the time of the *Cormorant Alpha* accident were stated [38] to be: a significant wave height of 7 to 8m, an average wave period of 8 to 10 seconds, with a wave direction of 340°, and a helicopter heading of 100°.

As in earlier investigations [39], it was assumed that the stated wave direction was that from which the waves were travelling, and that the so-called 'average' wave period was the zero-crossing period T_z . These conditions were therefore represented by a synthesised scatter table of significant wave heights, H_s , and zero-crossing periods, T_z , centred on the mean condition $H_s = 7.5\text{m}$, $T_z = 9.0\text{s}$, and with a variation of about $\pm 0.5\text{m}$ in H_s and $\pm 1.0\text{s}$ in T_z .

The wave scatter table assumed during these calculations is shown in Table A2-3. This distribution was based on an uncorrelated bi-variate normal distribution with standard deviations equal to 0.5m in H_s and 1.0s in T_z .

Table A2-3: Assumed scatter table representing the uncertainty in wave conditions at the time of the *Cormorant Alpha* accident.

| | | | | | | | |
|-----------|-----|-----|-----|-----|------|------|------|
| H_s (m) | | | | | | | |
| 9.0 | 0 | 0 | 0 | 0 | 0 | 0 | 0 |
| 8.5 | 0 | 1 | 3 | 5 | 3 | 1 | 0 |
| 8.0 | 0 | 3 | 15 | 24 | 15 | 3 | 0 |
| 7.5 | 0 | 5 | 24 | 40 | 24 | 5 | 0 |
| 7.0 | 0 | 3 | 15 | 24 | 15 | 3 | 0 |
| 6.5 | 0 | 1 | 3 | 5 | 3 | 1 | 0 |
| 6.0 | 0 | 0 | 0 | 0 | 0 | 0 | 0 |
| T_z (s) | 6.0 | 7.0 | 8.0 | 9.0 | 10.0 | 11.0 | 12.0 |

A3 Results from the Brent Spar Investigation

The main results from the *Brent Spar* investigation are shown in Figures 113 to 116. These four figures show exceedance probability distributions for the maximum impact load on the side and base panels in full-speed and half-speed impacts. Three sets of results are shown on each figure:

- The solid curve shows the range of loads occurring when all parameters were subject to the levels of uncertainty shown in the above tables.
- The dashed curve shows the variability associated with the wave environment alone, due to variations in the significant wave height and zero-crossing period, in the heading of the helicopter relative to the waves, and in the height and local slope of the individual wave at the instant of impact. The helicopter speed, descent angle and attitude were fixed in this case at their mean values.
- The vertical bar represents the fully deterministic scenario, with completely calm water, and all impact parameters set at their mean values.

The shapes of the curves are very similar for both panels at both impact speeds, with a fairly broad spread of values when all parameters were allowed to vary.

The impact loads occurring during a half-speed incident are a quarter of those occurring during the corresponding full-speed incident. This result is consistent with the theoretical formulation, which predicts that the impact load will vary with the square of the impact speed.

The amount of variability was much reduced when only the wave parameters were allowed to vary, confirming an earlier conclusion that the impact loads occurring in a vertical descent incident are insensitive to wave conditions.

The results obtained using the deterministic model are summarised in Table A3-1. The forces on the base panel are over three times the magnitude of those on the side panel. This result is not surprising, because the base panel was inclined at only 16°

to the horizontal. Even higher loads are possible if the panel is closer to the horizontal on impact.

| Table A3-1: The maximum impact force predicted in each deterministic <i>Brent Spar</i> impact scenario. | | |
|--|-------------------|-------------------|
| | Side panel | Base panel |
| Full-speed impact | 176 kN | 594 kN |
| Half-speed impact | 44 kN | 149 kN |

A4

Results from the Cormorant Alpha Investigation

Figures 118 and 119 show exceedance distributions of the maximum total impact force on the base panel and side panel respectively, based on the *Cormorant Alpha* accident scenario described above. Five sets of results are shown on each figure:

- The solid curve shows the range of loads occurring when all parameters were subject to the levels of uncertainty shown in the above tables.
- The dashed curve shows the variability associated with the surface slope and velocity at the point of impact when all other parameters (including the sea state itself) were fixed at their mean values.
- The chain-dashed curve shows the variability associated with the helicopter speed, descent angle and attitude alone, and represent impacts onto calm water.
- The two vertical bars represent results obtained using alternative fully deterministic scenarios, which are described in Section A4.1.

The solid lines demonstrate the wide range of impact loads that can occur when the calculations represent uncertainties in all the parameters describing the helicopter and the environment. These calculations indicate that there is a 5% probability of exceeding 350 kN on the base panel, and 89 kN on the side panel.

The dashed lines on these two figures show that there were still substantial variations in the impact loads when the helicopter's speed, descent angle, attitude and heading were all set at their mean values, and the significant wave height ($H_s = 7.5\text{m}$) and zero up-crossing wave period ($T_z = 9\text{s}$) were also fixed. Even though the sea state was fixed, the wave surface represented by this sea state was irregular, and the helicopter could make contact at any point on this surface. The dashed curves in Figures 118 and 119 show the range of impact loads that occurred in this scenario, due entirely to variations in the local water surface slope and surface velocity at different points of contact.

Both figures show a fairly broad spread of impact loads associated with variations in the local water surface slope and velocity. There are also noticeable differences between the distributions obtained using the original *Cormorant Alpha* sea state data and assuming 'calm water'. These results appear at first sight to be at variance with corresponding results from the main sensitivity study (see Section 6.2 in the main part

of this report and Figure 68), where wave conditions were found to have no noticeable effect on the impact load distribution corresponding to a loss of control incident. The key difference is that the sensitivity study was intended to be generic, covering a range of possible loss of control incidents, occurring randomly throughout the year. The majority of these simulated incidents occurred in fairly calm sea conditions. The *Cormorant Alpha* scenario was based on one particular incident, which occurred during rough sea conditions. The high sea state at the time of the *Cormorant Alpha* accident therefore gave the wave parameters more significance than they had during the generic study.

The sea state, surface slope and velocity have a particularly marked effect on base panel loads, as shown in Figure 118. The load distribution obtained by varying the surface slope and velocity alone is close to that obtained when all parameters are allowed to vary. Furthermore the 'calm water' load distribution has markedly less spread than when the simulation was based on sea states representative of the *Cormorant Alpha* accident. Sea state was more significant in this respect than variations in the helicopter's speed, descent angle, attitude and heading. This result is again at variance with those obtained from the main sensitivity study (see Section 6.2 in the main part of this report and Figure 68), which apply to loads on a side-facing panel, and are not necessarily valid for loads on a base panel.

A4.1 *The Deterministic Cormorant Alpha Scenario*

The dashed lines in Figures 118 and 119 show that impact forces on both the base panel and side panel are sensitive to variations in the water surface slope and velocity at the point of impact. The results from these simulations therefore had to be processed further in order to determine the maximum impact force associated with a deterministic impact scenario, where the wave surface slope and velocity are fixed at the instant of impact.

The contour plots in Figures 120 and 121 show how the maximum total impact forces on the base panel and side panel vary with the water surface angle β_w and the normal water surface velocity u_w . These contour plots are based on results from Monte Carlo simulations with fixed mean helicopter and sea state parameters. As expected, the force generally increases when the water surface rises (i.e. as the surface velocity becomes more negative), and when it is inclined towards the helicopter (a negative surface angle). The contour plot for the base panel shows a large peak centred around a water surface angle of about -18 degrees, this being the angle at which the water surface is parallel to the panel itself.

BMT had previously recommended [39] that a wave slope angle of 10 degrees, and a wave phase speed between 12 and 16 m/s should be assumed in WSA's deterministic model. The damage report suggested that the helicopter involved in the *Cormorant Alpha* accident had come down onto the rear flank of a wave travelling in approximately the same direction. The deterministic model therefore represents a wave surface, moving at an angle of 60° to the helicopter's own heading (see Figure 117), inclined towards it, and receding at the instant of impact.

Assuming that the water surface moves horizontally with the mean wave phase speed (14 m/s), the velocity of the water surface normal to itself is $14 \sin 10^\circ = 2.4$ m/s. The deterministic scenario should therefore represent the following: a surface slope angle equal to -10° , inclined towards the helicopter as it approaches, and a normal water surface velocity (downwards) equal to +2.4 m/s.

This particular deterministic scenario is represented by the symbol ● in Figures 120 and 121. The maximum total impact force on the base panel in this scenario is 160 kN, and the corresponding force on the side panel is 45 kN. These two ('deterministic, receding') values are shown as solid vertical bars in Figures 118 and 119.

The assumed phase speed of the wave surface is comparable in magnitude with the speed of the helicopter on impact, but its value is very uncertain. The deterministic calculation procedure predicts a much higher impact load if it is based on a regular wave with the same surface slope, but a shorter period, and therefore a lower wave phase speed. The symbol ○ in Figures 120 and 121 represents the scenario where the water surface is assumed to be stationary at the point of impact. The maximum total impact forces on the base panel and side panel are then increased to 250 kN and 59 kN respectively. These alternative ('deterministic, stationary') estimates are shown as light vertical bars on Figures 118 and 119. Substantially lower deterministic estimates of the impact load are therefore obtained when the water surface is assumed to be receding away from the helicopter at the point of impact, compared with the loads obtained assuming a stationary surface.

There are significant differences between the probabilities of exceeding these alternative deterministic estimates, when all the uncertainties in the helicopter and sea conditions are taken into account. The probability of exceeding the deterministic load on the base panel with a 'receding' water surface is over 20%, but this probability is reduced to only 9% if the water surface is assumed to be stationary at the point of impact. There are much larger probabilities of exceeding the deterministic loads on the side panel: 50% and 25% respectively. Whereas both deterministic estimates for the base panel may be regarded as reasonably conservative, this is not true of corresponding estimates for the side panel. More conservative estimates are obtained if the water surface is assumed to be stationary at the point of impact than if it is assumed to be receding away from the helicopter.

The results obtained using the deterministic model are summarised in Table A4-1. The force on the base panel is over six times the magnitude of the corresponding value for the side panel. This result is not surprising, because the base panel was inclined at only 8° relative to the water surface on impact. Significantly higher loads may occur if the panel is more nearly parallel to the water surface on impact.

| Table A4-1: The maximum impact force predicted in each deterministic <i>Cormorant Alpha</i> impact scenario. | | |
|---|-------------------|-------------------|
| | Side panel | Base panel |
| Receding water surface
($u_w = 2.4$ m/s) | 45 kN | 160 kN |
| Stationary water surface
($u_w = 0.0$ m/s) | 59 kN | 250 kN |

**Results from the Study based on the
Brent Spar Accident Scenario**

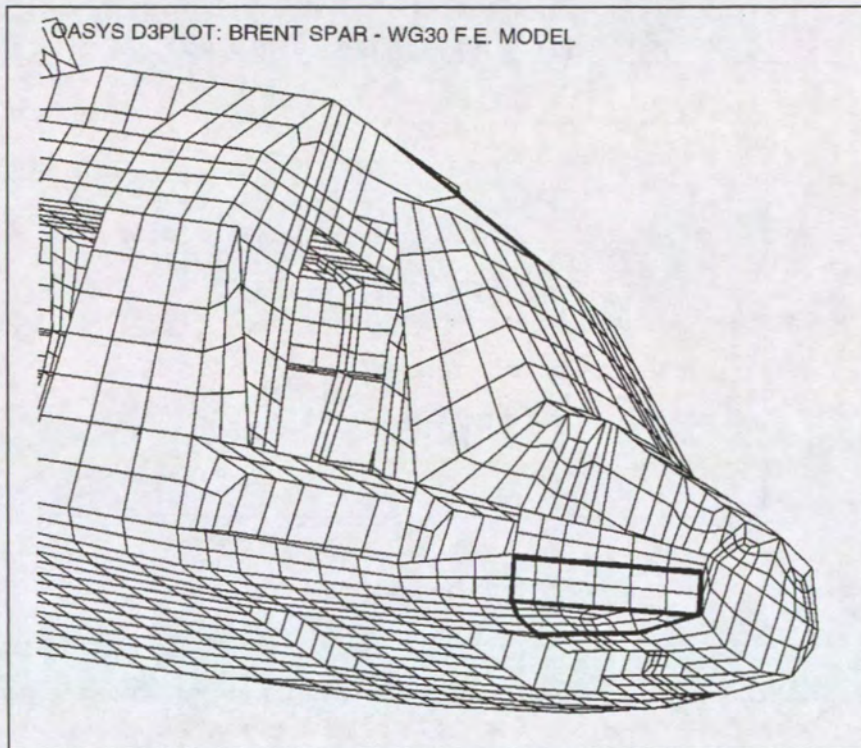


Figure 111: Forward part of WSA's finite element model, highlighting panels identified for investigation.

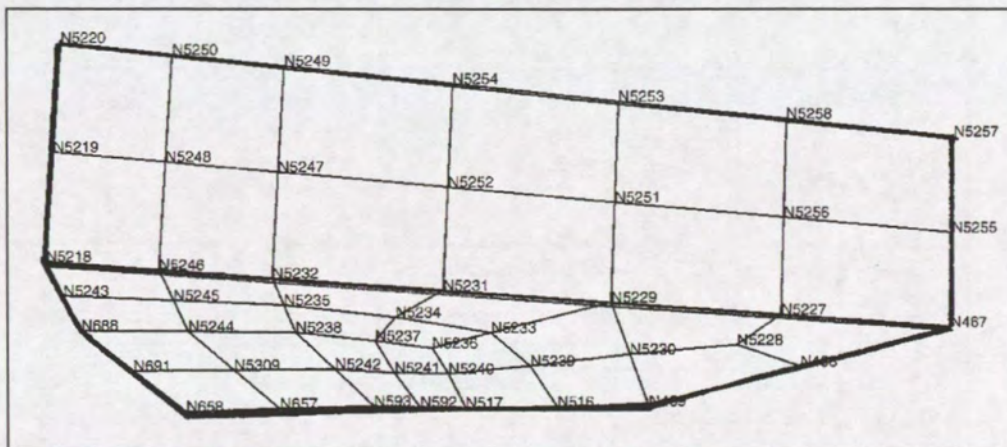


Figure 112: Enlargement of panels identified for investigation.

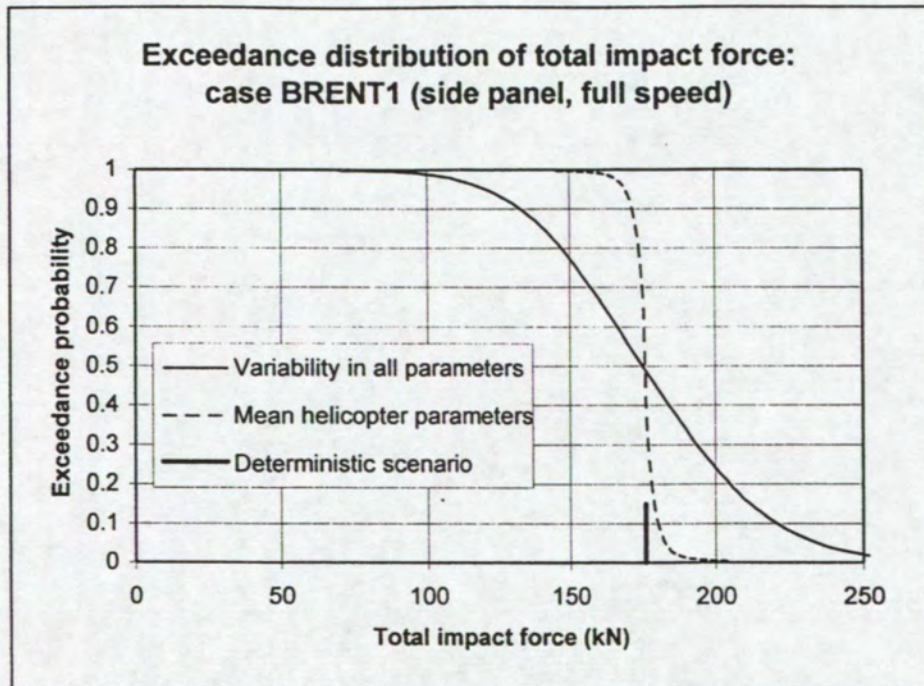


Figure 113: Exceedance distribution of the maximum total impact force: side panel in *Brent Spar* full-speed accident scenario.

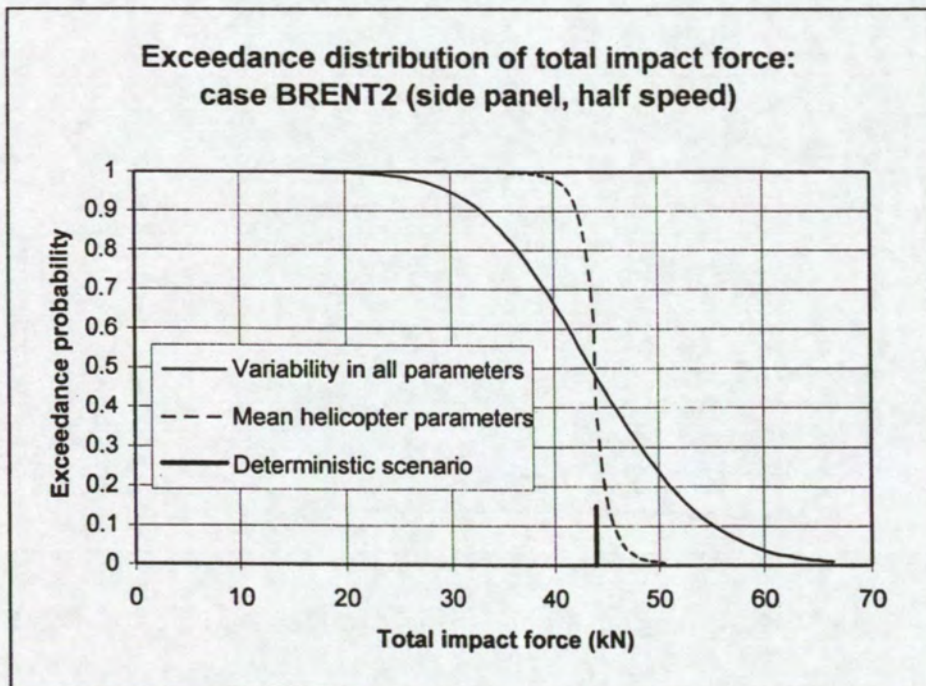


Figure 114: Exceedance distribution of the maximum total impact force: side panel in *Brent Spar* half-speed accident scenario.

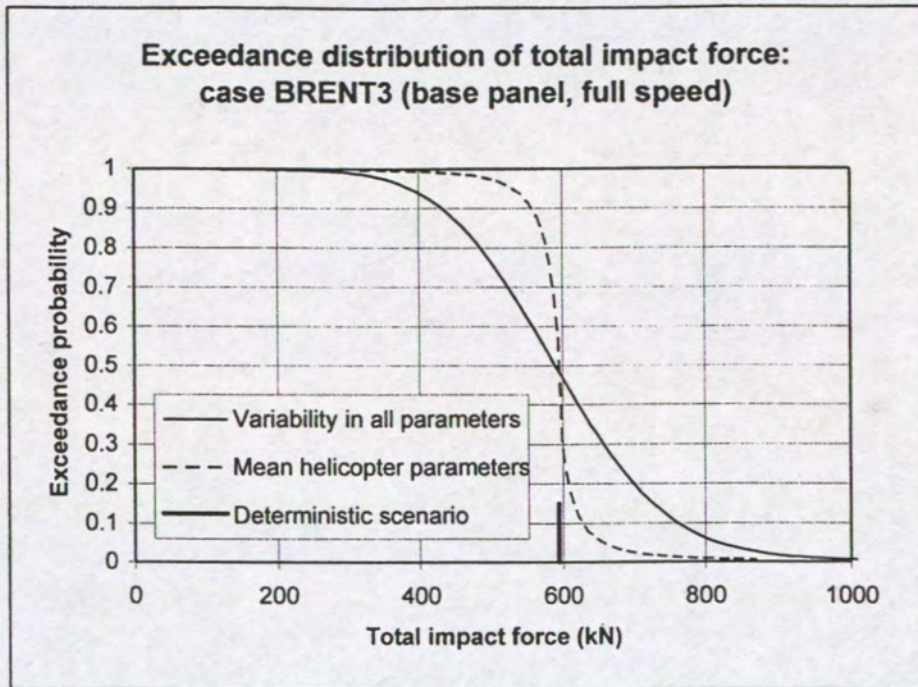


Figure 115: Exceedance distribution of the maximum total impact force: base panel in *Brent Spar* full-speed accident scenario.

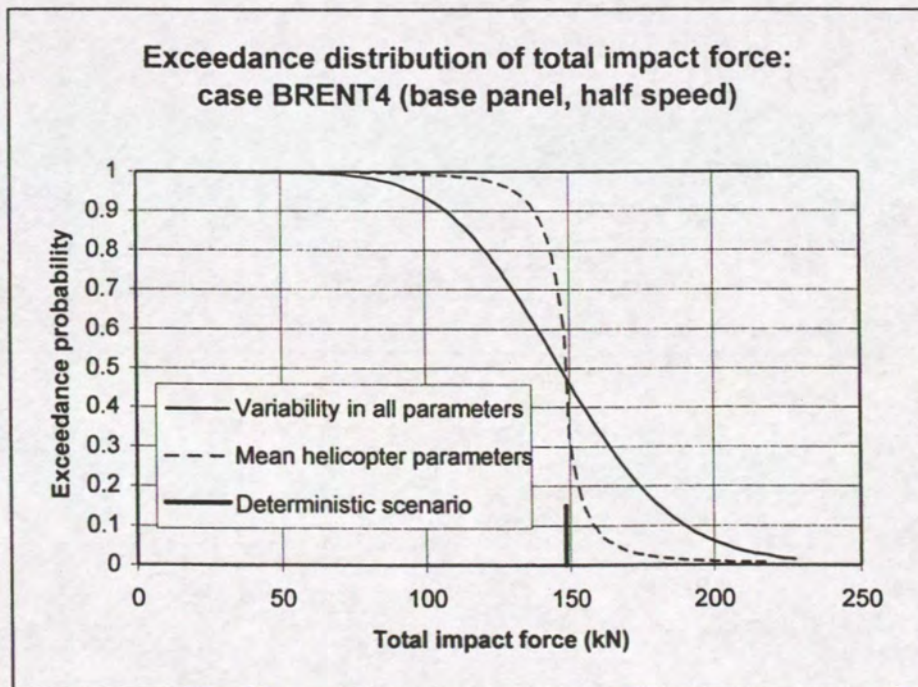


Figure 116: Exceedance distribution of the maximum total impact force: base panel in *Brent Spar* half-speed accident scenario.

**Results from the Study based on the
Cormorant Alpha Accident Scenario**

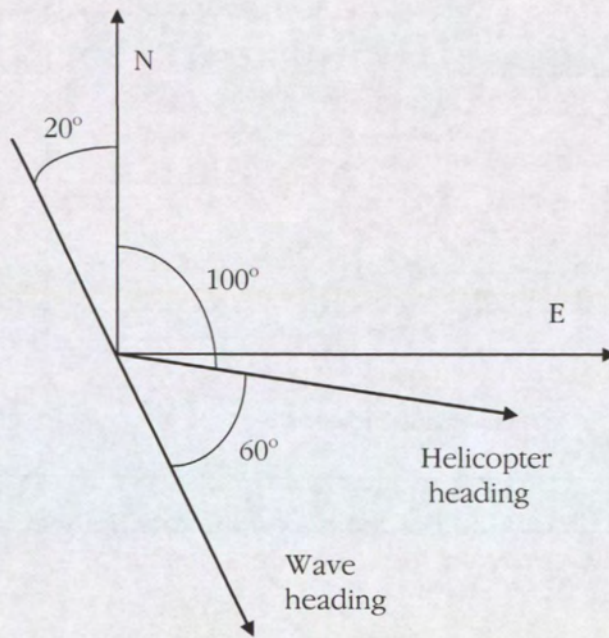


Figure 117: Mean wave heading and helicopter heading directions assumed during the *Cormorant Alpha* investigation.

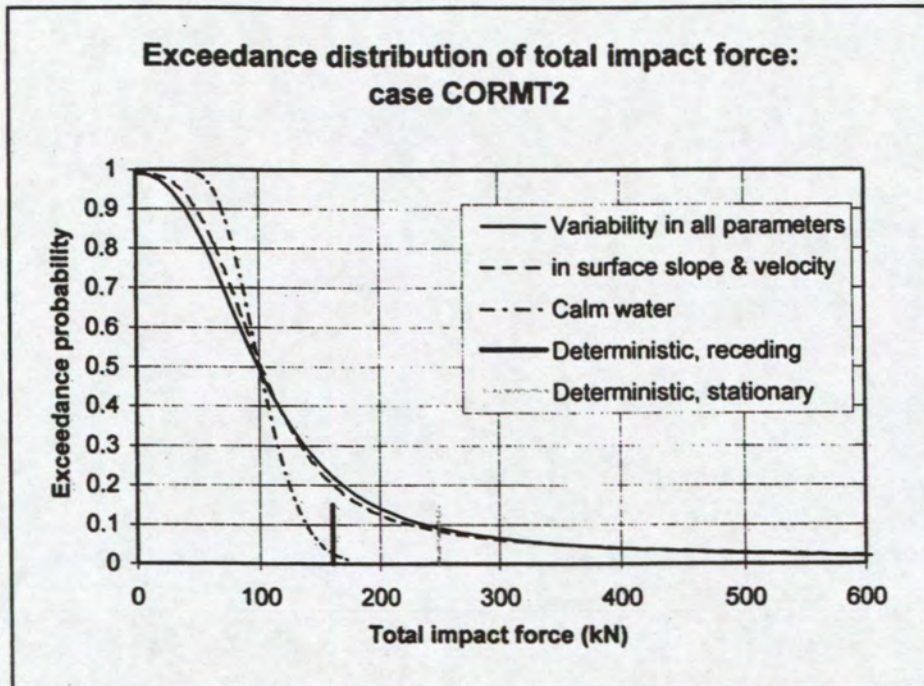


Figure 118: Exceedance distribution of the maximum total impact force: base panel in *Cormorant Alpha* accident scenario.

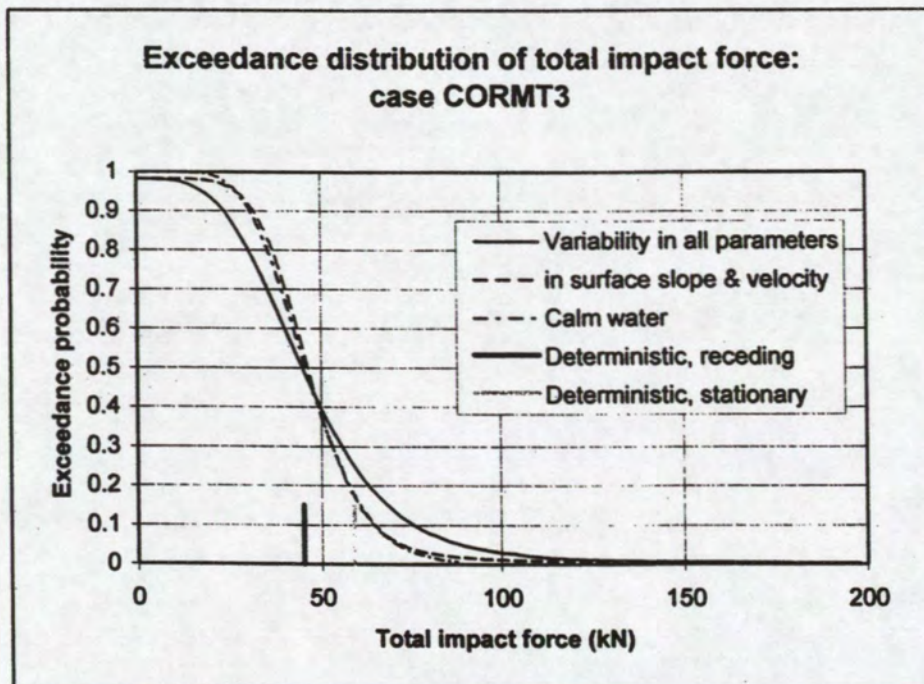


Figure 119: Exceedance distribution of the maximum total impact force: side panel in *Cormorant Alpha* accident scenario.

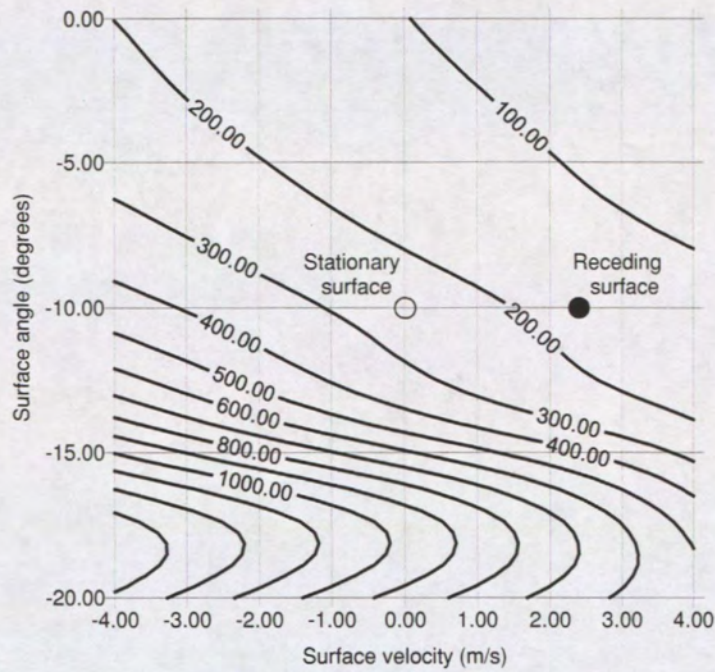


Figure 120: Contour plot of maximum total impact force against water surface angle and velocity, with other parameters fixed: *Cormorant Alpha* base panel.

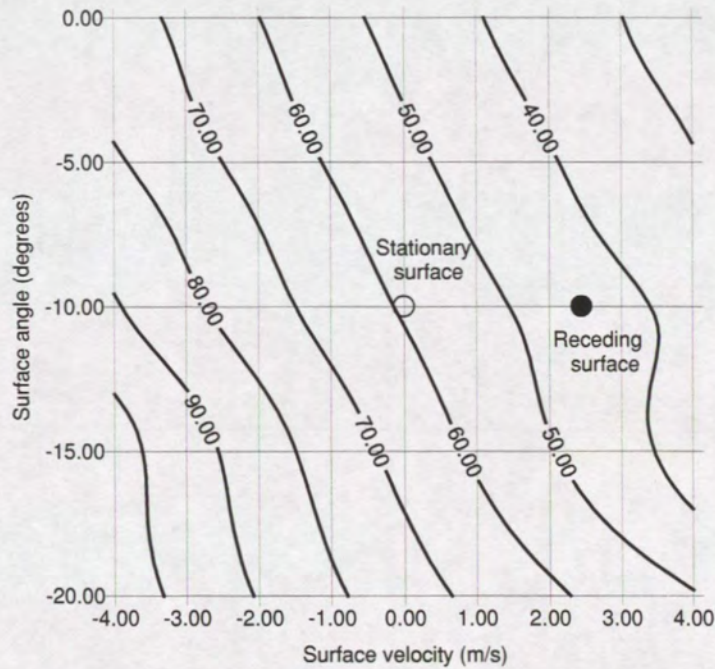


Figure 121: Contour plot of maximum total impact force against water surface angle and velocity, with other parameters fixed: *Cormorant Alpha* side panel.

